FELIPE DE MEDEIROS MAGALHÃES

FILOGEOGRAFIA E LIMITE ESPECÍFICO DO COMPLEXO *LEPTODACTYLUS LATRANS* DE ESPÉCIES (AMPHIBIA, ANURA, LEPTODACTYLIDAE) NA AMÉRICA DO SUL

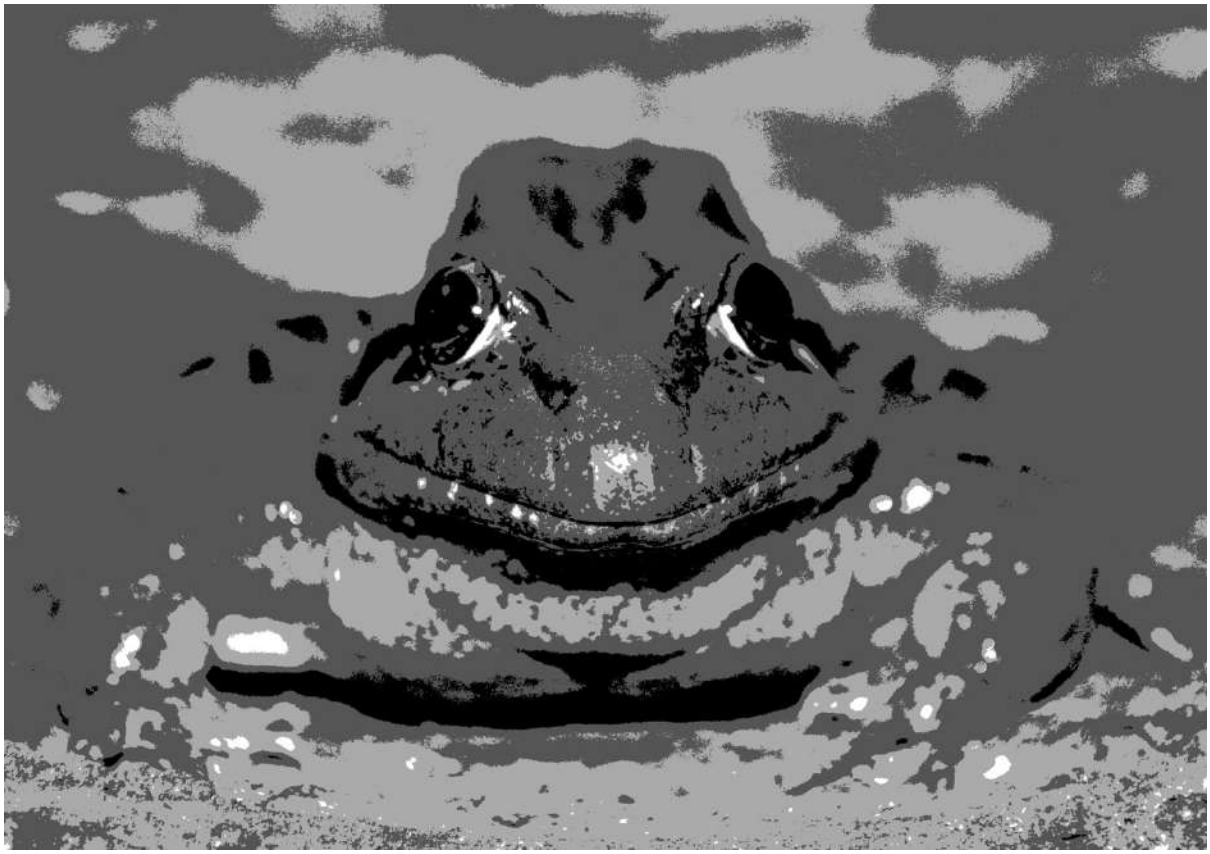

João Pessoa

Paraíba – Brasil

2019

FELIPE DE MEDEIROS MAGALHÃES

FILOGEOGRAFIA E LIMITE ESPECÍFICO DO COMPLEXO *LEPTODACTYLUS LATRANS* DE ESPÉCIES (AMPHIBIA, ANURA, LEPTODACTYLIDAE) NA AMÉRICA DO SUL

Tese apresentada à Universidade Federal da Paraíba, como parte de exigências do Programa de Pós-Graduação em Ciências Biológicas (Zoologia), para obtenção do título de Doutor

Orientador:
Dr. Adrian Antonio Garda

Catalogação na publicação
Seção de Catalogação e Classificação

M188f Magalhães, Felipe de Medeiros.
Filogeografia e limite específico do complexo Leptodactylus latrans de espécies (Amphibia, Anura, Leptodactylidae) na América do Sul / Felipe de Medeiros Magalhães. - João Pessoa, 2019.
231 f. : il.

Orientação: Adrian Antonio Garda.
Tese (Doutorado) - UFPB/CCEN.

1. Anura. 2. Biogeografia. 3. Delimitação multi-locus. 4. Taxonomia integrativa. 5. Bioacústica. 6. Genética de populações. 7. Leptodactylus. I. Garda, Adrian Antonio. II. Título.

UFPB/BC

FELIPE DE MEDEIROS MAGALHÃES

FILOGEOGRAFIA E LIMITE ESPECÍFICO DO COMPLEXO *LEPTODACTYLUS LATRANS* DE ESPÉCIES (AMPHIBIA, ANURA, LEPTODACTYLIDAE) NA AMÉRICA DO SUL

Tese apresentada à Universidade Federal da Paraíba, como parte de exigências do Programa de Pós-Graduação em Ciências Biológicas (Zoologia), para obtenção do título de Doutor

Dr. Henrique Batalha-Filho
Membro titular externo
UFBA

Dr. Pedro Ivo Simões
Membro titular externo
UFPE

Dr. Pedro C. E. de A. Pinto
Membro titular interno
UFPB

Dr. Gustavo H. C. Vieira
Membro titular interno
UFPB

Dr. Adrian Antonio Garda
Orientador
UFPB

Ata da 123ª Apresentação e Banca de Defesa de Doutorado de Felipe de Medeiros Magalhães

Ao(s) Trinta e um dias do mês de maio de dois mil e dezenove, às 13:00 horas, no(a) Sala do PPGCB, da Universidade Federal da Paraíba, reuniram-se, em caráter de solenidade pública, membros da banca examinadora para avaliar a tese de doutorado de **Felipe de Medeiros Magalhães**, candidato(a) ao grau de Doutor em Ciências Biológicas. A banca foi composta pelos seguintes professores/pesquisadores: **Dr. Adrian Antonio Garda (Orientador), Dr. Henrique Batalha Filho, Dr. Pedro Ivo Simões, Dr. Hélder Farias Pereira de Araújo e Dr. Diego José Santana Silva.** Compareceram à solenidade, além do(a) candidato(a) e membros da banca examinadora, alunos e professores do PPGCB. Dando início à sessão, a coordenação fez a abertura dos trabalhos, apresentando o(a) discente e os membros da banca. Foi passada a palavra para o(a) orientador(a), para que assumisse a posição de presidente da sessão. A partir de então, o(a) presidente, após declarar o objeto da solenidade, concedeu a palavra a **Felipe de Medeiros Magalhães**, para que dissertasse, oral e sucintamente, a respeito de seu trabalho intitulado **"Filogeografia e limite específico do complexo Leptodactylus latrans de espécies (Amphibia, Anura, Leptodactylidae) na América do Sul"**. Passando então a discorrer sobre o aludido tema, dentro do prazo legal, o(a) candidato(a) foi a seguir arguido(a) pelos examinadores na forma regimental. Em seguida, passou a Comissão, em caráter secreto, a proceder à avaliação e julgamento do trabalho, concluindo por atribuir-lhe o conceito Aprovado. Perante a aprovação, declarou-se o(a) candidato(a) legalmente habilitado(a) a receber o grau de **Doutor em Ciências Biológicas**, área de concentração **Zoologia**. Nada mais havendo a tratar eu, **Dr. Adrian Antonio Garda**, como presidente, lavrei a presente ata que, lida e aprovada, assino juntamente com os demais membros da banca examinadora.

João Pessoa, 31/05/2019.

Dr. Adrian Antonio Garda (Orientador)

Dr. Henrique Batalha Filho

Dr. Pedro Ivo Simões

Dr. Hélder Farias Pereira de Araújo

Dr. Diego José Santana Silva

Ciente do Resultado:

Felipe de Medeiros Magalhães

Felipe de Medeiros Magalhães

À toda população brasileira: balbúrdia para sempre…

Agradecimentos

Gostaria de agradecer a todos que de alguma forma contribuíram para a minha formação e para a realização deste trabalho. Aos meus pais Paulo Henrique Freire Magalhães e Inailde Maria de Medeiros Magalhães, meu irmão Bruno de Medeiros Magalhães, minha avó Cleide de Medeiros Queiroz, meu tio Junior (Juninho) Magalhães e meus demais familiares por todo apoio incondicional que me deram durante toda a minha vida, sempre apoiando minhas decisões e me dando forças para conquistar dia a dia todos os meus objetivos.

A minha companheira Renaly da Costa Rodrigues que me apoiou em todos os momentos difíceis e esteve ao meu lado sempre que eu precisei durante praticamente todos os anos de doutorado. Seu amor e carinho me mantiveram focado e determinado e, sem eles, não teria chegado aonde eu cheguei. Serei sempre grato por ter você na minha vida.

Ao meu orientador Adrian Antonio Garda pelas críticas e ensinamentos valiosos, que certamente ajudaram na minha formação como pesquisador.

Aos meus amigos e colegas do laboratório de Anfíbios e Répteis: Felipe Camurugi (Camura), Ricardo Rodrigues (xyrley/maislindo), Ricardo Marques, Felipe Coelho, Willianilson (Will), Alan Filipe (Neguin), David Lucas (Lucão), Leandro Alves, Marcelo Gehara, Emanuel Fonseca e Flávia Mol (Manel e Flavinha), Vinícius São-Pedro, Eliana Faria, Diego Santana e Sarah Mângia, André Bruinjé, Juan Pablo (Juanpy e família) por todo apoio, conselhos e companheirismo, me ajudando sempre que possível em todas atividades de laboratório ou de campo ou até mesmo com o bate papo descontraído nos corredores e fora do ambiente de trabalho. Em especial ao Will e Flavinha que me acompanharam nas viagens de campo que, apesar das adversidades, deram super certo.

Aos professores e colegas da UFPB. Em especial agradeço a Lucas Libélula, Izabel Regina, Gustavo Vieira e Daniel Mesquita que sempre me receberam de forma calorosa em João Pessoa.

A todos os alunos e técnicos das coleções das universidades de Brasilia (UnB), Uberlândia (UFU), Campo Grande (UFMS), UNESP-Rio Claro (CFBH), Salvador (UFBA) e Misiones (LGE-UNaM/Argentina) por seu apoio e companheirismo, em especial ao Arthur Senna, Cássio Rachid, Thiago Ribeiro de Carvalho e Mariana Lyra, pelas caronas e por me esperarem no laboratório um pouco mais que o usual para que eu pudesse examinar todos os exemplares a tempo. São muitos os nomes a agradecer, mas quero que saibam que sem o suporte de todos não teria conseguido realizar esse trabalho em tempo hábil. Vocês foram fundamentais!

Sumário

Resumo

MAGALHÃES, Felipe de Medeiros, Universidade Federal da Paraíba, Maio de 2019. **Filogeografia e limite específico do complexo *Leptodactylus latrans* de espécies (Amphibia, Anura, Leptodactylidae) na América do Sul.**
Orientador: Adrian Antonio Garda

O grupo *Leptodactylus latrans* de espécies (Anura: Leptodactylidae) compreende táxons morfologicamente crípticos com ampla distribuição na América do Sul (da Venezuela até o norte da Argentina, leste dos Andes), ocorrendo em todos os biomas brasileiros e ao longo de um gradiente altitudinal variando desde 0 à ~1500m de altitude. A delimitação das espécies desse grupo é historicamente problemática devido, principalmente, a ampla distribuição geográfica e a existência de possíveis sintopias entre espécies sem caracteres morfológicos diagnósticos discretos (por exemplo, *L. latrans/chaquensis/macrosternum*). Ainda, a falta de dados moleculares e acústicos também dificulta uma melhor compreensão acerca dos limites específicos e da diversidade existente neste grupo. Com isso, o objetivo da presente tese é: 1 – delimitar de forma integrativa (utilizando múltiplas fontes de evidência) o limite específico das espécies do complexo *Leptodactylus latrans*; 2 – investigar cenários de diversificação para o grupo. Para tanto, montei um extenso banco de dados incluindo informações genéticas (717 espécimes sequenciados e seis marcadores moleculares, sendo dois mitocondriais e quatro nucleares), morfométricas (com 811 indivíduos mensurados) e acústicas (gravações para todas as espécies) abrangendo toda a potencial distribuição geográfica do grupo. Dentre os principais resultados, proponho a ampla distribuição de *L. macrosternum* na América do Sul, suportada pela ausência de estruturação filogeográfica (linhagem geneticamente coesa). Em contrapartida, dados moleculares, acústicos e morfológicos corroboram a existência de quatro linhagens com alta divergência genética e padrão geográfico coerente (incluindo a linhagem nominal *L. latrans*). Portanto, restrinjo a ocorrência de *L. latrans* para a Mata Atlântica costeira do Brasil (norte de São Paulo à Bahia), proponho a revalidação de uma espécie e descrevo duas novas espécies para o grupo. Por fim, reforço a importância da abordagem integrativa para resolução taxonômica de táxons morfologicamente crípticos e amplamente distribuídos, demonstrando que o conhecimento acerca dos padrões de diversidade de espécies na região neotropical ainda é depreciado.

Palavras-chave: Anura, Biogeografia, delimitação multi-locus, filogeografia, taxonomia integrativa, bioacústica, genética de populações

Abstract

MAGALHÃES, Felipe de Medeiros, Universidade Federal da Paraíba, Maio de 2019. **Filogeografia e limite específico do complexo *Leptodactylus latrans* de espécies (Amphibia, Anura, Leptodactylidae) na América do Sul.**
Orientador: Adrian Antonio Garda

The *Leptodactylus latrans* species group (Anura: Leptodactylidae) includes morphologically cryptic taxa widely distributed in South America (from Venezuela to northern Argentina, east of Andes), occurring along all Brazilian biomes and along an altitudinal gradient ranging from 0 to ~1500m above sea level. The delimitation of the species in this group is historically problematic due to the wide geographical distribution and the existence of morphologically cryptic species that do not exhibit discrete diagnostic morphological characters (for instance, *L. latrans*/*chaquensis*/*macrosternum*). Moreover, the lack of molecular and acoustic data also hampers a better understand concerning the species limit and diversity existing in this group. Therefore, the objective of this thesis is: 1 – to delimit in an integrative approach (using several sourcers of evidence) the specific limits of the *Leptodactylus latrans* complex species; 2 – investigate diversification scenarios for this group. To do so, I assambled an extensive database including genetic information (717 sequenced specimens and six molecular markers, two mitochondrial and four nuclear), morphometric (with 811 measured specimens) and acoustic (recordings for all species) covering the entire geographical distribution range of the *L. latrans* group. Among the main results, we propose a wide geographic distribution of *L. macrosternum* in South America, supported by the absence of phylogeographic structure (cohesive genetic lineage). In contrast, molecular, acoustic and morphological data corroborate the existence of four lineages with high genetic divergence and coherent geographic pattern (including the nominal *L. latrans* lineage). Therefore, I restrict the occurrence of *L. latrans* to the coastal Atlantic Forest of Brazil (from north of São Paulo to Bahia), also propose the revalidation of one species (*L. luctator*) and describe two new species for the complex. Finally, these results reinforce the importance of an integrative approach for taxonomic resolutions in a morphologically cryptic and widely distributed taxa, demonstrating that the knowledge on patterns of species diversity in the neotropical region is still depreciated.

Key-words: Anura, Biogeography, multi-locus species delimitation, phylogeography, integrative taxonomy, bioacoustics, population genetics

INTRODUÇÃO GERAL

1. Introdução

Anfíbios anuros são um grupo bastante diversificado e com distribuição cosmopolita e a região Neotropical é a mais diversa e rica em espécies (Fritz & Rahbek 2012). Apesar de serem bastante diversos, os anfíbios anuros também representam um dos maiores grupos de vertebrados ameaçados de extinção, seja por influência antrópica ou por ação de patógenos (Stuart *et al.* 2004). Um compilado feito pela "Global Amphibian Assessment" (Stuart *et al.* 2004) estimou que 7.4% das espécies de anfíbios conhecidas estão sob ameaça crítica de extinção e aproximadamente 22.5% apresentam deficiência de dados sobre sua distribuição e status de conservação, o que subestima a confiabilidade de tais dados. Ainda, há indícios de que muitas espécies estão em declínio (Stuart *et al.* 2004), o que é agravado pelo fato de que muitas delas ainda não serem conhecidas.

Estudos recentes abordando filogenia e delimitação de espécies amplamente distribuídas em regiões altamente diversas têm demonstrado que grande parte da diversidade encontrada é críptica, ou seja, ocorre diversificação e separação de linhagens, porém, a morfologia dos táxons resultantes se mantém conservada (Chek *et al.* 2001; Fouquet *et al.* 2007a; Fouquet *et al.* 2007b). Espécies crípticas são morfologicamente indistinguíveis ou bastante similares e a ocorrência dessas formas em simpatria pode ocasionar, por exemplo, estimativas imprecisas de diversidade ou gerar dados incorretos em trabalhos ecológicos e etológicos, uma vez que espécies distintas podem ser tratadas como a mesma se não forem corretamente examinadas (Bickford *et al.* 2007; Pfenninger & Schwenk 2007).

Casos recém-estudados que envolvem estudos que identificaram vários desses complexos (Fouquet *et al.* 2007b; Padial & de La Riva 2009), ou que determinaram a relação de entidades biológicas em grupos taxonomicamente problemáticos (Fouquet *et al.* 2014; Vallinoto *et al.* 2010) só foram evidenciados devido, principalmente, ao avanço das técnicas moleculares. Entretanto, apenas uma pequena parte do complexo de espécies existentes foi estudada até hoje, o que torna o problema de espécies crípticas especialmente grave para anfíbios (Bickford *et al.* 2007). Além disso, recentes reconstruções filogenéticas (Faivovich *et al.* 2005; Pyron & Wiens 2011), baseadas principalmente em dados moleculares, conseguiram estabelecer as relações evolutivas entre diversos clados, modificando drasticamente a sistemática dos anfíbios Neotropicais. Essa revolução molecular levou a uma revitalização da taxonomia atual dos anfíbios, principalmente com as recentes descobertas de espécies crípticas (Fouquet *et al.* 2007a; McLoed 2010)

1.2 Taxonomia integrativa e o uso de múltiplos caracteres para delimitação de espécies

O avanço das técnicas moleculares tem mudado a forma de como a diversidade biológica de anfíbios anuros vem sendo descrita (Fouquet *et al.* 2007b; Padial & de La Riva 2009). Em combinação com outros tipos de dados (como dados acústicos, dados sobre larvas ou ainda comportamentais), o uso de sequencias de DNA como caractere taxonômico tem tornado mais precisa a delimitação de espécies e aumentou consideravelmente o número de descrições de espécies, principalmente as morfologicamente crípticas (Angulo & Icochea 2010; Fouquet *et al.* 2014). Além disso, a partir de uma avaliação filogenética molecular prévia, é possível identificar novas espécies candidatas que, posteriormente, são diagnosticadas através de caracteres morfológicos ou acústicos (Bruschi *et al.* 2014; Fouquet *et al.* 2014).

Assim, a taxonomia integrativa (Schlick-Steiner *et al.* 2010) utiliza diversas fontes de evidências como caracteres taxonômicos para "testar" a validade de uma espécie e ajuda a compreender os processos evolutivos que moldaram a estruturação genética dessas diferentes linhagens evolutivas, que antes não eram possíveis ser identificadas utilizando, apenas, uma fonte de evidência (por exemplo, baseadas apenas na morfologia). Muitas vezes, o estudo de caracteres independentes pode levar a conclusões imprecisas ou incongruentes sobre a delimitação de espécies num contexto evolutivo, pois estes podem evoluir em taxas diferente durante o processo de especiação (Padial *et al.* 2010; Sites & Marshall 2004). Portanto, a multidisciplinaridade da taxonomia integrativa tem tentado identificar espécies de forma mais precisa devido à uma maior confiabilidade em delimitar linhagens evolutivas distintas pela combinação de informações de diferentes naturezas e, geralmente, independentes (Daryat 2005).

Estudos moleculares têm sido eficazes na delimitação de espécies morfologicamente crípticas, principalmente com o desenvolvimento da teoria coalescente (Fujita *et al.* 2012). Com essa abordagem, a delimitação é possível mesmo quando a divergência entre as espécies é recente (Camargo & Sites 2013). Entretanto, caracteres morfológicos ainda são, tradicionalmente, os mais aceitos para separar espécies distintas em anfíbios. Além disso, as características do canto de anúncio emitido pelos machos adultos (que atua como um isolamento pré-zigótico impedindo ou diminuindo as chances de hibridização; Gerhardt 1994), assim como a morfologia dos girinos, também podem ser utilizados para tal propósito (McDiarmid & Altig 1999). Por serem espécie-específicas, apresentam grande importância taxonômica para descrição de novas espécies (Anstis *et al.* 2010; Magalhães *et al.* 2014). Portanto, a utilização destes caracteres é imprescindível quando se está estudando a taxonomia ou sistemática de algum grupo de anuro (Fouquet *et al.* 2014).

Como mencionado anteriormente, os anfíbios apresentam uma morfologia conservada e com pouca variação mesmo apresentando alta diferenciação genética (Gehara *et al.* 2013). Embora se tenha a noção que espécies de anfíbios com ampla distribuição sejam fortes candidatas a complexos de espécies crípticas (Angulo & Icochea 2010), a magnitude da diversidade críptica ainda é desconhecida, especialmente em regiões altamente diversas (Funk *et al.* 2012). Desse modo, quanto mais ferramentas taxonômicas comparativas forem usadas, mais precisos serão os resultados encontrados e mais claramente estabelecida será a relação entre grupos ou complexo de espécies que se está estudando (Padial & de La Riva 2009). Com isso, podemos nos aproximar de uma compreensão mais precisa da real diversidade dos anfíbios anuros, que trabalhos recentes indicam ser muito maior do que nós previamente acreditávamos (Fouquet *et al.* 2007a; Pfenninger & Schwenk 2007).

1.3 Filogeografia e o reconhecimento de linhagens e padrões evolutivos

Filogeografia corresponde a uma abordagem altamente integrativa utilizada para investigar a relação entre eventos geológicos históricos, ecológicos e a diversificação biótica (Avise 2000). A filogeografia combina informações sobre genética de populações, filogenia, flutuações geoclimáticas, paleontologia, evolução molecular e padrões biogeográficos a fim de relacionar a distribuição geográfica de linhagens genealógicas ao longo de uma paisagem geográfica, gerando um padrão filogeográfico que pode ser comparável mesmo entre organismos com histórias evolutivas completamente distintas (Avise 2000). Além disso, o uso dessa ferramenta nos permite inferir os processos evolutivos, demográfico e biogeográficos que moldam padrões gerais de diversificação (Turchetto-Zolet *et al.* 2013).

Por exemplo, a filogeografia permite o estudo independente de cada espécie ou linhagens evolutivas, onde diversas hipóteses geográficas ou barreiras históricas podem ser testadas a partir da relação genealógica das populações examinadas (Nascimento *et al.* 2013). Assim, estudos filogeográficos têm contribuído para a compreensão dos processos históricos da distribuição de genealogias, integrando as diversas áreas de conhecimento citadas previamente (Avise 2000). Avanços teóricos, computacionais, estatísticos e metodológicos tem permitido uma maior robustez nas inferências históricas e, atrelado ao uso de múltiplos lócus gênicos, diferentes cenários evolutivos alternativos podem ser testados estatisticamente (Fujita *et al.* 2012).

Apesar de relativamente recente, a associação entre estudos filogeográficos com a biogeografia é crescente e algumas teorias sobre a origem e diversificação da fauna Neotropical já podem ser testadas. Por exemplo, uma das hipóteses mais discutidas sobre a diversificação

nos Neotrópicos é a Teoria dos Refúgios Pleistocênicos (Haffer 1969): as florestas úmidas retraiam durante períodos frios e secos, isolando vários fragmentos de floresta úmidos ao longo de uma paisagem árida, resultando no isolamento geográfico de diversas linhagens. Com isso, eventos vicariantes promoveriam a diferenciação genética e completo isolamento reprodutivo originando, assim, novas espécies. Diversos estudos têm suportado essa teoria de refúgios, principalmente ao longo de florestas tropicais para diversos grupos de animais que ocorrem em áreas de floresta fechada (Carnaval *et al.* 2009; Fitzpatrick *et al.* 2009; Thomé *et al.* 2010). Controversamente, existem poucos estudos que focam na busca por padrões que deram origem a diversa fauna associada a ambientes abertos (ao longo da Diagonal Seca, por exemplo), possivelmente pela dificuldade de se estabelecer ou definir refúgios (Werneck 2011; Nascimento *et al.* 2013). Espera-se que exista uma alta diversidade genética dentro dos refúgios e uma alta estruturação filogeográfica quando diferentes refúgios são comparados (Carnaval *et al.* 2009).

Espécies com ampla distribuição, teoricamente, são mais tolerantes à degradação de hábitat e mais plásticas quanto ao uso de recursos tanto para reproduzir ou se alimentar e, em sua maioria, são atribuídas como "menos preocupantes" para conservação. Entretanto, estas podem se tratar de complexos de espécies crípticas com distribuições mais restritas do que se pensava (Fouquet *et al.* 2014; Gehara *et al.* 2013). Algumas dessas espécies, ou mesmo linhagens, podem estar inclusive altamente ameaçadas (Gehara *et al.* 2013). A perda ou não inclusão de uma linhagem pode afetar o resultado final de um estudo filogeográfico em grande escala, pois parte da história evolutiva da espécie está sendo perdida, podendo gerar resultados incongruentes ou não conclusivos (Gehara *et al.* 2014). Logo, é imprescindível a conservação destas linhagens, mesmo que se trate de uma espécie que não é considerada ameaçada. Tais estudos trazem uma nova percepção sobre a riqueza de espécies potencial na região tropical e geram dados mais robustos que podem afetar diretamente ações conservacionistas locais (Gehara *et al.* 2013).

1.4 O grupo *Leptodactylus latrans* e o complexo de espécies

O complexo de espécies do grupo *Leptodactylus latrans/chaquensis/macrosternum* está amplamente distribuído na América do Sul (da Colômbia até o norte da Argentina, leste dos Andes), ocorrem em uma variedade de biomas (Amazônia, Chaco, Pampas, Pantanal, Mata Atlântica, Cerrado e Caatinga) e gradientes altitudinais (0–1400m de altitude) e está, principalmente, associado a áreas abertas e bordas de floresta (de Sá *et al.* 2014). De acordo com os critérios de conservação da IUCN, estas espécies são consideradas "estável" e podem

ser encontradas em habitats degradados e áreas urbanas e, no geral, apresentam hábitos alimentares generalistas. Além disso, é descrita para a Mata Atlântica do Estado da Bahia, no município de Salvador, *Leptodactylus macrosternum* (Miranda-Ribeiro 1926), espécie cuja validade taxonômica é questionada, uma vez que os autores que o descreverem utilizaram apenas um indivíduo (aparentemente jovem) que está em más condições de conservação (Gallardo 1964; Sá *et al*. 2014), o que dificulta a inferência de sua identidade e relações taxonômicas frente as demais espécies do grupo *L. latrans* de espécie.

A falta em delimitar precisamente a distribuição dessas espécies está diretamente relacionada à morfologia críptica desses táxons (Cei 1962; Gallardo 1964; Heyer & de Sá 2014; de Sá *et al*. 2014). Por exemplo, em uma recente revisão sobre a sistemática do grupo, de Sá *et al*. (2014) restringiram a distribuição de *L. latrans* para sua localidade tipo (região costeira da Mata Atlântica do Estado do Rio de Janeiro no município de Teresópolis), já que não há dados robustos e precisos o suficiente (morfológicos e acústicos) para delimitar sua distribuição. Entretanto, neste mesmo trabalho, vários táxons associados ao grupo *L. latrans* não foram incluídos na análise e, atualmente, não estão atribuídos à nenhum táxon válido, como por exemplo, as espécies distribuídas ao longo do bioma da Caatinga no nordeste brasileiro. Da mesma forma, a distribuição de *L. chaquensis* ainda é discutida por diversos autores. Atualmente, *L. chaquensis* tem sua distribuição restrita ao ecossistema árido do Chaco (Norte da Argentina, Oeste do Uruguai, Paraguay e Sul da Bolívia) e áreas adjacentes nos estados de Mato Grosso do Sul e Rio Grande do Sul (de Sá *et al.* 2014). Entretanto, a distribuição de *L. chaquensis* já foi considerada bem mais abrangente do que esta proposta por de Sá et al. (2014). Cei (1962) propôs que *L. chaquensis* ocorreria em toda a diagonal de formações abertas, amplamente distribuído ao longo dos biomas da Caatinga, Cerrado e Chaco.

Ainda, a falta de dados acústicos dificulta a delimitação apropriada das espécies deste complexo. Por exemplo, até o momento o canto de anúncio de *L. latrans* e *L. macrosternum* ainda não é descrito (de Sá *et al.* 2014), dificultando a apreciação da real diversidade existente nesse complexo. Logo, apenas com o uso da morfologia, não é possível distinguir ou identificar o limite das referidas espécies com precisão, sendo necessária a implementação de dados moleculares (incluindo amostras que englobem, de preferência, toda a distribuição geográfica desses táxons) e dados acústicos para delimitação correta e precisa das espécies, visto que pouco avanço foi feito desde a descrição de *L. macrosternum* na década de 30, e das revisões taxonômicas feitas por Cei (1962) e Gallardo (1964).

Objetivo Geral

O objetivo desta tese é definir o limite específico das espécies do complexo *Leptodactylus latrans/chaquensis* utilizando dados moleculares, morfológicos e acúticos, além de revisitar todo o histórico taxonômico do grupo (Capítulo I). A partir da definição dos clados e estrutura genética, pretendo analisar quais possíveis eventos históricos (por exemplo, efeito de flutuações climáticas do Pleistoceno, barreiras geográficas e introgressões marinhas) influenciaram na estruturação genética e distribuição geográfica das espécies do complexo *L. latrans* (Capítulo II).

Referências Bibliográficas

Angulo, A. & Icochea, J. (2010) Cryptic species complexes, widespread species and conservaion: lessons from Amazonian frogs of the *Leptodactylus marmoratus* group. *Systematics and Biodiversity*, 8, 357–370.

Anstis, M., Tyler, M.J., Roberts, D., Price, L.C. & Doughty, P. (2010) A new species of *Litoria* (Anura: Hylidae) with a highly distinctive tadpole from the north-western Kimberley region of Western Australia. *Zootaxa*, 2550, 39–57.

Avise, J.C. (2000) *Phylogeography: the history and formation of species*. Harvard University Press, Cambridge, Massachusetts, 447 pp.

Bickford, D., Lohman, D.J., Sodhi, N.S., Ng, P.K.L., Meier, R., Winker, K., Ingram, K.K. & Das, I. (2007) Cryptic species as a window on diversity and conservation. *Trends in Ecology and Evolution*, 22, 148–155.

Bruschi, D.P., Lucas, E.M., Garcia, P.C.A. & Recco-Pimentel, S.M. (2014) Molecular and morphological evidence reveals a new species in the *Phyllomedusa hypochondrialis* group (Hylidae, Phyllomedusinae) from the Atlantic Forest of the highlands of southern Brazil. *Plos One*, 9, e105608.

Camargo, A. & Sites, J.W. (2013) Species Delimitation: A Decade After the Renaissance. *In:* Pavlinov, Y.I. & Rijeka, H.R. (Eds.) *The Species Problem - Ongoing Issues*. INTECH225–247.

Carnaval, A.C., Hickerson, M.J., Haddad, C.F.B., Rodrigues, M.T. & Moritz, C. (2009) Stability predicts genetic diversity in the Brazilian Atlantic forest hotspot. *Science*, 323, 785–789.

Cei, J.M. (1962) Mapa preliminar de la distribuition continental de las "sibling species" del grupo ocellatus (Genero *Leptodactylus*). *Revista de la Sociedad Argentina de Biología*, 38:258–265.

Chek, A.A., Lougheed, S.C., Bogart, J.P. & Boag, P. (2001) Perception and history: molecular phylogeny of a diverse droup of neotropical grogs, the 30-Chromosome *Hyla* (Anura: Hylidae). *Molecular Phylogenetics and Evolution*, 18, 370–385.

Daryat, B. (2005) Toward integrative taxonomy. *Biological Journal of Linnean Society*, 85, 407–415.

De Queiroz, K. (2007) Species concepts and species delimitation. *Systematic Biology*, 56, 879–886.

Domingos, F.M., Bosque R.J., Cassimiro J., Colli G.R., Rodrigues M.T., Santos M.G., Beheregaray L.B. (2014) Out of the deep: cryptic speciation in a Neotropical gecko

(Squamata, Phyllodactylidae) revealed by species delimitation methods. *Molecular Phylogenetics and Evolution*, 80:113–124.

de Sá, R.O., Grant, T., Camargo, A., Heyer, W.R., Ponssa, M.L. & Stanley, E. (2014) Systematics of the Neotropical genus *Leptodactylus* Fitzinger, 1826 (Anura: Leptodactylidae): phylogeny, the relevance of non-molecular evidence, and species accounts. *South American Journal of Herpetology*, 9, S1-S100.

Faivovich, J., Haddad, C.F.B., Garcia, P.C.A., Frost, D.R., Campbell, J.A. & Wheeler, W.C. (2005) Systematic review of the frog family *Hylidae*, with special reference to *Hylinae*: phylogenetic analysis and taxonomic revision. *Bulletin of the American Museum of Natural History*, 294, 1–240.

Fitzpatrick, S.W., Brasileiro, C.A., Haddad, C.F. & Zamudio, K.R. (2009) Geographical variation in genetic structure of an Atlantic Coastal Forest frog reveals regional differences in habitat stability. *Molecular Ecology*, 18, 2877–2896.

Fouquet, A., Cassini, C., Haddad, C.F.B., Pech, N. & Rodrigues, M.T. (2014) Species delimitation, patterns of diversification and historical biogeography of a Neotropical frog genus *Adenomera* (Anura, Leptodactylidae). *Journal of Biogeography*, 41, 855–870.

Fouquet, A., Gilles, A., Vences, M., Marty, C., Blanc, M. & Gemmell, N. (2007a) Underestimation of species richness in Neotropical frogs revealed by mtDNA analyses. *Plos One*, 2, e1109.

Fouquet, A., Vences, M., Salducci, M.D., Meyer, A., Marty, C., Blanc, M. & Gilles, A. (2007b) Revealing cryptic diversity using molecular phylogenetics and phylogeography in frogs of the *Scinax ruber* and *Rhinella margaritifera* species groups. *Molecular Phylogenetics and Evolution*, 43, 567–582.

Fritz, S.A. & Rahbek, C. (2012) Global patterns of amphibian phylogenetic diversity. *Journal of Biogeography*, 39, 1373–1382.

Fujita, M.K., Leaché, A.D., Burbrink, F.T., McGuire, J.A. & Moritz, C. (2012) Coalescent-based species delimitation in an integrative taxonomy. *Trends in Ecology & Evolution*, 27, 480–488.

Funk, W.C., Caldwell, J.P., Peden, C.E., Padial, J.M., De la Riva, I., Cannatella, D.C. (2007) Tests of biogeographic hypotheses for diversification in the Amazonian forest frog, *Physalaemus petersi*. *Molecular Phylogenetics and Evolution*, 44:825–837.

Funk, W.C., Caminer, M. & Ron, S.R. (2012) High levels of cryptic species diversity uncovered in Amazonian frogs. *Proceedings of the Royal Society B: Biological Sciences*, 279, 1806–1814.

Gallardo, J.M. (1964) Consideraciones sobre *Leptodactylus ocellatus* (L.) (Amphibia, Anura) y species aliadas. Physis, 24, 373–384.

Gamble, T., Colli G.R., Rodrigues M.T., Werneck F.P., Simons A.M. (2012) Phylogeny and cryptic diversity in geckos (*Phyllopezus*; Phyllodactylidae; Gekkota) from South America's open biomes. *Molecular Phylogenetics and Evolution*, 62:943–953.

Gehara, M., Crawford, A.J., Orrico, V.G., Rodriguez, A., Lotters, S., Fouquet, A., Barrientos, L.S., Brusquetti, F., De la Riva, I., & Kohler, J. (2014) High levels of diversity uncovered in a widespread nominal taxon: continental phylogeography of the neotropical tree frog *Dendropsophus minutus*. *Plos One*, 9, e103958.

Gehara, M.C., Canedo, C., Haddad, C.F.B. & Vences, M. (2013) From widespread to microendemic: molecular and acoustic analyses show that *Ischnocnema guentheri* (Amphibia: Brachycephalidae) is endemic to Rio de Janeiro, Brazil. *Conservation Genetics*, 2013, 1–10.

Gerhardt, H.C. (1994) The evolution of vocalization in frogs and toads. *Annual Review of Ecology and Systematics*, 25, 293–324.

Haffer, J. (1969) Speciation in Amazonian forest birds. *Science*, 165, 131–137.

Heyer, W.R. (1978) Systematics of the *fuscus* group of the frogs genus *Leptodactylus* (Amphibia, Leptodactylidae). *Natural History Museum of Los Angeles County Science Bulletin*, 29, 1–84.

Heyer, W.R., & de Sá, R.O. (2011) Variation, systematics, and relationships of the *Leptodactylus bolivianus* complex (Amphibia: Anura: Leptodactylidae). *Smithsonian Contributions to Zoology*, 635:1–58.

Heyer, W.R. (2014) Morphological analyses of frogs of the *Leptodactylus latrans* complex (Amphibia, Leptodactylidae) from selected localities in South America. *Proceedings of the Biological Society of Washington*, 126:369–378.

Lötters, S., Schmitz, A., Reichle, S., Rödder, D., Quennet, V. (2009) Another case of cryptic diversity in poison frogs (Dendrobatidae: *Ameerega*)—description of a new species from Bolivia. *Zootaxa,* 2028:20–30.

Magalhães, I.L.F., Oliveira, U., Santos, F.R., Vidigal, T.H.D.A., Brescovit, A.D., Santos A.J. (2014a). Strong spatial structure, Pliocene diversification and cryptic diversity in the Neotropical dry forest spider *Sicarius cariri*. *Molecular Ecology*, 23:5323–5336.

Magalhães, F.M., Loebmann, D., Kokubum, M.N.C., Haddad, C.F.B. & Garda, A.A. (2014b) A new species of *Pseudopaludicola* (Anura: Leptodactylidae: Leiuperinae) from northeastern Brazil. *Herpetologica*, 70, 77–88.

Miranda-Ribeiro, A. (1926) Notas para servirem ao estudo dos Gymnobatrachios (Anura) Brasileiros. *Arquivos do Museu Nacional. Rio de Janeiro*, 27:1–227.

McDiarmid, R.W. & Altig, R. (1999) *Tadpoles: The Biology of Anuran Larvae*. The University of Chicago Press, Chicago, 337 pp.

McLoed, D.S. (2010) Of least concern? systematics of a cryptic species complex: *Limnonectes kuhlii* (Amphibia: Anura: Dicroglossidae). *Molecular Phylogenetics and Evolution*, 56, 991–1000.

Nascimento, F.F., Lazar, A., Menezes, A.N., Durans Ada, M., Moreira, J.C., Salazar-Bravo, J., D'Andrea, P.S. & Bonvicino, C.R. (2013) The role of historical barriers in the diversification processes in open vegetation formations during the Miocene/Pliocene using an ancient rodent lineage as a model. *Plos One*, 8, e61924.

Oliveira, E.F., Gehara M., São-Pedro V.A., Chen X., Myers E.A., Burbrink F.T., Mesquita D.O., Garda A.A., Colli G.R., Rodrigues M.T., Arias F.J., Zaher H., Santos R.M.L., Costa G.C. (2015) Speciation with gene flow in whiptail lizards from a Neotropical xeric biome. *Molecular Ecology* 24:5957–5975.

Padial, J.M. & de La Riva, I. (2009) Integrative taxonomy reveals cryptic Amazonian species of *Pristimantis* (Anura: Strabomantidae). *Zoological Journal of the Linnean Society*, 155, 97–122.

Padial, J.M., Miralles, A., de la Riva, I. & Vences, M. (2010) The integrative future of taxonomy. *Frontiers in Zoology*, 7, 16.

Pennington, R.T., Lewis G.P., & Ratter J.A. (2006) An overview of the plant diversity, biogeography and conservation of neotropical savannas and seasonally dry forests. *Neotropical Savannas and Seasonally Dry Forests: Plant Diversity, Biogeography, and Conservation*, 69:1–29.

Pfenninger, M. & Schwenk, K. (2007) Cryptic animal species are homogeneously distributed among taxa and biogeographical regions. *Bmc Evolutionary Biology*, 7, http://www.biomedcentral.com/1471-2148/7/121.

Pyron, R.A. & Wiens, J.J. (2011) A large-scale phylogeny of Amphibia including over 2800 species, and a revised classification of extant frogs, salamanders, and caecilians. *Molecular Phylogenetics and Evolution*, 61, 543–583.

R Core Team (2014): R: A language and environment for statistical computing. – R Foundation for Statistical Computing, Vienna, Austria. Version 3.0.1. – Available at http://www.R-project.org/

Recoder, R.S., Werneck F.P., Teixeira-Jr M., Colli G.R., Sites-Jr J.W., & Rodrigues M.T. (2014) Geographic variation and systematic review of the lizard genus Vanzosaura (Squamata, Gymnophthalmidae), with the description of a new species. *Zoological Journal of the Linnean Society*, 171:206–225.

Reid, N., & Carstens, B. (2012) Phylogenetic estimation error can decrease the accuracy of species delimitation: a Bayesian implementation of the general mixed Yule-coalescent model. *BMC Evolutionary Biology*, 12:196.

Ron, S.R., Coloma, L.A., & Cannatella, D.C. (2005) A new cryptic species of *Physalaemus* (Anura: Leptodactylidae) from western Ecuador with comments on the call structure of the P. pustulosus species group. *Herpetologica*, 61:178–198

Santos, M.G., Nogueira C., Giugliano L.G., & Colli G.R. (2014) Landscape evolution and phylogeography of Micrablepharus atticolus (Squamata, Gymnophthalmidae), an endemic lizard of the Brazilian Cerrado. *Journal of Biogeography*, 41:1506–1519.

Schlick-Steiner, B.C., Steiner, F.M., Seifert, B., Stauffer, C., Christian, E. & Crozier, R.H. (2010) Integrative taxonomy: a multisource approach to exploring biodiversity. *Annual Review of Entomology*, 55, 421–438.

Sites, J.W. & Marshall, J.C. (2004) Operational criteria for delimiting species. *Annual Review of Ecology and Systematics*, 35, 199-227.

Stuart, S.N., Chanson, J.S., Cox, N.A., Young, B.E., Rodrigues, A.S.L., Fischman, D.L. & Waller, R.W. (2004) Status and trends of amphibian declines and extinctions worldwide. *Science*, 306, 1783–1786.

Tamura, K. & Nei, M. (1993) Estimation of the number of nucleotide substitutions in the control region of mitochondrial DNA in humans and chimpanzees. *Molecular Biology and Evolution*, 10:512–526.

Thomé, M.T., Zamudio, K.R., Giovanelli, J.G., Haddad, C.F.B., Baldissera, F.A., & Alexandrino, J. (2010) Phylogeography of endemic toads and post-Pliocene persistence of the Brazilian Atlantic Forest. *Molecular Phylogenetics and Evolution,* 55:1018–1031.

Turchetto-Zolet, A.C., Pinheiro, F., Salgueiro, F. & Palma-Silva, C. (2013) Phylogeographical patterns shed light on evolutionary process in South America. *Molecular Ecology*, 22, 1193–1213.

Vallinoto, M., Sequeira, F., Sodre, D., Bernardi, J.A.R., Sampaio, I. & Schneider, H. (2010) Phylogeny and biogeography of the *Rhinella marina* species complex (Amphibia, Bufonidae) revisited: implications for Neotropical diversification hypotheses. *Zoologica Scripta*, 39, 128–140.

Werneck, F.P. (2011) The diversification of eastern South American open vegetation biomes: Historical biogeography and perspectives. *Quarterly Science Reviews*, 30, 1630–1648.

Werneck, F.P., Leite, R.N., Geurgas, S.R., & Rodrigues, M.T. (2015) Biogeographic history and cryptic diversity of saxicolous Tropiduridae lizards endemic to the semiarid Caatinga. *BMC Evolutionay Biology,* 15:94.

Capítulo I

Taxonomic Review of South American Butter Frogs: Phylogeny, Biogeographic Patterns, and Species Delimitation in the *Leptodactylus latrans* Species Group (Anura: Leptodactylidae)

FELIPE DE M. MAGALHÃES[1,*], MARIANA L. LYRA[2], THIAGO R. DE CARVALHO[2], DIEGO BALDO[3], FRANCISCO BRUSQUETTI[4], PAMELA BURELLA[5], GUARINO R. COLLI[6], MARCELO C. GEHARA[7], ARIOVALDO A. GIARETTA[8], CÉLIO F.B. HADDAD[2], JOSÉ A. LANGONE[9], JAVIER A. LÓPEZ[5,10], MARCELO F. NAPOLI[11], DIEGO J. SANTANA[12], RAFAEL O. DE SÁ[13], AND ADRIAN A. GARDA[1,14]

[1] Programa de Pós-Graduação em Ciências Biológicas, Universidade Federal da Paraíba (UFPB), Centro de Ciências Exatas e da Natureza, Cidade Universitária, CEP 58000-000, João Pessoa, Paraíba, Brazil

[2] Universidade Estadual Paulista (UNESP), Instituto de Biociências, Campus Rio Claro, Departamento de Zoologia e Centro de Aquicultura (CAUNESP), Av 24A, N1515, CEP 13506-900, Rio Claro, São Paulo, Brazil

[3] Instituto de Biología Subtropical (IBS, CONICET-UNaM), Laboratorio de Genética Evolutiva, Facultad de Ciencias Exactas, Universidad Nacional de Misiones, Félix de Azara 1552, CPA N3300LQF, Posadas, Misiones, Argentina

[4] Instituto de Investigación Biológica del Paraguay (IIBP), Del Escudo 1607, CP 1429 Asunción, Paraguay

[5] Departamento de Ciencias Naturales, Facultad de Humanidades y Ciencias, Universidad Nacional del Litoral. Ciudad Universitaria UNL, Paraje El Pozo S/N, 3000, Santa Fe, Argentina

[6] Departamento de Zoologia, Universidade de Brasília (UNB), CEP 70910-900, Brasília, Distrito Federal, Brazil

[7] Department of Herpetology, American Museum of Natural History, New York, NY, USA

[8] Laboratório de Taxonomia e Sistemática de Anuros Neotropicais (LTSAN), Instituto de Ciências Exatas e Naturais do Pontal (ICENP), Universidade Federal de Uberlândia (UFU). Ituiutaba, Minas Gerais, Brazil

[9] Departamento de Herpetología, Museo Nacional de Historia Natural, Casilla de Correo 399, CP 11.000, Montevideo, Uruguay

[10] Instituto Nacional de Limnología (CONICET-UNL). Ciudad Universitaria UNL, Paraje El Pozo S/N, 3000, Santa Fe, Argentina

[11] Laboratório de Taxonomia e História Natural de Anfíbios (AMPHIBIA), Museu de História Natural, Instituto de Biologia, Universidade Federal da Bahia (UFBA), Campus Universitário de Ondina, Rua Barão de Jeremoabo S/N, CEP 40170–115, Salvador, Bahia, Brazil

[12] Mapinguari - Laboratório de Biogeografia e Sistemática de Anfíbios e Répteis, Universidade Federal de Mato Grosso do Sul (UFMS), CEP 79002-970 Campo Grande, Mato Grosso, Brazil

[13] Department of Biology, University of Richmond, Richmond, Virginia, 23173, USA

[14] Laboratório de Anfíbios e Répteis (LAR), Departamento de Botânica e Zoologia da Universidade Federal do Rio Grande do Norte (UFRN), Campus Universitário. Lagoa Nova, CEP 59078-900, Natal, Rio Grande do Norte, Brazil

[*] CORRESPONDENCE: e-mail, felipemm17@gmail.com

ABSTRACT: The *Leptodactylus latrans* species group (LLSG) currently comprises eight medium- to large-sized frog species with a convoluted taxonomic history, largely related to the specific limits of *L. latrans*, *L. chaquensis* and *L. macrosternum* (LCM complex). The homogeneous external morphology and continental geographic distribution in South America have posed severe limitations to a comprehensive revision of the LCM complex, such that taxonomic consensus and species limits remain uncertain. This is further worsened by the presence of chromatic polymorphism among coexisting species that can hardly be distinguished by external morphology. Based on a large-scale geographic sampling including multilocus DNA analyses, acoustic and morphological data, we provide a comprehensive evaluation of the taxonomic status and species limits of the LLSG, focusing on the resolution of the LCM complex. We gathered 717 mitochondrial sequences (COI based) from 421 localities, encompassing the group's entire geographic distribution. Both bGMYC and ABGD species delimitation methods recovered five major mitochondrial evolutionary lineages within the LCM complex supported by geographic concordance, multilocus molecular, morphologic and/or bioacoustics data. One lineage clustered the nominal *L. latrans*, and a second lineage encompasses all specimens previously assigned to *L. chaquensis*-*L. macrosternum*, clustered as a single evolutionary entity. Of the three remaining lineages, one was revalidated as *L. luctator*, and other two formally named. We provide a revised diagnosis for the LCM complex, based on acoustic data for all species, morphological/color variation and phylogenetic relationships of all species currently included in the LLSG. Our findings reinforce the view that Neotropical diversity is highly underestimated and stress that appropriate geographic sampling in an integrative framework is crucial for the establishment of specific limits among broadly distributed and morphologically cryptic Neotropical frogs.

Key words: ABGD; Bioacoustics; Cryptic species; Geographic distribution; GMYC; Morphology; Morphometrics; Systematics

THE GENUS *Leptodactylus* Fitzinger 1826 currently comprises 74 small- to large-sized species arranged in four groups supported by morphological, behavioral, and genetic data: *L. fuscus*, *L. pentadactylus*, *L. latrans*, and *L. melanonotus* species groups (see Heyer 1969; de Sá et al. 2014 and references therein). The *Leptodactylus latrans* species group (LLSG), also known as butter frogs because of their slippery skin, includes eight species: *L. bolivianus* Boulenger 1898, *L. chaquensis* Cei 1950, *L. guianensis* Heyer and de Sá 2011, *L. insularum* Barbour 1906, *L. latrans* (Steffen 1815), *L. macrosternum* Miranda-Ribeiro 1926, *L. silvanimbus* McCranie Wilson and Porras 1980, and *L. viridis* Jim and Spirandeli-Cruz 1973. Members of this species group occur from Central America (e.g., *L. insularum* and *L. silvanimbus*) to Argentina (e.g., *L. latrans* and *L. chaquensis*), and inhabit all South American biomes east of the Andes (de Sá et al. 2014). Most species are conspicuous, abundant and active (although not necessarily breeding) throughout most of the year in pristine or disturbed open habitats, making them some of the most common frogs in South America (Lutz 1930; Cei 1962; de Sá et al. 2014). Species from the LLSG are mainly recognized based on thumb spines and vocal sac morphology (both characteristics absent in females and non-active/juvenile males), arrangement of body dermal longitudinal folds, pigmentation patterns of body and thighs, and advertisement call (Cei 1980; Heyer and de Sá 2011; de Sá et al. 2014). However, species in the LLSG are morphologically cryptic and two species complexes are recognized (de Sá et al. 2014): The *L. bolivianus* complex, which encompasses *L. bolivianus*, *L. guianensis* and *L. insularum* (thoroughly revised by Heyer and de Sá 2011) and the *L. latrans*-*L. chaquensis*-*L. macrosternum* complex (hereafter LCM complex). The LCM complex likely harbors

undescribed taxa and has been for long known as a group that needs a thorough taxonomic revision (De la Riva and Maldonado 1999; de Sá et al. 2014; Heyer 2014).

The taxonomic history of the LCM complex is challenging. It dates back to the beginning of the nineteenth century, when many scientific expeditions took place in Brazil (Lavilla et al. 2010; Frost 2019). During this period, many representatives of the LCM complex were deposited in European and North American collections (Boulenger 1882; Cochran 1961; Glaw and Franzen 2006) and subsequently described (Raddi 1823; Spix 1824; Girard 1853). Nowadays, ca. 15 names are in the synonymy of *L. latrans* (Lavilla et al. 2010; de Sá et al. 2014; Frost 2019). Unfortunately, many species descriptions are brief and uninformative, lacking illustrations and precise geographic information, and type specimens were either lost or poorly preserved (Hoogmoed and Gruber 1983, Lavilla et al. 2010), precluding the use of morphological or geographic evidence for appropriate species identification. Moreover, the broad geographic distribution (spanning more than 30º of latitude) and the existence of cryptic species in syntopy (Cei 1950, 1962; Gallardo 1964) hampered the advance of the group's taxonomy and the establishment of clear species limits.

An essential contribution towards the taxonomic resolution of the LCM complex was provided by Lavilla et al. (2010). They elucidated the identity of *Leptodactylus ocellatus* (now *L. latrans*), designated and described a neotype from municipality of Teresópolis, Rio de Janeiro state, Brazil (Lavilla et al. 2010). Specimens attributed to *L. latrans* are widely distributed across ca. 3500 km, mostly on the eastern coastal zone in South America, from southern Buenos Aires province in Argentina to northeastern Brazil (Miranda-Ribeiro 1927; Cei 1962; Gallardo 1964). However, considering an uncertainty related to the geographic distribution and that *L. latrans* might correspond to a complex of morphologically cryptic species, de Sá et al. (2014) considered the range distribution beyond type locality as unknown

until further evidence is brought to light. No further advances on this topic have been made ever since, and the species limits remain uncertain to date.

A second major issue involving the LCM complex is the specific limits of the species pair "*Leptodactylus chaquensis-L. macrosternum*" and whether *L. macrosternum* is a valid species in relation to *L. chaquensis* (De la Riva et al. 2000; de Sá et al. 2014). These two species are considered morphologically cryptic, because there are no reliable morphological traits that could distinguish one from the other besides their geographic distributions (Gallardo 1964). For instance, *L. chaquensis* was described from Tucumán province, northwestern Argentina, and is a well-known (considering aspects of reproduction and morphology) and abundant species distributed from the South American Gran Chaco (hereafter Chaco) and also in adjacent regions outside Chaco in Bolivia and Brazil (Cei 1950, 1962; De la Riva and Maldonado 1999; de Sá et al. 2014). This species is distinguished from *L. latrans* by a few morphological characteristics (Gallardo 1964; Cei 1980; Langone 1995; Teixeira et al. 2017), but there are striking differences in their advertisement calls (Barrio 1966; Heyer and Giaretta 2009), male gametogenesis cycles (Cei 1948, 1950), physiological (e.g., Cei and Bertini 1961; Cei and Cohen 1965) and biochemical aspects (Maxson and Heyer 1988).

Meanwhile, there are few evidences to help elucidate the identity and geographic distribution of *Leptodactylus macrosternum*, as its type locality information is vague (Bahia province; Miranda-Ribeiro 1926). Bokermann (1966) stated that the type locality of *L. macrosternum* should probably correspond to the municipality of Salvador (Bahia state, in northeastern Brazil) or somewhere around the region of Salvador, where Mr. Bicego (a naturalist hired by the former Museu Paulista, currently Museu de Zoologia of the University of São Paulo; MZUSP) conducted field expeditions in 1896 and collected 13 representatives of the LCM complex (see Miranda-Ribeiro 1926, 1927). Interestingly, the presence of 10

dermal longitudinal folds is a feature that distinguishes *L. macrosternum* from all other morphs of "*L. latrans*" (exhibiting up to eight dermal longitudinal folds; Miranda-Ribeiro 1926) collected by Mr. Bicego in Bahia, but this was only discussed much later in Gallardo's (1964) review. However, the holotype of *L. macrosternum* (MZUSP 448, from a lot collected in 1896 by Mr. Bicego) is in fairly poor conditions of preservation and no longer exhibits such feature (Fig. 1), rendering us to rely solely on Miranda-Ribeiro's (1926) original description.

Cei (1950, 1962) and Gallardo (1964) analyzed several specimens belonging to the LCM complex from Argentina, Brazil, and Uruguay. They identified two clearly distinct morphotypes that co-occur in Brazil and Argentina: a large-sized morphotype with longer legs, single-lobed vocal sac, up to eight dermal longitudinal folds, and associated with humid areas in eastern South America (which is undoubtedly *L. latrans*; referred as *L. ocellatus* therein); and a relatively smaller morphotype with shorter legs, bilobed vocal sac, 10 dermal longitudinal folds, and widely distributed across xeric environments in South America (features of specimens assigned to *L. chaquensis*-*L. macrosternum*; Gallardo 1964). Despite reaching similar conclusions regarding the distribution and specific limits of *L. latrans* ("the larger morphotype"), they did not agree to the identity and distribution of *L. chaquensis*-*L. macrosternum*.

Based on morphology and histological data, Cei (1962) identified the widespread "smaller morphotype" from the diagonal belf of open formations (DOF, encompassing the Chaco, Cerrado and Caatinga biomes; see Vanzolini 1968; Werneck 2011) and Amazonia (which he referred to as "*forma amazonica*" or Amazonian morph) as *L. chaquensis*, a claim that has recently been substantiated by acoustic data (Camurugi et al. 2017). Conversely, Gallardo (1964) concluded that the "smaller morphotype" from central, northern (e.g., northern Cerrado and Amazonia) and northeastern Brazil, also reaching the coast and Llanos

of Venezuela, should be identified as *L. macrosternum* and elevated this name to full species status, restricting the occurrence of *L. chaquensis* to Chaco and surrounding areas. At that time, the holotype of *L. macrosternum* was already in poor conditions and Gallardo (1964) based his conclusions on the analysis of topotypical specimens collected in Salvador (Bahia state) that differed from *L. latrans* (e.g., presence of bilobed vocal sac) and matched the original description of *L. macrosternum* (e.g., presence of 10 dermal longitudinal folds; Miranda-Ribeiro 1926). In many of his contributions on the identity and specific limits of *L. latrans-L. chaquensis*, Cei did not address the taxonomic status of *L. macrosternum* directly. After Gallardo's (1964) review, Cei (1970) corroborated the species status of *L. macrosternum* by means of biochemical and serological data, which also indicated a closer relationship between *L. chaquensis-L. macrosternum* in comparison to *L. latrans* (see also Cei 1962; Cei et al. 1967). Moreover, considering the shared morphological, histological and physiological features between *L. chaquensis* and *L. macrosternum* (Gallardo 1964; Cei et al. 1967; Cei 1970), it is not surprising that these two taxa were recovered as sister groups in a recent molecular phylogenetic analysis (de Sá et al. 2014), although it is still not clear how these related taxa can be distinguished morphologically, nor which are their precise geographical ranges (De la Riva and Maldonado 1999).

As mentioned earlier, *Leptodactylus latrans* and *L. chaquensis-L. macrosternum* are distinguished by morphological (vocal sac, dermal longitudinal folds and coloration patterns; Cei 1950, 1962; Gallardo 1964; de Sá et al. 2014) and reproductive features (gametogenesis cycles and calls; Cei 1948, 1950; Barrio 1966). The most comprehensive studies on the specific limits of the LCM complex are those of Cei (1950, 1962) and Gallardo (1964), which were mostly concordant regarding the distribution of *L. latrans* and the existence of a widespread "smaller morphotype" (*L. chaquensis-L. macrosternum*) that partially overlaps its distribution with that of *L. latrans*. Only one subsequent work attempted to establish specific

limits of the LCM complex by assessing morphological variation for a set of specimens from sparse localities in South America (Heyer 2014). However, the existence of highly variable morphotypes and lack of genetic background hampered the recognition of species-specific traits on such a broad geographic scale. During the past decades, mitochondrial DNA has been used as a primer to establish genetic structure in zoological studies, especially if dealing with highly complex taxonomic groups with poorly understood specific limits (e.g., Barley et al. 2013; Fouquet et al. 2014; Gehara et al. 2014). Additionally, genetic information allows researchers to infer how morphological traits vary according to the genetic structure across the landscape (Posso-Terranova and Andrés 2018), and also test for specific limits (Pons et al. 2006; Funk et al. 2012).

Considering the intricate taxonomic history of the LCM complex, herein we (1) assess the evolutionary lineages within the LLSG (focusing on the LCM complex) and their geographic distribution, using samples obtained throughout their currently known geographic range; (2) test for species limits of populations/lineages using morphological, bioacoustics, and multilocus molecular data; (3) propose a molecular phylogeny including all species in the LLSG using mitochondrial and nuclear genes; and (4) reassess the taxonomic status of the LCM complex using an integrative framework.

MATERIAL AND METHODS

Taxon and Gene Sampling and Laboratory Procedures

Considering that specific limits of *Leptodactylus chaquensis-L. macrosternum* are not clear and that *L. latrans* may represent a species complex, our first strategy was to identify monophyletic evolutionary lineages through extensive mitochondrial DNA barcode sequencing. We amplified a 650 base-pair (bp) fragment of cytochrome c oxidase I (COI) mitochondrial gene (which is commonly used for such purposes; Hebert et al. 2003; Lyra et

al. 2017) for all our 656 samples. Because cryptic species coexist along several localities in Brazil and Argentina (Cei 1962; Gallardo 1964), we sequenced from one to five individuals per locality to enhance the detectability of all lineages occurring in each locality. Additionally, we also gathered COI and 16S ribosomal RNA mitochondrial genes sequences available in GenBank for the LLSG, including that of the *L. latrans* neotype (MNRJ 30733; GenBank number KM091606) and all other sequences previously provided by Heyer and de Sá (2011) and de Sá et al. (2014). Our final genetic database (considering GenBank samples) includes an extensive representation of the LLSG in South America (focusing on the LCM complex), with 717 sequenced specimens from 421 localities encompassing the entire currently know distribution of the LLSG (see Fig. 2 and Appendix I for all sampled localities and GenBank accession number). Additionally, we included samples from relevant localities considering the taxonomic history of LCM complex, such as: *L. latrans* samples from the type locality, Teresópolis municipality, Rio de Janeiro state, samples from Salvador municipality, Bahia state and vicinities (*L. macrosternum* most likely type locality), and samples covering the Chaco (including *L. chaquensis* type locality).

We extracted DNA from muscle or liver tissues using ammonium (Maniatis et al. 1982) or sodium chloride (Bruford et al. 1992) salt precipitation methods. We conducted polymerase chain reaction (PCR) amplifications using Taq DNA Polymerase Master Mix (Ampliqon S/A, Denmark). For PCR protocols, we started with an initial denaturation cycle of 95ºC for 3 min and finished with an extension cycle of 68ºC for 5 min (specific annealing temperature and extension time for each primer pairs are given in Table 1). In most occasions, we cleaned PCR products using enzymatic purifications (shrimp alkaline phosphatase and exonuclease I; Werle et al. 1994). We sent purified or unpurified PCR products to Macrogen Inc. (South Korea) for purification (when needed) and sequencing. We aligned all sequences using the MAFFT algorithm (Katoh et al. 2002) with the default

parameters in Geneious v1.8.7 (Kearse et al. 2012). When needed, we pruned genes alignment to fit our shortest sequences prior to analyses.

Mitochondrial Evolutionary Lineages

To objectively establish major mitochondrial evolutionary lineages (and therefore our putative species) based on the COI dataset, we implemented both tree-based and distance-based methods broadly used to delimit species based on single locus mitochondrial DNA datasets. We used the Bayesian implementation of the Generalized Mixed Yule-Coalescent (GMYC) model to account for uncertainty in genealogy and model estimation with package bGMYC (Reid and Carstens 2012), in R v3.0.2 (R Core Team 2018). The GMYC method runs a model-based analysis to locate threshold points (or nodes) on the genealogy where there are transitions in branching rates, reflecting either inter- or intraspecific evolutionary processes, using ultrametric gene tree as input (Pons et al. 2006). Because the inclusion of identical sequences results in many zero length branches at the tip of the tree, which can cause the model to overpartition the data set (Reid and Carstens 2012), we maintained only unique haplotypes for the final BEAST gene tree (resulting in 235 terminals in the COI final alignment). To generate ultrametric trees used as input for the GMYC analysis, we ran the uncorrelated lognormal relaxed clock analyses for a 507 bp COI data set using BEAST v1.10.4 (Suchard et al. 2018), setting a fixed prior distribution of 0.01 for the *ucld.mean* parameter. For the bGMYC analysis, we used a post-burn-in sample of 100 trees to calculate the posterior distribution of the GMYC model. We set an upper bound for yule and coalescent processes priors to 0.5 and 1.0, respectively, to obtain coalescence-to-yule rates above 0, indicating a good model approximation to the reality of the data (Reid and Carstens 2012). We ran the bGMYC analysis for 100,000 generations, with a burn-in of 90,000 generations and a thinning interval of 100 samples. We used a threshold of 50% of conspecific probability to recognize genetic clusters

delimited by the bGMYC model. We also implemented the Automatic Barcode Gap Discovery (ABGD) method, which relies on the overall pairwise differences of a given genetic distance matrix to automatically detect barcode gaps, using a range of intraspecific divergence priors, and sort sequences into candidate species (Puillandre et al. 2012). We used the same COI alignment employed in bGMYC and BEAST as input for ABGD. We set priors for minimum and maximum intraspecific divergence as 0.01 and 0.1, respectively, and relative gap width was set as 1.5. We used the default values for the remaining configuration settings. We selected the most constantly recovered groupings in the recursive partitions, as proposed by Puillandre *et al*. (2012).

In search for all supported monophyletic clusters (posterior probability [PP] = 1.0), we generated a COI gene tree under a Bayesian framework with BEAST v.1.10.4. We split the 507 bp COI alignment in three partitions, according to codon position (CP; 1st, 2nd and 3rd positions, 169 bp each), and used PartitionFinder2 (Lanfear et al. 2016) with the greedy algorithm, linked branch lengths and the Bayesian Information Criterion (BIC) to select the best-fit partitioning scheme model of nucleotide substitution (Table 2). We then ran BEAST for 20 million generations, sampling every 2 x 10^3 generations, discarded the initial 25% generations and trees as burn-in, and assessed convergence (ESS > 200) with Tracer v1.7 (Rambaut et al. 2018). To generate the Maximum credibility tree, we used TreeAnnotator v1.10.4 (http://beast.community/treeannotator) and FigTree v1.4.2 (Rambaut 2014). We recognized major evolutionary lineages as those that: (1) were supported as candidate species by both distance and tree-based species delimitation analyses, (2) represented monophyletic groupings with significant posterior probability (PP = 1.0), and (3) exhibited cohesive geographic distributions (e.g., distributed within a contiguous geographic range). This approach resulted in concordant sets of putative species, which we used in subsequent analyses (see Results).

For further examination of species boundaries, we sequenced fragments of the mitochondrial 16S gene (ca. 550 bp), and nuclear tyrosinase precursor (TYR, ca. 550 bp) and proopiomelanocortin (POMC, ca. 450 bp) genes for a sub-sample (112 specimens) of the COI dataset representing both the genetic structure (including individuals from all divergent lineages) and geographic distribution (evenly sampling specimens along lineages geographic range). We provide all primer pairs and PCR protocols used for amplification of previously mentioned genes in Table 1.

Phylogenetic Relationships and Genetic Distances

To infer phylogenetic relationships and further investigate species boundaries, we created a final DNA alignment for 180 specimens (112 sequenced individuals plus GenBank available sequences) encompassing all species currently included in the LLSG (*L. bolivianus*, *L. chaquensis*, *L. guianensis*, *L. insularum*, *L. latrans*, *L. macrosternum*, *L. silvanimbus*, and *L. viridis*) and putative species identified early using the COI dataset (see Results). As outgroups, we used nine species representing the *L. fuscus* (*L. fuscus*, *L. longirostris* and *L. mystaceus*), *L. pentadactylus* (*L. knudseni*, *L. labyrinthicus*, *L. pentadactylus* and *L. rhodomystax*) and *L. melanonotus* species groups (*L. natalensis* and *L. podicipinus*). We built the full dataset alignment based on the availability of the 16S rRNA gene because *L. latrans* neotype and *L. silvanimbus* lack the COI mitochondrial marker. The proportion of missing data for the whole dataset is 30% (Appendix I). We split the full dataset of 1945 bp into 10 partitions according to genome and transcript type (16S rRNA 520 bp; COI protein-coding mRNA 507 bp; TYR protein-coding nuDNA 511 bp; POMC protein-coding nuDNA 407 bp) and all protein-coding genes subdivided into codon position (1st; 2nd and 3rd CP). We used PartitionFinder2 with the greedy algorithm, linked branch lengths and the BIC to select the best-fit partitioning scheme model of nucleotide substitution **(**Table 2).

We generated hypotheses of phylogenetic relationships among species of the *Leptodactylus latrans* group using maximum likelihood (ML) in RAxML v8.2.10 (Stamatakis 2014) and Bayesian inference in BEAST v1.10.4, with the best PartitionFinder2 scheme. We obtained maximum likelihood tree estimates with nodal support assessed via 1000 rapid bootstrap replicates. We considered nodal support significant or moderate for bootstrap (BS) values over 95% (Felsenstein and Kishino 1993) and 70% (Hillis and Bull 1993), respectively. For Bayesian inference, we ran BEAST analyses for 50 million generations, sampling every 5000 generations and discarding the initial 25% as burn-in. We assessed convergence (ESS > 200) with Tracer v1.7, generated the maximum credibility tree with TreeAnnotator v1.10.1, and drew all phylogenetic trees using FigTree v1.4.2. We considered Bayesian posterior probability (PP) > 0.95 as significant (Suchard et al. 2018). We regarded as valid those lineages recovered with significant nodal support, indicating reciprocal monophyly.

Additionally, we computed between-lineage mean distances using the Tamura-Nei (Tamura and Nei 1993) corrected p-distances with MEGA v6.0.6 (Tamura et al. 2013). For that, we employed the 507 bp COI alignment (235 specimens) and the 510 bp 16S alignment including all available sequences (180 specimens). We defined groups by combining the results of both ABGD and bGMYC species delimitation methods (see below). GenBank accession numbers for all sequences are given in Appendix I.

Morphology

We measured and analyzed 811 specimens belonging to the LCM complex, of which 272 corresponded to molecular vouchers (34% of our dataset). Specimens without molecular data were assigned to the correct species based on combined information of morphology and geographic distribution (see Results). We excluded from subsequent analyses those

individuals that lacked molecular confirmation, occurred in sympatry zones, were juveniles or lacked any reliable diagnostic feature. We took the following measurements to the nearest 0.1 mm with Mitutoyo digital calipers: snout-vent length (SVL), head width (HW, between the membranes of the tympanum), head length (HL, from the tip of the snout to the posterior margin of the tympanum), eye-to-snout distance (ESD, from the anterior margin of the eye to the tip of snout), eye-to-nostril distance (END, from the anterior margin of the eye to the posterior margin of the nostril), eye-to-eye distance (EED, between the posterior margins of the eyes), eye diameter (ED, taken horizontally between anterior and posterior margins of the eye), tympanum diameter (TD, taken horizontally between anterior and posterior margins of the tympanum), hand length (HAL, from the wrist to the tip of finger III), forearm length (FAL, from the elbow to the tip of finger III), tibia length (TL, from the outer edge of the knee to the outer edge of the heel), and foot length (FTL, from the distal border of the inner metatarsal tubercle to the tip of the toe IV). We used the presence of thumb spines and vocal sacs/slits in males and presence of egg masses or absence of vocal slits in females for sex determination. Morphological nomenclature follows previous literature on Leptodactylidae (Heyer 1978; Heyer and de Sá 2011; de Sá et al. 2014). Specifically, nomenclature for dermal longitudinal folds (glandular crests on the dorsal surface of body and flank) follows de Sá et al. (2014), which arranged as dorsal (fold F1–3), dorsolateral (fold F4), and lateral folds (fold F5–6). Dorsal fold F3 is also recognized as auxiliary fold (de Sá et al. 2014). Museum acronyms follow Sabaj (2016) and we provide a full list of specimens examined in Appendix II. Museum acronyms not included in Sabaj (2016) are: Amphibian collection of Universidade Federal de Uberlândia, Minas Gerais, Brazil (AAG-UFU) and Universidade Federal do Triângulo Mineiro teaching collection, Uberaba, Minas Gerais, Brazil (UFTM).

Morphometry

To morphologically discriminate among the species sets (in the LCM complex) validated by our genetic dataset and to identify which variables contributed the most to their separation, we used a machine learning approach based on a random forest of decision trees (Breiman 2001). For such purpose, we created two datasets using only males: one dataset with 177 individuals encompassing only measured individuals whose identity was confirmed by DNA barcoding (conservative approach), and another dataset with 538 individuals encompassing both molecular and non-molecular vouchers. The random forest algorithm implemented in the R package randomForest (Liaw and Wiener 2002) generates random classification trees by using bootstrap samples from the original dataset to grow unpruned classification trees (usually 1000). Next, these trees are used to generate classifiers choosing the best splits based on a random sample of predictors. At last, the algorithm uses these predictors aggregated to classify new data based on a majority rule. At each bootstrap step, it predicts the data not present in the bootstrap sample ("out of the bag" samples, or OOB) and aggregates these results at the end to generate an error estimate of the classification (for more detail see Liaw and Wiener 2002). The analysis also generates a measure of importance for each variable and a measure of the internal structure of the data. Variable importance is estimated based on the effect of permuting a variable while leaving others unchanged on prediction error. Our dataset was inspected for univariate and multivariate outliers. A few values (HAL for two individuals and END for one individual) were substituted by NA values and imputed using missForest package in R (Stekhoven 2011). We detected three multivariate outliers (CFBH42701, CHUNB45658, and UFBA14331, which were dropped from further analyses.

Because classification error of preliminary analysis was high, we adjusted morphometric variables proportionally to body size favoring shape differences. For that, we defined body size as an isometric size variable (Rohlf and Bookstein 1987) following the

procedure described by Somers (1986). We calculated an isometric eigenvector, defined a priori with values equal to $p^{-0.5}$, where p is the number of variables (Jolicoeur 1963), and obtained scores from this eigenvector, hereafter called Body Size, by post-multiplying the n × p matrix of $\log_{10}$-transformed data, where n is the number of observations, by the p × 1 isometric eigenvector. Then, we removed the effect of size from the $\log_{10}$-transformed variables using Burnaby's method (Burnaby 1966). We post-multiplied the n × p matrix of the $\log_{10}$-transformed data by a p × p symmetric matrix, L, defined as: $L = I_p - V(V^TV)^{-1}V^T$, where I_p is a p × p identity matrix, V is the isometric size eigenvector defined above, and V^T is the transpose of matrix V (Rohlf and Bookstein 1987). This procedure lead to a better discrimination among groups, decreasing the OOB estimates of error rate from 30% to 17% (results not shown).

Bioacoustics

We recorded advertisement calls using Sennheiser K6/ME66 or K6/ME67 unidirectional microphones and digital recorders (Marantz PMD 670, 671; M-audio Microtrack 2; Tascam DR 40) set at sampling rates of 44.1 or 48.0 kHz and sample size of 16 bits. We deposited the recordings as uncompressed wave files in the acoustic repositories of AAG-UFU and CFBH collections, and Arquivos Sonoros da UFRN (ASUFRN). We provide additional information on sound recordings, including vouchers associated with calls, in Appendix III. We conducted acoustic analyses in Soundruler (Gridi-Papp 2007), built as a package interfacing with Matlab scripts (Matlab 2004) through automated procedures that allow for unbiased quantification of acoustic traits. We present acoustic traits as averaged means for the males analyzed, and their corresponding standard deviation as standard deviations of the averaged mean values. We calculated ranges based on the total amplitude of values from the raw dataset. We set parameters as follows: fast Fourier transform (FFT) size = 1024 samples, FFT overlap = 90%, window type = Hanning, contrast = 70%. Unless

otherwise stated, we defined settings for automated recognition of signals as follows: detection smoothing = 400, resolution = 1; delineation smooth factor = 5, smoothing = 150, resolution = 1; critical amplitude ratio = -1 (disabled). For the "*Leptodactylus* aff. *latrans* CS1" lineage, we set the following parameters: detection smoothing = 500, resolution = 1; delineation smooth factor = 1, smoothing = 100, resolution = 1; critical amplitude ratio = 0.8. For the growl-type note of *L. macrosternum*, we set the following parameters: detection smoothing = 800, resolution = 1; delineation smooth factor = 1, smoothing = 50, resolution = 1; critical amplitude ratio = -1 (disabled).

We applied two band-pass filters (80-Hz high pass and 2000-Hz low pass) to sound files in Soundruler before conducting acoustic analyses to reduce background noise caused by rain, wind, roads, or insects and other frog species. We produced sonograms using seewave 2.1.0 (Sueur et al. 2008) and tuneR 1.3.2 (Ligges et al. 2017) in R 3.5.0 (R Core Team 2018), with the following settings: window = Hann, FFT size = 1024 samples, FFT overlap = 90% (except for the call of *L. viridis*: FFT size = 512 samples; FFT overlap = 99%); the intensity of frequency components is indicated by their darkness in a relative 36-dB scale. We quantified the following acoustic traits: note length (time from 10% attack minus that at 10% decay, relative to call maximum amplitude, i.e. 100%), note rise time (time from beginning of call to point of maximum amplitude; given in %), dominant frequency (frequency with the greatest energy), frequency modulation (dominant frequency at 10% attack minus that at 10% decay, relative to the maximum amplitude of the note, i.e. 100%); pulse rate (pulse number minus 1, divided by the duration of peak-to-peak from first to last pulse of the note). The acoustic terminology used in call descriptions follows Littlejohn (2001).

South American States/Provinces Acronyms

To avoid unnecessary repetition of provinces/states names along the manuscript, we used the following acronyms:

Brazilian states.—AC: Acre, AL: Alagoas, AM: Amazonas, AP: Amapá, BA: Bahia, CE: Ceará, ES: Espírito Santo, GO: Goiás, MA: Maranhão, MG: Minas Gerais, MS: Mato Grosso do Sul, MT: Mato Grosso, PA: Pará, PB: Paraíba, PE: Pernambuco, PI: Piauí, PR: Paraná, RJ: Rio de Janeiro, RN: Rio Grande do Norte, RO: Roraima, RR: Rondônia, RS: Rio Grande do Sul, SC: Santa Catarina, SE: Sergipe, SP: São Paulo, TO: Tocantins.

Argentinian provinces.—BU: Buenos Aires, CA: Catamarca, CH: Chaco, CB: Córdoba, CO: Corrientes, ER: Entre Ríos, FO: Formosa, JY: Jujuy, LR: La Rioja, ME: Mendoza, MI: Misiones, SA: Salta, SJ: San Juan, SL: San Luís, SF: Santa Fe, ST: Santiago del Estero, TC: Tucumán.

RESULTS

Mitochondrial Evolutionary Lineages

We identified five major mitochondrial lineages belonging to the LCM complex with significant node supports in the Bayesian analysis (PP = 1.0), cohesive geographic distributions (mostly non-overlapping, with few sympatry zones), and supported as independently evolving species in the delimitation analyses (Fig. 2, 3). Two lineages within *Leptodactylus viridis* and three lineages from the *L. bolivianus* complex were also well-supported (Fig. 3), totaling 10 major evolutionary lineages in the LLSG (*L. silvanimbus* not included in the COI dataset). These results support the following taxonomic arrangement:

The nominal *Leptodactylus latrans*.—We sampled 91 individuals assigned to the nominal lineage of *L. latrans*, including samples from the type locality (Teresópolis municipality, RJ; Fig. 2). Individuals belonging to this lineage are mostly distributed along the coastal Atlantic Forest, from Salvador (BA) to Bertioga (SP) municipalities. This lineage is found from sea level to higher altitudinal zones (~600–900 m above sea level [a.s.l]) in the

Serra do Mar range in RJ, and in the Serra da Mantiqueira range, in the region known as "*Zona da Mata Mineira*" in southeastern MG.

The *Leptodactylus* aff. *latrans* CS1 lineage.—We sampled a total of 50 individuals assigned to the *L.* aff. *latrans* CS1 lineage. Individuals belonging to this lineage are restricted to Chapada Diamantina range and vicinities, east of the São Francisco river in BA, with single records in MG and PE.

The *Leptodactylus* aff. *latrans* CS2 lineage.—We sampled 163 individuals assigned to the *L.* aff. *latrans* CS2 lineage. Individuals belonging to this lineage are distributed from SJ, southwestern Chaco through the Humid Pampas in Argentina, Uruguay and southern Brazil (all low altitudinal areas below 100 m a.s.l), and across the Atlantic Forest through high altitude localities (west of Serra do Mar; reaching 1400 m a.s.l.) from SC to southern Chapada Diamantina in BA. This taxon apparently exhibits a disjunct distribution in the Pantanal (MS), considering that the closest locality with taxa related to this population is located about 600 km (e.g., areas of Cerrado in western MG).

The *Leptodactylus* aff. *latrans* CS3 lineage.—We sampled 31 individuals assigned to the *L.* aff. *latrans* CS3 lineage. Individuals belonging to this lineage are restricted to a narrow zone within the southeastern coastal Atlantic Forest region from Santos municipality (SP) to northeastern RS, mostly associated with low altitudes (up to 500 m a.s.l.), east to the Serra do Mar mountain range.

The *Leptodactylus chaquensis/macrosternum* lineage.—Samples identified as *L. chaquensis* (Chaco) and *L. macrosternum* (Salvador municipality and vicinities) were clustered into a single clade. We sampled a total of 343 individuals assigned to a single geographically cohesive and broadly distributed lineage, with a range spanning more than 4,000 km from southern SF province (Argentina) to the Guiana Shield in RR (Brazil), also reaching the northern and northeastern Brazilian coast. This lineage is associated with biomes

along the DOF in South America (Cerrado, Chaco, Pantanal and Caatinga), as well as many sites within the Amazon and Atlantic Forest.

The *Leptodactylus bolivianus* complex clade.—Samples sequenced by us from RO and those from RR states clustered with *L. guianensis* and *L. bolivianus*, respectively, and are within the known range of these species, while all our *L. insularum* samples were retrieved from GenBank. Accordingly, our delimitation analyses supported the existence of three distinct species, corroborating the recent taxonomic arrangement for the *L. bolivianus* complex (Heyer and de Sá 2011).

The *Leptodactylus viridis* clade.—We only sampled three specimens of *L. viridis*: two from BA (nominal *L. viridis* lineage) and one from MG. Surprisingly, these populations are genetically and geographically (by the Jequitinhonha river) structured and the population from MG (*L*. aff. *viridis* lineage) was recovered as a putative new species.

Hereafter, we will also use the following subgroups definition within the LCM complex: "*Leptodactylus latrans* complex", formed by the nominal *L. latrans* and three candidate species CS1–3; "*L. chaquensis/macrosternum*", formed by the species pair *L. chaquensis*-*L. macrosternum*, now treated as a single evolutionary entity (these groupings are depicted in Fig. 2).

Phylogenetic Relationships and Genetic Distances

Phylogenetic relationships.—Both Bayesian and ML approaches yielded phylogenies with identical topologies (Fig. 4), which overall matched the COI topology and the previously published phylogeny for the LLSG (de Sá et al. 2014), except that de Sá et al. (2014) did not include representatives of *Leptodactylus viridis* from MG, nor *L. guianensis*, and *L*. aff. *latrans* CS1 and CS3 lineages. In de Sá et al. (2014), their *L. macrosternum* (lineages 1 and 2) and *L. chaquensis* were considered distinct entities, which instead clustered

within a single lineage in our topology. Likewise, both *L. latrans* neotype and their *L. latrans* lineage 1 clustered within our nominal *L. latrans* lineage, while their *L. latrans* lineage 2 clustered within our *L*. aff. *latrans* CS2 lineage. However, differences in phylogenetic inference methods, molecular markers, partitioning schemes, and geographic sampling renders further comparisons of phylogenetic relationships and node support between de Sá et al. (2014) and our results inappropriate.

The Bayesian topology was highly supported (all ingroup nodes with PP = 1.0), except for the relationships between *Leptodactylus silvanimbus* and other ingroups (PP = 0.56). Likewise, we obtained moderate to significant bootstrap scores in the ML analysis, except for the phylogenetic relationships within the *L. bolivianus* complex clade (BS = 60). Compared to the COI dataset, we also recovered as monophyletic the *L. bolivianus* complex (PP = 1.0/BS = 100) and the clade formed by *L. viridis*, *L. chaquensis/macrosternum* and *L. latrans* complex (PP = 1.0/BS = 94). Within this last clade, *L. viridis* was recovered as sister to the clade containing *L. chaquensis/macrosternum* and the *L. latrans* complex (PP = 1.0/BS = 75), and the *L. latrans* complex monophyly was highly supported (PP= 1.0/BS = 96). All ten mitochondrial lineages (putative species) recovered in the COI dataset had high support values (PP = 1.0/BS = 100) in both analyses (Bayesian and likelihood), therefore confirming that these clades are reciprocally monophyletic and supported as distinct evolutionary entities.

Genetic distances.—The average genetic distance between species in the LLSG was 8% and 14% for the 16S and COI mitochondrial genes, respectively. The lowest average genetic distances within the whole dataset were between *Leptodactylus latrans* and *L.* aff. *latrans* CS3 (~4% and 8% for 16S and COI, respectively), while the overall average genetic distance within the *L. latrans* complex varied between 4–9% and 8–16% for 16S and COI, respectively (Table 3). Within all lineages, the genetic distance did not exceed 2% and 5% for

16S and COI, respectively. Unexpectedly, this also occurred in the *L. chaquensis/macrosternum* lineage in which taxa are separated by almost 4,000 km (e.g., from southern Chaco in Argentina to Guiana Shield populations in Brazil) and genetic distance for COI mitochondrial gene only varied between 2–3%. Moreover, the ABGD analyses identified that the most likely transition point between intra-interspecific genetic distances is around 5–6% for the COI dataset (see Fig. 5).

Morphology

After establishing our evolutionary lineages, we searched for morphological and morphometric traits that could support genetic clusters and aid in species identification in the LCM complex. Considering that external morphology is highly conserved and that species in the LCM complex exhibit several polychromatic patterns (making difficult to discriminate between patterns), we attempted to identify which features are present or absent in each lineage qualitatively.

Dermal longitudinal folds.—Dermal longitudinal folds have for long been used as diagnostic characteristics in Leptodactylidae (Heyer 1978; de Sá et al. 2014) and are useful for the recognition of species in the LLSG (Miranda-Ribeiro 1926; Gallardo 1964). For instance, all species belonging to the *Leptodactylus bolivianus* complex lack folds F1–3, distinguishing them from species in the *L. latrans* complex and *L. chaquensis/macrosternum* lineage (folds F1–3 present; see Heyer and de Sá 2011; de Sá et al. 2014) and *L. viridis* (dorsal folds F1–2 poorly developed and F3 absent; Jim and Spirandeli-Cruz 1973; de Sá et al. 2014). Gallardo (1964) mentioned that all specimens associated with *L. latrans* (referred as *L. ocellatus* therein) exhibited four dermal longitudinal folds on each side of the body, whereas *L. chaquensis* and *L. macrosternum* exhibited five. Upon the examination of >800 specimens and several pictures of live specimens of both clades (e.g., the *L. latrans* complex

and *L. chaquensis/macrosternum*), we noticed that all individuals belonging to the *L. latrans* complex clade exhibit eight well-developed dermal longitudinal folds (F2, F4, F5 and F6; Fig. 6) and predominantly lack the auxiliary fold (F3; de Sá et al. 2014). If present, the auxiliary fold is short, not reaching the middle of body (Fig. 6A). Further, similarly to the fold F1, the auxiliary fold F3 is followed or formed entirely by a row of tubercles in the *L. latrans* complex clade (see Fig. 6A). Conversely, specimens of the *L. chaquensis/macrosternum* lineage exhibit eight well-developed dermal longitudinal folds (F2, F4, F5 and F6) and a long and well-developed (usually complete, but interrupted or weakly developed in some individuals) auxiliary row that extends from behind the eyes to midbody in all individuals we analyzed (see fold F3; Fig. 6B), totaling 10 folds (not considering F1, which is formed by a row of tubercles). These results reinforce Gallardo's (1964) observations that the arrangement of dermal longitudinal folds (specifically the auxiliary fold) is useful for species recognition in the LCM complex. Moreover, fold F2 extends from the interocular ocellated blotch region (as depicted in Fig. 6A) or posteriorly to the interocular ocellated blotch region (as depicted in Fig. 5B) to the pelvic region. The lateral folds (F5–6) can be either complete or interrupted. Lateral fold F5 can be further characterized as long (extending from above arm insertion to groin; Fig. 6A) or short (extending from midbody to groin; Fig 6B). Variation in the dermal folds F2, F5 and F6 was observed in specimens from all lineages in the LCM complex and are not useful to diagnose species. It is worth mentioning that these dermal structures seem to fade in preserved specimens, especially those already preserved for decades (e.g., the holotype of *L. macrosternum*). Therefore, it is desirable to assess this morphological feature from live (including live pictures) or recently preserved specimens for a more accurate species identification.

Thigh coloration.—The thigh posterior surface coloration in live specimens is highly variable within clades of the LCM complex. We found at least 15 distinct coloration hues varying among blue, gray, green and yellow shades (Fig. 7A–L). Nevertheless, we were able to associate exclusive color shades to the evolutionary lineages in the LCM complex. The thigh posterior surface coloration of nominal *Leptodactylus latrans* ranges from blue to gray shades with black maculated patches on the background (see Fig. 7A, B), which might be absent in some individuals (Fig. 7C). The black maculated patch is also observed in specimens of *L.* aff. *latrans* CS2 and CS3 lineages (Fig. 7E, F). However, yellow shades on thigh posterior surface is an exclusive feature of *L.* aff. *latrans* CS2 (see Fig. 7L, K). The green coloration on thigh posterior surface without black maculated patches on the background (Fig. 7G) is a feature that has for long been associated with the *L. chaquensis/macrosternum* lineage (Cei 1950; Gallardo 1964). However, we found that the shades of green on thigh posterior surface is a feature shared with specimens of the *L.* aff. *latrans* CS1 (Fig. 7H). This feature was also observed among specimens in the CS2 lineage (only observed in one unvouchered specimen from MG; Fig. 7J), but the green coloration is not as distinctive in respect to remaining brown shades of thigh upperside surface as exhibited by *L. chaquensis/macrosternum* and *L*. aff. *latrans* CS1 (Fig. 7G, H). Finally, *L.* aff. *latrans* CS1 only exhibited green/gray shades on thigh posterior surface with few black blotches (not maculated patches) on the background (Fig. 7H, I).

Dorsal coloration.—Dorsal body pigmentation (including dorsolateral regions) is also a highly variable feature within and among the evolutionary lineages in the LCM complex. All specimens exhibit a conspicuous interocular ocellated blotch variable in shape and size. Such blotches are also present along the dorsal and dorsolateral regions of the body. We identified three main body pigmentation patterns related to the arrangement of the blotches for specimens in the LCM complex: (1) blotches overall absent, with only a few

scattered light brown and poorly marked blotches or ocellated blotches on dorsum (smooth pattern, Fig. 8A); (2) light to dark brown blotches (with distinct shapes) or ocellated blotches sparsely and evenly distributed on dorsum (Fig. 8B); and (3) several well-marked dark brown ocellated blotches outlined by a light-cream colored "ring" and evenly distributed on dorsum (Fig. 8C, D). As with thigh posterior surface coloration, we were able to associate exclusive patterns to evolutionary lineages. For instance, we identified that *Leptodactylus latrans* and *L.* aff. *latrans* CS3 only exhibited patterns 1 and 2, with pattern 1 mostly exclusive to these lineages (only two specimens out of hundreds *L.* aff. *latrans* CS2 specimens [AAG-UFU 1680, and an unvouchered individual from Araguari, MG] exhibited pattern 1. Likewise, pattern 3 was only observed in specimens of the *L.* aff. *latrans* CS2 and *L. chaquensis/macrosternum* lineages. The *L.* aff. *latrans* CS1 lineage only exhibited pattern 2.

Ventral coloration.—We considered the coloration of the underside thigh as part of ventral color patterns described here. Patterns are also highly variable within and among lineages. Overall, ventral pigmentation can be entirely light beige (as depicted in Fig. 9A–C) or mottled with dark gray/brown patches and blotches densely distributed along ventral body and thigh surfaces (as depicted in Fig. 9D). Two distinct patterns were only observed in representatives of the *Leptodactylus* aff. *latrans* CS2 lineage: (1) specimens exhibit a gray or light beige mottled pigmentation pattern, with several circular yellowish melanophores from the gular region to the belly (Fig. 9E, F); and (2) specimens exhibit a well-marked black maculated pattern along the ventral surface of thighs; (Fig. 9E). This last feature is mostly seen in specimens from southernmost populations (e.g., Argentina, Uruguay, and southern Brazil) and Pantanal populations of lineage CS2. Moreover, *L. chaquensis/macrosternum* does not exhibit patterns depicted in Figures 9D–F, as pigmentation is mostly light beige on belly and underside thigh surfaces.

Thumb spines.—The number and shape of thumb spines has also been used as a diagnostic trait for some species in the LLSG. For instance, both *Leptodactylus bolivianus* and *L. guianensis* exhibit one thumb spine on each hand (Heyer and de Sá 2011), distinguishing them from *L. insularum*, which has two spines on each thumb, while spine shape is the main external character that morphologically distinguishes these closely related species (Heyer and de Sá 2011). However, males of all clades in the LCM complex always exhibit two spines on hand. We found three distinct shapes for thumb spines in the LCM complex: (1) thumb spines with triangular shape and pointed tips (Fig. 10A); (2) thumb spines longer than wide with rounded tips (e.g., conical shape, Fig. 10B, D); (3) thumb spines wider than long with flattened and slightly rounded tips (e.g., rectangular shape, Fig. 10C). These patterns are variable within individuals and among lineages and not unique to any of them.

Vocal sac.—As proposed by Gallardo (1964), the vocal sac morphology is a useful characteristic that helps distinguish species belonging to the *Leptodactylus latrans* complex clade and *L. chaquensis/macrosternum*, but it is barely evident externally, especially in preserved specimens. All males from the *L. latrans* complex clade exhibit a single-lobed vocal sac that do not expand laterally, whereas males from the *L. chaquensis/macrosternum* lineage exhibit a bilobed vocal sac that slightly expands laterally (Fig. 10D; see also Santos and Cechin 2008). Moreover, throat coloration of adult males is also useful for discriminating specimens belonging to the *L. latrans* complex clade from *L. chaquensis/macrosternum*. For instance, the anterior throat is homogeneously dark gray in male specimens from the *L. latrans* complex (Fig. 10A–C), and without homogeneous dark gray pigmentation or exhibiting brown or gray blotches in *L. chaquensis/macrosternum* (Fig. 10D).

Morphometric variation.—We found no diagnostic morphometric trait that would help to recognize any of the lineages, as all variables measured for species in the LLSG

largely ovelap between lineages and sexes (Table 4). However, we found that, on average, specimens from *Leptodactylus latrans* complex clade have larger body sizes (SVL) compared to *L. chaquensis/macrosternum.* Likewise, although overlapping, tibia and foot length/SVL average ratios are slightly higher in specimens from *L. latrans* complex clade compared to specimens from *L. chaquensis/macrosternum* lineage (Table 4). Both morphometric datasets yielded identical results regarding variable importance to discriminate among groups. Therefore, we present the following results based on the full dataset (538 individuals). Our random forest classification also indicated large overlap between specimens in the scatter plot (Figure 11A). The variables that most contributed to the separation between species were body size and tympanum diameter (Figure 11B). Likewise, hand length and foot legth are also among best predictors, but discriminate better individuals of the *L. latrans* complex clade from those assigned to *L. chaquensis/macrosternum* lineage. Furthermore, the confusion matrix shows no fit of the data to correctly classify *L*. aff. *latrans* CS1 and CS3 lineages (71% and 100% error, respectively), and moderate errors to identify *L. latrans* and *L*. aff *latrans* CS2 lineage (ca. 15%; Figure 11C), while *L. chaquensis/macrosternum* fit the data well (3% error).

Advertisement Calls

Major acoustic patterns.—Lineages in the *Leptodactylus latrans* complex have such similar calls that some of them could not be distinguished based on acoustic data. Calls are single, low-pitched notes, emitted at irregular intervals (Fig. 12A–D). A major difference (detectable by the human ear) is related to the call envelope: the presence of weak/irregular amplitude modulations in the calls of *L.* aff. *latrans* CS2 and CS3 lineages (Fig. 12B, and D, respectively), resembling a harsh-like sound. These amplitude modulations were detected qualitatively, but quantification was not possible because amplitude oscillations are usually

weak and irregular within calls and among individuals. By contrast, amplitude modulations were almost always absent in the call of nominal *L. latrans* (only one individual among nine recorded individuals exhibited weak irregular amplitude modulations), which sounds like a hoot-sound instead (Fig. 12A). A third pattern is the presence of more homogeneous and well-marked amplitude modulations along the call, an acoustic pattern exclusive to CS1 lineage, which is regarded herein as a partly fused multi-pulsed call (Fig. 12C). These major patterns are described in detail in the Species Account section. The calls of *Leptodactylus chaquensis/macrosternum* are complex, including three distinct note types: grunts, growls, and trills (see Heyer and Giaretta 2009; Camurugi et al. 2017; Fig. 13A–C). Despite being more complex, the calls of this lineage are highly stereotyped throughout South America, from northern Argentina, the Cerrado savanna in central Brazil, northern Atlantic Forest, and Amazonia (Heyer and Giaretta 2009; Tárano 2010; Camurugi et al. 2017). A quantitative description and comparative sounds are provided in the next section.

With respect to the other species in the *Leptodactylus latrans* group, calls of the three species recognized in the *L. bolivianus* complex clade (*L. bolivianus*, *L. guianensis*, and *L. insularum*) were described in Heyer and de Sá (2011). All three species have a stereotyped whistle-like calls defined as single, nonpulsed notes with upsweep frequency modulation (Fig. 13D). The call of the Honduran *L. silvanimbus* (Heyer et al. 1996a) is unique in the *L. latrans* clade by being broad-bandwidth and lacking frequency modulation, giving the impression of a honk-like sound (Fig. 13E). The bubbling call of *Leptodactylus viridis* was described in Rocha et al. (2016) and can also be regarded as unique mainly because of its brief duration (< 50 ms) and strong frequency upsweep (Fig. 13F). Unfortunately, the low availability of calls precluded us to use statistical tools to compare the variation in acoustic parameters (see Discussion section).

Nomenclature History

Currently, there are 15 names (emendations or incorrect spelling not included) available in the synonym of *Leptodactylus latrans* (Lavilla et al. 2010; Frost 2019). Considering that our results corroborate the existence of four distinct species in the *L. latrans* complex and that *L. chaquensis* and *L. macrosternum* correspond to a single species, a reassessment of the nomenclature of this clade is needed. Although morphologically cryptic, the geographic range of lineages in the *L. latrans* complex are mostly not overlapping with few sympatry zones throughout their distribution (Fig. 2), enabling the association of previously available names with lineages if geographic information is available. Next, we discuss names available for the *L. latrans* complex and the *L. chaquensis*/*macrosternum* lineage.

Names under nominal *Leptodactylus latrans*.—Because *Leptodactylus latrans* is the only species restricted to the Atlantic Forest from northern SP to Salvador municipality (BA), all species names whose type locality is assigned to the same region were kept as synonyms of *L. latrans*: *Rana gibbosa* Raddi 1823 (type locality: Rio de Janeiro, Brazil), *Rana fusca* Raddi 1823 (type locality: "Rio-Janeiro", Brazil. Junior homonym of *Rana fusca* Schneider 1799; Lavilla et al. 2010), *Rana pachypus* Spix 1824 (type locality: "Habitat in locis humidis Provinciae Rio de Janeiro" [var. 1]; while [var. 2] from "locis humidis Bahiae" is a junior synonym of *Rana fusca* Schneider 1799; Peters 1872), *L. serialis* Girard 1853 (type locality: "Rio de Janeiro", Rio de Janeiro, Brazil), and *L. caliginosus* Girard 1853 (type locality: "Rio de Janeiro", Rio de Janeiro, Brazil).

***Rana pygmaea* Spix, 1824.—**Spix (1824) described a juvenile leptodactylid specimen collected from Bahia province (which is now part of BA) that differed from *Rana pachypus* mainly in body size. There was much discussion about the true identity of this taxon (see Hoogmoed and Gruber 1983), which has been considered as a juvenile of *R. pachypus* by

Peters (1872) and subsequently a synonym of *Leptodactylus latrans* (Hoogmoed and Gruber 1983), or an allied species to *L. mystacinus* (Miranda-Ribeiro 1926, 1927). Although geographic information is not accurate, Spix (1824) explicitly distinguishes specimens collected along "locis humidis" (a reference to sites located within the Atlantic Forest) as he did with *R. pachypus*, from those that were collected along the interior or mountainous regions, which might be the case of *R. pygmaea*. According to Vanzolini (1981), Spix's expedition crossed several municipalities in the inlands of BA (e.g., Caetité, Maracás), where three distinct lineages of the LCM complex occur in sympatry/syntopy (e.g., *L. chaquensis/macrosternum*, *L.* aff. *latrans* CS1 and CS2 lineages). Additionally, the *R. pygmaea* illustration provided by Spix (1824) does not exhibit the interocular ocellated blotch (plate VI, Fig. 2 in Spix 1824), a conspicuous feature exhibited by all species in the LLSG (even in post metamorphic individuals; FMM, personal observation). For instance, the ocellated blotch was depicted by him in adult and juvenile *R. pachypus* illustrations (see plate II, Fig.1 and plate III, Fig. 2 in Spix 1824), but not in *R. pygmaea*. The only feature depicted in *R. pygmaea* illustration that is shared by all *L. latrans* species is the dark brown transversal bars in the dorsal surface of thigh and tibia, a feature also observed in other leptodactylid frogs (e.g., species in the *L. fuscus* group) that occur in interior BA, such as *L. mystaceus* and *L. mystacinus* (Leite et al. 2008). Considering Spix's (1824) vague description and illustration and that the type specimen is now considered lost (Glaw and Franzen 2006), it is not possible to unambiguously assign this name to any species of the LLSG. Therefore, *R. pygmaea* is here regarded as a *nomen dubium* (a name of unknown or doubtful application; ICZN 1999), and associated with a *species inquirenda* (a species of doubtful identity needing further investigation; ICZN 1999).

***Rana pachybrachion* Wied-Neuwied, 1824.—**Lavilla et al. (2010) and Vanzolini and Myers (2015) mentioned that *Rana pachybrachion* is possibly an incorrect subsequent

spelling or emendation of *R. pachypus* (Spix 1824). Vanzolini and Myers (2015) further argued that Wied-Neuwied obtained specimens of *R. pachypus/pachybrachion* from Espírito Santo and Jucu rivers (which are now part of ES). As mentioned previously, *Leptodactylus latrans* is the only lineage occurring along ES and, therefore, this name is here kept as a synonym of *L. latrans*.

***Rana macrocephala* Wied-Neuwied, 1825.—**As mentioned in Lavilla et al. (2010) and Vanzolini and Myers (2015), this species might correspond to *Ceratophrys aurita* (Raddi 1823) instead of *Leptodactylus*, but the holotype is currently lost. The specimen described by Wied-Neuwied was collected from southern BA, Lagoa d'Arara, lower Mucuri river (Vanzolini and Myers 2015), and was tentatively placed in the synonymy of *L. ocellatus* by Bokermann (1966), because of its geographic distribution and description. In any case, *L. latrans* in the only lineage occurring in southernmost BA and, therefore, this name is here kept as a synonym of *L. latrans*.

***Rana pachypus octolineatus* Mayer, 1835.—**Lavilla et al. (2010) mentioned that this name was subjectively included as *Rana pachypus* synonym (and thereafter *R. ocellata*) by Tschudi (1838). There is no information regarding the geographic origin of the type series (and how many individuals compose it), which is presumably lost (Lavilla et al. 2010). Lavilla et al. (2010) further mentioned that Tschudi's decision to keep *R. pachypus octolineatus* in the synonymy of *Leptodactylus latrans* remains valid until the type specimens are found. Nevertheless, even if specimens were located, it is unlikely that one could correctly assign it to any of the four *L. latrans* lineages (considering their cryptic morphology and sympatric condition along some localities in Brazil). Considering the impossibility to undoubtedly associate the name with an actual lineage, and to avoid taxonomic confusion with other currently well-known species name, *R. pachypus octolineatus* is here considered a *nomen dubium*, and associated to a *species inquirenda*.

***Rana luctator* Hudson, 1892.—**The name *Rana luctator* was first assigned to *Leptodactylus ocellatus* (= *L. latrans* complex clade) by Serié (1935) and later confirmed by Gallardo (1964). This specimen was collected around the vicinities of Buenos Aires municipality by Hudson (1892), and lost along the course of his expedition. Nevertheless, he clearly intended to investigate the taxon identity, and explicitly stated that it might be new to science:

> *"Believing that I had discovered a frog differing in structure from all known species, and possessing a strange unique instinct of self-preservation, I carried my captive home, intending to show it to Dr. Burmeister, the director of the National Museum at Buenos Ayres. Unfortunately, after I had kept it some days, it effected its escape by pushing up the glass cover"* (Hudson 1892, p76).

Hudson did not provide a proper morphological description of the taxon but the illustration on page 77 (by J. Smid) overall resemble *L. latrans*, except that it shows a frog with palmate feet (character absent in members of genus *Leptodactylus*). Anyhow, he described an aggressive behavior exhibited by this specimen that is worthy of note. He explicitly stated that the frog attempted to clasp his fingers as he tried to capture it:

> "*Before I was sufficiently near to make a grab, it sprang straight at my hand, and, catching two of my fingers round with its fore legs, administered a hug so sudden and violent as to cause an acute sensation of pain*" (Hudson 1892, p76).

Then, he continues describing his encounter with this frog mentioning what would be a male with hypertrophied arms:

> "*I then noticed the enormous development of the muscles of the fore legs, usually small in frogs, bulging out in this individual, like a second pair of thighs, and giving it a strangely bold and formidable appearance*." (Hudson 1892, p76).

Considering all these statements (exhibiting clasping behavior and hypertrophied arms), it is certain that the referred specimen can only be associated with a member of the LLSG among all anurans occurring in BU province. This name fits all requirements of the International Code of Zoological Nomenclature (Articles 5, 8, 10, 11 and 12; ICZN 1999), which consider as valid those names without an associated type-specimen provided in scientific works published before 1999. Because the only lineage occurring in this region is *L.* aff. *latrans* CS2 (*L. chaquensis/macrosternum* does not reach such region; see Fig. 2), *Rana luctator* is the oldest available name applicable to this candidate species and has priority over other names that are also available for this lineage such as: *Cystignathus oxycephalus* Philippi 1902 (type locality: "ad Montevideo", Uruguay), *L. ocellatus* var. *reticulata* Cei 1948 (type locality: "Arroyo, Isla Apipé, Ituzaingó [Corrientes]" and "Puerto Bemberg [Misiones]", Argentina), and *L. ocellatus* var. *bonairensis* Cei 1949 (type locality: "Río Colorado y Bahía Blanca", Argentina). Because all our samples belonging to the *L. latrans* complex from Uruguay (Montevideo municipality), and Argentina (CO, MI and BU provinces) cluster within the CS2 lineage, we now regard these previously mentioned names as synonyms of *R. luctator*. *Leptodactylus chaquensis/macrosternum* also occurs in sympatry with *L.* aff. *latrans* CS2 in northeastern Argentina (Cei 1962). However, Cei (1948) clearly distinguishes "*Leptodactylus ocellatus* var. *typica*" (which he later described as *L. chaquensis*; Cei 1950) from those specimens belonging to the *L. latrans* complex clade (referred as var. *reticulata*; Cei 1948). Moreover, although we did not have access to samples from Bahía Blanca, southern BU, it is unlikely that populations are genetically structured if compared to localities from northern BU we sequenced because of climatic similarity and lack of major geographic barriers (mountains or rivers) along these two regions.

The *Leptodactylus chaquensis/macrosternum* case.—As mentioned previously, information regarding the type locality of *Leptodactylus macrosternum* is vague, but it is

certain that the specimens collected by the naturalist Mr. Bicego (and later described by Miranda-Ribeiro 1926) were obtained somewhere around the vicinities of Salvador municipality (Brazilian state of Bahia; Bokermann 1966). We now have enough evidence supporting the sympatric/syntopic condition of *L. latrans* and the "smaller morph" (=*L. chaquensis/macrosternum*) in some localities of BA coastal zone, especially in the vicinities of Salvador (Fig. 2). Hence, it is very likely that Mr. Bicego collected within sympatry zones in BA, although only a single individual among 13 was described by Miranda-Ribeiro (1926) as the morphotype *L. ocellatus macrosternum*. Nevertheless, Miranda-Ribeiro's (1926) description states that *L. ocellatus* (now *L. latrans*) and *L. ocellatus macrosternum* are distinguished by the arrangement of dermal longitudinal folds, a feature that we now confirm and that was also highlighted by Gallardo (1964) as diagnostic between these two morphologically cryptic species. Later, Cei (1950) described the Chacoan population from Argentina as *L. chaquensis*, but he did not mention differences on the arrangement of dermal folds and listed mostly reproductive and physiological features to diagnose *L. chaquensis* from *L. latrans*. We inferred that the widespread lineage distributed across xeric environments of South America (including Chacoan and BA populations) consists of a single species, because of the low genetic differentiation (which agrees with the overall intraspecific divergence reported for the LLSG; Fig. 5) and absence of morphological/morphometric and acoustic variation. Therefore, we herein regard *L. chaquensis* Cei 1950 as a junior synonym of *L. macrosternum* Miranda-Ribeiro 1926.

In the following section we provide the taxonomic accounts and formally name lineages CS1 and CS3 evidenced as new species by our integrative approach. There is more than one century of published literature using the names attributed to representatives of the LLSG, specifically those assigned to the LCM complex. Because members of this species group are widely distributed in South America and easily detected in nature, they are cited in

virtually any species list. Therefore, in the cases of *L. latrans*, *L. luctator* and *L. macrosternum* (which exhibit broad geographic ranges) we list only those synonyms originally published as species description.

Species Accounts

Leptodactylus macrosternum Miranda-Ribeiro 1926

(Figs. 1, 14)

Leptodactylus macrosternum Miranda-Ribeiro 1926: Miranda-Ribeiro (1926:147 [his Fig. 79]), species description; Gallardo (1964:379, 380 [Plate II, Figs. 8–9]).

Leptodactylus ocellatus var. *typica* Cei 1948: Cei (1984:308–312), species description.

Leptodactylus chaquensis Cei 1950: Cei (1950:403 [his Fig. 2], 417, 418–420 [his Table C], 421, 422, [Plates I–III, Figs. 3–4]), species description; Gallardo (1964:375 [Plate I, Figs. 3–4], 381 [Plate III, Figs. 10–11], 382–383).

Holotype.—MZUPS 446, a juvenile collected by Mr. Beniamino Bicego on June 1896 around the vicinities of Salvador municipality, Bahia province (now Bahia state), Brazil.

Diagnosis.—Assigned to the *Leptodactylus latrans* species group by phylogenetic placement and the following combination of features: (1) adult male SVL = 48.7–98.9 mm ($\bar{X}$ = 74.4 mm) and adult female SVL = 55.9–90.8 mm ($\bar{X}$ = 74.0 mm); (2) adult males with a pair of black keratinized thumb spines on hand; (3) adult males with chest spicules (no spines); (4) two pairs of complete and well-developed dorsal longitudinal folds (folds F2 and F4) extending from behind the eye or posterior interocular region to the pelvic region; (5) pair of auxiliary folds (fold F3) long extending from behind eye to midbody; (6) bilobed vocal sac in adult males; (7) toes and fingers laterally fringed; (8) single longitudinal row of spicules on posterior surface of tibia; (9) in life, thigh posterior surface coloration varying from gray to greenish hues without black maculated background pattern; (10) dark-brown

ocellated blotches evenly distributed on dorsum; (11) vocal repertoire made up of three distinct note types; (12) growl dominant frequency 366–445 Hz ($\overline{X}$ = 389 Hz).

Coloration of the holotype in preservative.—The overall holotype coloration is completely faded (Fig. 1), without any recognizable pigmentation pattern.

Measurements of holotype (in mm).—SVL 65. The poor preservation conditions of the holotype prevent us from taking reliable morphometric measurements.

Variation.— Most of the variation lies on the auxiliary fold F3 (which may be complete or interrupted) and on the coloration of thigh posterior surface (in life), which is usually distinctively green without black maculated patches on the background, but some individuals may exhibit gray shades. In life, body dorsal coloration is overall reddish-brown (Fig. 14A–C), but may also exhibit green shades (Fig. 14D). All other variations in morphological features are mentioned in the "Morphology" section of Results.

Advertisement call.—Redescription is based on a small sample of calls recorded by us (n = 2 males) to allow direct comparisons with calls of species in the *Leptodactylus latrans* complex. Previous descriptions can be found in Heyer and Giaretta (2009) and Camurugi et al. (2017). See Appendix III for locality and recording information. Descriptive statistics (mean and standard deviation) are given in Table 5. The call is composed of up to three distinct note types (referred as growl, grunt, and trill in Heyer and Giaretta 2009), which differ from each other in temporal (note duration, pulse number and rate) and frequency (dominant frequency and frequency modulation) traits, as well as differences in their envelopes (Table 5; Fig. 13A–C). Call notes are given at highly variable rates as single notes, in sequences of a same note type (mainly growl and trill notes) or combinations of more than one note type. The growl note type (Fig. 13A) is the most commonly emitted by males of *L. macrosternum*, which led Camurugi et al. (2017) to classify this note into a main reproductive context (i.e., advertisement call note). The growl-type note (n = 21) has pulses

(*n* = 455) separated by brief silence gaps in-between (in most cases) or partially fused in a few cases. Growl notes have their rise time at 26–63% of their length. Note length ranges from 316–591 ms. Each note is composed of 15–27 pulses, emitted at a rate of 48–57 pulses per second. The dominant frequency ranges from 366–445 Hz. Notes have modest frequency modulation, either positive or negative, which ranges from 215–188 Hz. The grunt-type note (*n* = 5) has a few amplitude modulations that could not be accurately quantified in the time domain, even though note subunits were visualized in the frequency domain (Fig. 13B). Grunt notes have their rise time at 27–48% of their length. Note length ranges from 81–117 ms. The dominant frequency ranges from 280–323 Hz. Notes have subtle negative frequency modulation ranging from -86 to -43 Hz. The trill-type note (*n* = 6) has complete pulses (*n* = 87), i.e., separated by silent gaps in-between along the note (Fig. 13C). Trill notes have their rise time at 59–78% of their length. Note length ranges from 537–667 ms. Pulse number is 14–15, emitted at a rate of 22–26 pulses per second. The dominant frequency ranges from 452–495 Hz. Notes have modest positive frequency modulation or completely lack modulation, which ranges from 0–172 Hz.

Comparisons with other species (characteristics from other species are given within parenthesis).—*Leptodactylus macrosternum* differs from *L. silvanimbus*, all species in the *L. bolivianus* complex (*L. bolivianus*, *L. guianensis* and *L. insularum*) and *L. viridis* by exhibiting well-developed and complete dorsal longitudinal folds F1–2 that extends from behind eye to the pelvic region (absent in *L. silvanimbus*, *L. bolivianus*, *L. guianensis* and *L. insularum*, Heyer and de Sá 2011; and poorly developed in *L. viridis*, Jim and Spirandeli-Cruz 1979). The bilobed vocal sac differs male *L. macrosternum* from those of *L. latrans* and *L. luctator* (single-lobed vocal sac, Gallardo 1964; Heyer and de Sá 2011; de Sá et al. 2014). The presence of two thumb spines on hand differs males of *L. macrosternum* from those of *L. bolivianus*, *L. guianensis* and *L. viridis* (one thumb spine on hand; Jim and Spirandeli-Cruz

1979; Heyer and de Sá 2011). By exhibiting a long auxiliary fold extending from behind eye to midbody (Fig. 6B), *L. macrosternum* differs from *L. latrans* and *L. luctator* (absent or, if present, short and restricted to the anterior third of body length; as depicted in Fig. 6A). The presence of a single longitudinal row of spicules on the posterior surface of tibia differs *L. macrosternum* from *L. viridis* (three longitudinal rows of spicules; Jim and Spirandeli-Cruz 1979). By its larger body size ($\bar{X}$ = 75.3 mm SVL), *L. macrosternum* differs from *L. silvanimbus* ($\bar{X}$ = 47.8 mm SVL; de Sá et al. 2014) and *L. viridis* ($\bar{X}$ = 63.4 mm SVL). In opposite, the smaller body size differs *L. macrosternum* from *L. latrans*, *L. luctator* and all species in the *L. bolivianus* complex clade (on average, the SVL of these species is larger than 84 mm; de Sá et. al. 2014; Table 4). Additionally, *L. macrosternum* differs from *L. viridis* by the overall reddish-brown body coloration in life (body coloration in life predominantly green; Jim and Spirandeli-Cruz 1979; de Sá et al. 2014). In life, coloration of groin and thigh posterior surface is generally distinctly green (not distinctly green in *L. latrans* and *L. luctator*). Moreover, *L. macrosternum* does not exhibit a black maculated background on the posterior surface of the thigh, distinguishing it from *L. latrans* and *L. luctator* (generally present in these species).

The complex call of *Leptodactylus macrosternum*, made up of three distinct note types, distinguishes this species from all congeners in the LLSG, which have single-note calls. Additionally, *L. macrosternum* is the only species in the clade having notes composed of complete pulses (growls and trills; Fig. 13A, and C, respectively). The rarest note type recorded, the grunt-type note (Fig. 13B), is not markedly pulsed as are growls and trills. This note type also differs from those of congeners in the LLSG by the absence of frequency upsweep (present in species of the *L. bolivianus* and *L. latrans* complexes; Heyer and de Sá 2011; Table 6). Furthermore, grunt notes' duration (81–117 ms) and dominant frequency (280–323 Hz) is shorter and lower-pitched, respectively, in comparison with calls of *L.*

silvanimbus (ca. 150 ms and 500 Hz on average; Heyer et al. 1996a), and longer and lower-pitched, respectively, in comparison with calls of *L. viridis* (16–31 ms and 560 Hz on average; Rocha et al. 2016).

Leptodactylus macrosternum exhibits from 69 to 92 bp (from 507 bp) differences in the COI mitochondrial gene (or approximately 17% to 20% of genetic distance) in comparison to all other species in the LLSG. This clade is supported as a distinct evolutionary entity with significant support in all phylogenetic (PP = 1.0/BS = 100) and delimitation (bGMYC; ABGD) analyses we performed.

Geographic distribution.—*Leptodactylus macrosternum* is broadly distributed across the DOF of South America (Fig. 2, 15). Its range spans more than 4,000 km from southern SF province in Argentina, through the Brazilian Guiana Shield in RR State, to the Llanos of Venezuela (Dixon and Staton 1976; Gorzula and Señaris 1998; Barrio 2004) and Guyana savannas (Cole et al. 2013), also reaching the coastal region of BA in Salvador municipality, and all northeastern and northern Brazilian coast. Although not sampled by us, there are records of *L. macrosternum* (referred as *L. chaquensis* therein) for the Brazilian states of RS (Santos and Cechin 2008; Teixeira et al. 2017), SC (Machado et al. 2014) and PR (Oda et al. 2014). Moreover, one of the *L. macrosternum* samples provided by de Sá et al. (2014) from Trinidad and Tobago also clustered with what we now regard as *L. macrosternum*, reinforcing the occurrence of this taxon in this continental island of South America (referred as *L. ocellatus* by Murphy 1997).

Remarks.—We did not evaluate the variation of some features previously used to distinguish *Leptodactylus macrosternum* from species in the *L. latrans* complex. For instance, the enlarged black triangular-shaped mark posterior to the tympanum provides a visual clue to distinguish living specimens of *L. luctator* from *L. macrosternum* collected in sympatry along Argentina, Uruguay and southernmost Brazil (Cei 1950, 1980; Langone

1995; Teixeira et al. 2017; referred therein as *L. latrans*/*L. ocellatus* and *L. chaquensis*, respectively). Accordingly, the green shades on posterior thigh surface may also provide a visual clue for identification of *L. macrosternum* living individuals, but if collected in northeastern Brazil this feature may not be useful (e.g., representatives of *L.* aff. *latrans* CS1 lineage also exhibit this characteristic). This species occurs in sympatry with almost all lineages in the LCM complex (except for representatives of *L.* aff. *latrans* CS3 lineage). Given the broad geographic distribution and that we may not fully assessed all morphological variation related to species in the LLSG, we highly recommend the combined use of distinct lines of evidence, including morphology (e.g., the arrangement of dermal longitudinal folds), geography, calls and genetic data for accurate species assignments.

Leptodactylus latrans (Steffen 1815)

(Fig. 16)

Rana gibbosa Raddi 1823: Raddi (1823:67), species description.

Rana fusca Raddi 1823: Raddi (1823:68), species description.

Rana pachypus Spix 1824: Spix (1824:26, [Plate II, Figs. 1–2; and Plate III, Fig. 2]), species description.

Rana pachybrachion Wied-Neuwied 1824: Wied-Neuwied (1824:671), species description; possible emendation or misspelling of *P. pachypus* by Vanzolini and Myers (2015:75–76).

Rana macrocephala Wied-Neuwied 1825: Wied-Neuwied (1825:544), species description.

Leptodactylus serialis Girard 1853: Girard (1853:421), species description.

Leptodactylus caliginosus Girard 1853: Girard (1853:422), species description; Girard (1858:31–33).

Leptodactylus ocellatus (non Linnaeus 1758): Girard (1858:29–31, [Plate III, Figs. 1–6]); Gallardo (1964:375 [Plate I, Figs. 1–2], 378–379), in part.

Holotype.—Presumably lost (see Lavilla et al. 2010; Frost 2019).

Neotype.—MNRJ 30733, an adult male collected by U. Caramaschi, H. de Niemeyer, and D.F. de Moraes Jr on 18 September 1999 at Vale dos Agriões, Teresópolis municipality, Rio de Janeiro state, Brazil (22°25'S, 42°58'W; 976 m a.s.l.).

Diagnosis.—Assigned to the *Leptodactylus latrans* species group by phylogenetic placement and the following combination of features: (1) adult male SVL = 63.2–124.9 mm ($\bar{X}$ = 95.8 mm) and adult female SVL = 61.4–104.7 mm ($\bar{X}$ = 89.8 mm); (2) adult males with a pair of black keratinized thumb spines on hand; (3) adult males with chest spicules (no spines); (4) two pairs of complete and well-developed dorsal longitudinal folds (folds F2 and F4) extending from behind the eye or posterior interocular region to the pelvic region; (5) pair of auxiliary folds (fold F3) absent or, if present, are short and restricted to the anterior third of the dorsum; (6) single-lobed vocal sac in adult males; (7) toes and fingers laterally fringed; (8) single longitudinal row of spicules on posterior surface of tibia; (9) in life, thigh posterior surface coloration varying from gray to blue shades; (10) dark or light brown ocellated blotches on dorsum varying from a smooth to sparsely scattered pattern**;** (11) advertisement call as single, nonpulsed notes with smooth envelope; (12) dominant frequency 280–455 Hz ($\bar{X}$ = 356 Hz).

Neotype description, coloration and measurements.—Provided by Lavilla et al. (2010).

Variation.—We observed that the distribution of ocellated blotches along the dorsal region varies from a smooth (ocellated blotches absent, Fig. 16B) to a sparsely scattered pattern (see Fig. 16A, C–D). The ocellated blotches are mostly restricted to dorsal and dorsolateral regions, while lateral regions mostly lack this feature. The supra-labial light

stripe that extends from below the eyes to the forelimb region (passing under the tympanum) can be well-marked (Fig. 16D) or poorly marked (Fig. 16A–C). A supratympanic dark stripe extending from below the eye to the forelimb insertion (posteriorly behind tympanum) can be well-marked (Fig. 16D) or poorly marked (Fig. 16B). Similarly, the supratympanic dark stripe may form a triangular-shaped feature posterior to the tympanum, which can be black (Fig. 16D), light to dark brown (Fig. 16A, C) or indistinct/absent (Fig. 16B). Some specimens may exhibit green shades along body dorsum, instead of the overall reddish-brown body coloration in life (Fig. 16A–D). All other variations in morphological features are mentioned in the "Morphology" section of Results.

Advertisement call.—Description is based on calls of nine males (n = 100 calls), of which three (n = 46 calls) are topotypes. See Appendix III for locality and recording information. Descriptive statistics (mean and standard deviation) are given in Table 6. Calls are given at irregular intervals. The call is composed of single, nonpulsed notes with rise time at 28–82% of their length (Fig. 12A). Note length ranges from 124–248 ms. Frequency range is mostly distributed across the first three harmonics, and the second harmonic often has more energy at the very onset, when the fundamental frequency is still barely detectable, but almost all sound energy is contained in the fundamental harmonic throughout the notes' duration. The dominant frequency is always associated with the fundamental harmonic, ranging from 280–445 Hz. Notes have a modest frequency upsweep, ranging from 43–301 Hz. An exception to this description is restricted to variation in the envelope of calls recorded from a topotype, in which we detected irregular amplitude modulations along the call. Without any other information, it is difficult to interpret the possible sources of variation related to such changes in the call envelope. We are aware that calling rate in the *L. latrans* complex clade, for instance, depends much on motivation state of nearby calling males, the presence of neighboring calling males and receptive females, among other factors. Call

envelope might also be modulated as a result of the combination of the extrinsic factors mentioned above and intrinsic factors (e.g., within-male variation/plasticity) and/or simply reflect interfering structures in the environment that could have affected sound propagation.

Comparisons with other species (characteristics from other species are given within parenthesis).—*Leptodactylus latrans* differs from *L. silvanimbus*, all species in the *L. bolivianus* complex (*L. bolivianus*, *L. guianensis* and *L. insularum*) and *L. viridis* by exhibiting well-developed and complete dorsal longitudinal folds F1–2 that extend from behind the eyes to the pelvic region (absent in *L. silvanimbus*, *L. bolivianus*, *L. guianensis* and *L. insularum*, Heyer and de Sá 2011; and poorly developed in *L. viridis*, Jim and Spirandeli-Cruz 1979). The presence of two thumb spines on hand differs males of *L. latrans* males from those of *L. bolivianus*, *L. guianensis* and *L. viridis* (one thumb spine on hand; Jim and Spirandeli-Cruz 1979; Heyer and de Sá 2011). The presence of a single longitudinal row of spicules on the posterior surface of tibia distinguishes *L. latrans* from *L. viridis* (three longitudinal rows of spicules; Jim and Spirandeli-Cruz 1979). By is larger body size ($\bar{X}$ = 93.8 mm SVL), *L. latrans* differs from *L. silvanimbus* ($\bar{X}$ = 47.8 mm SVL; de Sá et al. 2014) and *L. viridis* ($\bar{X}$ = 63.4 mm SVL). By its proportionally longer tibia and foot ($\bar{X}$ = 52% and 56% of SVL, respectively), *L. latrans* differs from *L. viridis* ($\bar{X}$ = 46% and 51% of SVL, respectively). Additionally, *L. latrans* differs from *L. viridis* by the overall reddish-brown body coloration in life (body coloration predominantly green; Jim and Spirandeli-Cruz 1979; de Sá et al. 2014). In life, coloration of the groin is not distinct from that of body's lateral regions (yellowish in *L. luctator*). In life, coloration of thigh posterior surface varies from blue to gray shades (yellowish in *L. luctator*).

Leptodactylus latrans is further distinguished from congeners in the LLSG by acoustic traits. From the closest related species (i.e., *L. latrans* complex clade), *L. latrans* differs in having nonpulsed notes with a smooth envelope, which is nonpulsed with

weak/irregular amplitude modulations in *L. luctator*. The three species of the *Leptodactylus bolivianus* complex (*L. bolivianus*, *L. guianensis* and *L. insularum*) have well-marked frequency upsweep in their calls, in contrast to modest frequency modulation in *L. latrans*. Also, calls in the *L. bolivianus* complex always have higher dominant frequencies than the call of *L. latrans* (Heyer and de Sá 2011; Table 6). *Leptodactylus silvanimbus* has a broad-band call without frequency sweeps, differing in both features from the call of *L. latrans*, which is relatively more well-tuned and with a frequency upsweep (Heyer et al. 1996a; Fig. 13E). *Leptodactylus viridis* has a short-length call (16–31 ms; Rocha et al. 2016; Fig. 13F) in comparison to *L. latrans* (124–248 ms).

Leptodactylus latrans has 32 to 110 bp (from 507 bp) differences in the COI mitochondrial gene (or approximately 8% to 26% of genetic distance) in comparison to all other species in the LLSG. This clade is supported as a distinct evolutionary entity with significant support in all phylogenetic (PP = 1.0/BS = 100) and delimitation analyses (bGMYC; ABGD).

Geographic distribution.—*Leptodactylus latrans* is endemic to the Atlantic Forest and occurs along the coastal zone from Mata de São João municipality (BA), all the way to northern SP in Bertioga municipality, also entering higher altitudinal zones (~700–900 m a.s.l) in RJ and "Zona da Mata Mineira", the Atlantic Forest zone in eastern MG. In SP state, we only recorded this species along coastal areas (> 100 m a.s.l) east of the Serra do Mar mountain range (Figs. 2, 17).

Remarks.—Both Cei (1962) and Gallardo (1964) identified individuals from AL and PE states in northeastern Brazil as *Leptodactylus latrans* (= *L. ocellatus* therein), occurring syntopically with the smaller morphotype *L. macrosternum*. Although all samples we sequenced from these regions clustered within *L. chaquensis/macrosternum* lineage, it is plausible that *L. latrans* occurs along the coastal zone of these states mostly because they are

under influence of Atlantic Forest, to which *L. latrans* is exclusively associated. Nevertheless, we have no further evidence supporting this geographic distribution.

Leptodactylus luctator (Hudson 1892) revalidated, new combination

(Figs. 18, 19)

Cystignathus oxycephalus Philippi 1902: Philippi (1902:105–106, [Plate VII, Fig. 3]), species description.

Leptodactylus ocellatus var. *reticulata* Cei 1948: Cei (1948:308–312), species description.

Leptodactylus ocellatus var. *bonairensis* Cei 1949: Cei (1949:127–132), species description; Cei (1950: 416 [Table B]).

Leptodactylus ocellatus (non Linnaeus 1758): Cei (1950:411–412 [his Table A], 413 [his Figs. 3.1–2], [Plates I–III, Figs. 1–2]); Gallardo (1964:375, 378–379), in part.

Holotype.—The holotype was not designated (Hudson 1892).

Neotype.—LGE 22146, an adult male collected by Diego Barrasso on March 2019 at Villa Elvira, La Plata municipality, Buenos Aires province, Argentina (34°58'36"S; 57°52'10"W; 14 m a.s.l.).

Diagnosis.—Assigned to the *Leptodactylus latrans* species group by phylogenetic placement and the following combination of features: (1) adult male SVL = 72.7–121.6 mm ($\bar{X}$ = 95.0 mm) and adult female SVL = 73.9–115.8 mm ($\bar{X}$ = 91.2 mm); (2) adult males with a pair of black keratinized thumb spines on hand; (3) adult males with chest spicules (no spines); (4) two pairs of complete and well-developed dorsal longitudinal folds (folds F2 and F4) extending from behind the eyes or posterior interocular regions to the pelvic region; (5) pair of auxiliary folds (fold F3) absent or, if present, are short and restricted to the anterior third of the dorsum; (6) single-lobed vocal sac in adult males; (7) toes and fingers laterally fringed; (8) single longitudinal row of spicules on posterior surface of tibia; (9) well-marked

dark brown ocellated blotches on dorsum varying from sparsely scattered to an evenly distributed pattern**;** (10) in life, thigh posterior surface coloration with yellow shades and black maculated background pattern; (11) advertisement call as single, nonpulsed notes with weak/irregular amplitude modulations; (12) dominant frequency 280–409 Hz ($\bar{X}$ = 343 Hz).

Neotype description.—Adult male, with strongly hypertrophied arms. Robust build; head slightly wider than long (HL/HW ratio about 93%), HL 34% of SVL, and HW 37% of SVL. Snout rounded from above (Fig. 18A), obtuse in profile (Fig. 18E); canthus rostralis indistinct and rounded; loreal region oblique, slightly concave. Nostril closer to tip of snout than to eyes. Eye to nostril distance larger than eye and tympanum diameters. Tympanum circular, annulus distinct, thick; distance from tympanum to eye smaller than TD; tympanum diameter slightly smaller than eye diameter (TD/ED ratio about 92%). Upper eyelid, head, and dorsal skin smooth; a thick supratympanic fold from posterior corner of eye, arching downwards posteriorly to tympanum, and reaching dorsal region of arm insertion; a thick, longitudinally elongated buccal fold posteriorly to mouth commissure; eight dermal longitudinal folds, four on each side of the body: fold F2 from posterior interocular region to urostyle region; fold F4 extends dorso-laterally from posterior corner of eye to groin; fold F1 (formed by small tubercles) poorly developed, mostly restricted to posterior region of dorsum; fold F5 slightly shorter than fold F6, interrupted and extending from above shoulder region to groin; fold F6 complete, from posterior corner of eye to groin. Ventral skin, dorsal and ventral surfaces of arms smooth; patch formed by small keratinized spicules overall absent on throat and along ventrolateral region of body; granular seat patch under thighs; cloacal region without expanded fringes; dorsal surface of thighs and tibiae with many small pointed spicules; on dorsal tibia surface these spicules align forming a longitudinal row. Vocal sac poorly developed, subgular, and single-lobed. Vocal slits present on each side of tongue; vomerine teeth in two transverse series almost contacting medially, laying between

and just posterior to choanae. Tongue large, free, slightly notched posteriorly. Hand (Fig. 18C) with slender fingers, not webbed, and with rounded and not expanded tips; weak lateral fringes without small keratinized spicules along their edges; finger lengths III < V < II < IV; subarticular tubercles rounded, and proximal tubercles more developed than distal ones; few rounded supernumerary tubercles present but not very developed; outer metacarpal tubercle large and cordiform; inner metacarpal tubercle small and rounded; a large and rounded keratinized black spine on thumb, lateral to proximal subarticular tubercle of finger I; a large and rounded keratinized spine on strongly developed prepollex. Legs robust, with long tibia and foot, representing about 48% and 54% of SVL, respectively. Foot (Fig. 18D) with slender toes and only basally webbed; lateral fringes without small keratinized spicules along edge; toe lengths I < II < V < III < IV; toe tips rounded; subarticular tubercles large and rounded; sole of foot with several distinct keratinized spicules; outer metatarsal tubercle very small, rounded and poorly developed; inner metatarsal tubercle large, elliptical, and slightly elevated; sole of tarsus with several evenly distributed keratinized spicules; inner tarsal fold developed, approximately the length of the tarsus.

Coloration of neotype.—In life, dorsal surface of body (dorsum and flanks) and limbs overall light brown with well-delimited dark brown blotches (Fig. 19A); on body, blotches are arranged longitudinally, running over dermal folds from behind eyes to cloacal region, while blotches are arranged transversally on thigh upperside and tibia posterior surfaces. Arms with small dark brown blotches, except for a larger circular blotch on elbow. Anterior surface of arms and groin beige. Posterior surface of thighs yellow mustard with brown maculated patches on the background. Dermal longitudinal folds (F1 to F5) dark brown, and F6 whitish. Dark brown stripe from snout, passing through nostrils, to the anterior corner of eye. Upper half of the loreal region light brown, while lower half with dark brown blotches above lip. Dark brown stripe running over the supratympanic fold. Tympanic

membrane homogeneously dark gray. Throat homogeneously pigmented in light gray. Ventral surface of arms, legs, and belly beige; underside surface of thighs with small and non-evident yellow melanophores. Ventral surface of hand, foot, and tarsus overall dark gray.

Measurements of Neotype (in millimeters).—SVL 99.7, HW 37.1, HL 34.4, ESD 17.1, END 9.2, EED 21.9, ED 9.5, TD 6.1, HAL 23.3, FAL 42.8, TL 47.7, FTL 51.9.

Variation.—We observed that the most predominant ocellated blotch patterns along the dorsal region are patterns 2 and 3 (Fig. 19). The supra-labial light stripe that extends from below eyes to the forelimb insertion (passing under the tympanum) can be well-marked (Fig. 19B–D) or indistinct (Fig. 19A). A supratympanic dark stripe extending from below the eye to the forelimb insertion (posteriorly behind tympanum) is generally well-marked and varies between black and brownish shades. Similarly, the supratympanic dark stripe may form a triangular-shaped mark posterior to the tympanum, which can be black (see Fig. 1B in Teixeira et al. 2017), light to dark brown (Fig. 19C, D) or indistinct/absent (Fig. 19A, B). Some specimens may exhibit green shades along body dorsum (Fig. 19B, C), instead of the overall reddish-brown body coloration in life. All other variations in morphological features are mentioned in the "Morphology" section of Results.

Advertisement call.—Description is based on calls of eight males (n = 134 calls; Table 6). See Appendix III for locality and recording information. Descriptive statistics (mean and standard deviation) are given in Table 6. Calls are given at irregular intervals. The call is made up of single, nonpulsed notes with rise time at 45–85% of their length (Fig. 12B). Although defined as nonpulsed, this species has weak/irregular amplitude modulations along the note, in contrast to the smooth envelope of nominal *L. latrans*. Note length ranges from 158–413 ms. Frequency range is mostly distributed across the first three harmonics, being that the second harmonic often has more energy at the very onset, when the fundamental frequency can still be barely detected, but almost all sound energy is contained

in the fundamental harmonic throughout notes' duration. The dominant frequency is always associated with the fundamental harmonic, ranging from 280–409 Hz. Notes have modest frequency upsweep ranging from 43–281 Hz.

Comparisons with other species (characteristics from other species are given within parenthesis).—*Leptodactylus luctator* differs from *L. silvanimbus*, all species in the *L. bolivianus* complex (*L. bolivianus*, *L. guianensis* and *L. insularum*) and *L. viridis* by exhibiting well-developed and complete dorsal longitudinal folds F1–2 that extends from behind eye to the pelvic region (absent in *L. silvanimbus*, *L. bolivianus*, *L. guianensis* and *L. insularum*, Heyer and de Sá 2011; and poorly developed in *L. viridis*, Jim and Spirandeli-Cruz 1979). The presence of two thumb spines on hand differs males of *L. luctator* from those of *L. bolivianus*, *L. guianensis* and *L. viridis* (one thumb spine on hand; Jim and Spirandeli-Cruz 1979; Heyer and de Sá 2011). The presence of single longitudinal row of spicules on the posterior surface of tibia differs *L. luctator* from *L. viridis* (three longitudinal rows of spicules; Jim and Spirandeli-Cruz 1979). By its larger body size ($\bar{X}$ = 94.0 mm SVL), *L. luctator* differs from *L. silvanimbus* ($\bar{X}$ = 47.8 mm SVL; de Sá et al. 2014) and *L. viridis* ($\bar{X}$ = 63.4 mm SVL). By its proportionally longer tibia and foot ($\bar{X}$ = 51% and 54% of SVL, respectively), *L. luctator* differs from *L. viridis* ($\bar{X}$ = 46% and 51% of SVL, respectively). Additionally, *L. luctator* differs from *L. viridis* by the overall reddish-brown body coloration in life (body coloration predominantly green; Jim and Spirandeli-Cruz 1979; de Sá et al. 2014).

Leptodactylus luctator is further distinguished from congeners in the LLSG based on acoustic traits. The three species of the *L. bolivianus* complex (*L. bolivianus*, *L. guianensis*, and *L. insularum*) have well-marked frequency upsweep in their calls, in contrast to modest frequency modulation in *L. luctator*. Also, calls in the *L. bolivianus* complex always have higher dominant frequencies than does the call of *L. luctator* (Heyer and de Sá 2011; Table

6). *Leptodactylus silvanimbus* has a broad-band call without frequency sweeps, differing in both features from the call of *L. luctator*, which is relatively more well-tuned and with a frequency upsweep (Heyer et al. 1996a; Fig. 13E). *Leptodactylus viridis* has a very short-length call (16–31 ms; Rocha et al. 2016; Fig. 13F) in comparison with that of *L. luctator* (158–413 ms).

Leptodactylus luctator exhibited from 42 to 106 bp (from 507 bp) differences in the COI mitochondrial gene (or approximately 10% to 24% of genetic distance) in comparison to all other species in the LLSG. This clade is supported as a distinct evolutionary entity with significant support in all phylogenetic (PP = 1.0/BS = 100) and delimitation (bGMYC; ABGD) analyses performed by us.

Geographic distribution.—This is the most geographically widespread taxa among species in the *Leptodactylus latrans* complex clade (Figs. 2, 20). It occurs in five countries of South America from low altitudinal and coastal zones (e.g., Argentina and Uruguay) to high altitudinal areas (e.g., above 1000 m a.s.l.) in eastern South America. It is distributed from southwestern Chaco in SJ, through the Argentinean and Uruguayan Pampas, across the Atlantic Forest from southeastern Paraguay and southern Brazil in RS through high altitudinal zones at SC, PR and SP (west to the Serra do Mar mountain range), also reaching rocky outcrop fields (known as "*campos rupestres*") within the Espinhaço mountain range in MG and BA. This species also occurs in areas under the influence of Cerrado (e.g., MT, GO and western MG) and apparently exhibit a disjoint distribution in areas under the influence of Pantanal in MS, with a single record at easternmost Bolivia (see De la Riva and Maldonado 1999).

Remarks.—According to Cei (1950, 1962), populations related to this species reaches the southernmost regions from BU (e.g., Bahía Blanca municipality; Cei 1950), but we did not assessed samples from these regions to confirm these populations identity.

Leptodactylus **CS1 lineage** sp. nov.

(Figs. 21, 22)

Leptodactylus latrans (non Steffen 1815): Magalhães et al. (2015:247 [Table 1], 255 [Fig. 9G], 261 [their Appendix I], in part.

Leptodactylus macrosternum non Miranda-Ribeiro 1926: Pedrosa et al. (2014:4 [Table 1], 5 [Fig. 3A].

Leptodactylus ocellatus (non Linaeus 1785): Juncá (2005:344 [Table 2]), in part; Nunes and Juncá (2006:152 [Table 1], 154 [Fig. 5]).

Holotype.—CHUFPB 28187, an adult male collected by F.M. Magalhães and W. Pessoa on 16 March 2018 at Chapada Diamantina, Jacobina Municipality, Bahia state, Brazil (11° 9'38.66"S, 40°32'6.60"W; 467 m a.s.l.).

Paratopotypes.—CHFUPB 28184, 28186, 28188–28192, adult males, and CHUFPB 28193, adult female, all collected with the holotype.

Diagnosis.—Assigned to the *Leptodactylus latrans* species group by phylogenetic placement and the following combination of features: (1) adult male SVL = 58.5–96.9 mm ($\bar{X}$ = 84.3 mm) and adult female SVL = 72.6–93.6 mm ($\bar{X}$ = 84.6 mm); (2) adult males with a pair of black keratinized thumb spines on hand; (3) adult males with chest spicules (no spines); (4) two pairs of complete and well-developed dorsal longitudinal folds (folds F2 and F4) extending from behind the eye or posterior interocular region to the pelvic region; (5) pair of auxiliary fold (fold F3) absent or, if present, are short and restricted to the first third of the dorsum; (6) single-lobed vocal sac in adult males; (7) toes and fingers laterally fringed; (8) single longitudinal row of spicules on the posterior surface of tibia; (9) in life, thigh posterior surface coloration varying from gray to green shades without black maculated background pattern; (10) dark-brown ocellated blotches evenly distributed on dorsum; (11)

advertisement call as a single type of partly fused, multi-pulsed note; (12) dominant frequency 398–633 Hz ($\bar{X}$ = 470 Hz).

Holotype description.—Adult male; arms strongly hypertrophied. Robust build; head slightly wider than long (HL/HW ratio about 95%), HL 35% of SVL, and HW 36% of SVL. Snout rounded from above (Fig. 21A), obtuse in profile (Fig. 21E); canthus rostralis indistinct and rounded; loreal region oblique, slightly concave. Nostril closer to tip of snout than to eye. Eye to nostril distance larger than eye and tympanum diameters. Tympanum circular, annulus distinct, thick; distance from tympanum to eye smaller than TD; tympanum diameter slightly smaller than eye diameter (TD/ED ratio about 84%). Upper eyelid, head, and dorsal skin smooth; a thick supratympanic fold from posterior corner of eye, arching downwards posteriorly to tympanum, and reaching dorsal region of arm insertion; a thick, longitudinally elongated buccal fold posteriorly to mouth commissure; eight dermal longitudinal folds, four on each side of body: fold F2 from posterior interocular region to urostyle region; fold F4 extends dorso-laterally from posterior corner of eye to groin; fold F1 (formed by small tubercles) poorly developed and not discernible in preservative; fold F5 slightly shorter than fold F6, interrupted, from above shoulder region to groin; fold F6 complete, from posterior corner of eye to groin; ventral skin, dorsal and ventral surfaces of arms smooth; a patch formed by small keratinized spicules from wrist to throat region, where more densely grouped spicules form a triangular shaped feature posteriorly to throat. Patch of keratinized spicules on each side of ventro-lateral region of body, extending from below arms to groin; a granular seat patch under thighs; cloacal region without expanded fringes; dorsal surface of thighs and tibia with many small pointed spicules; on dorsal tibia surface spicules align forming longitudinal row. Vocal sac poorly developed, subgular, and single-lobed. Vocal slits present on each side of tongue; vomerine teeth in two transverse series almost contacting medially, laying between and just posterior to choanae. Tongue large, free,

slightly notched behind. Hand (Fig. 21C) with slender fingers, not webbed, and with rounded and not expanded tips; weak lateral fringes with small keratinized spicules along their edges; finger lengths III < V < II < IV; subarticular tubercles rounded, and proximal tubercles more developed than distal ones; few rounded supernumerary tubercles present but not very developed; outer metacarpal tubercle large and cordiform; inner metacarpal tubercle small and rounded; a large and triangular keratinized black spine on thumb, lateral to proximal subarticular tubercle of finger I; a large, triangular, keratinized spine on strongly developed prepollex. Legs robust with long tibia and foot, representing about 49% and 47% of SVL, respectively. Foot (Fig. 21D) with slender toes and only basally webbed; lateral fringes with small keratinized spicules along edges; toe lengths I < II < V < III < IV; toe tips rounded; subarticular tubercles large and rounded; sole of foot with several distinct keratinized spicules; outer metatarsal tubercle very small, rounded and poorly developed; inner metatarsal tubercle large, elliptical, slightly elevated; sole of tarsus with several evenly distributed keratinized spicules; inner tarsal fold developed, approximately the length of tarsus also exhibiting keratinized spicules along its edge.

Coloration of holotype.—In life, dorsal surface of body (dorsum and flanks) and limbs overall reddish-brown with well-marked dark brown circular blotches (Fig. 22A); on body, blotches are sparsely scattered on dorsum, while on posterior members blotches are arranged transversally on thigh surface and mostly indistinct on tibia posterior surface Arms mostly lacking dark brown blotches; anterior surface of arms, groin and thighs posterior surface with green shades; posterior surface of thighs without strongly marked black maculated patches. Dermal longitudinal folds (F1 to F5) dark brown, and F6 whitish. Dark brown stripe between nostrils and anterior corner of eye. Loreal region homogeneously reddish-brown, with a light brown stripe above lip, running over the buccal fold posteriorly to mouth commissure, reaching arm insertion. Thin dark brown stripe running over the

supratympanic fold. Tympanic membrane homogeneously dark gray. Throat homogeneously pigmented in dark gray; Ventral surface of arms, legs, and belly beige. Ventral surface of hand, foot, and tarsus overall dark gray.

Measurements of holotype (in millimeters).—SVL 95.0, HW 34.5, HL 32.8, ESD 16.2, END 9.0, EED 19.4, ED 7.5, TD 6.3, HAL 22.1, FAL 40.1, TL 46.3, FTL 44.7.

Variation.—The supra-labial light stripe that extends from below eyes to the forelimb region (passing under the tympanum) can be well-marked (Fig. 22B–C) or barely indistinct (Fig. 22A). A supratympanic dark stripe extending from below eye to the forelimb (posteriorly behind tympanum) can also be well-marked (Fig. 22B, C) or indistinct (Fig. 22A). Similarly, the supratympanic dark stripe may form a triangular-shaped mark posterior to the tympanum, which can be black (Fig. 22B), light to dark brown (see Fig. 22B) or poorly defined (Fig. 22A, D). All other variations in morphological features are mentioned in the "Morphology" section of Results.

Advertisement call.—Description is based on calls of four males (n = 49 calls and 416 pulses; Table 6), including the holotype. See Appendix III for locality and recording information. Descriptive statistics (mean and standard deviation) are given in Table 6. Calls are given at irregular intervals. The call is made up of single, multi-pulsed (partly fused) notes with rise time at 56–86% of their length (Fig. 12C). Note length ranges from 158–245 ms. Pulse number is 6–10, which are emitted at a rate of 42–62 pulses per second. Frequency range is mostly distributed across the first three harmonics, being that the fundamental harmonic always has more sound energy along the call, therefore containing the call dominant frequency. The dominant frequency ranges from 398–633 Hz. Notes have frequency upsweep ranging from 94–609 Hz and sinusoidal modulations associated with the note pulsing.

Comparisons with other species (characteristics from other species are given within parenthesis).—*Leptodactylus* CS1 lineage differs from *L. silvanimbus*, all species in the *L. bolivianus* complex (*L. bolivianus*, *L. guianensis* and *L. insularum*) and *L. viridis* by exhibiting well-developed and complete dorsal longitudinal folds F1–2 that extends from behind eye to the pelvic region (absent in *L. silvanimbus*, *L. bolivianus*, *L. guianensis* and *L. insularum*, Heyer and de Sá 2011; and poorly developed in *L. viridis*, Jim and Spirandeli-Cruz 1979). The single-lobed vocal sac differs males of *L.* CS1 lineage from *L. macrosternum* males (bilobed vocal sac; Gallardo 1964). The presence of two thumb spines on hand differs males of *L.* CS1 lineage from those of *L. bolivianus*, *L. guianensis* and *L. viridis* (one thumb spine on hand; Jim and Spirandeli-Cruz 1979; Heyer and de Sá 2011). *Leptodactylus* CS1 lineage lacks the long auxiliary dorsal fold (or if present is short and restricted to body's anterior third; Fig. 6A) distinguishing it from *L. macrosternum* (long auxiliary fold extending from behind the eye to midbody; Fig. 6B). The presence of single longitudinal row of spicules on the posterior surface of tibia differs *L.* CS1 lineage from *L. viridis* (three longitudinal rows of spicules; Jim and Spirandeli-Cruz 1979). By its larger body size ($\bar{X}$ = 84.4 mm SVL), *L.* CS1 lineage differs from *L. macrosternum* ($\bar{X}$ = 74.3 mm SVL), *L. silvanimbus* ($\bar{X}$ = 47.8 mm SVL; de Sá et al. 2014), and *L. viridis* ($\bar{X}$ = 63.4 mm SVL). By its proportionally longer tibia and foot ($\bar{X}$ = 51% and 54% of SVL, respectively), *L.* CS1 lineage differs from *L. viridis* ($\bar{X}$ = 46% and 51% of SVL, respectively). Additionally, *L.* CS1 lineage differs from *L. viridis* by the overall brownish body coloration in life (body coloration predominantly green; Jim and Spirandeli-Cruz 1979; de Sá et al. 2014). In life, coloration of groin and thigh posterior surface is generally distinctly green (groin and thigh posterior regions are not distinctly green in *L. latrans* and *L. luctator*). Moreover, *L.* CS1 lineage does not exhibit a black maculated background on the posterior surface of the thigh, distinguishing it from *L. latrans* and *L. luctator* (generally present in these species).

Leptodactylus CS1 lineage is further distinguished from congeners in the LLSG based on acoustic traits. By having multi-pulsed notes (unique feature within the *L. latrans* complex clade), *L.* CS1 lineage differs from *L. latrans* and *L. luctator*, as well as species in the *L. bolivianus* complex, *L. silvanimbus*, and *L. viridis* (nonpulsed notes; Heyer et al. 1996a; Heyer and de Sá 2011; Rocha et al. 2016; Table 6). The single note acoustic repertoire distinguishes *L.* CS1 lineage from *L. macrosternum*, which have three distinct note types in its acoustic repertoire (referred as *L. chaquensis* in Heyer and Giaretta 2009, Camurugi et al. 2017).

Leptodactylus CS1 lineage has from 52 to 108 bp (from 507bp) differences in the COI mitochondrial gene (or approximately 13% to 24% of genetic distance) in comparison to all other species in the LLSG. This clade is supported as a distinct evolutionary entity with significant support in all phylogenetic (PP = 1.0/BS = 100) and delimitation (bGMYC; ABGD) analyses we performed.

Geographic distribution.—This species is widely distributed across open fields of Chapada Diamantina mountain range and surrounding areas in BA, east to the São Francisco River, with single records in Caatinga/Atlantic Forest ecotonal areas from MG and PE (Fig. 2, 23).

Leptodactylus **CS3 lineage** sp. nov.

(Figs. 24, 25)

Leptodactylus latrans (non Steffen 1815): Wachlevski and Rocha (2010:603 [Table 1 and Fig. 2E]); Zina et al. (2012:254 [Table 2]).

Leptodactylus ocellatus (non Linnaeus 1758): Silva et al. (2000:27 [Table 1]), in part; Bertoluci et al. (2007:368 [Table 1]), in part; Narvaes et al. (2009:120 [Table 1]).

Holotype.—CFBH 42804, an adult male collected by F.M. Magalhães and F.M. Lanna on 27 January 2018 at Peruíbe municipality, São Paulo state, Brazil (24°22'43.42"S, 47°4'31.04"W; 14 m above sea level).

Paratopotypes.—CFBH 42805 and 42807, adult males collected along with the holotype. CFBH 12455, an adult female collected by M.T. Thomé and K. Zamudio on 25 February 2006; CFBH 24121, an adult male collected by R.J Sawaya, F.E. Barbo and M.G. Rodrigues on 01 October 2008; and CFBH 38572, an adult male collected by F.R Silva and A.Z. Boaratti on 11 December 2014.

Diagnosis.—Assigned to the *Leptodactylus latrans* species group by phylogenetic placement and the following combination of features: (1) adult male SVL = 78.9–126.3 mm ($\bar{X}$ = 100.0 mm) and adult female SVL = 75.2–106.3 mm ($\bar{X}$ = 89.9 mm); (2) adult males with a pair of black keratinized thumb spines on hand; (3) adult males with chest spicules (no spines); (4) two pairs of complete and well-developed dorsal longitudinal folds (folds F2 and F4) extending from behind eye or posterior interocular region to pelvic region; (5) pair of auxiliary folds (fold F3) absent or, if present, short and restricted to first third of the dorsum; (6) single-lobed vocal sac in adult males; (7) toes and fingers laterally fringed; (8) single longitudinal row of spicules on posterior surface of tibia; (9) in life, thigh posterior surface coloration varying from gray to blue shades; (10) dark or light brown ocellated blotches on dorsum, varying smooth to sparsely scattered pattern**;** (11) advertisement call as single, nonpulsed notes with weak/irregular amplitude modulations; (12) dominant frequency 323–366 Hz ($\bar{X}$ = 340 Hz).

Holotype description.—Adult male; arms strongly hypertrophied. Robust build; head slightly wider than long (HL/HW ratio about 91%), HL 37% of SVL, and HW 40% of SVL. Snout rounded from above (Fig. 24A), obtuse in profile (Fig. 24E); canthus rostralis slightly marked and rounded; loreal region oblique, slightly concave. Nostril closer to tip of snout

than to eye. Eye to nostril distance larger than eye and tympanum diameter. Tympanum circular, annulus distinct, thick; distance from tympanum to eye smaller than TD; tympanum diameter slightly smaller than eye diameter (TD/ED ratio about 82%). Upper eyelid, head, and dorsal skin smooth; a thick supratympanic fold from posterior corner of eye, arching downwards posteriorly to tympanum, and reaching dorsal region of arm insertion; a thick, longitudinally elongated buccal fold posteriorly to mouth commissure; eight dermal longitudinal folds, four on each side of body: fold F2 from posterior interocular region to urostyle region; fold F4 dorso-laterally from posterior corner of eye to groin; fold F1 (formed by small tubercles) poorly developed and not discernible in preservative; fold F5 slightly shorter than fold F6, interrupted and extending from above shoulder region to groin; fold F6 interrupted, from posterior corner of eye to groin; ventral skin, dorsal and ventral surfaces of arms smooth; very few keratinized small spicules from wrist to throat region. A patch of keratinized spicules on each side of ventro-lateral region of body, from below arms to groin; a granular seat patch under thighs; cloacal region without expanded fringes; dorsal surface of thighs and tibiae with many small pointed tubercles or spicules; on dorsal tibia surface these spicules align forming a longitudinal row. Vocal sac poorly developed, subgular, and single-lobed; no lateral vocal folds. Vocal slits present; vomerine teeth in two transverse series, almost contacting medially, laying between and just posterior to choanae. Tongue large, free, slightly notched behind. Hand (Fig. 24C) with slender fingers, not webbed, and with rounded and not expanded tips; weak lateral fringes without keratinized spicules along their edges; finger lengths III < V < II < IV; subarticular tubercles rounded, and proximal tubercles more developed than distal ones; few rounded supernumerary tubercles present but not very developed; outer metacarpal tubercle large and cordiform; inner metacarpal tubercle small and rounded; a large and slightly rectangular keratinized black spine on thumb, lateral to proximal subarticular tubercle of finger I; a large and triangular keratinized spine on strongly

developed prepollex. Legs robust; tibia and foot long, representing about 55% and 60% of SVL, respectively. Foot (Fig. 24D) with slender toes and only basally webbed; lateral fringes without keratinized spicules along their edges; toe lengths I < II < V < III < IV; toe tips rounded; subarticular tubercles large and rounded; sole of foot with several distinct keratinized spicules; outer metatarsal tubercle very small, rounded and poorly developed; inner metatarsal tubercle large, elliptical, slightly elevated; sole of tarsus with several evenly distributed keratinized spicules; inner tarsal fold developed, approximately the length of tarsus without keratinized spicules along edge.

Coloration of holotype.— In life, dorsal surface of body (dorsum and flanks) and limbs overall light brown with greenish shades (Fig. 25A); on body, poorly marked brown circular blotches sparsely scattered along dorsum and upperside thighs, and arranged transversally on tibia posterior surface. Arms mostly lacking brown blotches; posterior surface of thighs with blue shades and well-marked black macular patches on the background. Dermal longitudinal folds (F1 to F5) brown, and F6 whitish. Dark brown stripe between nostrils and anterior corner of eye. Loreal region homogeneously light brown, forming a stripe that runs above lip, over the buccal fold posteriorly to mouth commissure, reaching arm insertion; lower lip with few white spots. Thin dark brown stripe running over the supratympanic fold. Tympanic membrane homogeneously dark gray. Throat homogeneously pigmented in dark gray; Ventral surface of arms, legs, and belly beige. Ventral surface of hand, foot, and tarsus overall dark gray.

Measurements of holotype (in mm).—SVL 87.2, HW 35.2, HL 31.9, ESD 16.0, END 9.2, EED 22.2, ED 8.3, TD 6.8, HAL 23.2, FAL 41.6, TL 48.3, FTL 52.1.

Variation.—We observed that the distribution of ocellated blotches along the dorsal region vary from a smooth to a sparsely scattered pattern (Fig. 25). The ocellated blotches are mostly restricted to the dorsal and dorsolateral regions, while body lateral region mostly lack

this feature. The supra-labial light stripe that extends from below eyes to the forelimb insertion (passing under the tympanum) can be well-marked or barely distinct (Fig. 25). A supratympanic dark stripe extending from below eye to the forelimb insertion (posteriorly behind tympanum) can be well-marked (Fig. 25B) or poorly marked (Fig. 25A). Similarly, the supratympanic dark stripe may form a triangular-shaped mark posterior to the tympanum, which can be light to dark brown (Fig. 25B) or indistinct/absent (Fig. 25A). In life, some specimens may exhibit green shades along body dorsum (Fig. 25A), instead of the overall reddish-brown body coloration (Fig. 25B). All other variations in morphological features are mentioned in the "Morphology" section of Results.

Advertisement call.—Description is based on calls of four males (n = 37 calls; Table 6), and the only vouchered recording represents the holotype. See Appendix III for locality and recording information. Descriptive statistics (mean and standard deviation) are given in Table 6. Calls are given at irregular intervals. The call is made up of single, nonpulsed notes with rise time at 59–82% of their length (Fig. 12D). Although defined as nonpulsed, this species has weak/irregular amplitude modulations along the note, in contrast to the smooth envelope of nominal *L latrans*. Note length ranges from 129–241 ms. Frequency range is mostly distributed across the first three harmonics, being that the second harmonic often has more energy at the very onset, when the fundamental frequency can still be barely detected, but almost all sound energy is contained in the fundamental harmonic throughout notes' duration. The dominant frequency is always associated with the fundamental harmonic, ranging from 323–366 Hz. Notes have subtle frequency modulation, either (mostly) positive or negative, ranging from -141–47 Hz.

Comparisons with other species (characteristics from other species are given within parenthesis).—*Leptodactylus* CS3 lineage differs from *L. silvanimbus*, all species in the *L. bolivianus* complex (*L. bolivianus*, *L. guianensis* and *L. insularum*) and *L. viridis* by

exhibiting well-developed and complete dorsal longitudinal folds F1–2 that extends from behind eye to the pelvic region (absent in *L. silvanimbus*, *L. bolivianus*, *L. guianensis* and *L. insularum*, Heyer and de Sá 2011; and poorly developed in *L. viridis*, Jim and Spirandeli-Cruz 1979). The single-lobed vocal sac differs males of *L.* CS3 lineage from *L. macrosternum* males (bilobed vocal sac; Gallardo 1964). The presence of two thumb spines on hand differs males of *L.* CS3 lineage from those of *L. bolivianus*, *L. guianensis* and *L. viridis* (one thumb spine on hand; Jim and Spirandeli-Cruz 1979; Heyer and de Sá 2011). *Leptodactylus* CS3 lineage lacks the auxiliary dorsal fold (or if present is short and restricted to body's anterior third) distinguishing it from *L. macrosternum* (long auxiliary fold extending from behind eye to midbody). The presence of a single longitudinal row of spicules on the posterior surface of tibia differs *L.* CS3 lineage from *L. viridis* (three longitudinal rows of spicules; Jim and Spirandeli-Cruz 1979). By its larger body size ($\bar{X}$ = 96.0 mm SVL), *L.* CS3 lineage differs from *L. macrosternum* ($\bar{X}$ = 74.3 mm SVL), *L. silvanimbus* ($\bar{X}$ = 47.8 mm SVL; de Sá et al. 2014), and *L. viridis* ($\bar{X}$ = 63.4 mm SVL). By its proportionally longer tibia and foot ($\bar{X}$ = 52% and 55% of SVL, respectively), *L.* CS3 lineage differs from *L. viridis* ($\bar{X}$ = 46% and 51% of SVL, respectively). Additionally, *L.* CS3 lineage differs from *L. viridis* by the overall brownish body coloration in life (body coloration predominantly green; Jim and Spirandeli-Cruz 1979; de Sá et al. 2014). In life, coloration of groin is generally not distinct to that of body lateral region in *L.* CS3 lineage (groin is distinctly green in *L.* CS1 lineage and *L. macrosternum*, or yellowish in *L. luctator*). In life, thigh posterior surface coloration varies from blue to gray shades in *L.* CS3 lineage (generally green in *L.* CS1 lineage and *L. macrosternum*, or yellowish in *L. luctator*).

Leptodactylus CS3 lineage is further distinguished from congeners in the LLSG based on acoustic traits. From the closest related species (i.e., *L. latrans* complex clade), *L.* CS3 lineage differs from *L.* CS1 lineage (pulsed notes) and *L. latrans* (nonpulsed notes with

smooth envelope) in having nonpulsed notes with weak/irregular amplitude modulations. From *L. luctator* (43–281 Hz), *L.* CS3 lineage differs in having negative frequency modulation (-141–47 Hz). By having a single-note call, *L.* CS3 lineage differs from *L. macrosternum* which has three distinct note types in its acoustic repertoire (referred as *L. chaquensis* in Heyer and Giaretta 2009, Camurugi et al. 2017). The three species of the *Leptodactylus bolivianus* complex (*L. bolivianus*, *L. guianensis*, and *L. insularum*) have well-marked frequency upsweep in their calls, in contrast to the negative frequency modulation in *L.* CS3 lineage (Table 6). Also, calls in the *L. bolivianus* complex always have higher dominant frequencies than does the call of *L.* CS3 lineage (Heyer and de Sá 2011; Table 6). *Leptodactylus silvanimbus* has a broad-band call without frequency sweeps (Heyer et al. 1996a; Fig. 13E), differing in both features from the call of *L.* CS3 lineage, which is relatively more well-tuned and usually with a negative frequency modulation. *Leptodactylus viridis* has a very short-length call (16–31 ms; Rocha et al. 2016; Fig. 13F) in comparison with that of *L.* CS3 lineage (129–241 ms).

Leptodactylus CS3 lineage exhibited from 32 to 112 base pair (from 507bp) differences in the COI mitochondrial gene (or approximately 8% to 27% of genetic distance) in comparison to all other species in the LLSG. This clade is supported as a distinct evolutionary entity with significant support in all phylogenetic (PP = 1.0/BS = 100) and delimitation (bGMYC; ABGD) analyses we performed.

Geographic distribution.—This species is endemic to a narrow zone within the southeastern coastal Atlantic Forest region from Santos municipality (SP) to northeastern RS through low altitudinal areas (but reaching up 500 m a.s.l.) located east of the Serra do Mar mountain range (Figs. 2, 26).

Remarks.—Silva et al. (2000) reported on a particular C-banding pattern in chromosomes for specimens of *L. latrans* complex from Guaratuba, PR (now *L.* CS3

lineage), indicating that they do not belong to the same species as that of individuals from the plateau areas (now *L. luctator*).

DISCUSSION

General Patterns of Genetic and Morphological Diversity

During the past two decades, the use of DNA sequence data has revealed an impressive number of morphologically cryptic anuran taxa that are potentially new species to science (e.g., Fouquet et al. 2007; Vieites et al. 2009; Funk et al. 2012), especially those distributed in the tropical regions. Despite of such discoveries, advances in taxonomy do not follow the pace at which researchers have uncovered cryptic diversity (Fiser et al. 2018). For instance, because most complexes of morphologically cryptic species revealed by molecular data lack discrete diagnostic morphological characters, formal descriptions are predominantly absent in such research papers (e.g., Gehara et al. 2013; Fouquet et al. 2014), even in cases that there is evidence of strong geographic structure and deep genetic divergences (e.g., Lanna et al. 2018; Oliveira et al. 2018; Sabbag 2018). Accordingly, the *Leptodactylus latrans* species complex, which includes conspicuous large-sized frogs, exhibits a strong pattern of geographic structure and high interspecific genetic distances compared to the average distances found for several currently recognized South American Neotropical amphibian species (Fouquet et al. 2007; Lyra et al. 2017). Nevertheless, their highly conserved morphology coupled with chromatic polymorphism (most of which are shared among all species) hampers discriminating species based solely on external morphology, as observed for species in the *L. bolivianus* complex (Heyer and de Sá 2011). On the other hand, advertisement calls have been increasingly employed as one of the most reliable diagnostic features for species discrimination in some anuran groups, specifically in *Leptodactylus* (e.g., Heyer et al. 1996b; Heyer and Juncá 2003; Carvalho et al. 2013). We found that most species

in the LLSG can be diagnosed based on acoustic features, except for *L. latrans* vs. *L. luctator/L.* CS3 lineage, for which differences are subtle and restricted to amplitude modulation patterns. Additionally, previous studies showed that species in the LLSG (mostly lacking discrete diagnostic morphological characters) can be distinguished by chromosomal arrangement (Silva et al. 2000) and biochemical, physiological and serological features of their skins (e.g., Cei and Bertini 1961; Cei and Cohen 1965; Maxson and Heyer 1988). Interestingly, species in the LLSG are strictly associated with aquatic environments during reproductive periods (e.g., males call with body partially submerged on water during breeding activity; Prado et al. 2000; Heyer and Giareta 2009; Camurugi et al. 2017). This indicates that aquatic biochemical communication may play an important role for species-specific recognition in this species group, thereby relaxing selection pressure towards distinct morphotypes (as proposed by Maxson and Heyer 1988). Although evidence supporting the existence of aquatic sex pheromones and chemical signaling among leptodactylid species is scarce (King et al. 2005), it is known that this could be an alternative channel for intraspecific communication in anurans (Belanger and Corkum 2009).

Recent studies have shown, mainly based on molecular data, that the geographic range of anuran species is generally narrower than previously reported in traditional taxonomic studies (Gehara et al. 2013) or show deep genetic divergences with strong geographic structure (Fouquet et al. 2014; Oliveira et al. 2018), as shown for species in the *Leptodactylus latrans* complex clade. For instance, *Dendropsophus minutus*, *L. fuscus* and *Physalaemus cuvieri*, three anuran species with broad geographic distribution in South America, have deep genetic structure across their distribution (Camargo et al. 2006; Gehara et al. 2014; Miranda et al. 2019). In opposite to our prediction, we found no evidence for strong regional genetic structure in *L. macrosternum* as intraspecific genetic divergence did not exceed 4% in the mitochondrial COI gene (as previously reported; Lyra et al. 2017). This

is the first reported case of a South American anuran species lacking strong regional structure or deep genetic divergences across a broad geographic range. It is very likely that the generalist habit, high tolerance to distinct environmental conditions and unique physiological adaptations explain why *L. macrosternum* populations are continuously distributed without noticeable genetic divergence throughout highly variable environmental gradients in South America.

Acoustics of the *Leptodactylus latrans* Species Group

Sound recordings for members in the LLSG are one of the rarest across the genus. This is because species may be explosive breeders (e.g., populations of *L. macrosternum*) or simply because vocal activity is scarcely observed in nature. In addition, these calls are often emitted at relatively lower amplitudes while many other frog species with louder sounds are also in calling activity at higher densities, such that obtaining good-quality recordings is a real challenge in the field. Members of the LLSG call from within the water, usually in dense vegetation, and are extremely wary: they perceive movements at the water surface and often stop calling and dive when approached (Heyer and Giareta 2009; Camurugi et al. 2017). On one hand, calls are low in pitch to the point low-pass filters could be applied to recordings; on the other, background noise at low frequencies caused by wind or rain usually has severe impacts on recordings. Hence, studies describing in detail vocal repertoires of species in the LLSG are still scanty in comparison with the volume of acoustic data already available for the other three *Leptodactylus* clades.

Nevertheless, a few call descriptions for species in the *Leptodactylus latrans* complex have been published, which we comment next (calls of other species in the LLSG were described elsewhere; see Fouquette 1960; Heyer et al. 1996a; Heyer and de Sá 2011; Tárano 2010; Rocha et al. 2016). To our knowledge, Barrio (1966), Straughan and Heyer (1976),

Straneck et al. (1993), and Nunes and Juncá (2006) are the only contributions (at least a brief quantitative description and/or sound figure provided) to the acoustics of the *L. latrans* complex, referred as *L. ocellatus* in those studies. Barrio (1966) presented only frequency call traits, which essentially agree with calls in the *L. latrans* complex. Straneck et al. (1993) provided spectrograms without associated quantitative data, which can also be associated with the *L. latrans* complex based on the low frequency range and frequency upsweep. According to the region (Santa Fe/Entre Ríos, Argentina), it is only possible to associate both above mentioned descriptions to *L. luctator*. Straughan and Heyer (1976) described calls from eastern Brazilian Amazonia (Belém, PA), far beyond the geographic range of the *L. latrans* complex (Fig. 2). These authors did not provide sonograms for the Amazonian calls, but we are aware that only *L. macrosternum* and species in the *L. bolivianus* complex are distributed in the Amazon Forest. However, based on dominant frequency (0.6–1.0 kHz), call duration (0.27 s on average), envelope (partially pulsed), and downward frequency modulation, it is clear that those calls are not from species of the *L. latrans* complex. Nunes and Juncá (2006) described multi-pulsed calls from BA, in northeastern Brazil. Based on the unique temporal envelope, we are certain that their description corresponds to the call of *L.* CS1 lineage. Moreover, we have genetic vouchers assigned to this species from the same locality where those authors recorded the calls (Serra de São João, municipality of Feira de Santana, BA).

The *Leptodactylus latrans* Species Group

The number of the *Leptodactylus latrans* species now encompasses 10 species, considering that we synonymized *L. chaquensis* with *L. macrosternum* and revalidated *L. luctator*. Still, the *L. viridis* population from MG showed a strong genetic structure in comparison with the nominal species from BA and was inferred as a putative new species in

our delimitation analyses, indicating that there might be additional unnamed lineages in the LLSG. However, the low sampling hampered us to precisely establish the taxonomic status of the MG population, which should be evaluated in a future study. Nevertheless, this is the less speciose clade among the four *Leptodactylus* groups proposed by Heyer (1969) and supported as monophyletic by de Sá et al. (2014). Historically, the LLSG is one of the less studied, mainly because the former *L. ocellatus* did not have an associated name-bearing type nor an exact type locality (Lavilla et al. 2010). For instance, publications regarding taxonomy and species limits in this group are scanty or restricted to punctual species descriptions (e.g., Jim and Spirandeli-Cruz 1937; McCranie et al. 1980), except for those of Cei (1950, 1962) and Gallardo (1964) using morphological and physiological data. We elucidated species limits and hidden diversity in the widespread LLSG by means of integrating distinct lines of evidence with comprehensive geographic/taxa sampling. Yet, high levels of cryptic morphology can be still more common than expected in *Leptodactylus* (e.g., Heyer 1978, 1994, 2005) and should be evaluated in the other three species groups of the genus.

Acknowledgments.—This work would never be possible without the help and collaboration of several individuals. We thank H. Batalha-Filho, P.I. Simões, H.F.P. Araújo and D. Baêta for suggestions and comments on the manuscript. FMM thanks the staff of Herpetology Laboratory and Zoology Museums from LGE (UNaM), UFBA, UFMS, UFPB, UNB, and UNESP-Rio Claro for their kind assistance and for all logistic support. We thank M. Jansen (Biodiversity and Climate Research Centre Laboratory), P.C.A. Garcia from UFMG, C. Ribas, F. Werneck and A.P. Lima from INPA institute for allowing the loan of genetic samples under their care. FMM and TRC are indebted to B.F.V. Teixeira, E.F. Oliveira, E.M. Fonseca, D.L. Bang, F.M. Lanna, F.S. de Andrade, L.B. Martins, R.M. Hoffmann, V.A. São-Pedro, and W. Pessoa for their support during field work. D. Barrasso for collecting the

specimen designated as *Leptodactylus luctator* Neotype. T. Grant and the Museu de Zoologia, Universidade de São Paulo for sharing and authorizing the use of *Leptodactylus macrosternum* holotype images. C. Marinho, F. Camurugi, L.A. Silva, M. Struett, R.O Abreu, and R. Marques for making available pictures of living specimens and/or tissue samples. We kindly thank L.R. Mariotto, A. Kwet, W.R. Heyer, Z. Tárano, P.C. Rocha, A. Wynn, J. Pointdexter (USNM recordings; Smithsonian institution), L.F. Toledo and S. Dena (FNJV recordings; Fonoteca Neotropical Jacques Vielliard) for granting us access to sound recordings. FMM thanks Conselho Nacional de Desenvolvimento Científico e Tecnológico (CNPq; #140649/2015-8) for his doctoral fellowship and Instituto Chico Mendes de Conservação da Biodiversidade (ICMBio, #53175-1) for scientific collection permits. TRC was funded through São Paulo Research Foundation with a doctoral fellowship (FAPESP, #2012/15763-7) and is currently supported by the same funding agency with a postdoctoral fellowship (#2017/08489-0). AAGiaretta thanks the financial support by CNPq and FAPEMIG. CFBH thanks FAPESP (#2013/50741-7), FAPESP/Fundação Grupo Boticário de Proteção à Natureza (#2014/50342-8), and CNPq (#306623/2018-8) for financial support. DJS thanks CNPq for his research fellowship (#311492/2017-7). FB thanks Programa Nacional de Incentivo a Investigadores from the Consejo Nacional de Ciencia y Tecnología (PRONII, CONACYT, Paraguay). GRC thanks Coordenação de Apoio à Formação de Pessoal de Nível Superior (CAPES), CNPq, Fundação de Apoio à Pesquisa do Distrito Federal (FAPDF), and USAID's PEER program under cooperative agreement AID-OAA-A-11-00012 for financial support. MFN thanks the Fundação de Amparo à Pesquisa do Estado da Bahia (FAPESB) for financial support (TO PAM 0005/2014), through the Rede Baiana de Pesquisa sobre Anfíbios (RBPA), and CNPq for productivity grants (#305849/2015-8 and #310490/2018-9). MLL thanks FAPESP for postdoctoral fellowship (#2017/26162-8). This research was supported by resources supplied by the High-Performance Computing Center

(NPAD) at Universidade Federal do Rio Grande do Norte-Brazil and Cyberinfrastructure for Phylogenetic Research (CIPRES).

LITERATURE CITED

Barley, A.J., J. White, A.C. Diesmos and R.M. Brown. 2013. The challenge of species delimitation at the extremes: diversification without morphological change in Philippine sun skinks. Evolution 67:3556–3572. DOI: 10.1111/evo.12219

Barrio, A. 1966. Divergencia acustica entre el canto nupcial de *Leptodactylus ocellatus* (Linne) y *L. chaquensis* Cei (Anura, Leptodactylidae). Physis 26:275–277.

Barrio-Amorós, C.L. 2004. Amphibians of Venezuela: systematic list, distribution and references; an update. Revista de Ecología Latino Americana 9:1–48.

Belanger, R.M. and L.D. Corkum. 2009. Review of aquatic sex pheromones and chemical communication in anurans. Journal of Herpetology 43:184–191. DOI: 10.1670/08-054R1.1

Bertoluci, J., R.A. Brassaloti, J.W.R. Júnior, V.M.F.N. Vilela and H.O. Sawakuchi. 2007. Species composition and similarities among anuran assemblages of forest sites in southeastern Brazil. Scientia Agricola 64:364–374. DOI: 10.1590/S0103-90162007000400007

Bokermann, W.C.A. 1966. Lista anotada das localidades tipo de anfíbios brasileiros. São Paulo, Serviço de Documentação, RUSP:1–183.

Boulenger, G.A. 1882. Catalogue of the Batrachia Salientia s. Ecaudata in the Collection of the British Museum. Second Edition. Taylor and Francis, London. DOI: 10.5962/bhl.title.54882

Breiman, L. 2001. Random forests. Machine learning 45:5–32. DOI: 10.1023/A:1010933404324

Bruford, M.W., O. Hanotte, J.F.Y. Brookfield and T. Burke. 1992. Single and multilocus DNA fingerprinting. Pp. 225–269 in Molecular Genetic Analysis of Populations: A Practical Approach (A.R. Hoelzel, ed.). I. R. L. Press, Oxford.

Burnaby, T.P. 1966. Growth-invariant discriminant functions and generalized distances. Biometrics 22:96–110. DOI: 10.2307/2528217

Camargo, A., R.O. de Sá and W.R. Heyer. 2006. Phylogenetic analyses of mtDNA sequences reveal three cryptic lineages in the widespread Neotropical frog *Leptodactylus fuscus* (Schneider, 1799) (Anura, Leptodactylidae). Biological Journal of the Linnean Society 87:325–341. DOI: 10.1111/j.1095-8312.2006.00581.x

Camurugi, F., F.M. Magalhães, M.H.C. Queiroz, T.C.S.O. Pereira, L. Tavares-Bastos, E.S. Lopes-Marinho, J.M.M. Neves and A.A. Garda. 2017. Reproduction, sexual dimorphism, and diet of *Leptodactylus chaquensis* (Anura, Leptodactylidae) in northeastern Brazil. Herpetological Conservation and Biology 12:498–508.

Carvalho, T.R., F.S.F. Leite and T.L. Pezzuti. 2013. A new species of *Leptodactylus* Fitzinger (Anura, Leptodactylidae, Leptodactylinae) from montane rock fields of the Chapada Diamantina, northeastern Brazil. Zootaxa 3701:349–364. DOI: 10.11646/zootaxa.3701.3.5

Cei, J.M. 1948. El ritmo estacional en los fenómenos cíclicos endocrino sexuales de la rana criolloa (*Leptodactylus ocellatus*) del norte Argentino. Acta Zoologica Lilloana 6:283–331.

Cei, J.M. 1949. La regulacion hormonal del ciclo sexual en *Leptodactylus ocellatus* (L.) de la Argentina. Acta Zoologica Lillloana 7:113–134.

Cei, J.M. 1950. *Leptodactylus chaquensis* n. sp. y el valor sistematico real de la especie Linneana *Leptodactylus ocellatus* en la Argentina. Acta Zoologica Lilloana 9:395–423.

Cei, J.M. 1962. Mapa preliminar de la distribución continental de las “sibling species” del grupo *ocellatus* (género *Leptodactylus*). Revista de la Sociedad Argentina de Biologia 38:258–265.

Cei, J.M. 1970. Relaciones serologicas entre los *Leptodactylus* del grupo *ocellatus-chaquensis* de la cuenca chaco-paranense y la forma *macrosternum*. Acta Zoologica Lilloana 27:299–306.

Cei, J.M. 1980. Amphibians of Argentina. Monitore Zoologico Italiano N. S. Monografia 2:1–609.

Cei, J.M. and F. Bertini. 1961. Serum proteins in allopatric and sympatric populations of *Leptodactylus ocellatus* and *L. chaquensis*. Copeia 1961:336–340. DOI: 10.2307/1439810

Cei, J.M. and R. Cohen. 1965. Serological relationships in the *Leptodactylus pachypus* species group (Amphibia, Salientia). Copeia 1965:155–158. DOI: 10.2307/1440717

Cei, J.M., V. Erspamer and M. Roseghini. 1967. Taxonomic and evolutionary significance of biogenic amines and polypeptides occurring in amphibian skin. I. Neotropical leptodactylid frogs. Systematic Zoology 16:328–342. DOI: 10.2307/2412152

Cochran, D.M. 1961. Type specimens of reptiles and amphibians in the U.S. National Museum. Bulletin of the United States National Museum 220:1–291. DOI: 10.5962/bhl.part.26967

Cole, C.J., C.R. Townsend, R.P. Reynolds, R.D. MacCulloch and A. Lathrop. 2013. Amphibians and reptiles of Guyana, South America: illustrated keys, annotated species accounts, and a biogeographic synopsis. Proceedings of the Biological Society of Washington 125:317–578. DOI: 10.2988/0006-324x-125.4.317

De la Riva, I., J. Köhler, S. Lötters and S. Reichle. 2000. Ten years of research on Bolivian amphibians: updated checklist, distribution, taxonomic problems, literature and iconography. Revista Española de Herpetología 14:19–164.

De la Riva, I. and M. Maldonado. 1999. First record of *Leptodactylus ocellatus* (Linnaeus, 1758) (Amphibia, Anura, Leptodactylidae) in Bolivia and comments on related species. Graellsia 55:193–197. DOI: 10.3989/graellsia.1999.v55.i0.328

de Queiroz, K. 2007. Species concepts and species delimitation. Systematic Biology 56:879–886. DOI: 10.1080/10635150701701083

de Sá, R.O., T. Grant, A. Camargo, W.R. Heyer, M.L. Ponssa and E. Stanley. 2014. Systematics of the Neotropical genus *Leptodactylus* Fitzinger, 1826 (Anura: Leptodactylidae): phylogeny, the relevance of non-molecular evidence, and species accounts. South American Journal of Herpetology 9:S1–S128. DOI: 10.2994/sajh-d-13-00022.1

Dixon, J.R. and M.A. Staton. 1976. Some aspects of the biology of *Leptodactylus macrosternum* Miranda-Ribeiro (Anura: Leptodactylidae) of the Venezuelan Llanos. Journal of Herpetology 32:227–232. DOI: 10.2307/3891743

Felsenstein, J. and H. Kishino. 1993. Is there something wrong with the bootstrap on phylogenies? A reply to Hillis and Bull. Systematic Biology 42:193–200. DOI: 10.1093/sysbio/42.2.193

Fiser, C., C.T. Robinson and F. Malard. 2018. Cryptic species as a window into the paradigm shift of the species concept. Molecular Ecology 27:613–635. DOI: 10.1111/mec.14486

Fouquet, A., C. Cassini, C.F.B. Haddad, N. Pech and M.T. Rodrigues. 2014. Species delimitation, patterns of diversification and historical biogeography of a Neotropical frog genus *Adenomera* (Anura, Leptodactylidae). Journal of Biogeography 41:855–870. DOI: 10.1111/jbi.12250

Fouquet, A., A. Gilles, M. Vences, C. Marty, M. Blanc and N. Gemmell. 2007. Underestimation of species richness in Neotropical frogs revealed by mtDNA analyses. PLoS ONE 2:e1109. DOI: 10.1371/journal.pone.0001109

Fouquet, A., B.P. Noonan, M.T. Rodrigues, N. Pech, A. Gilles and N.J. Gemmell. 2012. Multiple Quaternary refugia in the eastern Guiana Shield revealed by comparative phylogeography of 12 frog species. Systematic Biology 61:461–489. DOI: 10.1093/sysbio/syr130

Fouquette, M.J., Jr. 1960. Call structure in frogs of the family Leptodactylidae. The Texas Journal of Science 12:201–215.

Frost, D.R. 2019. Amphibian species of the world: an online reference. Version 6.0 (25 March 2019). American Museum of Natural History, USA. Accessible at: http://research.amnh.org/herpetology/amphibia/index.html.

Funk, W.C., M. Caminer and S.R. Ron. 2012. High levels of cryptic species diversity uncovered in Amazonian frogs. Proceedings of the Royal Society B: Biological Sciences 279:1806–1814. DOI: 10.1098/rspb.2011.1653

Gallardo, J.M. 1964. Consideraciones sobre *Leptodactylus ocellatus* (L.) (Amphibia, Anura) y species aliadas. Physis 24:373–384.

Gehara, M., A.J. Crawford, V.G. Orrico, A. Rodriguez, S. Lotters, A. Fouquet, L.S. Barrientos, F. Brusquetti, I. De la Riva, R. Ernst, G.G. Urrutia, F. Glaw, J.M. Guayasamin, M. Holting, M. Jansen, P.J. Kok, A. Kwet, R. Lingnau, M. Lyra, J. Moravec, J.P. Pombal, Jr., F.J. Rojas-Runjaic, A. Schulze, J.C. Senaris, M. Sole, M.T. Rodrigues, E. Twomey, C.F. Haddad, M. Vences and J. Kohler. 2014. High levels of diversity uncovered in a widespread nominal taxon: continental phylogeography of the Neotropical tree frog *Dendropsophus minutus*. PLoS One 9:e103958. DOI: 10.1371/journal.pone.0103958

Gehara, M.C., C. Canedo, C.F.B. Haddad and M. Vences. 2013. From widespread to microendemic: molecular and acoustic analyses show that *Ischnocnema guentheri* (Amphibia: Brachycephalidae) is endemic to Rio de Janeiro, Brazil. Conservation Genetics 2013:1–10.

Girard, C. 1853. Descriptions of new species of reptiles, collected by the U.S. Exploring Expedition, under the command of Capt. Charles Wilkes, U.S.N. Second part—including the species of batrachians, exotic to North America. Proceedings of the Academy of Natural Sciences of Philadelphia 6:420–424. DOI: 10.5962/bhl.part.9360

Girard, C. 1858. United States Exploring Expedition During the Years 1838, 1839, 1840, 1841, 1842, Under the Command of Charles Wilkes, U.S.N. Vol. 20 (Herpetology). C. Sherman, USA. https://biodiversitylibrary.org/page/40418548

Glaw, F. and M. Franzen. 2006. Type catalogue of amphibians in the Zoologische Staatsammlung München. Spixiana 29:153–192. http://www.biodiversitylibrary.org/page/28195131

Gorzula, S. and J.C. Señaris. 1998. Contribution to the herpetofauna of the Venezuelan Guayana I. A data base. Scientia Guaianae 8:1–268.

Gridi-Papp, M. 2007. SoundRuler: acoustic analysis for research and teaching. Available at: http://soundruler.sourceforge.net.

Hebert, P.D.N., A. Cywinska, S.L. Ball and J.R. deWaard. 2003. Biological identifications through DNA barcodes. Proceedings of the Royal Society B 270:313–321. DOI: 10.1098/rspb.2002.2218

Heyer, W.R. 1969. The adaptive ecology of the species groups of the frog genus *Leptodactylus* (Amphibia, Leptodactylidae). Evolution 23:421–428. DOI: 10.2307/2406697

Heyer, W.R. 1978. Systematics of the *fuscus* group of the frog genus *Leptodactylus* (Amphibia, Leptodactylidae). Science Bulletin. Natural History Museum of Los Angeles County 29:1–85.

Heyer, W.R. 1994. Variation within the *Leptodactylus podicipinus-wagneri* complex of frogs (Amphibia: Leptodactylidae). Smithsonian Contributions to Zoology 546:1–124. DOI: 10.5479/si.00810282.546.i

Heyer, W.R. 2005. Variation and taxonomic clarification of the large species of the *Leptodactylus pentadactylus* species group (Amphibia, Leptodactylidae) from Middle America, Northern South America, and Amazonia. Museu de Zoologia da Universidade de São Paulo 37:269–348.

Heyer, W.R. 2014. Morphological analyses of frogs of the *Leptodactylus latrans* complex (Amphibia, Leptodactylidae) from selected localities in South America. Proceedings of the Biological Society of Washington 126:369–378. DOI: 10.2988/0006-324X-126.4.369

Heyer, W.R. and R.O. de Sá. 2011. Variation, systematics, and relationships of the *Leptodactylus bolivianus* complex (Amphibia: Anura: Leptodactylidae). Smithsonian Contributions to Zoology 635:1–58. DOI: 10.5479/si.00810282.635.1

Heyer, W.R., R.O. de Sá, J.R. McCranie and L.D. Wilson. 1996a. *Leptodactylus silvanimbus* (Amphibia: Anura: Leptodactylidae): natural history notes, advertisement call, and relationships. Herpetological Natural History 4:169–174.

Heyer, W.R., J.M. García-Lopez and A.J. Cardoso. 1996b. Advertisement call variation in the *Leptodactylus mystaceus* complex (Amphibia: Leptodactylidae) with a description of a new sibling species. Amphibia-Reptilia 17:7–31. DOI: 10.1163/156853896X00252

Heyer, W.R. and A.A. Giaretta. 2009. Advertisement calls, notes on natural history, and distribution of *Leptodactylus chaquensis* (Amphibia: Anura: Leptodactylidae) in Brasil. Proceedings of the Biological Society of Washington 122:292–305. DOI: 10.2988/08-42.1

Heyer, W.R. and F.A. Juncá. 2003. *Leptodactylus caatingae*, a new species of frog from eastern Brazil (Amphibia: Anura: Leptodactylidae). Proceedings of the Biological Society of Washington 116:317–239.

Hillis, D.M. and J.J. Bull. 1993. An empirical test of bootstrapping as a method for assessing confidence in phylogenetic analysis. Systematic Biology 42:182–192. DOI: 10.1093/sysbio/42.2.182

Hoogmoed, M.S. and U. Gruber. 1983. Spix and Wagler type specimens of reptiles and amphibians in the Natural History Musea in Munich (Germany) and Leiden (the Netherlands). Spixiana 9:319–415.

Hudson, W.H. 1892. The naturalist in La Plata. Chapman and Hall, Ltd. DOI: 10.5962/bhl.title.13554

ICZN – International Commission on Zoological Nomenclature, 1999. International Code of Zoological Nomenclature. 4th Edition. International Trust for Zoological Nomenclature.

Jim, J. and E.F. Spirandeli-Cruz. 1979. Uma nova espécie de *Leptodactylus* do estado da Bahia, Brasil (Amphibia, Anura). Revista Brasileira de Biologia 39:707–710.

Jolicoeur, P. 1963. The multivariate generalization of the allometry equation. Biometrics 19:497–499. DOI: 10.2307/2527939

Juncá, F.A. 2005. Anfíbios e Répteis. Pp. 337–356 in Biodiversidade e Conservação da Chapada Diamantina (F.A. Juncá, L. Funch and W. Rocha, eds.). Ministério do Meio Ambiente (MMA), Brasil.

Katoh, K., K. Misawa, K. Kuma and T. Miyata. 2002. MAFFT: a novel method for rapid multiple sequence alignment based on fast Fourier transform. Nucleic Acids Research 30:3059–3066. DOI: 10.1093/nar/gkf436

Kearse, M., R. Moir, A. Wilson, S. Stones-Havas, M. Cheung, S. Sturrock, S. Buxton, A. Cooper, S. Markowitz, C. Duran, T. Thierer, B. Ashton, P. Meintjes and A. Drummond. 2012. Geneious basic: an integrated and extendable desktop software platform for the organization and analysis of sequence data. Bioinformatics 28:1647–1649. DOI: 10.1093/bioinformatics/bts199

King, J.D., L.A. Rollins-Smith, P.F. Nielsen, A. John and J.M. Conlon. 2005. Characterization of a peptide from skin secretions of male specimens of the frog *Leptodactylus fallax* that stimulates aggression in male frogs. Peptides 26:597–601. DOI: 10.1016/j.peptides.2004.11.004

Lanfear, R., P.B. Frandsen, A.M. Wright, T. Senfeld and B. Calcott. 2016. PartitionFinder 2: New methods for selecting partitioned models of evolution for molecular and morphological phylogenetic analyses. Molecular Biology and Evolution 34:772–773. DOI: 10.1093/molbev/msw260

Langone, J.A. 1995. Ranas y sapos del Uruguay (reconocimiento y aspectos biológicos). Museo Dámaso Antonio Larrañaga. Intendencia Municipal de Montevideo. Serie Divulgación 5:1–127.

Lanna, F.M., F.P. Werneck, M. Gehara, E.M. Fonseca, G.R. Colli, J.W. Sites Jr., M.T. Rodrigues and A.A. Garda. 2018. The evolutionary history of *Lygodactylus* lizards in the South American open diagonal. Molecular Phylogenetics and Evolution 127:638–645. DOI: 10.1016/j.ympev.2018.06.010

Lavilla, E.O., J.A. Langone, U. Caramaschi, W.R. Heyer and R.O. de Sá. 2010. The identification of *Rana ocellata* Linnaeus, 1758. Nomenclatural impact on the species

currently known as *Leptodactylus ocellatus* (Leptodactylidae) and *Osteopilus brunneus* (Gosse, 1851) (Hylidae). Zootaxa 2346:1–16. DOI: 10.5281/zenodo.275558

Leite, F.S.F., F.A. Juncá and P.C. Eterovick. 2008. Status do conhecimento, endemismo e conservação de anfíbios anuros da Cadeia do Espinhaço, Brasil. Megadiversidade 4:158–176.

Liaw, A. and M. Wiener. 2002. Classification and regression by randomForest. R News 2:18–22.

Ligges, U., S. Krey, O. Mersmann and S. Schnackenberg. 2018. tuneR: analysis of music and speech. Available at: https://CRAN.R-project.org/package=tuneR.

Littlejohn, M.J. 2001. Patterns of differentiation in temporal properties of acoustic signals of anurans. Pp. 102–120 in Anuran Acoustic Communication (M.J. Ryan, ed.). Smithsonian Institution Press, USA.

Lutz, A. 1930. Segunda memoria sobre espécies brasileiras do gênero *Leptodactylus*, incluindo outras alliadas. Memorias Do Instituto Oswaldo Cruz 23:1–20. DOI: 10.1590/S0074-02761930000100001

Lyra, M.L., C.F.B. Haddad and A.M.L. Azeredo-Espin. 2017. Meeting the challenge of DNA barcoding Neotropical amphibians: polymerase chain reaction optimization and new COI primers. Molecular Ecology Resources 17:966–980. DOI: 10.1111/1755-0998.12648

Machado, I.F., R.G. Becker and A.S. Mesquita. 2014. Geographic distribution: *Leptodactylus chaquensis*. Herpetological Review 45:277.

Magalhães, F.M., D.O. Laranjeiras, T.B. Costa, F.A. Juncá, D.O. Mesquita, D.L. Rohr, W.P. Silva, G.H.C. Vieira and A.A. Garda. 2015. Herpetofauna of protected areas in the Caatinga IV: Chapada Diamantina National Park, Bahia, Brazil. Herpetology Notes 8:243–261.

Maniatis, T., E.F. Fritsch and J. Sambrook. 1982. Molecular cloning: a laboratory manual. Cold Spring Harbour Laboratory, USA.

Matlab. 2004. The language of technical computing, version 6.5.2. The MathWorks Inc, USA.

Maxson, L.R. and W.R. Heyer. 1988. Molecular systematics of the frog genus *Leptodactylus* (Amphibia: Leptodactylidae). Fieldiana: Zoology 41:1–13. DOI: 10.5962/bhl.title.3187

Mayer, A.F.J.C. (1835) Analecten für vergleichende Anatomie. Eduard Weber, Bonn, 93 pp. + 71 pl.

McCranie, J.R., L.D. Wilson and L. Porras. 1980. A new species of *Leptodactylus* from the cloud forests of Honduras. Journal of Herpetology 14:361–367. DOI: 10.2307/1563691

Meyer, C. 2003. Molecular systematics of cowries (Gastropoda: Cypraeidae) and diversification patterns in the tropics. Biological Journal of Linnean Society 79:401–459. DOI: 10.1046/j.1095-8312.2003.00197.x

Miranda, N.E.O., N.M. Maciel, M.S. Lima-Ribeiro, G.R. Colli, C.F.B. Haddad and R.G. Collevatti. 2019. Diversification of the widespread Neotropical frog *Physalaemus cuvieri* in response to Neogene-Quaternary geological events and climate dynamics. Molecular Phylogenetics and Evolution 132:67–80. DOI: 10.1016/j.ympev.2018.11.003

Miranda-Ribeiro, A. 1926. Notas para servirem ao estudo dos Gymnobatrachios (Anura) brasileiros. Arquivos do Museu Nacional 27:1–227.

Miranda-Ribeiro, A. 1927. Os Leptodactylidae do Museu Paulista. Revista do Museu Paulista 15:113–134.

Murphy, J.C. 1997. Amphibians and reptiles of Trinidad and Tobago. Krieger Publishing Company.

Narvaes, P., J. Bertoluci and M.T. Rodrigues. 2009. Composição, uso de hábitat e estações reprodutivas das espécies de anuros da floresta de restinga da Estação Ecológica Juréia-Itatins, sudeste do Brasil. Biota Neotropica 9:117–123. DOI: 10.1590/S1676-06032009000200011

Nunes, I. and F.A. Juncá. 2006. Advertisement calls of three leptodactylid frogs in the state of Bahia, northeastern Brazil (Amphibia, Anura, Leptodactylidae), with considerations on their taxonomic status. Arquivos do Museu Nacional 64:151–157.

Oda, F.H., D.L. Santos, P.G. Gambale, V.A. Campos, V.G. Batista, I.P. Affonso and C. Strüssmann. 2014. New Brazilian records of *Leptodactylus chaquensis* Cei, 1950, at the species' southern range limit. Herpetozoa 26:195–200.

Oliveira, E.F., M. Gehara, V.A. São-Pedro, G.C. Costa, F.T. Burbrink, G.R. Colli, M.T. Rodrigues and A.A. Garda. 2018. Phylogeography of Muller's termite frog suggests the vicariant role of the Central Brazilian Plateau. Journal of Biogeography 45:2508–2519. DOI: 10.1111/jbi.13427

Palumbi, S.R., A. Martin, S. Romano, W.O. McMillan, L. Stice and G. Grabowski. 1991. The Simple Fool's Guide to PCR, Version 2.0. Department of Zoology, Kewalo Marine Laboratory, University of Hawaii.

Pedrosa, I.M.M.C., T.B. Costa, R.G. Faria, F.G.R. França, D.O. Laranjeiras, T.C.S.P. Oliveira, C.N.S. Palmeira, S. Torquato, T. Mott, G.H.C. Vieira and A.A. Garda. 2014. Herpetofauna of protected areas in the Caatinga III: the Catimbau National Park, Pernambuco, Brazil. Biota Neotropica 14:1–12. DOI: 10.1590/1676-06032014004614

Peters, W.C.H. 1872. Über die von Spix in Brasilien gesammelten Batrachier des Königl. Naturalienkabinet zu München. Monatsberichte der Königlichen Preussische Akademie des Wissenschaften zu Berlin 1872:196–227.

Philippi, R.A. (1902) Suplemento a los batraquios chilenos descritos en la historia física y politica de Chile de Don Claudio Gay. E.Blanchard–Chessi, Santiago, xi + 161 pp.

Pons, J., T.G. Barraclough, J. Gomez-Zurita, A. Cardoso, D.P. Duran, S. Hazell, S. Kamoun, W.D. Sumlin and A.P. Vogler. 2006. Sequence-based species delimitation for the DNA taxonomy of undescribed insects. Systematic Biology 55:595–609. DOI: 10.1080/10635150600852011

Posso-Terranova, A. and J. Andrés. 2018. Multivariate species boundaries and conservation of harlequin poison frogs. Molecular Ecology 27:3432–3451. DOI: 10.1111/mec.14803

Prado, C.P.A., M. Uetanabaro and F.S. Lopes. 2000. Reproductive strategies of *Leptodactylus chaquensis* and *L. podicipinus* in the Pantanal, Brazil. Journal of Herpetology 34:135–139.

Puillandre, N., A. Lambert, S. Brouillet and G. Achaz. 2011. ABGD, Automatic barcode gap discovery for primary species delimitation. Molecular Ecology 21:1864–1877. DOI: 10.1111/j.1365-294X.2011.05239.x

R Core Team. 2018. R: A language and environment for statistical computing. Vienna, R Foundation for Statistical Computing, Austria. Available at: http://www.R-project.org.

Raddi, G. 1823. Continuazione della descrizione dei rettili Brasiliani. Memorie della Societa Italiana delle Scienze 19:58–73.

Rambaut, A. 2014. FigTree: a graphical viewer of phylogenetic trees, version 1.4.2. Available at: http://tree.bio.ed.ac.uk/software/figtree/.

Rambaut, A., A.J. Drummond, D. Xie, G. Baele and M.A. Suchard. 2018. Posterior summarisation in Bayesian phylogenetics using Tracer 1.7. Systematic Biology 67:901–904. DOI: 10.1093/sysbio/syy032

Reid, N. and B. Carstens. 2012. Phylogenetic estimation error can decrease the accuracy of species delimitation: a Bayesian implementation of the general mixed Yule-coalescent model. BMC Evolutionary Biology 12:196. DOI: 10.1186/1471-2148-12-196

Rocha, P.C., T.L. Pezzuti and P.C.A. Garcia. 2016. Advertisement call of *Leptodactylus viridis* (Anura: Leptodactylidae) from Minas Gerais, Brazil. Salamandra 52:342–344.

Rohlf, F.J. and F.L. Bookstein. 1987. A comment on shearing as a method for "size correction". Systematic Zoology 36:356–367. DOI: 10.2307/2413400

Sabaj, M.H. 2016. Standard symbolic codes for institutional resource collections in herpetology and ichthyology: An online reference, version 6.5 (16 August 2016). American Society of Ichthyologists and Herpetologists, USA. Accessible at: http://www.asih.org/.

Sabbag, A.F., L.M. Lyra, K.R. Zamudio, C.F.B. Haddad, R.N. Feio, F.S.F. Leite, J.L. Gasparini and C.A. Brasileiro. 2018. Molecular phylogeny of Neotropical rock frogs reveals a long history of vicariant diversification in the Atlantic forest. Molecular Phylogenetics and Evolution 2018:142–156. DOI: 10.1016/j.ympev.2018.01.017

Santos, T.G. and S.Z. Cechin. 2008. Amphibia, Anura, Leptodactylidae, *Leptodactylus chaquensis*: Distribution extension in the state of Rio Grande do Sul, Brazil. Check List 4:142–144. DOI: 10.15560/4.2.142

Serié, P. 1935. Observaciones de Hudson sobre algunos saurios y batrachios. Physis 11: 493–494.

Silva, A.P., C.F.B. Haddad and S. Kasahara. 2000. Chromosomal studies on five species of the genus *Leptodactylus* Fitzinger, 1826 (Amphibia, Anura) using differential staining. Cytobios 103:25–38.

Somers, K.M. 1986. Multivariate allometry and removal of size with principal component analysis. Systematic Zoology 35:359–368. DOI: 10.1093/sysbio/35.3.359

Spix, J.B. 1824. Animalia nova sive Species novae Testudinum et Ranarum quas in itinere per Brasiliam annis MDCCCXVII–MDCCCXX jussu et auspiciis Maximiliani Josephi I. Bavariae Regis. Typis Franc. Seraph. Hübschmanni, Monachii. DOI: 10.5962/bhl.title.3665

Stamatakis, A. 2014. RAxML version 8: a tool for phylogenetic analysis and post-analysis of large phylogenies. Bioinformatics 30:1312–1313. DOI: 10.1093/bioinformatics/btu033

Stekhoven, D.J. 2011. Using the missForest Package. R package:1–11

Straneck, R., E.V. Olmedo and G.R. Carrizo. 1993. Catálogo de voces de anfíbios argentinos. Tomo I, Ediciones LOLA, Argentina.

Straughan, I.R. and W.R. Heyer. 1976. A functional analysis of the mating calls of the Neotropical frog genera of the *Leptodactylus* complex (Amphibia, Leptodactylidae). Papéis Avulsos de Zoologia 29:221–245.

Suchard, M.A., P. Lemey, G. Baele, A.D. L., A.J. Drummond and A. Rambaut. 2018. Bayesian phylogenetic and phylodynamic data integration using BEAST 1.10. Virus Evolution 4:vey016. DOI: 10.1093/ve/vey016

Sueur, J., T. Aubin and C. Simonis. 2008. Seewave: a free modular tool for sound analysis and synthesis. Bioacoustics 18:213–226. DOI: 10.1080/09524622.2008.9753600

Tamura, K. and M. Nei. 1993. Estimation of the number of nucleotide substitutions in the control region of mitochondrial DNA in humans and chimpanzees. Molecular Biology and Evolution 10:512–526. DOI: 10.1093/oxfordjournals.molbev.a040023

Tamura, K., G. Stecher, D. Peterson, A. Filipski and S. Kumar. 2013. MEGA6: Molecular Evolutionary Genetics Analysis version 6.0. Molecular Biology and Evolution 30:2725–2729. DOI: 10.1093/molbev/mst197

Tárano, Z. 2010. Advertisement calls and calling habitats of frogs from a flooded savanna of Venezuela. South American Journal of Herpetology 5:221–240. DOI: 10.2994/057.005.0308

Teixeira, V.H.S., F.M. Quintela and D. Loebmann. 2017. *Leptodactylus chaquensis* Cei, 1950 (Leptodactylidae, Leptodactylinae): extension of the distribution in state of Rio Grande do Sul, southern Brazil. Brazilian Journal of Biology 77:893–894. DOI: 10.1590/1519-6984.04316

Tschudi, J.J. 1838. Classification der Batrachier mit Berücksichtigung der fossilen Thiere dieser Abtheilung der Reptilien. Neuchâtel: Petitpierre.

Vanzolini, P.E. 1968. Geography of the South American Gekkonidae (Sauria). Arquivos de Zoologia 17:85–112. DOI: 10.11606/issn.2176-7793.v17i2p85-112

Vanzolini, P.E. 1981. Introduction: the scientific and political contexts of the Bavarian expedition to Brazil. Pp. 9–29 in Herpetology of Brazil by Johan Baptist von Spix and Johann Georg Wagler (K.A. Adler, ed.). Society for the Study of Amphibians and Reptiles, USA.

Vanzolini, P.E. and C.W. Myers. 2015. The herpetological collection of Maximilian, Prince of Wied (1782–1867), with special reference to Brazilian materials. Bulletin of the American Museum of Natural History 395:1–155. DOI: 10.5531/sd.sp.9

Vieites, D.R., M.-S. Min and D.B. Wake. 2007. Rapid diversification and dispersal during periods of global warming by plethodontid salamanders. Proceedings of the National Academy of Sciences of the USA 104:19903–19907. DOI: 10.1073/pnas.0705056104

Vieites, D.R., K.C. Wollenberg, F. Andreone, J. Kohler, F. Glaw and M. Vences. 2009. Vast underestimation of Madagascar's biodiversity evidenced by an integrative amphibian inventory. Proceedings of the National Academy of Sciences USA 106:8267–8272. DOI: 10.1073/pnas.0810821106

Wachlevski, M. and C.F.D. Rocha. 2010. Amphibia, Anura, restinga of Baixada do Maciambu, municipality of Palhoça, state of Santa Catarina, southern Brazil. Check List 6:602–604.

Werle, E., C. Schneider, M. Renner, M. Völker and W. Fiehn. 1994. Convenient single-step, one tube purification of PCR products for direct sequencing. Nucleic Acids Research 22:4354–4355.

Werneck, F.P. 2011. The diversification of eastern South American open vegetation biomes: historical biogeography and perspectives. Quarterly Science Reviews 30:1630–1648. DOI: 10.1016/j.quascirev.2011.03.0

Wied-Neuwied, M.A.P. 1824. Verzeichniss der Amphibien, welche im zweiten Bande der Naturgeschichte Brasiliens vom Prinz Max. Von Neuwied beschrieben werden. Isis von Oken 14:661–673.

Wied-Neuwied, M.A.P. 1825. Beitrage zur Naturgeschichte von Brasilien. Vol. 1. Verzeichniss de Amphibien. Gr. H.S. priv. Landes–Industrie–Comptoir, Germany.

Zina, J., C.P.A. Prado, C.A. Brasileiro and C.F.B. Haddad. 2012. Anurans of the sandy coastal plains of the Lagamar Paulista, state of São Paulo, Brazil. Biota Neotropica 12:251–260. DOI: 10.1590/S1676-06032012000100020

APPENDIX I

Molecular Samples and Localities. *Individuals included in the phylogenetic analyses are highlighted in bold.

#SEQ	Sample ID*	Associated voucher	Species	GenBank ID	COI	16S	TYR	POMC	Municipality	State/Province	Country
1	**45mc**	NA	*macrosternum*	as *L. ocellatus*	NA	EU201124	NA	NA	Guatemala	Cayenne	Frech Guiana
2	AAGARDA00651	NA	*luctator*	Correct	**seq**	NA	NA	NA	Santo Antônio da Patrulha	Rio Grande do Sul	Brazil
3	**AAGARDA00660**	NA	*luctator*	Correct	**seq**	**seq**	**seq**	**seq**	Lagoa Santa	Minas Gerais	Brazil
4	AAGARDA02000	NA	*macrosternum*	Correct	**seq**	NA	NA	NA	Tailândia	Pará	Brazil
5	AAGARDA02635	NA	*macrosternum*	Correct	**seq**	NA	NA	NA	Canguaretama	Rio Grande do Norte	Brazil
6	AAGARDA02723	NA	*macrosternum*	Correct	**seq**	NA	NA	NA	Crato	Ceará	Brazil
7	AAGARDA02724	NA	*macrosternum*	Correct	**seq**	NA	NA	NA	Crato	Ceará	Brazil
8	AAGARDA02726	NA	*macrosternum*	Correct	**seq**	NA	NA	NA	Crato	Ceará	Brazil
9	AAGARDA02727	NA	*macrosternum*	Correct	**seq**	NA	NA	NA	Crato	Ceará	Brazil
10	AAGARDA03106	NA	*macrosternum*	Correct	**seq**	NA	NA	NA	Goianinha	Rio Grande do Norte	Brazil
11	AAGARDA03110	NA	*macrosternum*	Correct	**seq**	NA	NA	NA	Goianinha	Rio Grande do Norte	Brazil
12	AAGARDA03111	NA	*macrosternum*	Correct	**seq**	NA	NA	NA	Goianinha	Rio Grande do Norte	Brazil
13	AAGARDA03126	NA	*macrosternum*	Correct	**seq**	NA	NA	NA	Canguaretama	Rio Grande do Norte	Brazil
14	**AAGARDA03281**	CHUFPB28110	*latrans*	Correct	**seq**	**seq**	**seq**	**seq**	Cataguases	Minas Gerais	Brazil
15	AAGARDA03282	CHUFPB28111	*latrans*	Correct	**seq**	NA	NA	NA	Cataguases	Minas Gerais	Brazil
16	AAGARDA03283	CHUFPB28112	*latrans*	Correct	**seq**	NA	NA	NA	Cataguases	Minas Gerais	Brazil
17	**AAGARDA03356**	CHUFPB28113	*luctator*	Correct	**seq**	**seq**	**seq**	**seq**	Bom Jardim da Serra	Santa Catarina	Brazil
18	AAGARDA03599	CHUFPB28114	*macrosternum*	Correct	**seq**	NA	NA	NA	Puxinanã	Paraiba	Brazil
19	AAGARDA03632	NA	*macrosternum*	Correct	**seq**	NA	NA	NA	Camacan	Bahia	Brazil
20	AAGARDA03634	CHUFPB28116	*latrans*	Correct	**seq**	NA	NA	NA	Camacan	Bahia	Brazil
21	**AAGARDA03688**	CHUFPB28117	*latrans*	Correct	**seq**	**seq**	**seq**	**seq**	Vicosa	Minas Gerais	Brazil
22	AAGARDA03834	CHUFPB28121	*macrosternum*	Correct	**seq**	NA	NA	NA	Areia	Paraiba	Brazil
23	AAGARDA03956	CHUFPB28130	*macrosternum*	Correct	**seq**	NA	NA	NA	Areia	Paraiba	Brazil
24	AAGARDA04008	CHUFPB28131	*macrosternum*	Correct	**seq**	NA	NA	NA	Areia	Paraiba	Brazil
25	AAGARDA04009	CHUFPB28132	*macrosternum*	Correct	**seq**	NA	NA	NA	Areia	Paraiba	Brazil
26	AAGARDA04040	NA	*macrosternum*	Correct	**seq**	NA	NA	NA	Puxinanã	Paraiba	Brazil
27	AAGARDA04267	NA	*macrosternum*	Correct	**seq**	NA	NA	NA	Paulo Afonso	Bahia	Brazil
28	AAGARDA04287	CHUFPB28137	*macrosternum*	Correct	**seq**	NA	NA	NA	Paulo Afonso	Bahia	Brazil

29	AAGARDA04506	CHUFPB28138	*macrosternum*	Correct	**seq**	NA	NA	NA	Paulo Afonso	Bahia	Brazil
30	AAGARDA05767	NA	*macrosternum*	Correct	**seq**	NA	NA	NA	Macaíba	Rio Grande do Norte	Brazil
31	AAGARDA06006	NA	*macrosternum*	Correct	**seq**	NA	NA	NA	Nísia Floresta	Rio Grande do Norte	Brazil
32	AAGARDA06098	NA	*macrosternum*	Correct	**seq**	NA	NA	NA	Parnamirim	Rio Grande do Norte	Brazil
33	AAGARDA06125	NA	*macrosternum*	Correct	**seq**	NA	NA	NA	Nísia Floresta	Rio Grande do Norte	Brazil
34	AAGARDA06126	NA	*macrosternum*	Correct	**seq**	NA	NA	NA	Nísia Floresta	Rio Grande do Norte	Brazil
35	AAGARDA06204	NA	*macrosternum*	Correct	**seq**	NA	NA	NA	Nísia Floresta	Rio Grande do Norte	Brazil
36	AAGARDA06243	NA	*macrosternum*	Correct	**seq**	NA	NA	NA	Nísia Floresta	Rio Grande do Norte	Brazil
37	AAGARDA06466	CHUFPB28140	*macrosternum*	Correct	**seq**	NA	NA	NA	João Câmara	Rio Grande do Norte	Brazil
38	AAGARDA06768	NA	*macrosternum*	Correct	**seq**	NA	NA	NA	Palmeiras	Bahia	Brazil
39	AAGARDA06769	NA	*macrosternum*	Correct	**seq**	NA	NA	NA	Palmeiras	Bahia	Brazil
40	AAGARDA06770	NA	*macrosternum*	Correct	**seq**	NA	NA	NA	Palmeiras	Bahia	Brazil
41	AAGARDA06782	CHUFPB28141	*macrosternum*	Correct	**seq**	NA	NA	NA	Palmeiras	Bahia	Brazil
42	AAGARDA06783	CHUFPB28142	*macrosternum*	Correct	**seq**	NA	NA	NA	Palmeiras	Bahia	Brazil
43	AAGARDA06784	CHUFPB28143	CS1	Correct	**seq**	NA	NA	NA	Palmeiras	Bahia	Brazil
44	AAGARDA06785	CHUFPB28144	*macrosternum*	Correct	**seq**	NA	NA	NA	Palmeiras	Bahia	Brazil
45	**AAGARDA07017**	CHUFPB28145	CS1	Correct	**seq**	**seq**	**seq**	**seq**	Palmeiras	Bahia	Brazil
46	**AAGARDA07244**	CHUFPB28146	*luctator*	Correct	**seq**	**seq**	**seq**	**seq**	Guiné	Bahia	Brazil
47	**AAGARDA07245**	NA	CS1	Correct	**seq**	**seq**	**seq**	**seq**	Guiné	Bahia	Brazil
48	AAGARDA08165	NA	CS1	Correct	**seq**	NA	NA	NA	Buíque	Pernambuco	Brazil
49	**AAGARDA08166**	NA	CS1	Correct	**seq**	**seq**	**seq**	**seq**	Buíque	Pernambuco	Brazil
50	AAGARDA08188	NA	CS1	Correct	**seq**	NA	NA	NA	Buíque	Pernambuco	Brazil
51	AAGARDA09008	NA	*macrosternum*	Correct	**seq**	NA	NA	NA	Taquaritinga do Norte	Pernambuco	Brazil
52	AAGARDA09035	NA	*macrosternum*	Correct	**seq**	NA	NA	NA	São Miguel dos Campos	Alagoas	Brazil
53	AAGARDA09060	NA	*macrosternum*	Correct	**seq**	NA	NA	NA	São José da Tapera	Alagoas	Brazil
54	**AAGARDA09084**	NA	CS1	Correct	**seq**	**seq**	**seq**	**seq**	Macajuba	Bahia	Brazil
55	**AAGARDA09098**	NA	CS1	Correct	**seq**	**seq**	**seq**	**seq**	Jaguaquara	Bahia	Brazil
56	**AAGARDA09102**	NA	*latrans*	Correct	**seq**	**seq**	**seq**	**seq**	Igrapiúna	Bahia	Brazil
57	AAGARDA09104	NA	*latrans*	Correct	**seq**	NA	NA	NA	Igrapiúna	Bahia	Brazil
58	AAGARDA09292	NA	*macrosternum*	Correct	**seq**	NA	NA	NA	Umarizal	Rio Grande do Norte	Brazil
59	AAGARDA09648	NA	*latrans*	Correct	**seq**	NA	NA	NA	Elísio Medrado	Bahia	Brazil
60	AAGARDA09722	CHUFPB28147	*latrans*	Correct	**seq**	NA	NA	NA	Varzedo	Bahia	Brazil

61	AAGARDA09723	CHUFPB28148	*latrans*	Correct	**seq**	NA	NA	NA	Varzedo	Bahia	Brazil
62	**AAGARDA10077**	MZFS4438	*luctator*	Correct	**seq**	**seq**	**seq**	**seq**	Piatã	Bahia	Brazil
63	AAGARDA10078	MZFS4439	*luctator*	Correct	**seq**	NA	NA	NA	Piatã	Bahia	Brazil
64	AAGARDA10079	MZFS4440	*luctator*	Correct	**seq**	NA	NA	NA	Piatã	Bahia	Brazil
65	AAGARDA10080	UFBA0000	*luctator*	Correct	**seq**	NA	NA	NA	Piatã	Bahia	Brazil
66	AAGARDA10081	UFBA0000	*luctator*	Correct	**seq**	NA	NA	NA	Piatã	Bahia	Brazil
67	AAGARDA10085	CHUFPB28149	*luctator*	Correct	**seq**	NA	NA	NA	Piatã	Bahia	Brazil
68	AAGARDA10086	CHUFPB28150	*luctator*	Correct	**seq**	NA	NA	NA	Piatã	Bahia	Brazil
69	AAGARDA10087	CHUFPB28151	*luctator*	Correct	**seq**	NA	NA	NA	Piatã	Bahia	Brazil
70	AAGARDA10372	NA	*macrosternum*	Correct	**seq**	NA	NA	NA	Jaguaribe	Ceará	Brazil
71	AAGARDA10373	NA	*macrosternum*	Correct	**seq**	NA	NA	NA	Jaguaribe	Ceará	Brazil
72	AAGARDA10374	NA	*macrosternum*	Correct	**seq**	NA	NA	NA	Jaguaribe	Ceará	Brazil
73	AAGARDA10403	NA	*macrosternum*	Correct	**seq**	NA	NA	NA	Jaguaribe	Ceará	Brazil
74	AAGARDA10438	CHUFPB28152	*macrosternum*	Correct	**seq**	NA	NA	NA	Angicos	Rio Grande do Norte	Brazil
75	AAGARDA10439	NA	*macrosternum*	Correct	**seq**	NA	NA	NA	Angicos	Rio Grande do Norte	Brazil
76	AAGARDA10449	NA	*macrosternum*	Correct	**seq**	NA	NA	NA	Condeúba	Bahia	Brazil
77	AAGARDA10450	NA	*macrosternum*	Correct	**seq**	NA	NA	NA	Condeúba	Bahia	Brazil
78	AAGARDA10787	NA	*macrosternum*	Correct	**seq**	NA	NA	NA	Ubajara	Ceará	Brazil
79	AAGARDA10788	NA	*macrosternum*	Correct	**seq**	NA	NA	NA	Ubajara	Ceará	Brazil
80	AAGARDA10792	NA	*macrosternum*	Correct	**seq**	NA	NA	NA	Ubajara	Ceará	Brazil
81	AAGARDA10794	NA	*macrosternum*	Correct	**seq**	NA	NA	NA	Ubajara	Ceará	Brazil
82	AAGARDA10795	NA	*macrosternum*	Correct	**seq**	NA	NA	NA	Ubajara	Ceará	Brazil
83	AAGARDA11288	CHUFPB28156	*macrosternum*	Correct	**seq**	NA	NA	NA	PARNA Serra das Confusões	Piaui	Brazil
84	AAGARDA11570	CHUFPB28157	*macrosternum*	Correct	**seq**	NA	NA	NA	Caracol	Piaui	Brazil
85	AAGARDA11571	CHUFPB28158	*macrosternum*	Correct	**seq**	NA	NA	NA	Caracol	Piaui	Brazil
86	AAGARDA11579	CHUFPB28165	*macrosternum*	Correct	**seq**	NA	NA	NA	Caracol	Piaui	Brazil
87	AAGARDA11580	CHUFPB28166	*macrosternum*	Correct	**seq**	NA	NA	NA	Caracol	Piaui	Brazil
88	AAGARDA11661	NA	*macrosternum*	Correct	**seq**	NA	NA	NA	Quixadá	Ceará	Brazil
89	AAGARDA11662	CHUFPB28167	*macrosternum*	Correct	**seq**	NA	NA	NA	Quixadá	Ceará	Brazil
90	AAGARDA11683	NA	*macrosternum*	Correct	**seq**	NA	NA	NA	Quixadá	Ceará	Brazil
91	AAGARDA12086	CHUFPB28183	*macrosternum*	Correct	**seq**	NA	NA	NA	Camacan	Bahia	Brazil
92	**AAGARDA12103**	CFBH42662	*luctator*	Correct	**seq**	**seq**	**seq**	**seq**	Lindoia	São Paulo	Brazil
93	AAGARDA12104	CFBH42663	*luctator*	Correct	**seq**	NA	NA	NA	Lindoia	São Paulo	Brazil
94	AAGARDA12142	CFBH42697	*latrans*	Correct	**seq**	NA	NA	NA	Ponte Nova	Minas Gerais	Brazil
95	AAGARDA12144	CFBH42699	*latrans*	Correct	**seq**	NA	NA	NA	Ponte Nova	Minas Gerais	Brazil
96	AAGARDA12145	CFBH42700	*latrans*	Correct	**seq**	NA	NA	NA	Ponte Nova	Minas Gerais	Brazil
97	AAGARDA12148	CFBH42703	*latrans*	Correct	**seq**	NA	NA	NA	Ponte Nova	Minas Gerais	Brazil
98	AAGARDA12181	CFBH42733	*latrans*	Correct	**seq**	NA	NA	NA	Ponte Nova	Minas Gerais	Brazil
99	AAGARDA12186	CFBH42737	*latrans*	Correct	**seq**	NA	NA	NA	Juiz de For a	Minas Gerais	Brazil
100	AAGARDA12187	CFBH42738	*latrans*	Correct	**seq**	NA	NA	NA	Juiz de For a	Minas Gerais	Brazil

101	**AAGARDA12212**	CFBH42763	*latrans*	Correct	**seq**	**seq**	**seq**	**seq**	Teresopolis	Rio de Janeiro	Brazil
102	AAGARDA12214	CFBH42765	*latrans*	Correct	**seq**	NA	NA	NA	Teresópolis	Rio de Janeiro	Brazil
103	AAGARDA12215	CFBH42766	*latrans*	Correct	**seq**	NA	NA	NA	Teresópolis	Rio de Janeiro	Brazil
104	AAGARDA12221	CFBH42772	*latrans*	Correct	**seq**	NA	NA	NA	Teresópolis	Rio de Janeiro	Brazil
105	AAGARDA12223	CFBH42774	*latrans*	Correct	**seq**	NA	NA	NA	Itatiaia	Rio de Janeiro	Brazil
106	AAGARDA12225	CFBH42776	*latrans*	Correct	**seq**	NA	NA	NA	Itatiaia	Rio de Janeiro	Brazil
107	**AAGARDA12226**	CFBH42777	*latrans*	Correct	**seq**	**seq**	**seq**	NA	Itatiaia	Rio de Janeiro	Brazil
108	**AAGARDA12233**	CFBH42813	*luctator*	Correct	**seq**	**seq**	**seq**	NA	Buri	São Paulo	Brazil
109	**AAGARDA12254**	CFBH42804	CS3	Correct	**seq**	**seq**	**seq**	**seq**	Peruibe	São Paulo	Brazil
110	AAGARDA12257	CFBH42807	CS3	Correct	**seq**	NA	NA	NA	Peruibe	São Paulo	Brazil
111	AAGARDA12263	CFBH42814	*luctator*	Correct	**seq**	NA	NA	NA	Buri	São Paulo	Brazil
112	AAGARDA12267	CHUFPB28184	CS1	Correct	**seq**	NA	NA	NA	Jacobina	Bahia	Brazil
113	AAGARDA12278	CHUFPB28185	*macrosternum*	Correct	**seq**	NA	NA	NA	Jacobina	Bahia	Brazil
114	AAGARDA12279	CHUFPB28186	CS1	Correct	**seq**	NA	NA	NA	Jacobina	Bahia	Brazil
115	**AAGARDA12302**	CHUFPB28187	CS1	Correct	**seq**	**seq**	**seq**	**seq**	Jacobina	Bahia	Brazil
116	AAGARDA12303	CHUFPB28188	CS1	Correct	**seq**	NA	NA	NA	Jacobina	Bahia	Brazil
117	AAGARDA12304	CHUFPB28189	CS1	Correct	**seq**	NA	NA	NA	Jacobina	Bahia	Brazil
118	**AAGARDA12310**	CHUFPB28192	CS1	Correct	**seq**	**seq**	NA	NA	Jacobina	Bahia	Brazil
119	AAGARDA12311	CHUFPB28193	CS1	Correct	**seq**	NA	NA	NA	Jacobina	Bahia	Brazil
120	AAGARDA12481	NA	*macrosternum*	Correct	**seq**	NA	NA	NA	RVS Tapacurá, São Lourenço da Mata	Pernambuco	Brazil
121	AAGARDACX84PE10	NA	*macrosternum*	Correct	**seq**	NA	NA	NA	Umarizal	Rio Grande do Norte	Brazil
122	AAGUFU1680	NA	*luctator*	Correct	**seq**	NA	NA	NA	Piatã	Bahia	Brazil
123	**AAGUFU2679**	NA	*macrosternum*	Correct	NA	KC477255	NA	NA	Vale do Paranã	Tocantins	Brazil
124	AAGUFU3573	NA	*macrosternum*	Correct	**seq**	NA	NA	NA	Macaíba	Rio Grande do Norte	Brazil
125	AAGUFU5272	NA	*macrosternum*	Correct	**seq**	NA	NA	NA	Costa Marques	Rondônia	Brazil
126	AAGUFU5273	NA	*macrosternum*	Correct	**seq**	NA	NA	NA	Costa Marques	Rondônia	Brazil
127	**AAGUFU5494**	NA	*guianensis*	Correct	**seq**	**seq**	**seq**	NA	Tepequém	Roraima	Brazil
128	AAGUFU5495	NA	*guianensis*	Correct	**seq**	NA	NA	NA	Tepequém	Roraima	Brazil
129	AAGUFU5558	NA	*macrosternum*	Correct	**seq**	NA	NA	NA	Cantá	Roraima	Brazil
130	AAGUFU6008	NA	*macrosternum*	Correct	**seq**	NA	NA	NA	Macapá	Amapá	Brazil
131	AAGUFU6023	NA	*macrosternum*	Correct	**seq**	NA	NA	NA	Alta Floresta D'oeste	Rondônia	Brazil
132	AAGUFU6024	NA	*macrosternum*	Correct	**seq**	NA	NA	NA	Alta Floresta D'oeste	Rondônia	Brazil
133	AAGUFU6128	NA	*macrosternum*	Correct	**seq**	NA	NA	NA	Ituiutaba	Minas Gerais	Brazil
134	AAGUFU6129	NA	*macrosternum*	Correct	**seq**	NA	NA	NA	Ituiutaba	Minas Gerais	Brazil
135	**AJC3509**	NA	*insularum*	Correct	KP149150	KP149348	NA	NA	San Vincente de Chucuri	Santander	Colombia

136	**AJC3517**	NA	*insularum*	Correct	KP14 9219	KP149424	NA	NA	San Vincente de Chucuri	Santander	Colombia
137	AK12	NA	*macrosternum*	Correct	**seq**	NA	NA	NA	Río San Francisco, Ledesma	Jujuy	Argentina
138	**AMNH145130 (JC7056)**	NA	*guianensis*	as *L. bolivianus*	NA	HQ232838	NA	NA	Dubulay Ranch	Corontyne Region	Guyana
139	**AMNH145131 (JC7057)**	NA	*guianensis*	as *L. bolivianus*	NA	HQ232834	NA	NA	Dubulay Ranch	Corontyne Region	Guyana
140	**AS288**	NA	*macrosternum*	as *L. chaquensis*	**seq**	JF789865	NA	NA	Hacienda and RPPN Caparú	Santa Cruz	Bolivia
141	**AS289**	NA	*macrosternum*	as *L. chaquensis*	**seq**	JF789870	NA	NA	Hacienda and RPPN Caparú	Santa Cruz	Bolivia
142	**AS290**	NA	*macrosternum*	as *L. chaquensis*	NA	JF789872	NA	NA	Hacienda and RPPN Caparú	Santa Cruz	Bolivia
143	**AS291**	NA	*macrosternum*	as *L. chaquensis*	NA	JF789869	NA	NA	Hacienda and RPPN Caparú	Santa Cruz	Bolivia
144	**AS292**	NA	*macrosternum*	as *L. chaquensis*	**seq**	JF789871	NA	NA	Hacienda and RPPN Caparú	Santa Cruz	Bolivia
145	**AS575**	NA	*macrosternum*	as *L. chaquensis*	NA	JF789867	NA	NA	Estancia Büchler	Santa Cruz	Bolivia
146	**AS580**	NA	*macrosternum*	as *L. chaquensis*	**seq**	JF789866	NA	NA	Estancia Büchler	Santa Cruz	Bolivia
147	**BKT273**	NA	*luctator*	Correct	**seq**	**seq**	NA	NA	Montevideo	Montevideo	Argentina
148	**BKT274**	NA	*luctator*	Correct	**seq**	**seq**	NA	NA	Montevideo	Montevideo	Argentina
149	**CAUFJF1350**	NA	*luctator*	Correct	**seq**	**seq**	**seq**	**seq**	Ponte Nova	Minas Gerais	Brazil
150	**CAUFJF1352**	NA	*latrans*	Correct	**seq**	**seq**	**seq**	**seq**	Ponte Nova	Minas Gerais	Brazil
151	CAUFJF1355	NA	*latrans*	Correct	**seq**	NA	NA	NA	Ponte Nova	Minas Gerais	Brazil
152	**CAUFJF1550**	NA	*latrans*	Correct	**seq**	**seq**	**seq**	**seq**	Ubá	Minas Gerais	Brazil
153	CAUFJF1551	NA	*latrans*	Correct	**seq**	NA	NA	NA	Ubá	Minas Gerais	Brazil
154	**CC06**	CFBH40853	*latrans*	Correct	**seq**	**seq**	**seq**	NA	Ilha Bela	São Paulo	Brazil
155	CFBH30078	NA	*macrosternum*	Correct	**seq**	NA	NA	NA	Contendas do Sincora	Bahia	Brazil
156	CFBH30092	NA	*luctator*	Correct	**seq**	NA	NA	NA	Mucugê	Bahia	Brazil
157	CFBH30113	NA	*luctator*	Correct	**seq**	NA	NA	NA	Mucugê	Bahia	Brazil
158	CFBH30152	NA	CS1	Correct	**seq**	NA	NA	NA	Palmeiras	Bahia	Brazil
159	CFBH30159	NA	CS1	Correct	**seq**	NA	NA	NA	Palmeiras	Bahia	Brazil
160	CFBH30247	NA	CS1	Correct	**seq**	NA	NA	NA	Jussiape	Bahia	Brazil
161	**CFBH31115**	NA	CS1	Correct	**seq**	**seq**	**seq**	NA	Araçuai	Minas Gerais	Brazil
162	CFBH31289	NA	*macrosternum*	Correct	**seq**	NA	NA	NA	Casa Nova	Bahia	Brazil
163	CFBH31432	NA	*macrosternum*	Correct	**seq**	NA	NA	NA	São Francisco do Piaui	Piaui	Brazil
164	CFBH31433	NA	*macrosternum*	Correct	**seq**	NA	NA	NA	São Francisco do Piaui	Piaui	Brazil
165	CFBHT00382	NA	*latrans*	Correct	**seq**	NA	NA	NA	Guarapari	Espirito Santo	Brazil

166	CFBHT00494	NA	*luctator*	Correct	**seq**	NA	NA	NA	São Luis do Paraitinga	São Paulo	Brazil
167	**CFBHT00832**	NA	*luctator*	as *L. latrans*	**seq**	KU495335	**seq**	NA	Camanducaia	Minas Gerais	Brazil
168	**CFBHT00969**	NA	*luctator*	Correct	**seq**	**seq**	**seq**	NA	Nova Itapirema	São Paulo	Brazil
169	**CFBHT01030**	CFBH06897	*luctator*	Correct	**seq**	**seq**	**seq**	NA	Ribeirao Branco	São Paulo	Brazil
170	**CFBHT01074**	NA	*macrosternum*	Correct	**seq**	KU495340	NA	NA	Costa Rica	Mato Grosso do Sul	Brazil
171	**CFBHT01146**	CFBH07325	*macrosternum*	Correct	**seq**	KU495341	NA	NA	Passo de Camarajibe	Alagoas	Brazil
172	**CFBHT01166**	NA	*luctator*	Correct	**seq**	**seq**	**seq**	NA	Capinzal	Santa Catarina	Brazil
173	CFBHT01169	NA	*luctator*	Correct	**seq**	NA	NA	NA	Ipuacu	Santa Catarina	Brazil
174	**CFBHT01339**	NA	*macrosternum*	Correct	**seq**	KU495342	NA	NA	Pontalina	Goias	Brazil
175	CFBHT01379	NA	*macrosternum*	Correct	**seq**	NA	NA	NA	Itaja	Goias	Brazil
176	CFBHT01611	CFBH08352	*luctator*	Correct	**seq**	NA	NA	NA	Pilar do Sul	São Paulo	Brazil
177	**CFBHT01723**	CFBH08446	*luctator*	as *L. latrans*	**seq**	KU495332	NA	NA	Tijucas do Sul	Paraná	Brazil
178	**CFBHT01758**	CFBH08481	CS3	Correct	**seq**	**seq**	**seq**	NA	Angelina	Santa Catarina	Brazil
179	**CFBHT01860**	CFBH08597	*luctator*	as *L. latrans*	**seq**	KU495334	**seq**	**seq**	Mafra	Santa Catarina	Brazil
180	CFBHT01926	CFBH08500	CS3	Correct	**seq**	NA	NA	NA	Treviso	Santa Catarina	Brazil
181	**CFBHT02022**	NA	*macrosternum*	Correct	**seq**	KU495344	NA	NA	Aguiarnopolis	Tocantins	Brazil
182	**CFBHT02037**	NA	*luctator*	Correct	**seq**	**seq**	**seq**	NA	Conceicao do Mato Dentro	Minas Gerais	Brazil
183	**CFBHT02050**	NA	*macrosternum*	Correct	**seq**	KU495345	NA	NA	Pirapora	Minas Gerais	Brazil
184	CFBHT02132	CFBH08197	*macrosternum*	Correct	**seq**	NA	NA	NA	Porto Franco	Maranhão	Brazil
185	**CFBHT02139**	CFBH08203	*macrosternum*	Correct	**seq**	KU495343	NA	NA	Porto Franco	Maranhão	Brazil
186	CFBHT02249	NA	CS3	Correct	**seq**	NA	NA	NA	Iguape	São Paulo	Brazil
187	CFBHT02265	CFBH09764	*latrans*	Correct	**seq**	NA	NA	NA	São Sebastião	São Paulo	Brazil
188	**CFBHT02266**	CFBH09765	*latrans*	Correct	**seq**	KU495328	**seq**	**seq**	São Sebastião	São Paulo	Brazil
189	**CFBHT02460**	CFBH10086	*macrosternum*	as *L. chaquensis*	**seq**	KU495311	NA	NA	Teodoro Sampaio	São Paulo	Brazil
190	CFBHT02485	NA	*latrans*	Correct	**seq**	NA	NA	NA	Bertioga	São Paulo	Brazil
191	CFBHT02486	NA	*latrans*	Correct	**seq**	NA	NA	NA	Bertioga	São Paulo	Brazil
192	CFBHT02518	CFBH10546	CS3	Correct	**seq**	NA	NA	NA	Cubatão	São Paulo	Brazil
193	**CFBHT02530**	NA	*luctator*	Correct	**seq**	**seq**	**seq**	NA	Bairro Alto	São Paulo	Brazil
194	**CFBHT02635**	NA	CS3	Correct	**seq**	**seq**	**seq**	NA	Eldorado	São Paulo	Brazil
195	**CFBHT02748**	NA	CS3	Correct	**seq**	**seq**	**seq**	NA	Cananeia	São Paulo	Brazil
196	**CFBHT02990**	NA	CS3	Correct	**seq**	**seq**	**seq**	NA	Botuvera	Santa Catarina	Brazil
197	CFBHT03039	CFBH11015	*luctator*	Correct	**seq**	NA	NA	NA	Bom Jardim da Serra	Santa Catarina	Brazil
198	CFBHT03070	CFBH11046	*luctator*	Correct	**seq**	NA	NA	NA	Piraquara	Paraná	Brazil
199	**CFBHT03087**	CFBH11064	CS3	Correct	**seq**	**seq**	**seq**	**seq**	Antonina	Paraná	Brazil
200	CFBHT03182	NA	*luctator*	Correct	**seq**	NA	NA	NA	Santa Isabel	São Paulo	Brazil
201	**CFBHT03259**	NA	CS3	Correct	**seq**	**seq**	**seq**	NA	Corupa	Santa Catarina	Brazil
202	CFBHT03283	CFBH12391	CS3	Correct	**seq**	NA	NA	NA	Treviso	Santa Catarina	Brazil
203	**CFBHT03296**	CFBH12415	*luctator*	Correct	**seq**	**seq**	**seq**	NA	Sapiranga	Rio Grande do Sul	Brazil
204	**CFBHT03698**	CFBH11320	*latrans*	Correct	**seq**	**seq**	**seq**	NA	Rio de Janeiro	Rio de Janeiro	Brazil

205	CFBHT03706	CFBH11322	*latrans*	Correct	**seq**	NA	NA	NA	Mimoso do Sul	Espirito Santo	Brazil
206	CFBHT04033	CFBH12455	CS3	Correct	**seq**	NA	NA	NA	Iguape	São Paulo	Brazil
207	**CFBHT04051**	NA	*latrans*	Correct	**seq**	**seq**	**seq**	NA	Caraiva	Bahia	Brazil
208	CFBHT04053	CFBH13377	*latrans*	Correct	**seq**	NA	NA	NA	Anchieta	Espirito Santo	Brazil
209	CFBHT04058	NA	*latrans*	Correct	**seq**	NA	NA	NA	Conceicao da Barra	Espirito Santo	Brazil
210	CFBHT04074	NA	*latrans*	Correct	**seq**	NA	NA	NA	Caraiva	Bahia	Brazil
211	CFBHT04086	CFBH13387	CS1	Correct	**seq**	NA	NA	NA	Feira de Santana	Bahia	Brazil
212	CFBHT04090	NA	*macrosternum*	Correct	**seq**	NA	NA	NA	Itabaiana	Sergipe	Brazil
213	CFBHT04091	NA	*macrosternum*	Correct	**seq**	NA	NA	NA	Itabaiana	Sergipe	Brazil
214	CFBHT04257	NA	*macrosternum*	Correct	**seq**	NA	NA	NA	Brejo do Piaui	Piaui	Brazil
215	**CFBHT04399**	CFBH13991	*luctator*	Correct	**seq**	**seq**	**seq**	NA	Pedregulho	São Paulo	Brazil
216	**CFBHT04560**	CFBH14243	*macrosternum*	as *L. chaquensis*	**seq**	KU495312	NA	NA	Bonito	Mato Grosso do Sul	Brazil
217	CFBHT04787	NA	*macrosternum*	Correct	**seq**	NA	NA	NA	Pocone	Mato Grosso	Brazil
218	CFBHT05235	NA	CS3	Correct	**seq**	NA	NA	NA	Ilha Comprida	São Paulo	Brazil
219	**CFBHT05417**	CFBH16121	*macrosternum*	Correct	**seq**	KU495337	NA	NA	Ubajara	Ceará	Brazil
220	**CFBHT06487**	NA	*luctator*	as *L. latrans*	**seq**	KU495329	**seq**	NA	Rio Claro	São Paulo	Brazil
221	CFBHT07639	NA	*luctator*	Correct	**seq**	NA	NA	NA	Assis	São Paulo	Brazil
222	CFBHT07640	NA	*luctator*	Correct	**seq**	NA	NA	NA	Assis	São Paulo	Brazil
223	**CFBHT07680**	NA	*latrans*	Correct	**seq**	**seq**	**seq**	NA	Prado	Bahia	Brazil
224	**CFBHT07725**	CFBH19761	*luctator*	as *L. latrans*	**seq**	KU495333	NA	NA	Bauru	São Paulo	Brazil
225	CFBHT07879	CFBH18294	*macrosternum*	Correct	**seq**	NA	NA	NA	Teodoro Sampaio	São Paulo	Brazil
226	CFBHT08134	CFBH18134	*luctator*	Correct	**seq**	NA	NA	NA	Quatro Barras	Paraná	Brazil
227	CFBHT08426	NA	*macrosternum*	Correct	**seq**	NA	NA	NA	Itamaraca	Pernambuco	Brazil
228	CFBHT08618	NA	CS3	Correct	**seq**	NA	NA	NA	Cananeia	São Paulo	Brazil
229	CFBHT08695	NA	CS3	Correct	**seq**	NA	NA	NA	Iguape	São Paulo	Brazil
230	CFBHT09137	CFBH21088	*macrosternum*	Correct	**seq**	NA	NA	NA	Dom Basilio	Bahia	Brazil
231	CFBHT09153	CFBH21060	*latrans*	Correct	**seq**	NA	NA	NA	Urucuca	Bahia	Brazil
232	CFBHT09155	NA	*macrosternum*	Correct	**seq**	NA	NA	NA	Caetite	Bahia	Brazil
233	CFBHT09167	CFBH21065	CS1	Correct	**seq**	NA	NA	NA	Jequie	Bahia	Brazil
234	**CFBHT09221**	NA	*latrans*	Correct	**seq**	**seq**	**seq**	NA	Linhares	Espirito Santo	Brazil
235	**CFBHT09245**	CFBH18730	*latrans*	Correct	**seq**	**seq**	**seq**	NA	Aurelino Leal	Bahia	Brazil
236	CFBHT09316	CFBH18807	CS1	Correct	**seq**	NA	NA	NA	Maracás	Bahia	Brazil
237	CFBHT09392	NA	CS1	Correct	**seq**	NA	NA	NA	Maracás	Bahia	Brazil
238	CFBHT09399	NA	CS1	Correct	**seq**	NA	NA	NA	Maracás	Bahia	Brazil
239	**CFBHT09416**	NA	*macrosternum*	Correct	**seq**	KU495338	NA	NA	Bonito	Pernambuco	Brazil
240	**CFBHT09428**	NA	*macrosternum*	Correct	**seq**	KU495339	NA	NA	Sanharo	Pernambuco	Brazil
241	CFBHT09560	NA	*luctator*	Correct	**seq**	NA	NA	NA	Cerro Largo	Rio Grande do Sul	Brazil
242	CFBHT09578	NA	*luctator*	Correct	**seq**	NA	NA	NA	São Sepé	Rio Grande do Sul	Brazil
243	CFBHT09612	CFBH18395	*luctator*	Correct	**seq**	NA	NA	NA	Teodoro Sampaio	São Paulo	Brazil
244	CFBHT09673	NA	*luctator*	Correct	**seq**	NA	NA	NA	Mato Castelhano	Rio Grande do Sul	Brazil
245	**CFBHT10455**	CFBH18470	*latrans*	Correct	**seq**	KU495331	**seq**	NA	Marataizes	Espirito Santo	Brazil
246	**CFBHT10542**	NA	*latrans*	Correct	**seq**	KU495336	NA	NA	Niteroi	Rio de Janeiro	Brazil

247	CFBHT10660	NA	CS3	Correct	**seq**	NA	NA	NA	Cananeia	São Paulo	Brazil
248	CFBHT10950	NA	*macrosternum*	Correct	**seq**	NA	NA	NA	Baixa Grande	Piaui	Brazil
249	CFBHT11476	NA	*macrosternum*	Correct	**seq**	NA	NA	NA	Figueiropolis	Tocantins	Brazil
250	CFBHT11565	CFBH23925	CS3	Correct	**seq**	NA	NA	NA	Santos	São Paulo	Brazil
251	**CFBHT11586**	NA	*macrosternum*	as *L. chaquensis*	**seq**	KU495313	NA	NA	Tres Lagoas	Mato Grosso do Sul	Brazil
252	**CFBHT11864**	NA	*luctator*	as *L. latrans*	**seq**	KU495330	**seq**	NA	Tibagi	Paraná	Brazil
253	CFBHT11881	NA	*luctator*	Correct	**seq**	NA	NA	NA	Jaguariaiva	Paraná	Brazil
254	CFBHT11883	CFBH24730	*luctator*	Correct	**seq**	NA	NA	NA	Jaguariaiva	Paraná	Brazil
255	CFBHT12438	NA	*macrosternum*	Correct	**seq**	NA	NA	NA	Camocim	Ceará	Brazil
256	CFBHT12451	NA	*macrosternum*	Correct	**seq**	NA	NA	NA	Barreirinhas	Maranhão	Brazil
257	**CFBHT12637**	NA	*luctator*	Correct	**seq**	**seq**	**seq**	**seq**	Brasilia	Distrito Federal	Brazil
258	CFBHT12657	NA	CS3	Correct	**seq**	NA	NA	NA	Governador Celso Ramos	Santa Catarina	Brazil
259	CFBHT12753	CFBH25493	*latrans*	Correct	**seq**	NA	NA	NA	Mimoso do Sul	Espirito Santo	Brazil
260	CFBHT12809	CFBH29492	*latrans*	Correct	**seq**	NA	NA	NA	Camamu	Bahia	Brazil
261	CFBHT12810	CFBH29493	*latrans*	Correct	**seq**	NA	NA	NA	Camamu	Bahia	Brazil
262	**CFBHT12812**	NA	*latrans*	Correct	**seq**	**seq**	**seq**	**seq**	Camamu	Bahia	Brazil
263	CFBHT12813	CFBH29496	*latrans*	Correct	**seq**	NA	NA	NA	Camamu	Bahia	Brazil
264	CFBHT12834	CFBH29497	*latrans*	Correct	**seq**	NA	NA	NA	Camamu	Bahia	Brazil
265	CFBHT12835	NA	*latrans*	Correct	**seq**	NA	NA	NA	Camamu	Bahia	Brazil
266	CFBHT12837	CFBH29500	*latrans*	Correct	**seq**	NA	NA	NA	Camamu	Bahia	Brazil
267	**CFBHT12845**	CFBH29506	*viridis*	Correct	**seq**	**KU495369**	**seq**	**seq**	Camamu	Bahia	Brazil
268	**CFBHT12846**	CFBH29505	*viridis*	Correct	**seq**	**KU495370**	**seq**	NA	Jequie	Bahia	Brazil
269	CFBHT12852	CFBH29507	*macrosternum*	Correct	**seq**	NA	NA	NA	Jequie	Bahia	Brazil
270	CFBHT12853	CFBH29508	*macrosternum*	Correct	**seq**	NA	NA	NA	Jequie	Bahia	Brazil
271	CFBHT12854	CFBH29509	*macrosternum*	Correct	**seq**	NA	NA	NA	Jequie	Bahia	Brazil
272	CFBHT12855	CFBH29510	CS1	Correct	**seq**	NA	NA	NA	Jequie	Bahia	Brazil
273	CFBHT12856	CFBH29511	*macrosternum*	Correct	**seq**	NA	NA	NA	Dário Meira	Bahia	Brazil
274	CFBHT12857	CFBH29512	*macrosternum*	Correct	**seq**	NA	NA	NA	Dário Meira	Bahia	Brazil
275	CFBHT13211	NA	*luctator*	Correct	**seq**	NA	NA	NA	Dom Pedro de Alcantara	Rio Grande do Sul	Brazil
276	CFBHT13404	NA	*macrosternum*	Correct	**seq**	NA	NA	NA	Barreiras	Bahia	Brazil
277	CFBHT13450	NA	CS1	Correct	**seq**	NA	NA	NA	Itiuba	Bahia	Brazil
278	CFBHT13479	CFBH27965	*latrans*	Correct	**seq**	NA	NA	NA	Gandu	Bahia	Brazil
279	CFBHT13480	CFBH27966	*latrans*	Correct	**seq**	NA	NA	NA	Gandu	Bahia	Brazil
280	CFBHT13860	CFBH28290	*macrosternum*	Correct	**seq**	NA	NA	NA	Porto Nacional	Tocantins	Brazil
281	CFBHT14222	CFBH28893	*macrosternum*	Correct	**seq**	NA	NA	NA	Porto Nacional	Tocantins	Brazil
282	**CFBHT14337**	NA	*luctator*	Correct	**seq**	**seq**	**seq**	**seq**	São Jose do Barreiro	São Paulo	Brazil
283	CFBHT14458	NA	*macrosternum*	Correct	**seq**	NA	NA	NA	Porangatu	Goias	Brazil
284	CFBHT14980	NA	CS3	Correct	**seq**	NA	NA	NA	Lauro Muller	Santa Catarina	Brazil
285	CFBHT14993	CFBH30351	CS3	Correct	**seq**	NA	NA	NA	Lauro Muller	Santa Catarina	Brazil
286	CFBHT15568	CFBH30905	*luctator*	Correct	**seq**	NA	NA	NA	Santana do Riacho	Minas Gerais	Brazil

287	CFBHT15673	NA	*latrans*	Correct	**seq**	NA	NA	NA	Linhares	Espirito Santo	Brazil
288	CFBHT15828	CFBH32117	*latrans*	Correct	**seq**	NA	NA	NA	Porto Seguro	Bahia	Brazil
289	CFBHT15840	NA	*latrans*	Correct	**seq**	NA	NA	NA	Itamaraju	Bahia	Brazil
290	CFBHT15844	NA	*latrans*	Correct	**seq**	NA	NA	NA	Itamaraju	Bahia	Brazil
291	CFBHT15877	NA	*macrosternum*	Correct	**seq**	NA	NA	NA	Manuel Vitorino	Bahia	Brazil
292	CFBHT15916	CFBH31074	*luctator*	Correct	**seq**	NA	NA	NA	São Paulo	São Paulo	Brazil
293	CFBHT16454	NA	*macrosternum*	Correct	**seq**	NA	NA	NA	Carinhanha	Bahia	Brazil
294	CFBHT17417	NA	*macrosternum*	Correct	**seq**	NA	NA	NA	Brumado	Bahia	Brazil
295	CFBHT17990	CFBH35883	*luctator*	Correct	**seq**	NA	NA	NA	Poços de Caldas	Minas Gerais	Brazil
296	CFBHT18461	CFBH37913	CS1	Correct	**seq**	NA	NA	NA	Brejinho das Ametistas	Bahia	Brazil
297	CFBHT18466	CFBH37918	CS1	Correct	**seq**	NA	NA	NA	Brejinho das Ametistas	Bahia	Brazil
298	**CFBHT18858**	CFBH36505	CS3	Correct	**seq**	**seq**	**seq**	NA	Sete Barras	São Paulo	Brazil
299	CFBHT18860	CFBH36507	*luctator*	Correct	**seq**	NA	NA	NA	Sacramento	Minas Gerais	Brazil
300	CFBHT19074	CFBH38950	*macrosternum*	Correct	**seq**	NA	NA	NA	Galia	São Paulo	Brazil
301	CFBHT19163	CFBH38481	*luctator*	Correct	**seq**	NA	NA	NA	Parelheiros	São Paulo	Brazil
302	CFBHT19178	CFBH38572	CS3	Correct	**seq**	NA	NA	NA	Peruibe	São Paulo	Brazil
303	CFBHT19193	CFBH38695	CS3	Correct	**seq**	NA	NA	NA	Apiai	São Paulo	Brazil
304	CFBHT19264	NA	*luctator*	Correct	**seq**	NA	NA	NA	Juquitiba	São Paulo	Brazil
305	CFBHT19344	CFBH38484	*luctator*	Correct	**seq**	NA	NA	NA	Parelheiros	São Paulo	Brazil
306	**CFBHT19433**	NA	CS3	Correct	**seq**	**seq**	**seq**	**seq**	Apiai	São Paulo	Brazil
307	**CFBHT19776**	CFBH39301	CS3	Correct	**seq**	**seq**	**seq**	**seq**	São Francisco do sul	Santa Catarina	Brazil
308	CFBHT20243	NA	*luctator*	Correct	**seq**	NA	NA	NA	Santana do Riacho	Minas Gerais	Brazil
309	CFBHT20248	CFBH40109	*luctator*	Correct	**seq**	NA	NA	NA	Santana do Riacho	Minas Gerais	Brazil
310	**CFBHT21008**	NA	*luctator*	Correct	**seq**	**seq**	**seq**	NA	Campo Alegre	Santa Catarina	Brazil
311	**CFBHT21063**	CFBH41677	CS3	Correct	**seq**	**seq**	**seq**	**seq**	Torres	Rio Grande do Sul	Brazil
312	CH215	NA	*macrosternum*	Correct	**seq**	NA	NA	NA	Porto Murtinho	Mato Grosso do Sul	Brazil
313	CH234	NA	*macrosternum*	Correct	**seq**	NA	NA	NA	Porto Murtinho	Mato Grosso do Sul	Brazil
314	CHUNB12432	NA	*macrosternum*	Correct	**seq**	NA	NA	NA	Vilhena	Rondônia	Brazil
315	CHUNB12433	NA	*macrosternum*	Correct	**seq**	NA	NA	NA	Vilhena	Rondônia	Brazil
316	**CHUNB25169**	NA	*luctator*	Correct	**seq**	**seq**	**seq**	NA	Paracatu	Minas Gerais	Brazil
317	CHUNB31189	CHUNB31189	*macrosternum*	Correct	**seq**	NA	NA	NA	Monte Alegre	Pará	Brazil
318	CHUNB33878	CHUNB33878	*macrosternum*	Correct	**seq**	NA	NA	NA	Alvorada do Norte	Goias	Brazil
319	CHUNB37707	NA	*macrosternum*	Correct	**seq**	NA	NA	NA	Paranã	Tocantins	Brazil
320	CHUNB42258	NA	*macrosternum*	Correct	**seq**	NA	NA	NA	Mateiros	Tocantins	Brazil
321	CHUNB42640	NA	*macrosternum*	Correct	**seq**	NA	NA	NA	Araçuai	Minas Gerais	Brazil
322	CHUNB42699	NA	*macrosternum*	Correct	**seq**	NA	NA	NA	Britânia	Goias	Brazil
323	CHUNB42841	NA	*macrosternum*	Correct	**seq**	NA	NA	NA	Corumbá	Mato Grosso do Sul	Brazil
324	CHUNB43112	NA	*macrosternum*	Correct	**seq**	NA	NA	NA	Conceição do Araguaia	Pará	Brazil
325	CHUNB43113	NA	*macrosternum*	Correct	**seq**	NA	NA	NA	Pirapora	Minas Gerais	Brazil

326	CHUNB43116	NA	*macrosternum*	Correct	**seq**	NA	NA	NA	Conceição do Araguaia	Pará	Brazil
327	CHUNB43117	NA	*macrosternum*	Correct	**seq**	NA	NA	NA	Sandolândia	Tocantins	Brazil
328	CHUNB43121	NA	*macrosternum*	Correct	**seq**	NA	NA	NA	Couto Magalhães	Tocantins	Brazil
329	CHUNB43122	NA	*macrosternum*	Correct	**seq**	NA	NA	NA	Corinto	Minas Gerais	Brazil
330	CHUNB43194	NA	*macrosternum*	Correct	**seq**	NA	NA	NA	Pirapora	Minas Gerais	Brazil
331	**CHUNB43427**	NA	*luctator*	Correct	**seq**	**seq**	**seq**	NA	Luziânia	Goias	Brazil
332	CHUNB44305	NA	*macrosternum*	Correct	**seq**	NA	NA	NA	Buritizeiro	Minas Gerais	Brazil
333	CHUNB44554	NA	*macrosternum*	Correct	**seq**	NA	NA	NA	Buritizeiro	Minas Gerais	Brazil
334	CHUNB45666	NA	*macrosternum*	Correct	**seq**	NA	NA	NA	Caseara	Tocantins	Brazil
335	CHUNB45667	NA	*macrosternum*	Correct	**seq**	NA	NA	NA	Caseara	Tocantins	Brazil
336	CHUNB50374	NA	*macrosternum*	Correct	**seq**	NA	NA	NA	Colinas do Sul	Goias	Brazil
337	CHUNB50923	NA	*macrosternum*	Correct	**seq**	NA	NA	NA	Colinas do Tocantins	Tocantins	Brazil
338	CHUNB51781	NA	*macrosternum*	Correct	**seq**	NA	NA	NA	Carolina	Maranhão	Brazil
339	CHUNB53011	NA	*macrosternum*	Correct	**seq**	NA	NA	NA	Pimenteiras do Oeste	Rondônia	Brazil
340	CHUNB53235	NA	*macrosternum*	Correct	**seq**	NA	NA	NA	Anagé	Bahia	Brazil
341	CHUNB53236	CHUNB53236	*macrosternum*	Correct	**seq**	NA	NA	NA	Anagé	Bahia	Brazil
342	**CHUNB53237**	NA	CS1	Correct	**seq**	**seq**	**seq**	**seq**	Dário Meira	Bahia	Brazil
343	CHUNB53238	CHUNB53238	CS1	Correct	**seq**	NA	NA	NA	Dário Meira	Bahia	Brazil
344	CHUNB53239	CHUNB53239	CS1	Correct	**seq**	NA	NA	NA	Dário Meira	Bahia	Brazil
345	CHUNB56587	NA	*macrosternum*	Correct	**seq**	NA	NA	NA	Mamanguape	Paraiba	Brazil
346	CHUNB56589	NA	*macrosternum*	Correct	**seq**	NA	NA	NA	Mamanguape	Paraiba	Brazil
347	CHUNB57253	CHUNB57253	*macrosternum*	Correct	**seq**	NA	NA	NA	Jacobina	Bahia	Brazil
348	CHUNB57258	CHUNB57258	*macrosternum*	Correct	**seq**	NA	NA	NA	Morro do Chapeu	Bahia	Brazil
349	CHUNB57259	NA	*macrosternum*	Correct	**seq**	NA	NA	NA	Santa Rita de Cássia	Bahia	Brazil
350	CHUNB57261	CHUNB57261	*macrosternum*	Correct	**seq**	NA	NA	NA	Jacobina	Bahia	Brazil
351	CHUNB57262	CHUNB57262	*macrosternum*	Correct	**seq**	NA	NA	NA	Barra	Bahia	Brazil
352	CHUNB57292	NA	*macrosternum*	Correct	**seq**	NA	NA	NA	Barra	Bahia	Brazil
353	CHUNB57658	NA	*luctator*	Correct	**seq**	NA	NA	NA	Poços de Caldas	Minas Gerais	Brazil
354	CHUNB57825	NA	*macrosternum*	Correct	**seq**	NA	NA	NA	Novo Santo Antônio	Mato Grosso	Brazil
355	CHUNB57894	NA	*macrosternum*	Correct	**seq**	NA	NA	NA	Novo Santo Antônio	Mato Grosso	Brazil
356	CHUNB61843	NA	*macrosternum*	Correct	**seq**	NA	NA	NA	Piripiri	Piaui	Brazil
357	CHUNB63992	CHUNB63992	*macrosternum*	Correct	**seq**	NA	NA	NA	Nova Xavantina	Mato Grosso	Brazil
358	CHUNB63994	NA	*macrosternum*	Correct	**seq**	NA	NA	NA	Nova Xavantina	Mato Grosso	Brazil
359	CHUNB65066	NA	*macrosternum*	Correct	**seq**	NA	NA	NA	Nossa Senhora do Livramento	Mato Grosso	Brazil
360	CHUNB65067	NA	*macrosternum*	Correct	**seq**	NA	NA	NA	Nossa Senhora do Livramento	Mato Grosso	Brazil

361	CHUNB67794	CHUNB67794	*macrosternum*	Correct	**seq**	NA	NA	NA	Ribeirão Cascalheira	Mato Grosso	Brazil
362	CHUNB67795	CHUNB67795	*macrosternum*	Correct	**seq**	NA	NA	NA	Ribeirão Cascalheira	Mato Grosso	Brazil
363	CHUNB67797	NA	*macrosternum*	Correct	**seq**	NA	NA	NA	Ribeirão Cascalheira	Mato Grosso	Brazil
364	CHUNB71350	NA	*macrosternum*	Correct	**seq**	NA	NA	NA	Iaciara	Goias	Brazil
365	CHUNB71684	NA	*macrosternum*	Correct	**seq**	NA	NA	NA	Paracatu	Minas Gerais	Brazil
366	CHUNB73955	CHUNB73955	*macrosternum*	Correct	**seq**	NA	NA	NA	Pium	Tocantins	Brazil
367	CHUNB73957	CHUNB73957	*macrosternum*	Correct	**seq**	NA	NA	NA	Pium	Tocantins	Brazil
368	**FC15**	MZFS5137	*latrans*	Correct	NA	**seq**	NA	NA	Terra Nova	Bahia	Brazil
369	**FC16**	MZFS5138	*latrans*	Correct	NA	**seq**	NA	NA	Terra Nova	Bahia	Brazil
370	**FC17**	MZFS5139	*latrans*	Correct	NA	**seq**	NA	NA	Terra Nova	Bahia	Brazil
371	**FC18**	MZFS5140	*macrosternum*	Correct	NA	**seq**	NA	NA	Terra Nova	Bahia	Brazil
372	**FC19**	MZFS5141	*macrosternum*	Correct	NA	**seq**	NA	NA	Terra Nova	Bahia	Brazil
373	FG16	NA	*macrosternum*	Correct	**seq**	NA	NA	NA	Flores de Goiás	Goias	Brazil
374	FG21	NA	*macrosternum*	Correct	**seq**	NA	NA	NA	Flores de Goiás	Goias	Brazil
375	FG72	NA	*macrosternum*	Correct	**seq**	NA	NA	NA	Flores de Goiás	Goias	Brazil
376	FRD1072	NA	*macrosternum*	Correct	**seq**	NA	NA	NA	Serra Talhada	Pernambuco	Brazil
377	FSCHUFPB0015	NA	*macrosternum*	Correct	**seq**	NA	NA	NA	Monte Alegre	Sergipe	Brazil
378	FSCHUFPB0016	NA	*macrosternum*	Correct	**seq**	NA	NA	NA	Monte Alegre	Sergipe	Brazil
379	FSCHUFPB3018	NA	*macrosternum*	Correct	**seq**	NA	NA	NA	Aiuaba	Ceará	Brazil
380	FSCHUFPB3019	NA	*macrosternum*	Correct	**seq**	NA	NA	NA	Aiuaba	Ceará	Brazil
381	FSCHUFPB3020	NA	*macrosternum*	Correct	**seq**	NA	NA	NA	Aiuaba	Ceará	Brazil
382	FSCHUFPB3202	NA	*macrosternum*	Correct	**seq**	NA	NA	NA	Aiuaba	Ceará	Brazil
383	FSCHUFPB4298	NA	*macrosternum*	Correct	**seq**	NA	NA	NA	Santa Rita	Paraiba	Brazil
384	FSCHUFPB4302	NA	*macrosternum*	Correct	**seq**	NA	NA	NA	Santa Rita	Paraiba	Brazil
385	FSCHUFPB4322	NA	*macrosternum*	Correct	**seq**	NA	NA	NA	Santa Rita	Paraiba	Brazil
386	FSCHUFPB4332	NA	*macrosternum*	Correct	**seq**	NA	NA	NA	Santa Rita	Paraiba	Brazil
387	FSCHUFPB4349	NA	*macrosternum*	Correct	**seq**	NA	NA	NA	Santa Rita	Paraiba	Brazil
388	FSCHUFPB5396	NA	*macrosternum*	Correct	**seq**	NA	NA	NA	Serra Negra do Norte	Rio Grande do Norte	Brazil
389	FSCHUFPB5412	NA	*macrosternum*	Correct	**seq**	NA	NA	NA	Serra Negra do Norte	Rio Grande do Norte	Brazil
390	FSCHUFPB5416	NA	*macrosternum*	Correct	**seq**	NA	NA	NA	Serra Negra do Norte	Rio Grande do Norte	Brazil
391	FSCHUFPB5418	NA	*macrosternum*	Correct	**seq**	NA	NA	NA	Serra Negra do Norte	Rio Grande do Norte	Brazil
392	FSCHUFPB5420	NA	*macrosternum*	Correct	**seq**	NA	NA	NA	Serra Negra do Norte	Rio Grande do Norte	Brazil
393	FSCHUFPB7132	CHUFPB28194	*macrosternum*	Correct	**seq**	NA	NA	NA	Paratinga	Bahia	Brazil
394	FSCHUFPB7133	NA	*macrosternum*	Correct	**seq**	NA	NA	NA	Paratinga	Bahia	Brazil
395	FSCHUFPB7134	NA	*macrosternum*	Correct	**seq**	NA	NA	NA	Paratinga	Bahia	Brazil

396	FSCHUFPB7135	NA	*macrosternum*	Correct	**seq**	NA	NA	NA	Paratinga	Bahia	Brazil
397	FSCHUFPB7136	NA	*macrosternum*	Correct	**seq**	NA	NA	NA	Paratinga	Bahia	Brazil
398	FSCHUFPB7143	NA	*macrosternum*	Correct	**seq**	NA	NA	NA	Barra	Bahia	Brazil
399	FSCHUFPB7146	NA	*macrosternum*	Correct	**seq**	NA	NA	NA	Barra	Bahia	Brazil
400	**FSCHUFPB7162**	CHUFPB28195	CS1	Correct	**seq**	**seq**	**seq**	**seq**	Morro do Chapeu	Bahia	Brazil
401	FSCHUFPB7168	CHUFPB28196	CS1	Correct	**seq**	NA	NA	NA	Campo Formoso	Bahia	Brazil
402	FSCHUFPB7169	CHUFPB28197	CS1	Correct	**seq**	NA	NA	NA	Campo Formoso	Bahia	Brazil
403	**FSCHUFPB7170**	CHUFPB28198	CS1	Correct	**seq**	**seq**	**seq**	**seq**	Campo Formoso	Bahia	Brazil
404	FSCHUFPB7171	CHUFPB28199	CS1	Correct	**seq**	NA	NA	NA	Campo Formoso	Bahia	Brazil
405	**FSCHUFPB7174**	CHUFPB28200	CS1	Correct	**seq**	**seq**	**seq**	**seq**	Jaguarari	Bahia	Brazil
406	FSCHUFPB7175	CHUFPB28201	CS1	Correct	**seq**	NA	NA	NA	Jaguarari	Bahia	Brazil
407	FSCHUFPB7176	CHUFPB28202	CS1	Correct	**seq**	NA	NA	NA	Jaguarari	Bahia	Brazil
408	FSCHUFPB7177	CHUFPB28203	*macrosternum*	Correct	**seq**	NA	NA	NA	Jaguarari	Bahia	Brazil
409	FSCHUFPB7899	NA	*macrosternum*	Correct	**seq**	NA	NA	NA	Poço Redondo	Sergipe	Brazil
410	FSCHUFPB7902	NA	*macrosternum*	Correct	**seq**	NA	NA	NA	Poço Redondo	Sergipe	Brazil
411	FSCHUFPB7905	NA	*macrosternum*	Correct	**seq**	NA	NA	NA	Poço Redondo	Sergipe	Brazil
412	FSCHUFPB9155	NA	*macrosternum*	Correct	**seq**	NA	NA	NA	Cruz do Espírito Santo	Paraiba	Brazil
413	HT0414	NA	*guianensis*	Correct	**seq**	NA	NA	NA	Parque Nacional do Viruá	Roraima	Brazil
414	HT0415	NA	*guianensis*	Correct	**seq**	NA	NA	NA	Parque Nacional do Viruá	Roraima	Brazil
415	HT0416	NA	*guianensis*	Correct	**seq**	NA	NA	NA	Parque Nacional do Viruá	Roraima	Brazil
416	**HT2683**	NA	*guianensis*	Correct	**seq**	**seq**	**seq**	**seq**	Ilha de Maracá	Roraima	Brazil
417	HT2689	NA	*guianensis*	Correct	**seq**	NA	NA	NA	Ilha de Maracá	Roraima	Brazil
418	HT2761	NA	*guianensis*	Correct	**seq**	NA	NA	NA	Ilha de Maracá	Roraima	Brazil
419	**HT3072**	NA	*bolivianus*	Correct	**seq**	**seq**	**seq**	**seq**	Rio Madeira-Ilha da Pedra	Rondônia	Brazil
420	**HT3253**	NA	*bolivianus*	Correct	**seq**	**seq**	**seq**	**seq**	Rio Madeira-Ilha do Bufalo	Rondônia	Brazil
421	**HT3348**	NA	*bolivianus*	Correct	**seq**	**seq**	**seq**	NA	Rio Madeira-Morrinho	Rondônia	Brazil
422	HT3349	NA	*bolivianus*	Correct	**seq**	NA	NA	NA	Rio Madeira-Morrinho	Rondônia	Brazil
423	HT3989	NA	*bolivianus*	Correct	**seq**	NA	NA	NA	Rio Madeira-Ilha da Pedra	Rondônia	Brazil
424	HT4060	NA	*macrosternum*	Correct	**seq**	NA	NA	NA	Rio Madeira-Morrinho	Rondônia	Brazil
425	HT4325	NA	*macrosternum*	Correct	**seq**	NA	NA	NA	Rio Madeira-Jirau Direito	Rondônia	Brazil

426	HT5935	NA	*macrosternum*	Correct	**seq**	NA	NA	NA	Rio Jatapu, São João do Lago da Velha	Amazônia	Brazil
427	HT6160	NA	*macrosternum*	Correct	**seq**	NA	NA	NA	Rio Purus, Igarapé do Jacinto, acampamento	Amazônia	Brazil
428	**HT7666**	NA	*guianensis*	Correct	**seq**	**seq**	**seq**	**seq**	PARNA Serra da Mocidade	Roraima	Brazil
429	IB01	NA	*macrosternum*	Correct	**seq**	NA	NA	NA	Iberá	Corrientes	Argentina
430	**IGA103**	NA	*luctator*	Correct	**seq**	**seq**	**seq**	NA	Atucha	Buenos Aires	Argentina
431	IGA106	NA	*luctator*	Correct	**seq**	NA	NA	NA	Atucha	Buenos Aires	Argentina
432	IGA108	NA	*luctator*	Correct	**seq**	NA	NA	NA	Lima	Buenos Aires	Argentina
433	IGA112	NA	*luctator*	Correct	**seq**	NA	NA	NA	Atucha	Buenos Aires	Argentina
434	IGA115	NA	*luctator*	Correct	**seq**	NA	NA	NA	Atucha	Buenos Aires	Argentina
435	IGA117	NA	*luctator*	Correct	**seq**	NA	NA	NA	Atucha	Buenos Aires	Argentina
436	IIBPH0095	NA	*macrosternum*	Correct	**seq**	NA	NA	NA	San Cosme y Damián	Itapua	Paraguay
437	IIBPH0368	NA	*macrosternum*	Correct	**seq**	NA	NA	NA	Refugio Biológico Limoy	Alto Paraná	Paraguay
438	**IIBPH0619**	NA	*luctator*	Correct	**seq**	**seq**	**seq**	NA	Yegros	Caazapa	Paraguay
439	IIBPH0746	NA	*macrosternum*	Correct	**seq**	NA	NA	NA	Concepción, Estancia Ybú	Concepción	Paraguay
440	IIBPH1038	NA	*macrosternum*	Correct	**seq**	NA	NA	NA	Estancia Pirá Potrero (Vierci)	Amambay	Paraguay
441	IIBPH1208	NA	*luctator*	Correct	**seq**	NA	NA	NA	Alto Vera	Itapua	Paraguay
442	IIBPH1548	NA	*macrosternum*	Correct	**seq**	NA	NA	NA	Golondrina	Presidente Hayes	Paraguay
443	IIBPH1570	NA	*luctator*	Correct	**seq**	NA	NA	NA	Alto Vera	Itapua	Paraguay
444	IIBPH1598	NA	*macrosternum*	Correct	**seq**	NA	NA	NA	Coronel Martínez, Estancia Yaca	Guairá	Paraguay
445	IIBPH1643	NA	*macrosternum*	Correct	**seq**	NA	NA	NA	Brazo del Rio Pilcomayo, General Díaz	Presidente Hayes	Paraguay
446	IIBPH1699	NA	*macrosternum*	Correct	**seq**	NA	NA	NA	Transchaco-Loma Plata	Boquerón	Paraguay
447	IIBPH1741	NA	*macrosternum*	Correct	**seq**	NA	NA	NA	Estancia Cotorrita	Boquerón	Paraguay
448	IIBPH2225	NA	*macrosternum*	Correct	**seq**	NA	NA	NA	Distrito Puerto Casado, Carmelo Peralta	Alto Paraguay	Paraguay
449	IIBPH3044	NA	*macrosternum*	Correct	**seq**	NA	NA	NA	25 de Diciembre	San Pedro	Paraguay
450	**JDL24816**	NA	*insularum*	as *L. bolivianus*	NA	HQ232843	NA	NA	San Marcos	Sucre	Colombia
451	**JDL24887**	NA	*insularum*	as *L. bolivianus*	NA	HQ232845	NA	NA	San Marcos	Sucre	Colombia
452	**JDL26573**	NA	*insularum*	as *L. bolivianus*	NA	HQ232844	NA	NA	Lorica	Cordoba	Colombia
453	**JDL26591**	NA	*insularum*	as *L. bolivianus*	NA	HQ232846	NA	NA	Lorica	Cordoba	Colombia

454	JL0023	NA	*luctator*	Correct	**seq**	NA	NA	NA	Monte Vera	Santa Fe	Argentina
455	JL1020	NA	*luctator*	Correct	**seq**	NA	NA	NA	Monte Vera	Santa Fe	Argentina
456	**JL2030**	NA	*luctator*	Correct	**seq**	**seq**	**seq**	NA	Monte Vera	Santa Fe	Argentina
457	**JLEjemp5**	NA	*luctator*	Correct	**seq**	**seq**	**seq**	NA	La Capital	Santa Fe	Argentina
458	**JLsj3**	NA	*luctator*	Correct	**seq**	**seq**	**seq**	**seq**	San Carlos	San Juan	Argentina
459	JLsj4	NA	*luctator*	Correct	**seq**	NA	NA	NA	San Carlos	San Juan	Argentina
460	**JMORAVEC66**	NA	*bolivianus*	Correct	NA	HQ232840	NA	NA	Nacebe	Pando	Bolivia
461	**JMP223 (MNCN-DNA4042)**	NA	*macrosternum*	as *L. chaquensis*	NA	EU192259	NA	NA	Lomas de Arena Regional Park	Santa Cruz	Bolivia
462	**KU289191**	NA	*luctator*	as *L. ocellatus*	NA	DQ158417	NA	DQ158259	National Reserve - San Rafael Park	Itapua	Paraguay
463	LCH01	NA	*macrosternum*	Correct	**seq**	NA	NA	NA	Pampa Blanca, El Carmen	Jujuy	Argentina
464	LGE00278	NA	*luctator*	Correct	**seq**	NA	NA	NA	El Piñalito, San Pedro	Misiones	Argentina
465	LGE00570	NA	*luctator*	Correct	**seq**	NA	NA	NA	Parque Provincial Moconá, San Pedro	Misiones	Argentina
466	LGE01210	NA	*luctator*	Correct	**seq**	NA	NA	NA	Cainguás	Misiones	Argentina
467	**LGE01211**	NA	*luctator*	Correct	**seq**	**seq**	**seq**	NA	Cainguás	Misiones	Argentina
468	LGE01215	NA	*luctator*	Correct	**seq**	NA	NA	NA	Cainguás	Misiones	Argentina
469	LGE01216	NA	*luctator*	Correct	**seq**	NA	NA	NA	Cainguás	Misiones	Argentina
470	LGE01335	NA	*luctator*	Correct	**seq**	NA	NA	NA	Itacaruaré, San Javier	Misiones	Argentina
471	LGE01567	NA	*luctator*	Correct	**seq**	NA	NA	NA	Osununú, San Ignacio	Misiones	Argentina
472	**LGE02007**	NA	*luctator*	Correct	**seq**	**seq**	**seq**	NA	Estero Carambola	Corrientes	Argentina
473	**LGE02278**	LGE02278	*luctator*	Correct	**seq**	**seq**	**seq**	NA	General Manuel Belgrano	Misiones	Argentina
474	**LGE03417**	NA	*luctator*	Correct	**seq**	**seq**	**seq**	**seq**	Estancia Macaca	Misiones	Argentina
475	LGE03418	LGE03418	*luctator*	Correct	**seq**	NA	NA	NA	Estancia Macaca	Misiones	Argentina
476	**LGE03574**	LGE03574	*luctator*	Correct	**seq**	**seq**	**seq**	NA	StoDomingo	Corrientes	Argentina
477	LGE03614	NA	*luctator*	Correct	**seq**	NA	NA	NA	StoDomingo	Corrientes	Argentina
478	LGE03618	LGE03618	*luctator*	Correct	**seq**	NA	NA	NA	StoDomingo	Corrientes	Argentina
479	**LGE03658**	NA	*luctator*	Correct	**seq**	**seq**	**seq**	NA	Garupá, Barrio Santa Helena, Capital	Misiones	Argentina
480	LGE03725	LGE03725	*luctator*	Correct	**seq**	NA	NA	NA	Garupá, Barrio Santa Helena, Capital	Misiones	Argentina
481	LGE04262	LGE04262	*luctator*	Correct	**seq**	NA	NA	NA	Colonia Villa Bonita, 25 de Mayo	Misiones	Argentina

482	LGE05045	LGE05045	*luctator*	Correct	**seq**	NA	NA	NA	Colonia Alemana, Leandro N. Alem	Misiones	Argentina
483	LGE05046	NA	*luctator*	Correct	**seq**	NA	NA	NA	Colonia Alemana, Leandro N. Alem	Misiones	Argentina
484	**LGE06178**	NA	*luctator*	Correct	**seq**	**seq**	**seq**	NA	ResStoTome	Corrientes	Argentina
485	LGE06182	LGE06182	*luctator*	Correct	**seq**	NA	NA	NA	Fachina, Capital	Misiones	Argentina
486	**LGE07305**	LGE07305	*luctator*	Correct	**seq**	**seq**	**seq**	NA	Arroyo Toribio, San Javier	Misiones	Argentina
487	LGE07805	NA	*luctator*	Correct	**seq**	NA	NA	NA	EstHollada	Cordoba	Argentina
488	**LGE09027**	LGE09027	*luctator*	Correct	**seq**	**seq**	**seq**	NA	StoTome	Corrientes	Argentina
489	LGE18675	LGE18675	*macrosternum*	Correct	**seq**	NA	NA	NA	Florencia	Santa Fe	Argentina
490	LGE18676	LGE18676	*macrosternum*	Correct	**seq**	NA	NA	NA	Florencia	Santa Fe	Argentina
491	LGE18703	LGE18703	*macrosternum*	Correct	**seq**	NA	NA	NA	San Javier, Ruta Provincial N° 39	Santa Fe	Argentina
492	LGE18717	NA	*luctator*	Correct	**seq**	NA	NA	NA	Luis Palacios	Santa Fe	Argentina
493	**LGE18721**	NA	*luctator*	Correct	**seq**	**seq**	**seq**	NA	Luis Palacios	Santa Fe	Argentina
494	LGE18740	LGE18740	*macrosternum*	Correct	**seq**	NA	NA	NA	Zavalla	Santa Fe	Argentina
495	LGE18857	LGE18857	*macrosternum*	Correct	**seq**	NA	NA	NA	Federal	Entre Ríos	Argentina
496	LGE18859	LGE18859	*macrosternum*	Correct	**seq**	NA	NA	NA	Federal	Entre Ríos	Argentina
497	**LGE22146**	NA	*luctator*	Correct	**seq**	**seq**	NA	NA	La Plata	Buenos Aires	Argentina
498	**LGE22147**	NA	*luctator*	Correct	**seq**	**seq**	NA	NA	Posadas	Misiones	Argentina
499	**LGE22148**	NA	*luctator*	Correct	**seq**	**seq**	NA	NA	Posadas	Misiones	Argentina
500	**MANC38648**	NA	*luctator*	as *L. ocellatus*	NA	AY843688	NA	KP295578	Loma Verde, Escobar	Buenos Aires	Argentina
501	MAP0204	NA	*macrosternum*	Correct	**seq**	NA	NA	NA	Campo Grande	Mato Grosso do Sul	Brazil
502	MAP0205	MAP0205	*macrosternum*	Correct	**seq**	NA	NA	NA	Campo Grande	Mato Grosso do Sul	Brazil
503	MAP0206	NA	*macrosternum*	Correct	**seq**	NA	NA	NA	Campo Grande	Mato Grosso do Sul	Brazil
504	MAP0524	MAP0524	*macrosternum*	Correct	**seq**	NA	NA	NA	Campo Grande	Mato Grosso do Sul	Brazil
505	MAP0821	NA	*macrosternum*	Correct	**seq**	NA	NA	NA	Itapagibe	Minas Gerais	Brazil
506	MAP0822	NA	*macrosternum*	Correct	**seq**	NA	NA	NA	Itapagibe	Minas Gerais	Brazil
507	MAP0823	MAP0823	*luctator*	Correct	**seq**	NA	NA	NA	Itapagibe	Minas Gerais	Brazil
508	MAP2019	NA	*macrosternum*	Correct	**seq**	NA	NA	NA	Terenos	Mato Grosso do Sul	Brazil
509	MAP2020	NA	*macrosternum*	Correct	**seq**	NA	NA	NA	Terenos	Mato Grosso do Sul	Brazil
510	MAP2370	MAP2370	*macrosternum*	Correct	**seq**	NA	NA	NA	Lagoa Grande	Minas Gerais	Brazil
511	MAP2371	MAP2371	*macrosternum*	Correct	**seq**	NA	NA	NA	Lagoa Grande	Minas Gerais	Brazil
512	MAP2376	MAP2376	*macrosternum*	Correct	**seq**	NA	NA	NA	Lagoa Grande	Minas Gerais	Brazil
513	MAP3582	NA	*latrans*	Correct	**seq**	NA	NA	NA	Miracema	Rio de Janeiro	Brazil
514	MAP3583	NA	*macrosternum*	Correct	**seq**	NA	NA	NA	São José do Rio Preto	São Paulo	Brazil
515	MAPT0235	NA	*macrosternum*	Correct	**seq**	NA	NA	NA	Camapuã	Mato Grosso do Sul	Brazil
516	MAPT0379	NA	*macrosternum*	Correct	**seq**	NA	NA	NA	Óbidos	Pará	Brazil
517	MAPT0799	NA	*macrosternum*	Correct	**seq**	NA	NA	NA	Guadalupe	Piaui	Brazil
518	MAPT0801	NA	*macrosternum*	Correct	**seq**	NA	NA	NA	Guadalupe	Piaui	Brazil

519	MAPT0899	NA	*macrosternum*	Correct	**seq**	NA	NA	NA	Selviria	Mato Grosso do Sul	Brazil
520	MAPT0902	NA	*macrosternum*	Correct	**seq**	NA	NA	NA	Selviria	Mato Grosso do Sul	Brazil
521	MAPT0965	NA	CS3	Correct	**seq**	NA	NA	NA	São Bonifacio	Santa Catarina	Brazil
522	MAPT0967	NA	CS3	Correct	**seq**	NA	NA	NA	São Bonifacio	Santa Catarina	Brazil
523	**MAPT0968**	NA	CS3	Correct	**seq**	**seq**	**seq**	NA	São Bonifacio	Santa Catarina	Brazil
524	MAPT1040	MAP0860	*macrosternum*	Correct	**seq**	NA	NA	NA	Corumbá	Mato Grosso do Sul	Brazil
525	MAPT1041	NA	*macrosternum*	Correct	**seq**	NA	NA	NA	Corumbá	Mato Grosso do Sul	Brazil
526	MAPT1088	NA	*macrosternum*	Correct	**seq**	NA	NA	NA	Rio Negro	Mato Grosso do Sul	Brazil
527	MAPT1146	NA	*macrosternum*	Correct	**seq**	NA	NA	NA	Aquidauana	Mato Grosso do Sul	Brazil
528	MAPT1147	NA	*macrosternum*	Correct	**seq**	NA	NA	NA	Aquidauana	Mato Grosso do Sul	Brazil
529	MAPT1176	NA	*macrosternum*	Correct	**seq**	NA	NA	NA	Lagoa da Confusão	Tocantins	Brazil
530	MAPT1177	NA	*macrosternum*	Correct	**seq**	NA	NA	NA	Lagoa da Confusão	Tocantins	Brazil
531	**MAPT1362**	NA	*luctator*	Correct	**seq**	**seq**	**seq**	**seq**	Corumbá	Mato Grosso do Sul	Brazil
532	**MAPT1372**	MAP1530	*luctator*	Correct	**seq**	**seq**	**seq**	NA	Corumbá	Mato Grosso do Sul	Brazil
533	MAPT1373	MAP1531	*luctator*	Correct	**seq**	NA	NA	NA	Corumbá	Mato Grosso do Sul	Brazil
534	MAPT2229	NA	*latrans*	Correct	**seq**	NA	NA	NA	Divino	Minas Gerais	Brazil
535	MAPT2231	NA	*latrans*	Correct	**seq**	NA	NA	NA	Divino	Minas Gerais	Brazil
536	MAPT2527	NA	*luctator*	Correct	**seq**	NA	NA	NA	Corumbá	Mato Grosso do Sul	Brazil
537	MAPT2529	NA	*luctator*	Correct	**seq**	NA	NA	NA	Corumbá	Mato Grosso do Sul	Brazil
538	**MCNAM17618**	NA	*luctator*	as *L. latrans*	NA	KY007126	NA	NA	Penedia district, Caeté	Minas Gerais	Brazil
539	MD2279	NA	*latrans*	Correct	KC603989	NA	KC604082	**KC604055**	Una	Bahia	Brazil
540	**MJ1325**	NA	*macrosternum*	as *L. chaquensis*	**seq**	JF789868	NA	NA	Los Lagos	Beni	Bolivia
541	MJ1692	NA	*macrosternum*	Correct	**seq**	NA	NA	NA	Hacienda San Sebastián	Santa Cruz	Bolivia
542	MLPDB2471	LGE14780	*macrosternum*	Correct	**seq**	NA	NA	NA	Perugorria	Corrientes	Argentina
543	**MLPDB2510**	NA	*luctator*	Correct	**seq**	**seq**	**seq**	NA	Perugorria	Corrientes	Argentina
544	**MLPDB2632**	LGE14942	*luctator*	Correct	**seq**	**seq**	**seq**	NA	Tulumba	Cordoba	Argentina
545	MLPDB2768	NA	*macrosternum*	Correct	**seq**	NA	NA	NA	9 de Julio	Chaco	Argentina
546	MLPDB2847	NA	*macrosternum*	Correct	**seq**	NA	NA	NA	Capital	Santa Fe	Argentina
547	**MLPDB3325**	NA	*luctator*	Correct	**seq**	**seq**	**seq**	NA	Vera	Santa Fe	Argentina
548	MLPDB3337	LGE14915	*luctator*	Correct	**seq**	NA	NA	NA	Vera	Santa Fe	Argentina
549	**MLPDB4190**	NA	*luctator*	Correct	**seq**	**seq**	**seq**	**seq**	Lujan	Buenos Aires	Argentina
550	MLPDB4250	NA	*luctator*	Correct	**seq**	NA	NA	NA	Ituzaingó	Corrientes	Argentina
551	**MLPDB4421**	NA	*luctator*	Correct	**seq**	**seq**	**seq**	NA	Candelario	Misiones	Argentina
552	MLPDB5612	NA	*macrosternum*	Correct	**seq**	NA	NA	NA	San Fernando	Chaco	Argentina
553	MLPDB5618	NA	*luctator*	Correct	**seq**	NA	NA	NA	General Paz	Corrientes	Argentina
554	MLPDB6067	NA	*luctator*	Correct	**seq**	NA	NA	NA	Ituzaingó	Corrientes	Argentina
555	**MLPDB6080**	NA	*luctator*	Correct	**seq**	**seq**	**seq**	NA	Chajari	Entre Rios	Argentina
556	MLPDB6255	LGE14839	*macrosternum*	Correct	**seq**	NA	NA	NA	Pilcomayo	Formosa	Argentina
557	MLPDB6268	LGE14864	*macrosternum*	Correct	**seq**	NA	NA	NA	Pilcomayo	Formosa	Argentina
558	MLPDB6271	NA	*macrosternum*	Correct	**seq**	NA	NA	NA	Pirané	Formosa	Argentina

559	MLPDB6318	NA	*macrosternum*	Correct	**seq**	NA	NA	NA	Patiño	Formosa	Argentina
560	MLPDB6365	LGE14813	*macrosternum*	Correct	**seq**	NA	NA	NA	General San Martín	Salta	Argentina
561	MLPDB6410	LGE14840	*macrosternum*	Correct	**seq**	NA	NA	NA	Iruya	Salta	Argentina
562	MLPDB6520	NA	*macrosternum*	Correct	**seq**	NA	NA	NA	General Paz	Corrientes	Argentina
563	MLPDB6678	NA	*luctator*	Correct	**seq**	NA	NA	NA	Juarez Celman	Cordoba	Argentina
564	**MLPDB6679**	NA	*luctator*	Correct	**seq**	**seq**	**seq**	NA	Juarez Celman	Cordoba	Argentina
565	MLPDB6748	NA	*luctator*	Correct	**seq**	NA	NA	NA	Ituzaingó	Corrientes	Argentina
566	MLPDB6825	LGE14724	*macrosternum*	Correct	**seq**	NA	NA	NA	General Güemes	Chaco	Argentina
567	MLPDB6934	LGE14715	*macrosternum*	Correct	**seq**	NA	NA	NA	General Güemes	Chaco	Argentina
568	MLPDB6993	LGE14711	*macrosternum*	Correct	**seq**	NA	NA	NA	General Güemes	Chaco	Argentina
569	MLPDB7748	LGE14842	*macrosternum*	Correct	**seq**	NA	NA	NA	General Güemes	Chaco	Argentina
570	MLPDB8042	NA	*macrosternum*	Correct	**seq**	NA	NA	NA	Avellaneda	Santiago del Estero	Argentina
571	**MLPDB8140**	NA	*luctator*	Correct	**seq**	**seq**	**seq**	NA	General Obligado	Santa Fe	Argentina
572	MLPDB8141	NA	*luctator*	Correct	**seq**	NA	NA	NA	General Obligado	Santa Fe	Argentina
573	MLPDB8155	NA	*luctator*	Correct	**seq**	NA	NA	NA	General Obligado	Santa Fe	Argentina
574	MLPDB8451	LGE14766	*macrosternum*	Correct	**seq**	NA	NA	NA	General Güemes	Chaco	Argentina
575	MLPDB8452	LGE14753	*macrosternum*	Correct	**seq**	NA	NA	NA	General Güemes	Chaco	Argentina
576	**MNKA10384**	NA	*macrosternum*	as *L. chaquensis*	NA	KF723156	NA	NA	Hacienda and RPPN Caparú	Santa Cruz	Bolivia
577	**MNRJ30733**	NA	*latrans*	Correct	NA	KM091606	NA	NA	Teresopolis	Rio de Janeiro	Brazil
578	**MUJ2187**	NA	*insularum*	as *L. bolivianus*	NA	HQ232842	NA	NA	NA	NA	Colombia
579	**MZFS4360**	NA	CS1	Correct	**seq**	**seq**	**seq**	**seq**	Elísio Medrado	Bahia	Brazil
580	MZFS4720	MZFS4720	CS1	Correct	**seq**	NA	NA	NA	Santa Terezinha	Bahia	Brazil
581	MZFS4957	MZFS4957	CS1	Correct	**seq**	NA	NA	NA	Feira de Santana	Bahia	Brazil
582	MZFS4960	NA	CS1	Correct	**seq**	NA	NA	NA	Feira de Santana	Bahia	Brazil
583	MZFS4974	NA	*macrosternum*	Correct	**seq**	NA	NA	NA	Mucugê	Bahia	Brazil
584	MZFS4980	NA	*macrosternum*	Correct	**seq**	NA	NA	NA	Mucugê	Bahia	Brazil
585	**NA (RdS)**	NA	*viridis*	Correct	NA	KM091622	NA	NA	NA	NA	NA
586	PB4	NA	*luctator*	Correct	**seq**	NA	NA	NA	Santa Rosa de Calchines	Santa Fe	Argentina
587	PBd066	MZFS##	CS1	Correct	**seq**	NA	NA	NA	Morro do Chapeu	Bahia	Brazil
588	PBd068	MZFS##	CS1	Correct	**seq**	NA	NA	NA	Morro do Chapeu	Bahia	Brazil
589	PBd140	MZFS##	CS1	Correct	**seq**	NA	NA	NA	Lençóis	Bahia	Brazil
590	PBd158	NA	*macrosternum*	Correct	**seq**	NA	NA	NA	Andaraí	Bahia	Brazil
591	PNCopo	NA	*macrosternum*	Correct	**seq**	NA	NA	NA	Copo	Santiago del Estero	Argentina
592	PR01	NA	*luctator*	Correct	**seq**	NA	NA	NA	Ponta Grossa	Paraná	Brazil
593	PR02	NA	*luctator*	Correct	**seq**	NA	NA	NA	Ponta Grossa	Paraná	Brazil
594	RM1	NA	*macrosternum*	Correct	**seq**	NA	NA	NA	Massarandupió	Bahia	Brazil
595	RM2	NA	*macrosternum*	Correct	**seq**	NA	NA	NA	Massarandupió	Bahia	Brazil
596	RM3	NA	*macrosternum*	Correct	**seq**	NA	NA	NA	Massarandupió	Bahia	Brazil
597	RM4	NA	*macrosternum*	Correct	**seq**	NA	NA	NA	Massarandupió	Bahia	Brazil
598	RPB108	CFBH42980	*latrans*	Correct	**seq**	NA	NA	NA	Ubatuba	São Paulo	Brazil

599	RPB151	CFBH42994	*latrans*	Correct	**seq**	NA	NA	NA	Ubatuba	São Paulo	Brazil
600	RPB156	CFBH42998	*latrans*	Correct	**seq**	NA	NA	NA	Ubatuba	São Paulo	Brazil
601	RPB243	CFBH43028	*luctator*	Correct	**seq**	NA	NA	NA	Marmelópolis	Minas Gerais	Brazil
602	RPB244	CFBH43029	*luctator*	Correct	**seq**	NA	NA	NA	Piquete	São Paulo	Brazil
603	RPB245	CFBH43030	*luctator*	Correct	**seq**	NA	NA	NA	Piquete	São Paulo	Brazil
604	RPB246	CFBH43031	*luctator*	Correct	**seq**	NA	NA	NA	Piquete	São Paulo	Brazil
605	RPB248	CFBH43033	*luctator*	Correct	**seq**	NA	NA	NA	Marmelópolis	Minas Gerais	Brazil
606	SB16	NA	*macrosternum*	Correct	**seq**	NA	NA	NA	São Bento do Norte	Rio Grande do Norte	Brazil
607	SB17	NA	*macrosternum*	Correct	**seq**	NA	NA	NA	São Bento do Norte	Rio Grande do Norte	Brazil
608	SB18	NA	*macrosternum*	Correct	**seq**	NA	NA	NA	São Bento do Norte	Rio Grande do Norte	Brazil
609	SIL68	NA	*macrosternum*	Correct	**seq**	NA	NA	NA	Riachão	Maranhão	Brazil
610	**SMF94261**	NA	*macrosternum*	as *L. chaquensis*	NA	KF723158	NA	NA	Estancia Büchler	Santa Cruz	Bolivia
611	**SMF94337**	NA	*macrosternum*	as *L. chaquensis*	NA	KF723157	NA	NA	Hacienda and RPPN Caparú	Santa Cruz	Bolivia
612	STAFE01	STAFE01	*macrosternum*	Correct	**seq**	NA	NA	NA	Campo Grande	Mato Grosso do Sul	Brazil
613	TG043	NA	*latrans*	Correct	**seq**	NA	NA	NA	Salvador	Bahia	Brazil
614	TG085	NA	*macrosternum*	Correct	**seq**	NA	NA	NA	Indiana	São Paulo	Brazil
615	TG266	NA	*macrosternum*	Correct	**seq**	NA	NA	NA	Fortaleza	Ceará	Brazil
616	TG369	NA	*latrans*	Correct	**seq**	NA	NA	NA	Rio de Janeiro	Rio de Janeiro	Brazil
617	TG370	NA	*latrans*	Correct	**seq**	NA	NA	NA	Rio de Janeiro	Rio de Janeiro	Brazil
618	**TRC011**	NA	*latrans*	Correct	**seq**	**seq**	**seq**	**seq**	Santa Tereza	Espirito Santo	Brazil
619	TRC012	NA	*latrans*	Correct	**seq**	NA	NA	NA	Santa Tereza	Espirito Santo	Brazil
620	**TRC116**	NA	*latrans*	Correct	**seq**	**seq**	**seq**	NA	Cachoeira de Macacu	Rio de Janeiro	Brazil
621	**UC128**	NA	*guianensis*	as *L. bolivianus*	NA	HQ232833	NA	NA	Vila Surumu	Roraima	Brazil
622	**UC130**	NA	*guianensis*	as *L. bolivianus*	NA	HQ232832	NA	NA	Vila Surumu	Roraima	Brazil
623	**UC171**	NA	*latrans*	Correct	NA	KM091605	NA	NA	NA	NA	NA
624	UFBA07402	NA	*macrosternum*	Correct	**seq**	NA	NA	NA	Mucugê	Bahia	Brazil
625	UFBA07403	NA	*macrosternum*	Correct	**seq**	NA	NA	NA	Mucugê	Bahia	Brazil
626	UFBA07522	NA	*macrosternum*	Correct	**seq**	NA	NA	NA	Barreirinhas	Maranhão	Brazil
627	UFBA07832	NA	*macrosternum*	Correct	**seq**	NA	NA	NA	Santa Rita de Cássia	Bahia	Brazil
628	UFBA07833	NA	*macrosternum*	Correct	**seq**	NA	NA	NA	Santa Rita de Cássia	Bahia	Brazil
629	UFBA08735	NA	*macrosternum*	Correct	**seq**	NA	NA	NA	Santa Rita de Cássia	Bahia	Brazil
630	UFBA08736	NA	*macrosternum*	Correct	**seq**	NA	NA	NA	Santa Rita de Cássia	Bahia	Brazil
631	UFBA09479	NA	*macrosternum*	Correct	**seq**	NA	NA	NA	Santa Rita de Cássia	Bahia	Brazil

632	UFBA11131	UFBA11131	*macrosternum*	Correct	**seq**	NA	NA	NA	Salvador, Unidunas	Bahia	Brazil
633	UFBA11707	NA	*macrosternum*	Correct	**seq**	NA	NA	NA	Conde	Bahia	Brazil
634	UFBA11830	NA	*macrosternum*	Correct	**seq**	NA	NA	NA	Conde	Bahia	Brazil
635	UFBA11832	UFBA11832	*macrosternum*	Correct	**seq**	NA	NA	NA	Conde	Bahia	Brazil
636	UFBA13106	UFBA13106	*macrosternum*	Correct	**seq**	NA	NA	NA	Arembepe, Camaçarí	Bahia	Brazil
637	UFBA13107	UFBA13107	*macrosternum*	Correct	**seq**	NA	NA	NA	Arembepe, Camaçarí	Bahia	Brazil
638	UFBA14177	NA	*macrosternum*	Correct	**seq**	NA	NA	NA	Guaratinga	Bahia	Brazil
639	UFBA14178	NA	*macrosternum*	Correct	**seq**	NA	NA	NA	Guaratinga	Bahia	Brazil
640	UFBA14209	UFBA14209	*macrosternum*	Correct	**seq**	NA	NA	NA	Jacinto	Minas Gerais	Brazil
641	UFBA14285	UFBA14285	*macrosternum*	Correct	**seq**	NA	NA	NA	Arembepe, Camaçarí	Bahia	Brazil
642	UFBA14287	UFBA14287	*macrosternum*	Correct	**seq**	NA	NA	NA	Arembepe, Camaçarí	Bahia	Brazil
643	UFBA14300	UFBA14300	CS1	Correct	**seq**	NA	NA	NA	Maracás	Bahia	Brazil
644	UFBA14301	UFBA14301	CS1	Correct	**seq**	NA	NA	NA	Maracás	Bahia	Brazil
645	UFBA14302	UFBA14302	CS1	Correct	**seq**	NA	NA	NA	Maracás	Bahia	Brazil
646	UFBA14331	UFBA14331	*macrosternum*	Correct	**seq**	NA	NA	NA	Belmonte	Bahia	Brazil
647	UFBA14444	UFBA14444	*macrosternum*	Correct	**seq**	NA	NA	NA	Almenara	Minas Gerais	Brazil
648	UFBA14455	UFBA14455	*macrosternum*	Correct	**seq**	NA	NA	NA	Almenara	Minas Gerais	Brazil
649	UFBA14457	UFBA14457	*macrosternum*	Correct	**seq**	NA	NA	NA	Almenara	Minas Gerais	Brazil
650	UFBA14557	UFBA14557	*macrosternum*	Correct	**seq**	NA	NA	NA	Jacinto	Minas Gerais	Brazil
651	UFBA14591	UFBA14591	CS1	Correct	**seq**	NA	NA	NA	Lençóis	Bahia	Brazil
652	UFBA14649	UFBA14649	*macrosternum*	Correct	**seq**	NA	NA	NA	Itapebi	Bahia	Brazil
653	**UFBA14650**	UFBA14650	*latrans*	Correct	**seq**	**seq**	**seq**	NA	Itapebi	Bahia	Brazil
654	UFBA15093	UFBA15093	*macrosternum*	Correct	**seq**	NA	NA	NA	Costa Azul, Jandaíra	Bahia	Brazil
655	UFBA15094	UFBA15094	*macrosternum*	Correct	**seq**	NA	NA	NA	Costa Azul, Jandaíra	Bahia	Brazil
656	**UFBA15099**	UFBA15099	*latrans*	Correct	**seq**	**seq**	**seq**	**seq**	Vale Encantado, Salvador	Bahia	Brazil
657	UFBA15101	UFBA15101	*latrans*	Correct	**seq**	NA	NA	NA	Vale Encantado, Salvador	Bahia	Brazil
658	UFBA15104	UFBA15104	*latrans*	Correct	**seq**	NA	NA	NA	Vale Encantado, Salvador	Bahia	Brazil
659	UFBA15105	UFBA15105	*latrans*	Correct	**seq**	NA	NA	NA	Vale Encantado, Salvador	Bahia	Brazil
660	UFBA15225	NA	*macrosternum*	Correct	**seq**	NA	NA	NA	Maracás	Bahia	Brazil
661	UFBA15226	NA	*macrosternum*	Correct	**seq**	NA	NA	NA	Maracás	Bahia	Brazil
662	UFES2865	NA	*latrans*	Correct	**seq**	NA	NA	NA	Cariacica	Espirito Santo	Brazil
663	UFES2866	NA	*latrans*	Correct	**seq**	NA	NA	NA	Cariacica	Espirito Santo	Brazil

664	UFES3137	NA	*latrans*	Correct	**seq**	NA	NA	NA	Serra	Espirito Santo	Brazil
665	**UFES3511**	NA	*latrans*	Correct	**seq**	**seq**	**seq**	NA	Castelo	Espirito Santo	Brazil
666	UFES3512	NA	*latrans*	Correct	**seq**	NA	NA	NA	Vila Velha	Espirito Santo	Brazil
667	UFMGT0112	NA	*luctator*	Correct	**seq**	NA	NA	NA	Santa Barbara	Minas Gerais	Brazil
668	UFMGT0127	NA	*luctator*	Correct	**seq**	NA	NA	NA	Mariana	Minas Gerais	Brazil
669	UFMGT0552	NA	*macrosternum*	Correct	**seq**	NA	NA	NA	Santa Barbara	Minas Gerais	Brazil
670	UFMGT0613	NA	*luctator*	Correct	**seq**	NA	NA	NA	Catas Altas	Minas Gerais	Brazil
671	UFMGT0648	NA	*luctator*	Correct	**seq**	NA	NA	NA	Brumal	Minas Gerais	Brazil
672	UFMGT1456	NA	*macrosternum*	Correct	**seq**	NA	NA	NA	Sebastião Laranjeiras	Bahia	Brazil
673	UFMGT1462	NA	*macrosternum*	Correct	**seq**	NA	NA	NA	Riacho Santana	Bahia	Brazil
674	UFMGT1463	NA	*macrosternum*	Correct	**seq**	NA	NA	NA	Riacho Santana	Bahia	Brazil
675	UFMGT1652	NA	*luctator*	Correct	**seq**	NA	NA	NA	Jaboticatubas	Minas Gerais	Brazil
676	UFMGT1656	NA	*luctator*	Correct	**seq**	NA	NA	NA	Jaboticatubas	Minas Gerais	Brazil
677	**UFMGT2137**	NA	*luctator*	Correct	**seq**	**seq**	**seq**	**seq**	Serra do salitre	Minas Gerais	Brazil
678	UFMGT2204	NA	*macrosternum*	Correct	**seq**	NA	NA	NA	Caarapó	Mato Grosso do Sul	Brazil
679	UFMGT2205	NA	*macrosternum*	Correct	**seq**	NA	NA	NA	Caarapó	Mato Grosso do Sul	Brazil
680	UFMGT2846	NA	*luctator*	Correct	**seq**	NA	NA	NA	Mariana	Minas Gerais	Brazil
681	UFMGT3008	NA	*luctator*	Correct	**seq**	NA	NA	NA	Itacambira	Minas Gerais	Brazil
682	**UFMGT3539**	NA	*luctator*	Correct	**seq**	**seq**	**seq**	**seq**	Botumirim	Minas Gerais	Brazil
683	UFMGT3957	NA	*luctator*	Correct	**seq**	NA	NA	NA	Brumadinho	Minas Gerais	Brazil
684	UFMGT4360	NA	*macrosternum*	Correct	**seq**	NA	NA	NA	Grão Mogol	Minas Gerais	Brazil
685	UFMGT4361	NA	*macrosternum*	Correct	**seq**	NA	NA	NA	Grão Mogol	Minas Gerais	Brazil
686	**UFMGT4377**	NA	*luctator*	Correct	**seq**	**seq**	**seq**	NA	Grão Mogol	Minas Gerais	Brazil
687	UFMGT4600	NA	*latrans*	Correct	**seq**	NA	NA	NA	Santa Barbara do Leste	Minas Gerais	Brazil
688	**UFMGT5160**	NA	*latrans*	Correct	**seq**	**seq**	**seq**	**seq**	Caratinga	Minas Gerais	Brazil
689	**UFMGT5744**	NA	*latrans*	Correct	**seq**	**seq**	**seq**	**seq**	Carlos Chagas	Minas Gerais	Brazil
690	**UFMGT5758**	NA	aff. *viridis*	Correct	**seq**	**seq**	**seq**	**seq**	Carlos Chagas	Minas Gerais	Brazil
691	UFMGT5982	NA	*macrosternum*	Correct	**seq**	NA	NA	NA	Santa Barbara	Minas Gerais	Brazil
692	UFMGT6167	NA	CS3	Correct	**seq**	NA	NA	NA	Benedito Novo	Santa Catarina	Brazil
693	**ULABG5111**	NA	*insularum*	as *L. bolivianus*	NA	HQ232836	NA	NA	Rio Limones	Merida	Venezuela
694	**ULABG5112**	NA	*insularum*	as *L. bolivianus*	NA	HQ232841	NA	NA	Rio Limones	Merida	Venezuela
695	**ULABG5113**	NA	*insularum*	as *L. bolivianus*	NA	HQ232837	NA	NA	Rio Limones	Merida	Venezuela
696	**ULABG5304**	NA	*insularum*	as *L. bolivianus*	NA	HQ232835	NA	NA	Rio Limones	Merida	Venezuela
697	**USNM268966 (USNM-FS 152368)**	NA	*bolivianus*	Correct	NA	HQ232831	NA	NA	Puerto Maldonado	Madre de Dios	Peru
698	**USNM287016**	NA	*macrosternum*	Correct	NA	KM091598	NA	NA	Icacos Point, Icacos Erin Beach Road	St. Patrick	Trindad
699	**USNM302459**	NA	*macrosternum*	Correct	NA	KM091599	NA	NA	Caracaranã	Roraima	Brazil

700	**USNM319708**	NA	*macrosternum*	as *L. chaquensis*	NA	EF632055/ AY943234	NA	NA	San Miguel de Tucuman	Tucuman	Argentina
701	**USNM348631**	NA	*silvanimbus*	Correct	NA	AY943232	NA	NA	Belen Gualcho	Ocotepeque	Honduras
702	**USNM565027 (CH4955)**	NA	*insularum*	Correct	NA	HQ232839	NA	NA	Rio Indio, Camino Hacia las Minas	Panamá	Panama
703	**USNM565028 (CH4956)**	NA	*insularum*	Correct	NA	AY943235	NA	NA	Rio Indio, Camino Hacia las Minas	Panamá	Panama
704	**USNM572730 (KRL1114)**	NA	*insularum*	Correct	FJ766 746	FJ784467	NA	NA	PN G. D. Omar Torrijos, El Cope	Cocle	Panama
705	ZUFG5826	NA	*macrosternum*	Correct	**seq**	NA	NA	NA	São Domingos	Goias	Brazil
706	ZUFG5829	NA	*macrosternum*	Correct	**seq**	NA	NA	NA	São Domingos	Goias	Brazil
707	ZUFG6133	NA	*macrosternum*	Correct	**seq**	NA	NA	NA	Paraúna	Goias	Brazil
708	ZUFG6804	NA	*macrosternum*	Correct	**seq**	NA	NA	NA	Paraúna	Goias	Brazil
709	ZVCB03777	NA	*luctator*	Correct	**seq**	NA	NA	NA	Colonia Esterella	Colonia	Uruguay
710	ZVCB04608	NA	*luctator*	Correct	**seq**	NA	NA	NA	Maldonado	Maldonado	Uruguay
711	**ZVCB04714**	NA	*luctator*	Correct	**seq**	**seq**	NA	NA	Maldonado	Maldonado	Uruguay
712	ZVCB04797	NA	*luctator*	Correct	**seq**	NA	NA	NA	Maldonado	Maldonado	Uruguay
713	ZVCB04798	NA	*luctator*	Correct	**seq**	NA	NA	NA	Maldonado	Maldonado	Uruguay
714	ZVCB11683	NA	*luctator*	Correct	**seq**	NA	NA	NA	Cerro Largo	Cerro Largo	Uruguay
715	**ZVCB11749**	NA	*luctator*	Correct	**seq**	**seq**	**seq**	NA	Durazno	Durazno	Uruguay
716	ZVCB19561	NA	*macrosternum*	Correct	**seq**	NA	NA	NA	Artigas	Artigas	Uruguay
717	ZVCB19566	NA	*macrosternum*	Correct	**seq**	NA	NA	NA	Artigas	Artigas	Uruguay

APPENDIX II

Specimens examined for morphometric analysis.

Leptodactylus latrans: BRAZIL: BAHIA: Aurelino Leal: CFBH18730 (-14.313, -39.334); Camacan: CHUFPB28115–16 (-15.401, -39.512); Camamu: CFBH29492–94, 29496–97, 29499–500 (-13.944, -39.124); Gandu: CFBH27965–66 (-13.744, -39.485); Ibirapitanga: UFBA03927 (-13.9, -39.454); Ilhéus: AAG-UFU0251, CFBH29514–15, UFBA10836, 10839–40 (-14.806, -39.053); Itamaraju: CFBH32137 (-17.028, -39.55); Itapebi: UFBA14648, 14650 (-15.889, -39.532); Ituberá: UFBA03146 (-13.723, -39.151); Mata de São João: UFBA03894 (-12.567, -38.039); Porto Seguro: CFBH32117 (-16.396, -39.049); Porto Seguro (Caraíva): CFBH13379 (-16.801, -39.152); Salvador: CFBH32167, UFBA04107, 12074, 15099, 15101, 15104–05 (-12.946, -38.398); Saubara: UFBA11730 (-12.752, -38.771); Terra Nova: MZFS5137–39 (-12.453, -38.678); Una: CFBH29517 (-15.187, -39.321); Uruçuca: CFBH21060, 32362, 32388–89, 34023, 37945 (-14.59, -39.296); Varzedo: CHUFPB28147–48 (-12.965, -39.438). ESPÍRITO SANTO: Alegre: CFBH25122 (-20.777, -41.533); Anchieta: CFBH13377 (-20.716, -40.774); Conceição da Barra: CFBH02435–40, 33324, 35399, 41604–05 (-18.355, -39.844); Linhares: CFBH11328, 26266–27 (-19.399, -40.074); Marataízes: CFBH18470 (-21.038, -40.845); Mimoso do Sul: CFBH11322, 25484, 25490–91, 25493–94 (-21.074, -41.369); São Mateus: CFBH01690–91 (-18.708, -39.843); Vargem Alta: CFBH25080 (-20.669, -41.016); Vitória: CFBH01994–95, 33277–78 (-20.331, -40.309). MINAS GERAIS: Cataguases: CHUFPB28110–12 (-21.377, -42.716); Chiador: AAG-UFU0667 (-22.006, -43.052); Divino: MAP0331, ZUFMS-AMP6455–56 (-20.605, -42.156); Juiz de Fora: CFBH42737–38 (-21.733, -43.37); Muriaé: MAP1264–67, 1272 (-21.155, -42.387); Ponte Nova: CFBH42697, 42699–703, 42731–33 (-20.285, -42.956); Viçosa: CHUFPB28117 (-20.775, -42.876). RIO DE JANEIRO: Duas Barras: AAG-UFU0501 (-22.058, -42.517); Itatiaia: CFBH42774–77 (-22.479, -44.57); Macaé:

AAG-UFU0527 (-22.38, -41.816); Rio de Janeiro: CFBH11320, UFBA00572 (-22.962, -43.289); Teresópolis: CFBH42763–69, 42772 (-22.32, -42.82). SÃO PAULO: Ilha Bela: CFBH40853 (-23.828, -45.383); São Sebastião: CFBH09764–65 (-23.748, -45.413); Ubatuba: AAG-UFU2147, 4406–14, CFBH01070, 01072, 01324, 01692 (-23.445, -45.089); Ubatuba (Picinguaba): CFBH11941, 30033, 42979–80, 42994–96, 42998–99, 43074 (-23.369, -44.826).

Leptodactylus CS1 lineage: BRAZIL: BAHIA: Andaraí: MZFS-PDB140 (-12.841, -41.316); Brejinho das Ametistas: CFBH37913, 37918 (-14.266, -42.522); Brotas de Macaúbas: UFBA11022–24 (-12.004, -42.624); Caetité: UFBA08971, 08974 (-14.041, -42.283); Campo Formoso: CHUFPB28196–99 (-10.509, -40.326); Cocos: CHUNB38811 (-14.176, -44.526); Dário Meira: CHUNB53236, 53238–39 (-14.437, -39.907); Feira de Santana: CFBH13387; MZFS4957 (-12.115, -39.043); Jacobina: CHUFPB28184, 28186–93 (-11.161, -40.535), UFBA00149; 00153, 00160, 00162, 00166, 00168–69 (-11.323, -40.469); Jaguarari: CHUFPB28200–02 (-10.267, -40.199); Jequié: CFBH21065, 29510 (-13.928, -40.077); Lençóis: UFBA14591 (-12.553, -41.383); Maracás: CFBH18807, UFBA14300–02 (-13.432, -40.405); Morro do Chapéu: CHUFPB28195, CHUNB57258 (-11.614, -41.155), MZFS-PDB066, 068 (-11.666, -41.131); Palmeiras: CHUFPB28143 (-12.572, -41.492); Santa Terezinha: MZFS4360, 4720 (-12.783, -39.513); Senhor do Bonfim: MZFS2282–83, 2286, 2801 (-10.466, -40.219).

Leptodactylus luctator: ARGENTINA: BUENOS AIRES: La Plata: LGE22146 (-34.977, -57.87); CHACO: San Fernando: LGE14928 (-27.439, -58.854); CÓRDOBA: Juárez Celman: LGE13299 (-33.511, -63.289); Punilla: LGE14945 (-31.383, -64.605); Tulumba (San Pedro Norte): LGE14942 (-30.083, -64.15). CORRIENTES: Corrientes: LGE11278 (-27.433, -58.75);

Ituzaingó: LGE07658, 07667 (-27.744, -56.475); Ituzaingó (Santo Domingo): LGE03574, 03618 (-27.671, -56.14); Ituzaingó (Yacryetá): LGE14931 (-27.563, -56.659); Santo Tomé (Garruchos): LGE09025, 09027–29 (-28.088, -55.747); Santo Tomé (Gdo Val Virasoro): LGE06340, 14887–88 (-28.046, -56). ENTRE RIOS: Federal: LGE18856 (-30.954, -58.771). MISIONES: 25 de Mayo: LGE04262 (-27.566, -54.838); 25 de Mayo (Arroyo Melo): LGE03444 (-27.421, -54.701); 25 de Mayo (Puerto Londero): LGE14946 (-27.37, -54.409); Candelaria (Barrio UCPN): LGE14878, 20110 (-27.482, -55.745); Candelaria (El Puma): LGE03361 (-27.461, -55.799); Candelaria (Isla): LGE20150 (-27.496, -55.775); Candelaria (Reserva EBY): LGE20229 (-27.495, -55.795); Capital (Fachinal): LGE06182, 14900 (-27.648, -55.816); Concepción: LGE13169–73 (-27.982, -55.531); Concepción (La Corita): LGE19995 (-27.896, -55.359); Eldorado: LGE14904 (-26.217, -54.601); Eldorado (Colonia Delicia): LGE13297 (-26.164, -54.251); Garupá: LGE09546, 09553–54, 09570–71 (-27.494, -55.821); Garupá (Santa Helena): LGE03720, 03725, 04909 (-27.465, -55.888); General Manuel Belgrano: LGE07486 (-26.116, -53.81); General Manuel Belgrano (Macaca): LGE03418 (-26.395, -53.723); General Manuel Belgrano (Ruta Nacional N14): LGE03974, 07487, 07524, 07629 (-26.116, -53.81); General Manuel Belgrano (San Sebastián): LGE14909–10 (-25.858, -53.975); General Manuel Belgrano (Tajamar): LGE02277–79 (-26.116, -53.81); Guaraní (El Soberbio): LGE14881 (-27.283, -54.2); Iguazú: LGE05860 (-25.972, -54.176); Ituzaingó: LGE03459 (-27.533, -56.6); Leandro N. Alem: LGE05045 (-27.56, -55.519); Posadas: LGE02630 (-27.463, -55.963); Posadas (Campus): LGE14917 (-27.437, -55.894); Posadas (Nacional N12): LGE22147–49 (-27.453, -56.022); San Ignacio (Gobernador Roca): LGE13296 (-27.183, -55.45); San Ignacio (Santo Pipó): LGE14919 (-27.127, -55.471); San Javier (Arroyo Toribio): LGE07305 (-27.841, -55.147); San Pedro: LGE08889 (-26.789, -53.907); San Pedro (El Piñalito): LGE16551, 18223–24, 20454 (-26.43, -53.852); San Pedro (Ruta Provincial N20): LGE00239, 21893 (-26.561, -54.066).

SANTA FÉ: General Obligado: LGE14947 (-28.485, -59.722); General Obligado (Florencia): LGE18681 (-28.031, -59.308); Rosario: LGE18741–42 (-32.991, -60.907); Vera: LGE14912, 14915–16 (-29.467, -60.233); Vera (Ruta Provincial N30): LGE20630 (-28.105, -60.167); Vera (Ruta Provincial N40, Fortín Olmos): LGE20669–70 (-29.096, -60.623). BRAZIL: BAHIA: Cocos: CHUNB38812 (-14.176, -44.526); Guiné: CHUFPB28146 (-12.827, -41.518); Jaborandi: CFBH20512 (-13.629, -44.464); Piatã: AAG-UFU1680, CHUFPB28149–51, MZFS4438–40, UFBA-AAGARDA10080–81 (-13.153, -41.787). MATO GROSSO: Alto Araguaia: CHUNB67030 (-17.32, -53.243). MATO GROSSO DO SUL: Corumbá - BEP: MAP1530–31, ZUFMS-AMP2081, ZUFMS-AMP2085–86, 2091–92, 2099–2100 (-19.577, -57.019). MINAS GERAIS: Araguari: AAG-UFU4918 (-18.624, -48.22); Fama: CFBH01763 (-21.402, -45.838); Itapagibe: MAP0823 (-19.913, -49.217); Marmelópolis: CFBH43028, 43033, 43045 (-22.501, -45.151); Poços de Caldas: AAG-UFU1173, 4801, CFBH35883 (-21.836, -46.531); Sacramento: CFBH36507 (-19.861, -47.46); Santana do Riacho: CFBH30905, 39825, 40109 (-19.257, -43.533); Tapira: AAG-UFU0612 (-19.919, -46.818); Uberlândia: AAG-UFU2146, 4478–79 (-18.986, -48.298). PARANÁ: Jaguariaiva: CFBH21025, CFBH24729–30 (-24.238, -49.712); Piraquara: CFBH11046 (-25.466, -49.053); Quatro Barras: CFBH18134 (-25.378, -49.085); Tijucas do Sul: CFBH08446 (-25.925, -49.174). RIO GRANDE DO SUL: São Sepé: CFBH12044 (-30.37, -53.664); Sapiranga: CFBH12415 (-29.552, -51.016). SANTA CATARINA: Bom Jardim da Serra: CFBH11015–16, 11029, CHUFPB28113 (-28.352, -49.599); Mafra: CFBH08597 (-26.114, -49.757). SÃO PAULO: Apiaí: CFBH25614–15 (-24.562, -48.67); Bauru: CFBH19761 (-22.346, -49.007); Buri: CFBH42813–14 (-23.612, -48.533); Campinas: CFBH00938, 35545 (-22.883, -46.935); Corumbataí: CFBH04186 (-22.216, -47.618); Cunha: CFBH43007, 43019 (-23.223, -44.962); Guará: CFBH39955 (-20.492, -47.859); Itirapina: CFBH06022, 06441 (-22.248, -47.826); Lindóia: CFBH42662–63 (-22.523, -46.643); Luís Antônio: CFBH31870–71 (-21.573, -

47.738); Mairiporã: CFBH13877 (-23.322, -46.562); Mogi das Cruzes: CFBH41881 (-23.719, -46.168); Parelheiros: CFBH38481, 38484 (-23.987, -46.743); Pedregulho: CFBH13991 (-20.254, -47.455); Pilar do Sul: CFBH08352 (-23.832, -47.713); Piquete: CFBH43029–32, 43044, 43064–65 (-22.596, -45.23); Ribeirão Branco: CFBH02323–25, 04463, 06897, 06899–900, 41603 (-24.217, -48.754); Rio Claro: CFBH08022 (-22.317, -47.697); São José do Barreiro: CFBH43068 (-22.722, -44.617); São Luis do Paraitinga: CFBH10773, 38731, 38760 (-23.335, -45.147); São Miguel Arcanjo: UFBA07977–78 (-23.986, -47.921); São Paulo: CFBH31074 (-23.675, -46.732); Teodoro Sampaio: CFBH18395 (-22.537, -52.125). URUGUAY: MONTEVIDEO: Montevideo: LGE22129–32 (-34.861, -56.249).

Leptodactylus CS3 lineage: BRAZIL: PARANÁ: Antonina: CFBH11064 (-25.419, -48.733); Morretes: UFBA09112 (-25.458, -48.818). RIO GRANDE DO SUL: Torres: CFBH41677 (-29.348, -49.748). SANTA CATARINA: Angelina: CFBH08481 (-27.566, -48.99) Corupá: CFBH12432 (-26.435, -49.245); Lauro Muller: CFBH30351 (-28.399, -49.504); São Francisco do Sul: CFBH39301 (-26.249, -48.635); Treviso: CFBH08500, 12391 (-28.519, -49.464). SÃO PAULO: Apiaí: CFBH38695 (-24.562, -48.67); Cubatão: CFBH10546, 11376 (-23.886, -46.453); Eldorado: CFBH30993 (-24.532, -48.122); Iguape: CFBH09752 (-24.379, -47.075); Peruíbe: CFBH12455, 24121, 38572, 42804–05, 42807 (-24.379, -47.075); Praia Grande: AAG-UFU4900–01 (-24.005, -46.485); Santos: CFBH23925 (-23.9, -46.26); São Vicente: CFBH38034 (-23.964, -46.366); Sete Barras: CFBH36494, 36505, 36555 (-24.384, -47.933).

Leptodactylus macrosternum: ARGENTINA: CHACO: Chacabuco (Charata): LGE05221 (-27.26, -61.198); Chacabuco (Mesón de Fierro): LGE05260, 05278 (-27.403, -60.932); Fray

Justo Santa María de Oro (Santa Sylvina): LGE05373 (-27.803, -61.088); General Güemes: LGE14712 (-25.078, -61.627); General Güemes (Comandancia Frias): LGE14709–11 (-24.491, -62.119); General Güemes (El Pintado): LGE14827 (-24.654, -61.472); General Güemes (El Sauzalito): LGE14722, 14724, 14733, 14842, 14857, 18722 (-24.439, -61.683); General Güemes (Fuerte Esperanza): LGE14714–15, 14717 (-25.085, -61.644); General Güemes (Misión Nueva Pompeya): LGE12209, 14704, 14753, 14762, 14766, 17012, 20698 (-24.78, -61.694); General Güemes (Paraje Zanjas): LGE14773–74 (-24.519, -61.811); General Güemes (Rio Bermejito): LGE14752, 14755 (-24.769, -61.808); General Güemes (Wichi): LGE14852 (-24.692, -61.431); Maipú (Tres Isletas): LGE10092, 10094, 10096 (-26.212, -60.329). CORRIENTES: Corrientes (Capital): LGE11272–73, 14765 (-27.433, -58.75); Curuzú Cuatiá (El Oscuro): LGE14780, 14784 (-29.168, -58.517); Ituzaingó (Santo Domingo): LGE04815 (-27.671, -56.14). ENTRE RIOS: Federal: LGE18857–59 (-30.954, -58.771); FORMOSA: Pilcomayo (Palma Sola): LGE14837–39, 14864 (-25.251, -57.999); Pirané (Campo Villafañe): LGE09409 (-26.158, -59.03); Pirané (Ruta Provincial N81): LGE14791 (-25.678, -59.081). MISIONES: Candelaria (Estancia San Juan): LGE14825 (-27.429, -55.622). SALTA: General José de San Martín (Embarcación): LGE14813 (-23.182, -64.076); Iruya (Isla de Cañas): LGE14840 (-22.918, -64.646); Orán (Hipólito Irigoyen): LGE21647 (-23.255, -64.273). SANTA FE: Nueve de Julio (Villa Minetti): LGE20717 (-28.613, -61.677); General Obligado (Florencia): LGE18675–76 (-28.028, -59.348); General Obligado (Villa Ana S): LGE14819 (-28.573, -59.641); Rosario (Zavalla): LGE18740 (-32.991, -60.907); San Javier (San Javier): LGE18703 (-30.551, -59.999); Santa Fé (Sauce Viejo): LGE14848–49 (-31.766, -60.836); Vera (Los Amores): LGE20623, 20631 (-28.107, -59.989); Vera (Ruta Provincial N40, Fortín Olmos): LGE20641–42, 20648 (-29.096, -60.623). SANTIAGO DEL ESTERO: General Taboada (Anatuya, Ruta Provincial N7): LGE20794–95 (-28.416, -62.603); General Taboada (Colonia Dora): LGE05499–501, 14801,

14803, 14809 (-28.516, -62.888); General Taboada (Los Juries): LGE05454, 05458, 05504–05, 05507–08, (-28.508, -62.134); Juan Felipe Ibarra (El Sobrante): LGE08345 (-27.643, -63.481); Juan Felipe Ibarra (Suncho Corral): LGE08348 (-27.822, -63.472); Moreno (Tintina): LGE08276, 08282 (-27.141, -63.056); Río Hondo: LGE00323, 20927, 20938–39 (-27.509, -64.838); Robles (Fernández): LGE14831 (-27.974, -63.8). TUCUMÁN: Lules: LGE14841, 14869 (-26.863, -65.299). BRAZIL: ACRE: Cruzeiro do Sul: CFBH00039–40 (-7.602; -72.658). ALAGOAS: Passo de Camaragibe: CFBH07325 (-9.262; -35.457). AMAPÁ: Macapá: AAG-UFU6008 (-0.007, -51.107). BAHIA: Amargosa: UFBA06440 (-13.085, -39.649); Barra: CHUNB57262 (-11.083, -43.142); Barreiras: UFBA12903, 12907–08, 12918, 13109–10, 13120–21 (-12.111, -44.967); Belmonte: UFBA14331 (-15.849, -38.878); Bom Jesus da Lapa: UFBA07692 (-13.267, -43.420); Brotas de Macaúbas: UFBA13119 (-12.004, -42.623); Caetité: UFBA08547 (-14.041, -42.282); Camacan: CHUFPB28183 (-15.400, -39.512); Camaçari: UFBA00633–35, 01049–54, 07809–10, 07815–16, 11824, 11827–28, 13103, 13106–07, 13104, A14285, 14287 (-12.762, -38.170); Conde: UFBA11829, 11831–32, 14060 (-11.853, -37.578); Condeúba: CHUFPB28153–55 (-14.907, -41.963); Curaçá: UFBA11359–60 (-9.009, -39.918); Dário Meira: CFBH29511–12 (-14.437, -39.907); Dom Basílio: CFBH21088 (-13.752, -41.768); Entre Rios: UFBA05902, 05957, 06065, 06076, 06109 (-12.365, -37.882); Ibiraba: UFBA02096, 02098, 02100–01 (-10.792, -42.824); Itapebi: UFBA14649 (-15.889, -39.532); Jacobina: CHUFPB28185 (-11.160, -40.534), CHUNB57253, 57261 (-11.189, -40.555), UFBA00142, 00154, 00157–58, 00161, 00163 (-11.323, -40.469); Jaguarari: CHUFPB28203 (-10.266, -40.198); Jandaíra: UFBA15093–95 (-11.663, -37.482); Jequié: CFBH29507–09 (-13.928, -40.077); Macaúbas: UFBA13116, 13118 (-13.026, -42.687); Mata de São João: UFBA02377, 08158 (-12.551, -38.000); Mucugê: UFBA07402–03, 07763 (-13.0125, -41.369); Palmeiras: CHUFPB28141–42, 28144–45 (-12.572, -41.491); Paratinga: CHUFPB28194 (-12.689, -43.190); Paulo Afonso:

CHUFPB28134–38 (-9.683, -38.630), UFBA07632, 07634–36 (-9.242, -38.125); Pilão Arcado: MZFS2500, 2584, 2586, 2588, UFBA07264–65, 07267–71 (-10.043, -42.416); Salvador: UFBA11131 (-12.919, -38.325); Santa Rita de Cássia: UFBA08735, 08737–42, 09478–79 (-11.016, -44.505); São Desidério: CFBH20514, UFBA12911–12 (-12.784, -45.943); Senhor do Bonfim: MZFS2284–85 (-10.466, -40.219); Serra do Ramalho: CFBH27663–64 (-13.550, -43.585); Terra Nova: MZFS5140–41 (-12.452, -38.678). CEARÁ: Quixadá: CHUFPB28167 (-4.958, -38.968), CHUFPB28168–82 (-4.958, -38.968); Ubajara: CFBH16121 (-3.841, -40.905). GOIÁS: Alvorada do Norte: CHUNB33867 (-14.584, -46.404), CHUNB33868–69, 33878, 33884, 33886 (-14.584, -46.404); Palmeiras de Goiás: CFBH26141–42 (-16.933, -50.002); Porangatu: CFBH27048 (-13.411, -49.108); Quirinópolis: CFBH04597, 26009 (-18.402, -50.455); São Domingos: CHUNB33876–77, 43865 (-13.396, -46.311). MARANHÃO: Alcântara: CFBH19229 (-2.406, -44.411); Humberto de Campos: CFBH24313 (-2.402, -43.51); Porto Franco: CFBH08197, 08203 (-6.337, -47.407); Riachão: ZUFMS-AMP/SIL37, 66–68, 82–83 (-7.362, -46.629). MATO GROSSO: Cuiabá: AAG-UFU2131 (-15.574, -56.128); Nova Xavantina: CHUNB63992 (-14.522, -52.181); Novo Santo Antônio: CHUNB57800–02, 57893, 57902, 57904 (-12.29, -50.967); Poconé: CHUNB35950 (-16.283, -56.641); Ribeirão Cascalheira: CHUNB22772, 22774, 67794–95, 67798, 67807, 67815, 67841, (-12.931, -51.814). MATO GROSSO DO SUL: Aquidauana: AAG-UFU4099 (-20.450, -55.621); Bela Vista: AAG-UFU0156–57 (-22.101, -56.545); Bonito: CFBH14243, CHUNB49276, ZUFMS-AMP5609 (-20.982, -56.51); Camapuã : ZUFMS-AMP/MAP1094, ZUFMS-AMP5565, 5567 (-19.013, -53.858); Campo Grande: ZUFMS-AMP/MAP0205, 0259, 0524–25, ZUFMS-AMP/STAFE01 (-20.538, -54.751); Corguinho: ZUFMS-AMP/MAP2426, ZUFMS-AMP5605–06 (-19.790, -54.931); Corumbá (BEP): ZUFMS-AMP/MAP1731, ZUFMS-AMP5583, 5585, 5587, 5594, 5600 (-19.576, -57.018); Corumbá (Nhumirim): MAP0860 (-18.988, -56.619); Porto Murtinho:

CFBH30534 (-21.668, -57.713), ZUFMS-AMP/MAP2432 (-20.999, -57.281); Selviria: MAP0653 (-20.384, -51.383). MINAS GERAIS: Almenara: UFBA14444, 14455, 14457 (-16.166, -40.671); Araguari: AAG-UFU4096 (-18.623, -48.220); Bambuí: AAG-UFU0297 (-19.986, -45.964). Jacinto: UFBA14209, 14557–59 (-16.194, -40.341); Lagoa Grande: ZUFMS-AMP/MAP2366, 2369–71, 2376 (-17.809, -46.496); Sacramento: AAG-UFU0886 (-19.861, -47.460). PARÁ: Monte Alegre: CHUNB31189 (-1.933, -54.032); PARAÍBA: Areia: CHUFPB28118–33 (-6.965, -35.718); Puxinanã: CHUFPB28114 (-7.148, -35.955). PERNAMBUCO: Igarassu: CFBH02488 (-7.823, -34.869). PIAUÍ: Brejo do Piauí: CFBH14023 (-8.195, -42.835); Caracol: CHUFPB28157–66 (-9.279, -43.338); Guadalupe: ZUFMS-AMP/MAP0536 (-6.762, -43.617); PARNA Serra das Confusões: CHUFPB28156 (-9.219, -43.49). RIO GRANDE DO NORTE: Angicos: CHUFPB28152 (-5.67, -36.642); Canguaretama: CHUFPB28108–09 (-6.386, -35.136); EAJ-Macaíba: AAG-UFU3573–74, CHUFPB28102–07 (-5.885, -35.368); Extremoz: CHUFPB28139 (-5.684, -35.241); João Câmara: CHUFPB28140 (-5.364, -35.884); Rafael Godeiro: CHUFPB28098–101 (-6.081, -37.716). RONDÔNIA: Costa Marques: AAG-UFU5272–76, 5281–84, CHUNB28978 (-12.454, -64.198). RORAIMA: Cantá: AAG-UFU5558 (2.61, -60.597). SÃO PAULO: Gália: CFBH38950 (-22.397, -49.681); Guararapes: AAG-UFU2019 (-21.213, -50.631); Teodoro Sampaio: CFBH10086, 18294 (-22.537, -52.125). TOCANTINS: Brejinho do Nazaré: AAG-UFU0916 (-11.026, -48.589); Caseara: CHUNB45653, 45658, 45660, 45662, 58158 (-9.372, -49.843); Colinas do Tocantins: CFBH19894, 28429 (-8.069, -48.487); Combinado: CHUNB62725 (-12.806, -46.547); Figueirópolis: CFBH28335 (-12.166, -48.988); Mateiros: CHUNB28843 (-10.702, -46.413); Pium: CHUNB73955, 73957 (-9.946, -49.792); Porto Nacional: CFBH28290, 28893 (-10.986, -48.561); Ribeirão Cascalheira: CHUNB73967 (-12.931, -51.815); Wanderlândia: CFBH28475 (-6.903, -47.923).

Leptodactylus viridis: BRAZIL: BAHIA: Dário Meira: CFBH29505–06, 29513 (-14.437, -39.907).

APPENDIX III

Sound Recordings and Associated Information

Sound file	Species	Voucher	Locality (State)	Air / Water
ASUFRN664	*latrans*	CFBH42763	Teresópolis (RJ)	21/– °C
ASUFRN666	*latrans*	Unvouchered	Teresópolis (RJ)	21/– °C
ASUFRN668	*latrans*	CFBH42772	Teresópolis (RJ)	22/– °C
AAG1a	*latrans*	Unvouchered	Ubatuba (SP)	23/23 °C
AAG2b	*latrans*	Unvouchered	Ubatuba (SP)	23/23 °C
AAG3b	*latrans*	Unvouchered	Ubatuba (SP)	25/24 °C
AAG5d	*latrans*	Unvouchered	Ubatuba (SP)	24/29 °C
AAG6e	*latrans*	Unvouchered	Ubatuba (SP)	25/– °C
TRC1a	*latrans*	AAG-UFU6148	Santa Teresa (ES)	22/– °C
AAG1b	*luctator*	AAG-UFU1680	Piatã (BA)	24/25 °C
AAG2a	*luctator*	Unvouchered	Piatã (BA)	24/25 °C
AAG1b	*luctator*	Unvouchered	Araguari (MG)	24/26 °C
AAG5c	*luctator*	Unvouchered	Uberlândia (MG)	23/23 °C
AAG6a	*luctator*	Unvouchered	Uberlândia (MG)	23/23 °C
AAG7a	*luctator*	Unvouchered	Uberlândia (MG)	24/27 °C
AAG8a	*luctator*	Unvouchered	Uberlândia (MG)	23/24 °C
AAG10a	*luctator*	Unvouchered	Uberlândia (MG)	22/23 °C
AAG2b	*macrosternum*	AAG-UFU4108	Araguari (MG)	25/31 °C
TRC1c	*macrosternum*	AAG-UFU3573	Macaíba (RN)	28/– °C
ASUFRN670	CS3	Unvouchered	Peruíbe (SP)	23/– °C
ASUFRN671	CS3	CFBH42804	Peruíbe (SP)	23/– °C
BNU25_95.01	CS3	Unvouchered	Blumenau (SC)	–/–
BNU25_95.02	CS3	Unvouchered	Blumenau (SC)	–/–
ASUFRN672	CS1	Unvouchered	Jacobina (BA)	26/– °C
ASUFRN673	CS1	CHUFPB28187	Jacobina (BA)	26/– °C
ASUFRN676.1	CS1	CHUFPB28189	Jacobina (BA)	27/– °C
ASUFRN676.2	CS1	CHUFPB28189	Jacobina (BA)	27/– °C

TABLE 1.—List of primers used in this study. COI = mitochondrial cytochrome c oxidase I; POMC = nuclear proopiomelanocortin; TYR = nuclear tyrosinase precursor. F = forward; R = reverse.

Primer		Gene	Sequence	PCR Protocol	Reference
dgLCO1490	F	COI	GGTCAACAAATCATAAAGAYATYG G	[94 (30”), 48 (30”), 72 (40”)] × 35	Meyer 2003
dgHCO2198	R	COI	TAAACTTCAGGGTGACCAAARAAY CA		
AnF1	F	COI	ACHAAYCAYAAAGAYATYGG		Lyra et al. 2017
AnR1	R	COI	CCRAARAATCARAADARRTGTTG		
16SA-L	F	16S	CGCCTGTTTATCAAAAACAT		Palumbi et al. 1991
16SB-H	R	16S	CCGGTCTGAACTCAGATCACGT		
Tyr I Lepto14	F	TYR	GTCSTGTCCAACTCTCCYGTG	[94 (30”), 58 (30”), 72 (40”)] × 40	Fouquet et al. 2012
Tyr E Lepto29	R	TYR	CGTTGCTGGTTGGGTGGKTTC		
POMC_DRV_F1	F	POMC	ATATGTCATGASCCAYTTYCGCTGG AA	[94 (30”), 56 (30”), 72 (40”)] × 40	Vieites et al. 2007
POMC_DRV_R1	R	POMC	GGCRTTYTTGAAWAGAGTCATTAG WGG		

TABLE 2.—Best-fitting partitioning scheme model of nucleotide substitution for COI gene tree and multilocus dataset. COI = mitochondrial cytochrome c oxidase I; POMC = nuclear proopiomelanocortin; TYR = nuclear tyrosinase precursor; GTR = general time-reversible; F81 = Felsenstein 1981; TrN, TrNef = Tamura and Nei 1993; K80 = Kimura 1981.

Dataset	Partition	Model
COI gene tree	COI 1st position	TrN + Γ
	COI 2nd position	F81 + I
	COI 3rd position	TrN + Γ
	16S	GTR + Γ + I
mtDNA + nuDNA	COI 1st position	TrN + Γ
	COI 2nd position	F81 + I
	COI 3rd position	TrN + Γ + I
	TYR and POMC 1st and 2nd positions	F81 + I
	TYR and POMC 3rd position	HKY + Γ + I

TABLE 3.—Average between-groups genetic distances of *Leptodactylus latrans* species group using the corrected p-distance Tamura-Nei model for the COI (below diagonal) and 16S (above diagonal) mitochondrial genes. gui = *L. guianensis*; bol = *L. bolivianus*; ins = *L. insularum*; lat = nominal *L. latrans*; CS1 = *L.* CS1 lineage; luc = *L. luctator* (CS2 lineage); CS3 = *L.* CS3 lineage; mac = *L. macrosternum* ("*chaquensis/macrosternum"* lineage); vir = nominal *L. viridis*; vir2 = *L.* aff. *viridis* MG; sil = *L. silvanimbus*. The lower line is empty because no COI sequences were available for *L. silvanimbus*. Genetic distances among species in the *L. latrans* complex are highlighted in bold.

	gui	bol	ins	CS1	luc	lat	CS3	mac	vir	vir2	sil
gui	–	0.07	0.09	0.16	0.16	0.17	0.17	0.15	0.19	0.18	0.22
bol	0.13	–	0.06	0.13	0.13	0.13	0.14	0.12	0.16	0.16	0.18
ins	0.15	0.16	–	0.14	0.14	0.14	0.15	0.11	0.15	0.15	0.15
CS1	0.24	0.23	0.26	–	**0.09**	**0.07**	**0.06**	0.09	0.14	0.15	0.19
luc	0.20	0.20	0.24	**0.16**	–	**0.06**	**0.06**	0.09	0.15	0.15	0.18
lat	0.21	0.21	0.26	**0.15**	**0.13**	–	**0.04**	0.08	0.15	0.14	0.19
CS3	0.21	0.21	0.27	**0.13**	**0.10**	**0.08**	–	0.09	0.17	0.16	0.18
mac	0.19	0.18	0.20	0.20	0.18	0.17	0.17	–	0.15	0.13	0.18
vir	0.19	0.23	0.24	0.20	0.18	0.19	0.18	0.19	–	0.06	0.19
vir2	0.22	0.22	0.24	0.19	0.21	0.20	0.20	0.20	0.09	–	0.19
sil	–	–	–	–	–	–	–	–	–	–	–

TABLE 4.— Descriptive statistics for 12 measurement variables and ratios for adult males (M) and females (F) of the *Leptodactylus latrans* complex, *L. chaquensis/macrosternum* and *L. viridis*. Values are presented as mean ± SD (range). *n* = total number of measured individuals/measured individuals being molecular vouchers; CM = "*chaquensis/macrosternum*". Abbreviations for measurements are in Material and Methods section. Measurements are in millimeters.

Variables	*L. latrans*		*L.* CS1 lineage		*L. luctator* (CS2 lineage)		*L.* CS3 lineage		*L. macrosternum* (CM lineage)		*L. viridis*	
	M (*n*=96/26)	**F (*n*=45/25)**	**M (*n*=42/23)**	**F (*n*=13/13)**	**M (*n*=136/44)**	**F (*n*=51/12)**	**M (*n*=17/9)**	**F (*n*=10/7)**	**M (*n*=247/75)**	**F (*n*=154/38)**	**M (*n*=2/1)**	**F (*n*=1/1)**
SVL	95.8 ± 13.9 (63.2–124.9)	89.8 ± 8.2 (61.4–104.7)	84.5 ± 8.2 (58.5–96.9)	84.0 ± 7.2 (72.6–93.6)	95.1 ± 10.3 (72.7–121.6)	91.2 ± 7.8 (73.9–115.8)	100 ± 12.7 (78.9–126.3)	88.7 ± 9.7 (75.2–106.3)	74.4 ± 9.0 (48.7–98.9)	74.0 ± 7.3 (55.9–90.8)	63.4 ± 0.7 (63.0–63.9)	66.96
HW	35.8 ± 6.2 (20.9–49.1)	31.1 ± 2.6 (24.5–37.2)	31.0 ± 3.3 (20.5–36.3)	29.5 ± 1.9 (26.5–32.2)	33.4 ± 4.2 (24.9–44.2)	30.2 ± 2.5 (24.0–36.8)	37.6 ± 5.1 (28.1–47.6)	31.0 ± 4.0 (25.9–37.9)	26.2 ± 3.2 (16.9–34.3)	25.3 ± 2.4 (18.6–32.3)	23.1 ± 0.3 (22.9–23.3)	24.74
HL	34.7 ± 4.0 (25.5–43.6)	32.3 ± 2.1 (26.7–36.9)	30.3 ± 2.6 (22.1–34.2)	29.7 ± 1.9 (26.0–32.6)	32.6 ± 3.1 (25.9–39.8)	30.8 ± 2.2 (25.1–37.1)	35.2 ± 3.7 (20.3–43.5)	31.8 ± 3.2 (27.8–36.6)	26.4 ± 2.6 (18.0–34.3)	25.9 ± 2.2 (21.3–32.4)	22.5 ± 1.8 (21.2–23.8)	25.36
ESD	17.2 ± 2.3 (10.1–22.5)	15.7 ± 1.9 (7.8–18.2)	15.2 ± 1.3 (10.8–17.4)	14.1 ± 2.3 (7.8–16.4)	16.0 ± 1.7 (11.3–20.7)	15.2 ± 1.2 (12.7–19.7)	17.4 ± 2.0 (14.5–22.5)	15.6 ± 1.9 (12.1–18.3)	12.8 ± 1.3 (9.3–16.9)	12.5 ± 1.1 (9.4–15.9)	9.9 ± 0 (9.9–10.0)	11.36
END	9.8 ± 1.5 (6.3–13.5)	9.0 ± 0.7 (7.4–10.2)	8.3 ± 0.9 (5.6–9.7)	7.9 ± 0.9 (6.3–9.4)	8.7 ± 1.0 (6.1–11.8)	8.1 ± 0.7 (6.5–9.7)	9.9 ± 1.5 (7.7–13.5)	8.6 ± 1.2 (6.6–10.4)	7.0 ± 0.9 (4.9–16.9)	6.9 ± 0.7 (5.4–8.9)	5.8 ± 0.2 (5.7–6.0)	5.77
EED	21.7 ± 2.8 (15.2–28.3)	20.2 ± 1.8 (15.3–23.9)	18.8 ± 1.8 (14.3–21.6)	18.4 ± 1.6 (15.6–20.9)	20.1 ± 2.0 (14.5–25.6)	19.1 ± 1.4 (16.1–21.7)	22.5 ± 2.5 (18.6–27.6)	19.8 ± 1.9 (17.2–23.2)	16.2 ± 1.7 (11.3–20.8)	16.2 ± 1.5 (12.3–20.6)	13.8 ± 0.8 (13.2–14.4)	14.58
ED	8.7 ± 0.9 (6.9–10.8)	8.4 ± 0.7 (6.9–10.0)	7.6 ± 0.7 (5.7–9.3)	7.8 ± 0.7 (6.4–8.9)	8.3 ± 0.8 (6.2–10.3)	8.2 ± 0.7 (6.9–10.1)	8.7 ± 0.9 (6.7–11.0)	8.3 ± 0.6 (7.7–9.1)	6.9 ± 0.7 (5.0–8.8)	7.0 ± 0.8 (5.7 ± 9.2)	6.1 ± 0.4 (5.8–6.4)	6.5
TD	6.5 ± 0.8 (4.4–8.9)	6.1 ± 0.5 (4.8–7.0)	6.1 ± 0.7 (4.7–7.7)	6.0 ± 0.6 (4.9–6.8)	7.0 ± 0.7 (5.3–8.8)	6.7 ± 0.4 (5.7–8.5)	6.9 ± 1.0 (5.3–9.3)	6.0 ± 0.8 (4.9–7.5)	5.8 ± 0.7 (4.0–7.8)	5.6 ± 0.6 (4.4–7.3)	4.8 ± 0.4 (4.5–5.1)	4.72

HAL	23.8 ± 3.2 (15.3–30.3)	21.7 ± 1.5 (17.2–24.5)	20.4 ± 1.8 (14.2–23.1)	19.2 ± 1.2 (17.5–20.8)	22.8 ± 2.5 (16.6–27.9)	21.1 ± 1.8 (17.2–26.1)	24.8 ± 3.2 (20.2–32.2)	21.3 ± 2.5 (16.8–25.0)	16.5 ± 1.8 (11.7–23.4)	16.2 ± 1.5 (12.3–21.1)	15.9 ± 0.5 (15.5–16.2)	16.07
FAL	42.8 ± 6.6 (25.4–57.4)	37.7 ± 2.6 (30.8–42.0)	36.7 ± 3.7 (24.1–42.5)	33.7 ± 2.0 (29.9–36.2)	40.9 ± 4.9 (29.0–53.8)	36.2 ± 3.4 (28.1–45.5)	44.6 ± 6.1 (33.9–59.1)	37.2 ± 4.6 (29.7–45.4)	29.9 ± 3.6 (20.3–43.0)	28.7 ± 2.8 (21.2–37.1)	25.8 ± 0.3 (25.6–26.1)	28.56
TL	49.4 ± 5.8 (32.4–61.3)	46.5 ± 3.0 (37.2–52.3)	43.5 ± 3.6 (30.9–48.1)	42.3 ± 2.7 (36.6–45.8)	48.0 ± 5.6 (34.6–65.2)	45.7 ± 3.9 (36.0–52.7)	52.4 ± 5.9 (43.5–65.9)	46.6 ± 4.9 (39.0–55.2)	36.2 ± 3.7 (26.1–48.7)	35.9 ± 3.2 (27.8–46.0)	28.5 ± 0.1 (28.4–28.6)	32.53
FTL	53.0 ± 6.2 (36.2–68.3)	49.7 ± 3.5 (40.0–55.0)	45.5 ± 3.6 (35.4–50.8)	43.7 ± 2.6 (39.4–48.2)	51.6 ± 5.3 (38.4–64.5)	49.5 ± 3.9 (41.4–58.2)	54.8 ± 6.2 (45.5–71.3)	49.0 ± 5.2 (40.1–56.8)	37.8 ± 3.7 (28.8–50.0)	37.4 ± 3.4 (27.5–46.2)	32.3 ± 0.8 (31.8–32.9)	34.14
TL/SVL ratio	0.52 ± 0.04 (0.46–0.59)	0.52 ± 0.04 (0.47–0.73)	0.52 ± 0.02 (0.46–0.55)	0.51 ± 0.03 (0.47–0.56)	0.51 ± 0.03 (0.43–0.59)	0.50 ± 0.03 (0.45–0.57)	0.53 ± 0.02 (0.49–0.56)	0.53 ± 0.02 (0.50–0.57)	0.49 ± 0.03 (0.42–0.55)	0.49 ± 0.03 (0.42–0.55)	0.45 ± 0.01 (0.44–0.45)	0.48
FTL/SVL ratio	0.56 ± 0.03 (0.48–0.65)	0.55 ± 0.03 (0.51–0.65)	0.54 ± 0.04 (0.44–0.61)	0.52 ± 0.04 (0.46–0.57)	0.54 ± 0.03 (0.44–0.62)	0.54 ± 0.03 (0.46–0.63)	0.55 ± 0.03 (0.49–0.60)	0.55 ± 0.03 (0.53–0.60)	0.51 ± 0.03 (0.42–0.60)	0.51 ± 0.04 (0.39–0.60)	0.51 ± 0.02 (0.50–0.52)	0.51

TABLE 5.—Comparative data for the three note types in the acoustic repertoire of *Leptodactylus macrosternum* ("*chaquensis/macrosternum*" lineage). Data are given as mean ± SD (range). The following traits were quantified from three note types (growls, trills, and grunts): note length (NL), note rise time (NRT), pulse number (PP), pulse rate (PR), dominant frequency (DF), and linear frequency modulation (LFM); *n* = number of males recorded (number of calls/pulses analyzed); NA = not applicable.

Trait	Growl	Trill	Grunt
	n = 2 (21 / 455)	*n* = 1 (6 / 87)	*n* = 1 (5 / NA)
NL (ms)	435.5 ± 64.6 (316–591)	593.8 ± 44.0 (537–667)	102.9 ± 14.6 (81–117)
NRT (%)	47.8 ± 5.4 (26–63)	70.3 ± 7.8 (59–78)	39.0 ± 8.5 (27–48)
PP/note	21.8 ± 1.0 (15–27)	14.5 ± 0.5 (14–15)	NA
PR/s	52.0 ± 5.4 (48–57)	24.0 ± 1.7 (22–26)	NA
DF (Hz)	388.5 ± 24.2 (366–445)	480.9 ± 22.2 (452–495)	314.4 ± 19.3 (280–323)
LFM (Hz)	-14.2 ± 86.4 (-215–188)	71.8 ± 64.8 (0–172)	-60.3 ± 23.6 (-86 to -43)

TABLE 6.—Advertisement call traits for the species in the *Leptodactylus latrans* complex clade. Data are given as mean ± SD (range). The following traits were quantified from notes of the advertisement call: note length (NL), note rise time (NRT), pulse number (PP), pulse rate (PR), dominant frequency (DF), and linear frequency modulation (LFM); *n* = number of males recorded (number of calls/pulses analyzed); NA = not applicable.

Trait	*L. latrans* (CS1 lineage)	*L.* CS1 lineage (CS1 lineage)	*L. luctator* (CS2 lineage)	*L.* CS3 lineage (CS3 lineage)
	n = 9 (100 / NA)	*n* = 4 (49 / 416)	*n* = 8 (134 / NA)	*n* = 4 (37 / NA)
NL (ms)	174.9 ± 29.7 (124–248)	191.9 ± 14.9 (158–245)	282.4 ± 58.4 (158–413)	181.0 ± 17.6 (129–241)
NRT (%)	53.5 ± 11.9 (28–82)	66.1 ± 9.2 (56–86)	67.6 ± 8.9 (45–85)	72.5 ± 8.1 (59–82)
PP/note	NA	8.4 ± 1.3 (6–10)	NA	NA
PR/s	NA	50.8 ± 8.1 (42–62)	NA	NA

DF (Hz)	355.7 ± 39.6 (280–445)	470.1 ± 69.2 (398–633)	342.8 ± 29.2 (280–409)	339.7 ± 14.3 (323–366)
LFM (Hz)	152.2 ± 58.4 (43–301)	359.8 ± 116.3 (94–609)	160.3 ± 52.0 (43–281)	-27.1 ± 32.4 (-141–47)

FIGURE CAPTIONS

FIG. 1.—Holotype of *Leptodactylus macrosternum*, MZUSP 448, from "Bahia province" (now, Bahia state), northeastern Brazil. (A) Dorsal, (B) ventral and (C) lateral views of body. Scale = 1 cm. Photo provided by T. Grant and Museu de Zoologia, Universidade de São Paulo.

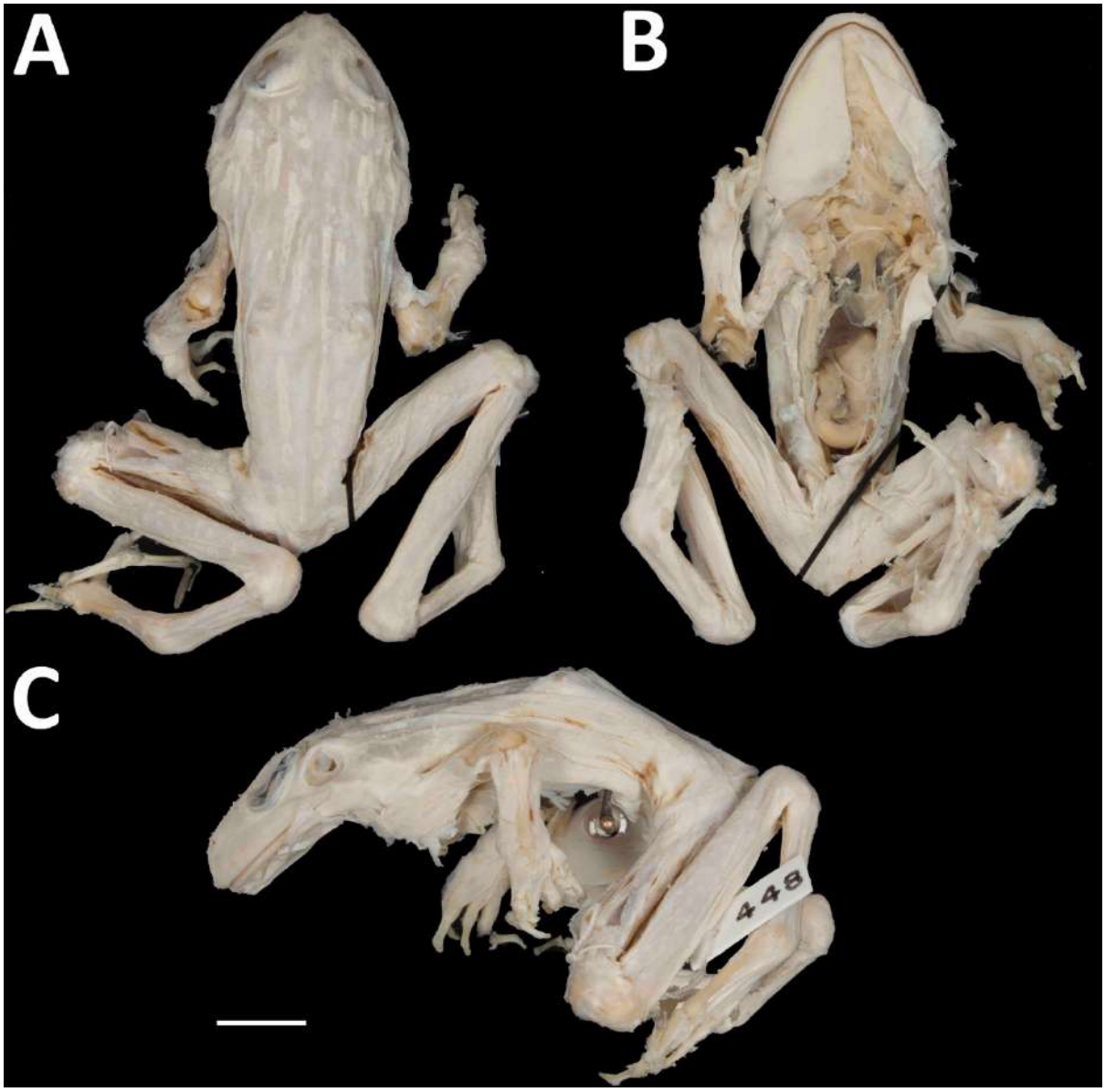

FIG. 2.—Geographic distribution of all genetic samples (mitochondrial+nuclear) from species belonging to the *Leptodactylus latrans* group in South America used herein (right); and COI mitochondrial gene tree recovered from a Bayesian inference analysis in BEAST (left). All clades highlighted are the major evolutionary lineages (putative species) recovered in both bGMYC and ABGD species delimitation analyses. Values on nodes indicate posterior probabilities. Asterisks on nodes denotes posterior probability = 1.0. Scale indicates rate of base substitutions per site. The municipalities of Salvador (Bahia state), Teresópolis (Rio de Janeiro state) and Buenos Aires (Buenos Aires province), relevant for the group taxonomic context, are indicated by arrows. *L. chaq*/*macro* = *L. chaquensis*/*macrosternum* lineage. South American countries acronyms. ARG: Argentina, BOL: Bolivia, BRA: Brazil, CHI: Chile, COL: Colombia, CTR: Costa Rica, ECU: Ecuador, FRG: French Guiana, HON: Honduras, GUY: Guyana, NIC: Nicaragua, PAN: Panama, PER: Peru, PAR: Paraguay, SUR: Suriname, TRI: Trinidad and Tobago, URU: Uruguay, VEN: Venezuela.

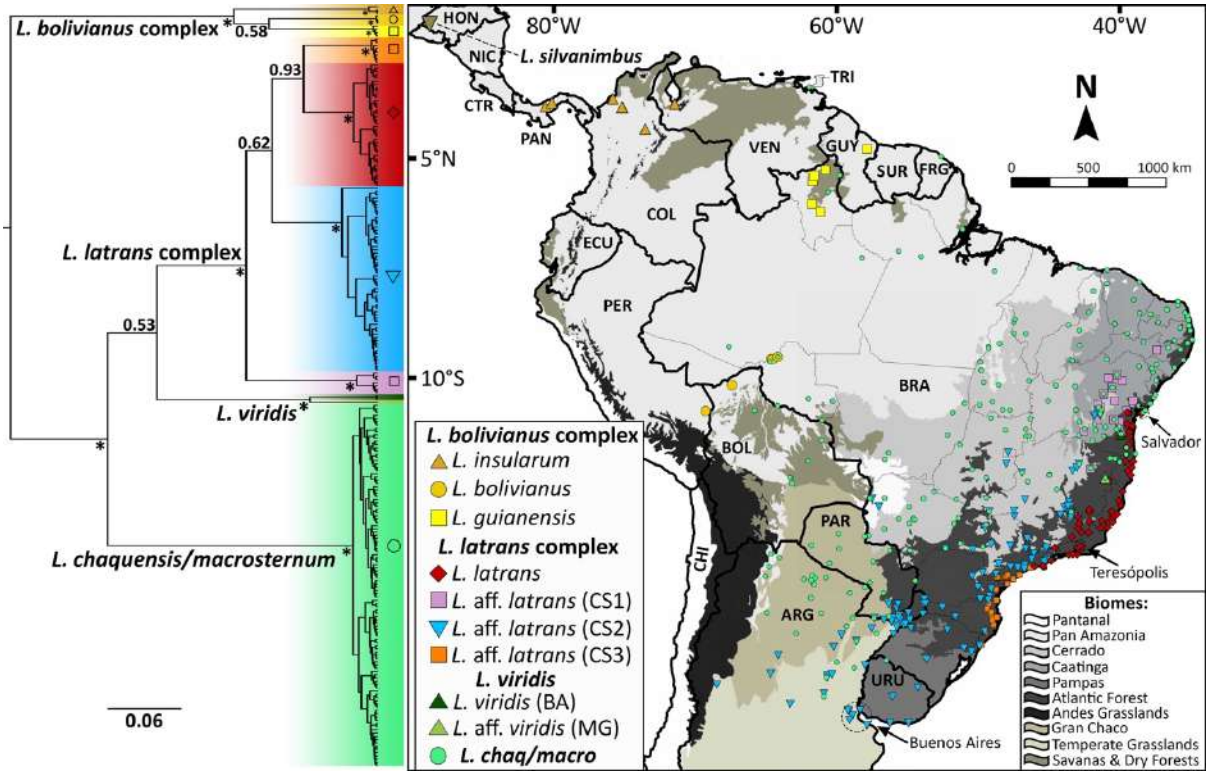

FIG. 3.—Summary of species delimitation analyses using Bayesian implementation of the Generalized Mixed Yule Coalescent model for species in the *Leptodactylus latrans* group. The topology represents the maximum clade credibility COI gene tree from BEAST. The genetic clusters identified by the ABGD analysis are outlined with dashed contours. Numbers are the posterior probability of species identities sampled from a posterior distribution of 100 trees generated in BEAST. The gray scale plot is a sequence-by-sequence matrix colored by pair-wise posterior probabilities of conspecificity, where off-diagonal patterns indicate uncertainty of species limits owing to topological variation of phylogenetic tree.

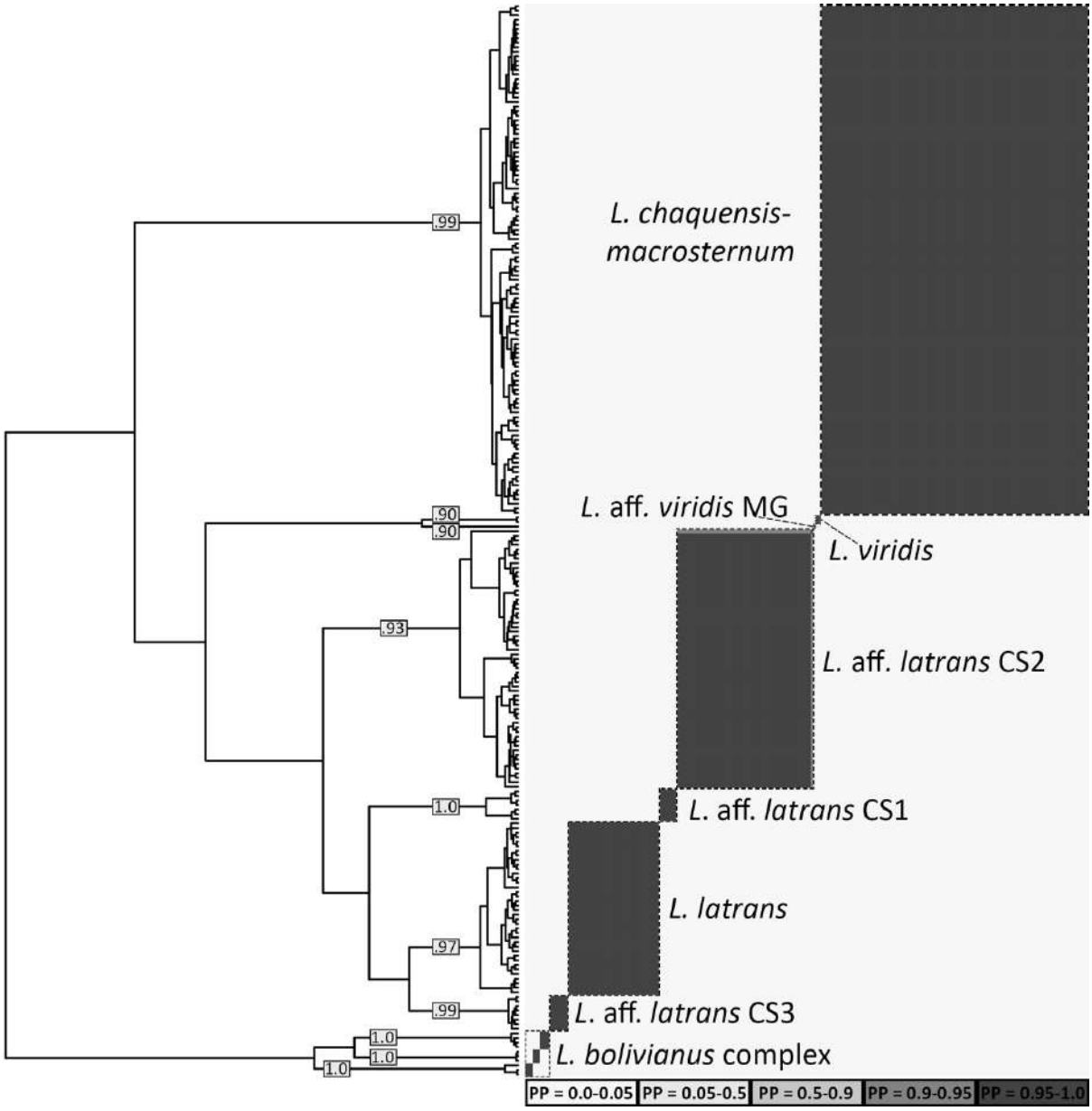

FIG. 4.—Phylogenetic relationships in the *Leptodactylus latrans* species group as estimated by a Bayesian inference (BEAST) and maximum-likelihood (RAxML) analyses of concatenated mitochondrial 16S rRNA, COI mRNA, nuclear tyrosinase precursor (TYR), and proopiomelanocortin (POMC) genes. Values below nodes indicate Bayesian posterior probabilities and bootstrap values from maximum likelihood analysis. Asterisks indicate posterior probabilities/bootstrap values = 1.0/100. Scale indicates rate of base substitutions per site. Colors on branches refer to the same evolutionary lineages recovered in the delimitation analyses.

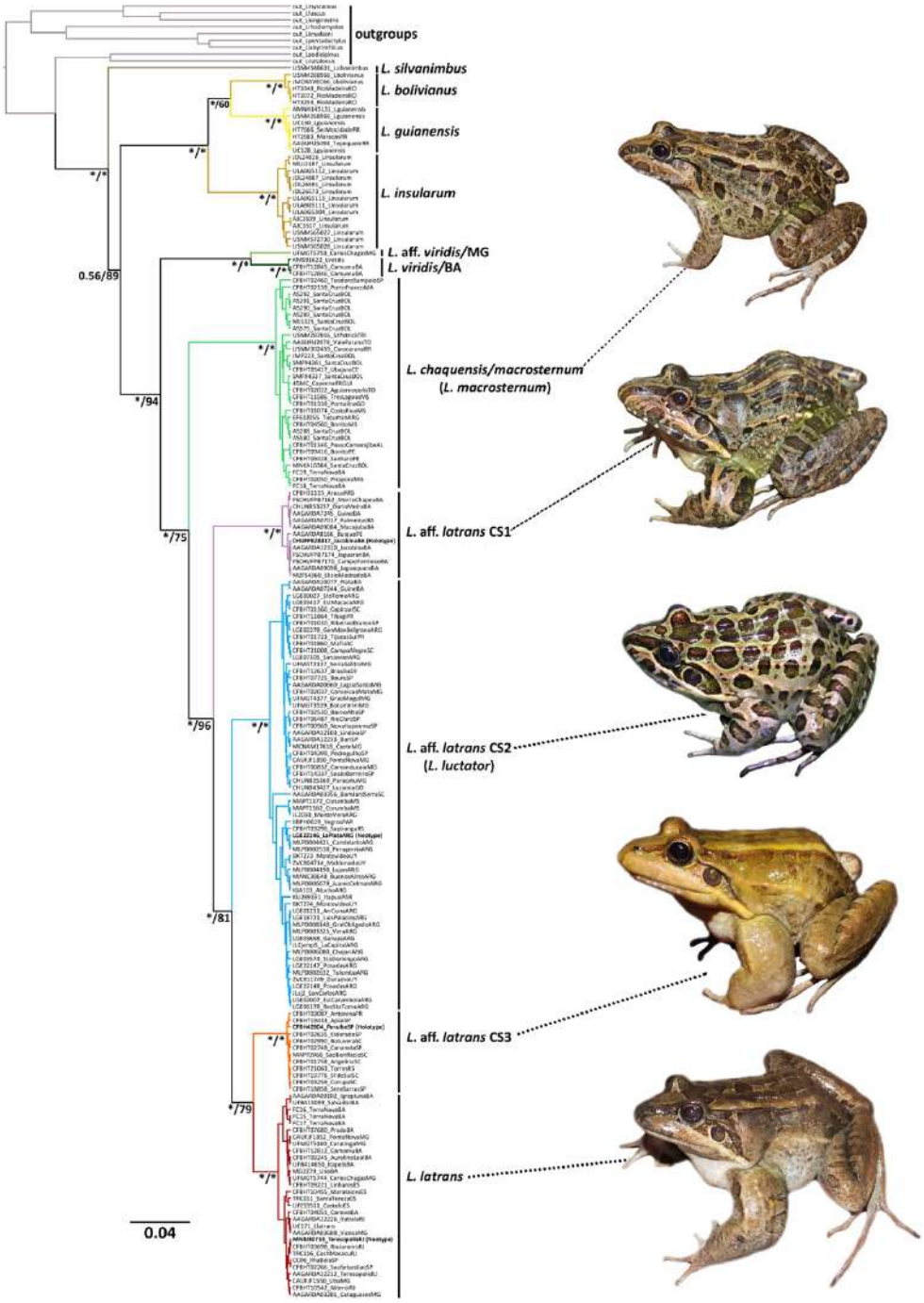

FIG. 5.—Pairwise genetic distances (x-axis) for all sequences of the COI dataset from the *Leptodactylus latrans* species group showing the transition point (gap pointed by arrow) between intraspecific (left) and interspecific genetic (right) distances as identified by the ABGD analysis.

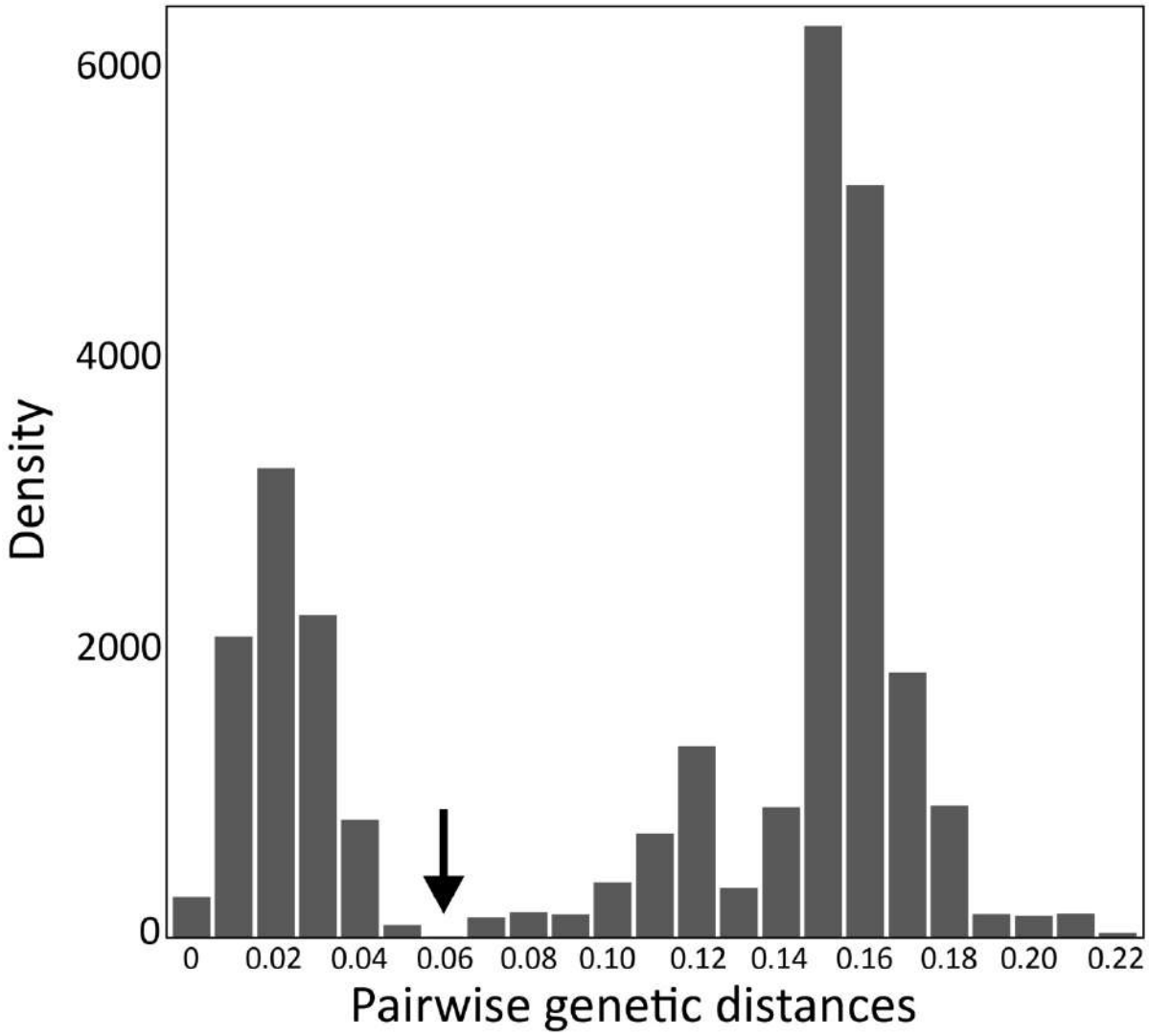

FIG. 6.—Variation on dorsal fold F3 (or auxiliary fold, depicted by red circles): (A) short auxiliary fold followed by rows of tubercles in *Leptodactylus* CS1 lineage (CS1 lineage, CHUFPB 28193); and (B) long and complete auxiliary folds in *L. macrosternum* ("*chaquensis/macrosternum"* lineage, CHUFPB 28185) collected syntopically in Jacobina municipality, Bahia state, Brazil. F1–3 are dorsal, F4 is dorsolateral and F5–6 are lateral folds as proposed by de Sá et al. (2014).

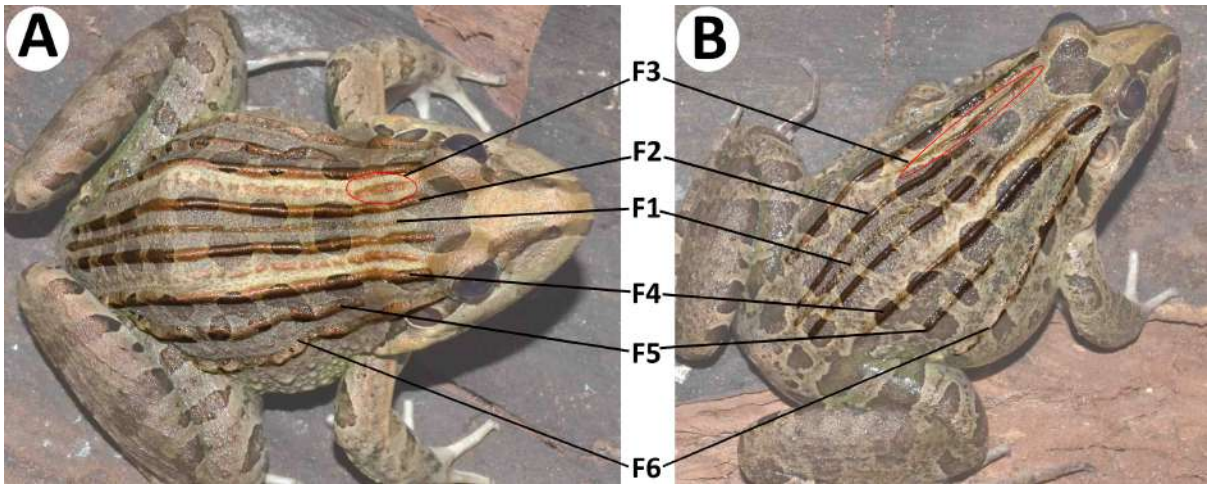

FIG. 7.—Thigh posterior surface coloration patterns. Localities are given as municipality, state/province (collection number): Gray/blue shades: (A) *Leptodactylus latrans* from Ponte Nova, Minas Gerais (CFBH 42697); (B) *L. latrans* from Terra Nova, Bahia (MZFS 5138), photo by F. Camurugi; (C) *L. latrans* from Santa Teresa, Espírito Santo (AAG-UFU 6148); (D) *L. latrans* from Ponte Nova, Minas Gerais (CFBH 42703); (E) *L.* CS3 lineage from Peruíbe, São Paulo (CS3 lineage, CFBH 42807); (F) *L. luctator* from Candelaria, Misiones (CS2 lineage, LGE 15019). Green shades: (G) *L. macrosternum* from Jacobina, Bahia ("*chaquensis/macrosternum"* lineage, CHUFPB 28815); (H) *L.* CS1 lineage from Jacobina, Bahia (CS1 lineage, CHUFPB 28192); (I) *L.* CS1 lineage from Maracás, Bahia (CS1 lineage, UFBA14300), photo by R.O. Abreu; (J) *L. luctator* from Araguari, Minas Gerais (CS2 lineage, unvouchered). Yellow shades: (K) *L. luctator* from La Plata, Buenos Aires (CS2 lineage, LGE 22146); (L) *L. luctator* from Buri, São Paulo (CS2 lineage, CFBH42813).

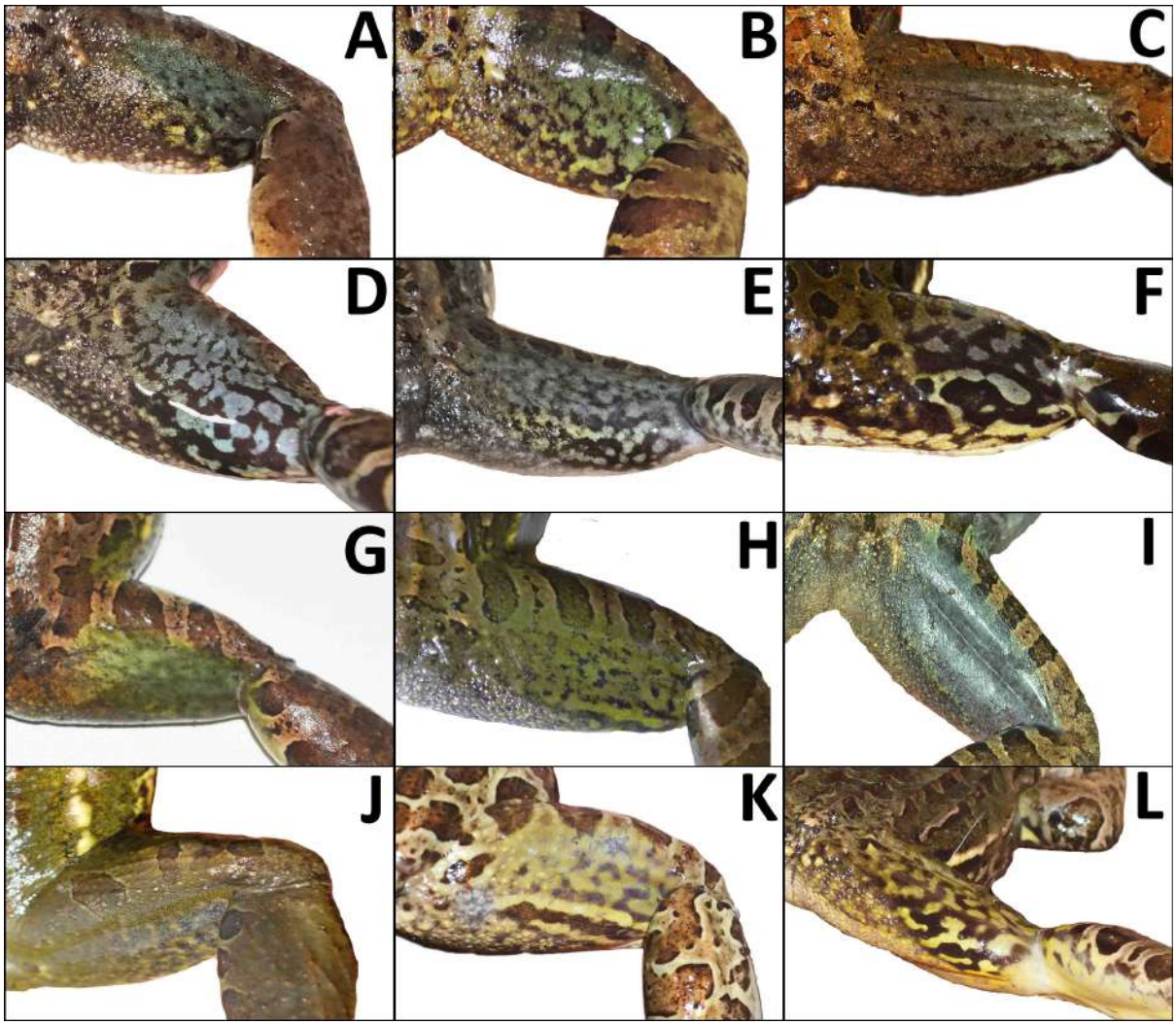

FIG. 8.—Dorsal coloration patterns. Localities are given as municipality, state/province (collection number): (A) *Leptodactylus latrans* from Terra Nova, Bahia (unvouchered) without ocellated blotches on dorsum (smooth, pattern 1), photo by F. Camurugi; (B) *L.* CS1 lineage from Maracás, Bahia (CS1 lineage, UFBA 14300) with light to dark-brown ocellated blotches evenly distributed on dorsum (pattern 2), photo by R.O. Abreu; and (C) *L. macrosternum* from Conceição das Alagoas, Minas Gerais ("*chaquensis/macrosternum*" lineage, UFTM teaching collection), and (D) *L. luctator* from Poços de Caldas, Minas Gerais (CS2 lineage, AAG-UFU 1173) with dark-brown ocellated blotches delimited by light colored rings (pattern 3).

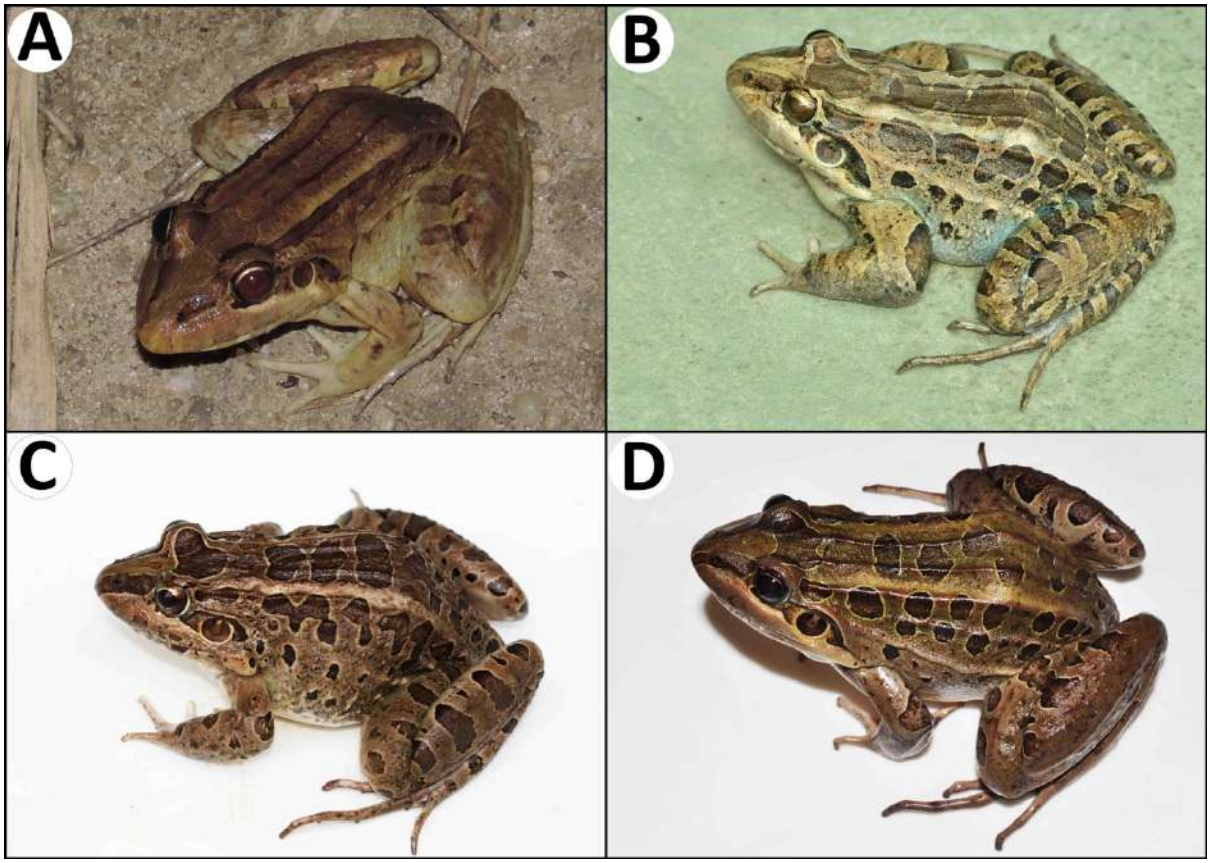

FIG. 9.—Ventral coloration patterns. Localities are given as municipality, state/province (collection number): (A) *Leptodactylus luctator* from La Plata, Buenos Aires (CS2 lineage, LGE 22146), (B) *L. latrans* from Teresópolis, Rio de Janeiro (CFBH 42763); (C) *L.* CS1 lineage from Maracás, Bahia (CS1 lineage, CFBH 42766) all generally lacking pigmentation on ventral body; (D) *L. latrans* from Teresópolis, Rio de Janeiro (CFBH 42766) exhibiting a mottled pattern; (E) *L. luctator* from Posadas, Misiones (CS2 lineage, LGE 22149) exhibiting a black maculated pattern along thigh surface (within red circle) and yellowish melanophores on belly (arrow); and (F) *L. luctator* from Buri, São Paulo (CS2 lineage, CFBH 42814) exhibiting well-marked yellowish melanophores on the belly (arrow).

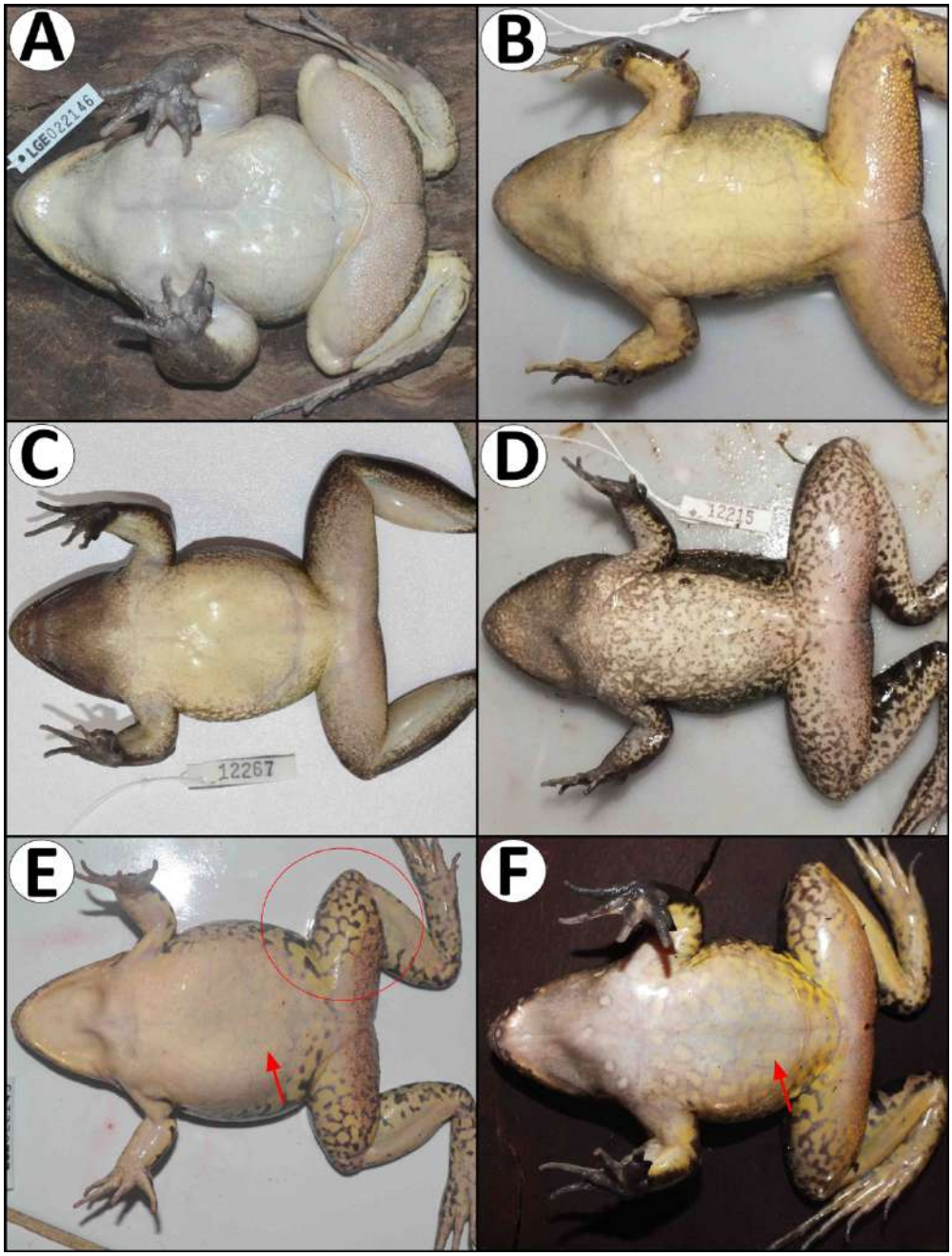

FIG. 10.—Vocal sac, throat coloration and thumb spine morphology. Localities are given as municipality, state/province (collection number): single-lobed vocal sac in (A) *Leptodactylus latrans* from Teresópolis, Rio de Janeiro (CFBH 42765) exhibiting triangular thumb spines; (B) *L.* CS1 lineage from Dário Meira, Bahia (CS1 lineage, CHUNB 53238) exhibiting conical thumb spines; (C) *L. luctator* from Piatã, Bahia (CS2 lineage, CHUFPB 28151) exhibiting rectangular thumb spines; and bilobed vocal sac in (D) *L. macrosternum* from Palmeiras de Goiás, Goiás ("*chaquensis/macrosternum*" lineage, CFBH 26142) exhibiting conical thumb spines.

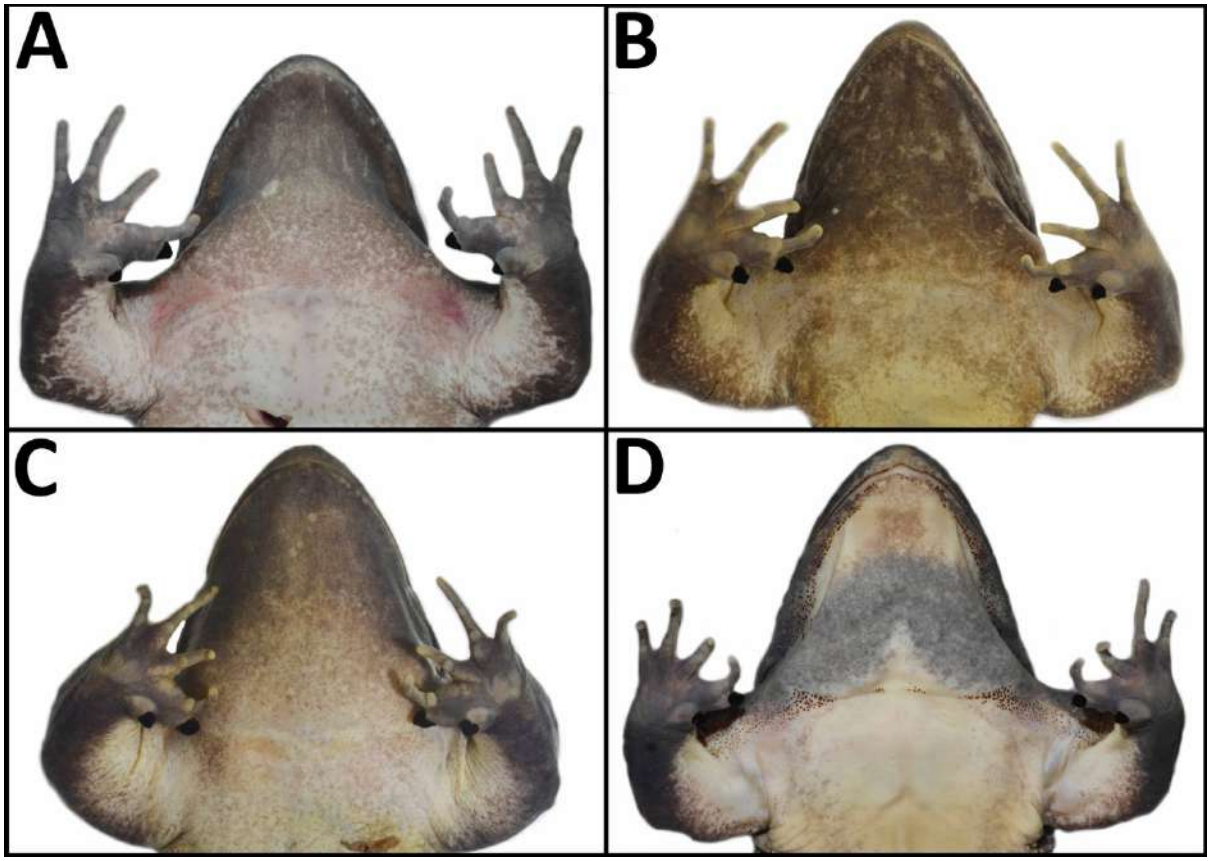

FIG. 11.—Random forest results for species in the *Leptodactylus latrans* complex and *L. macrosternum* based on morphometric variables. (A) Variation in body size and tympanum diameter, the two best predictors of differences among species/lineages. (B) Dotcharts of variable importance scores based on mean decrease of random forest models. The higher the mean decrease in Gini accuracy, the higher the predictor importance. (C) Confusion matrix showing individual classification error. Species abbreviations are the first three letters of the specific epithet shown in letter A legend. Lineages are CS1–3 and CM (*chaquensis*/*macrosternum*). Abbreviations for measurements are in Material and Methods section

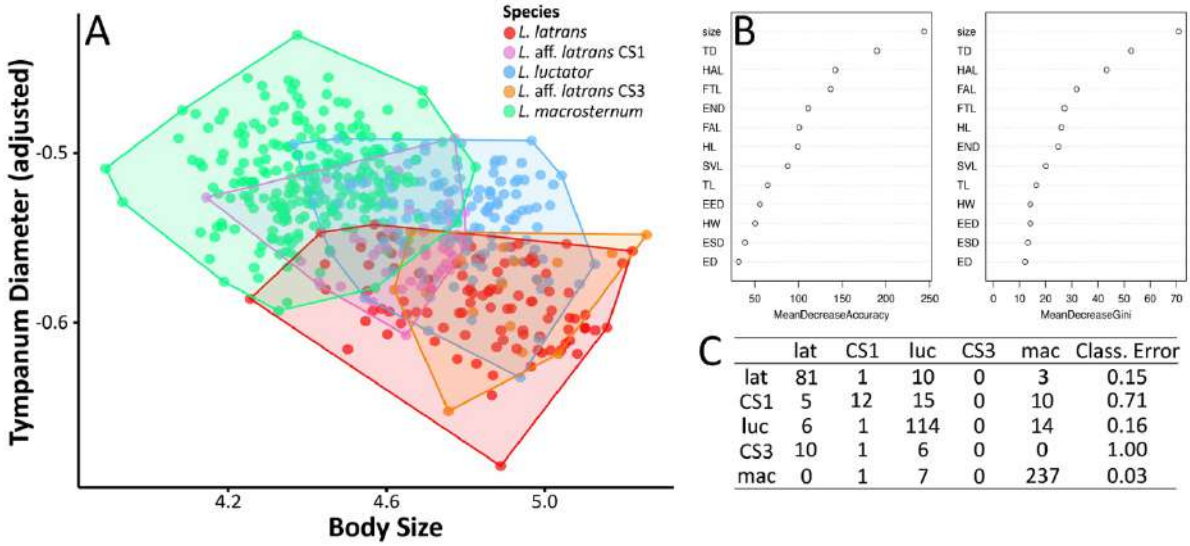

C

	lat	CS1	luc	CS3	mac	Class. Error
lat	81	1	10	0	3	0.15
CS1	5	12	15	0	10	0.71
luc	6	1	114	0	14	0.16
CS3	10	1	6	0	0	1.00
mac	0	1	7	0	237	0.03

FIG. 12.—Advertisement calls (spectrogram and oscillogram from top to bottom) of species in the *Leptodactylus latrans* complex. (A) nonpulsed note with a smooth envelope of a *L. latrans* topotype (CFBH 42772) recorded from Teresópolis, Rio de Janeiro, Brazil (recording ASUFRN668); (B) nonpulsed note of *L. luctator*, with weak amplitude modulations (CS2 lineage, unvouchered), recorded from Uberlândia, Minas Gerais, Brazil (recording Leptod_luctatorUberlandiaMG8aAAGm); (C) an eight-pulse note of *L.* CS1 lineage holotype (CS1 lineage, CHUFPB 28187) recorded from Jacobina, Bahia, Brazil (recording ASUFRN674); and (D) nonpulsed note of *L.* CS3 lineage holotype, exhibiting amplitude modulations (CS3 lineage, CFBH 42804), recorded from Peruíbe, São Paulo, Brazil (recording ASUFRN671). Figures are equally scaled.

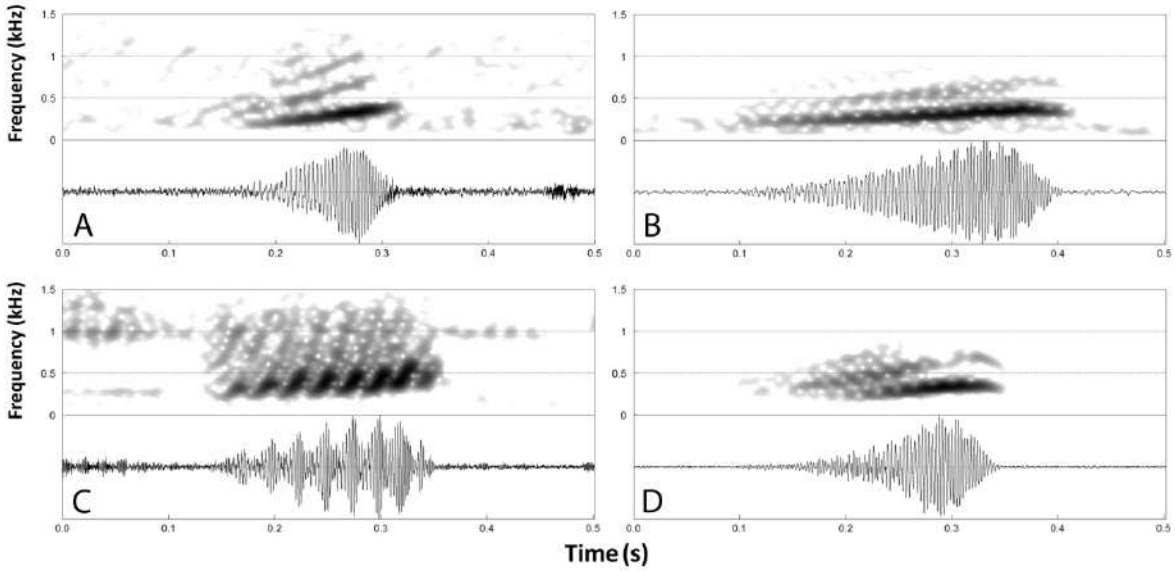

FIG. 13.— Advertisement calls (spectrogram and oscillogram from top to bottom) of species in the *Leptodactylus latrans* species group. (A–C) The three distinct note types (growl, grunt, and trill, respectively) of the vocal repertoire of *L. macrosternum* ("*chaquensis/macrosternum*" lineage, AAG-UFU 4108) recorded from Araguari, Minas Gerais, Brazil (recording Leptod_macrosternumAraguariMG2bAAGm); (D) nonpulsed, frequency-modulated call of *L. insularum* (unvouchered) recorded from Guárico province, Venezuela, by Z. Tárano (recording from Tárano 2010); (E) broad-bandwidth call of *L. silvanimbus* (unvouchered) recorded from Ocotepeque province, Honduras (recording USNM Tape 317, cut 6); and (F) nonpulsed, frequency-modulated call of *L. viridis* (UFMG 15127) recorded from Carlos Chagas, Minas Gerais, Brazil, by P.C. Rocha (recording CBUFMG 139).

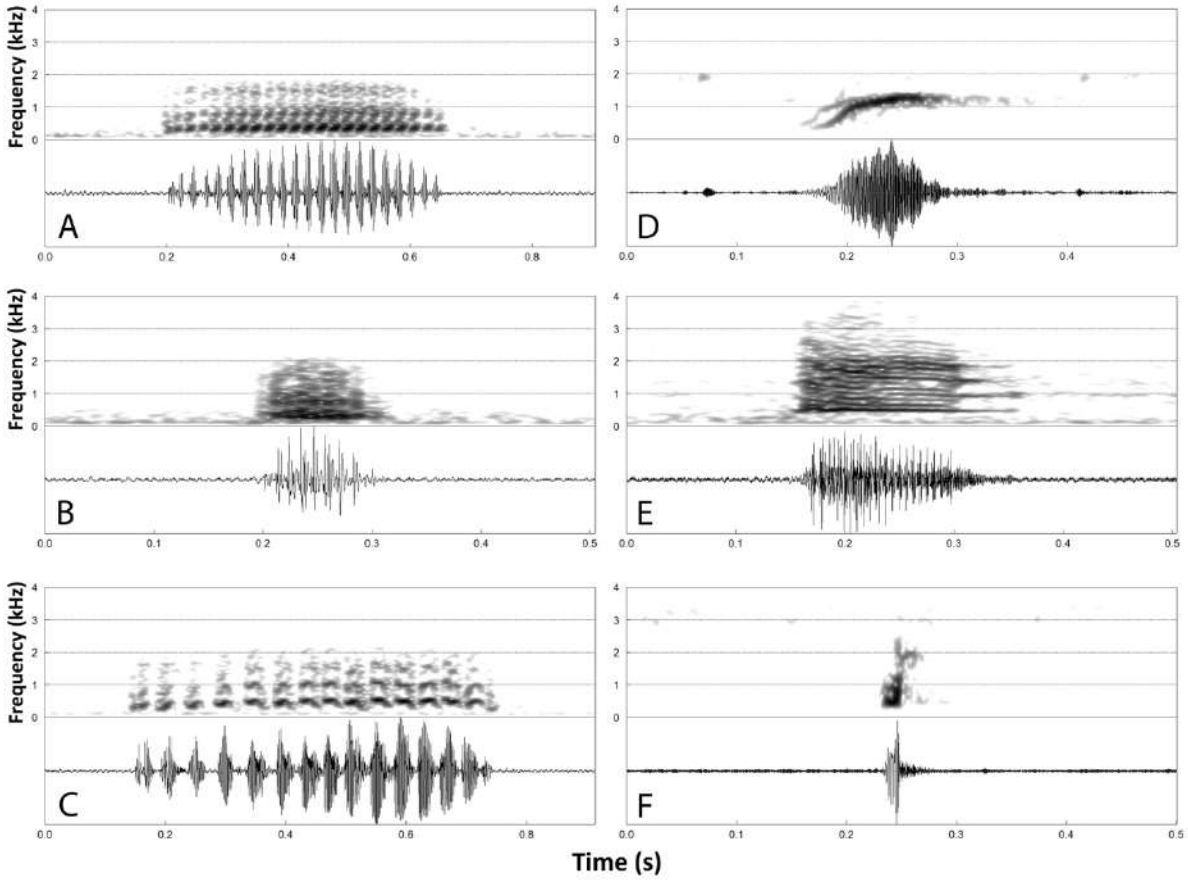

FIG. 14.—Representatives of *Leptodactylus macrosternum*: (A) adult male (MZFS 5141) from Terra Nova Municipality, Bahia, Brazil (Salvador vicinities), photo by F. Camurugi; (B) adult male (MAP-T 379) from Óbidos municipality, Pará, Brazil (Amazonia); (C) adult male (unvouchered) from Macaíba, Rio Grande do Norte, Brazil (Caatinga biome); and (D) adult male (LGE 14821) from Nueve de Julio municipality, Chaco, Argentina (Chaco biome). Note the developed dermal auxiliary fold (F3) of *L. macrosternum* (a diagnostic characteristic), which is absent in species of the *L. latrans* complex.

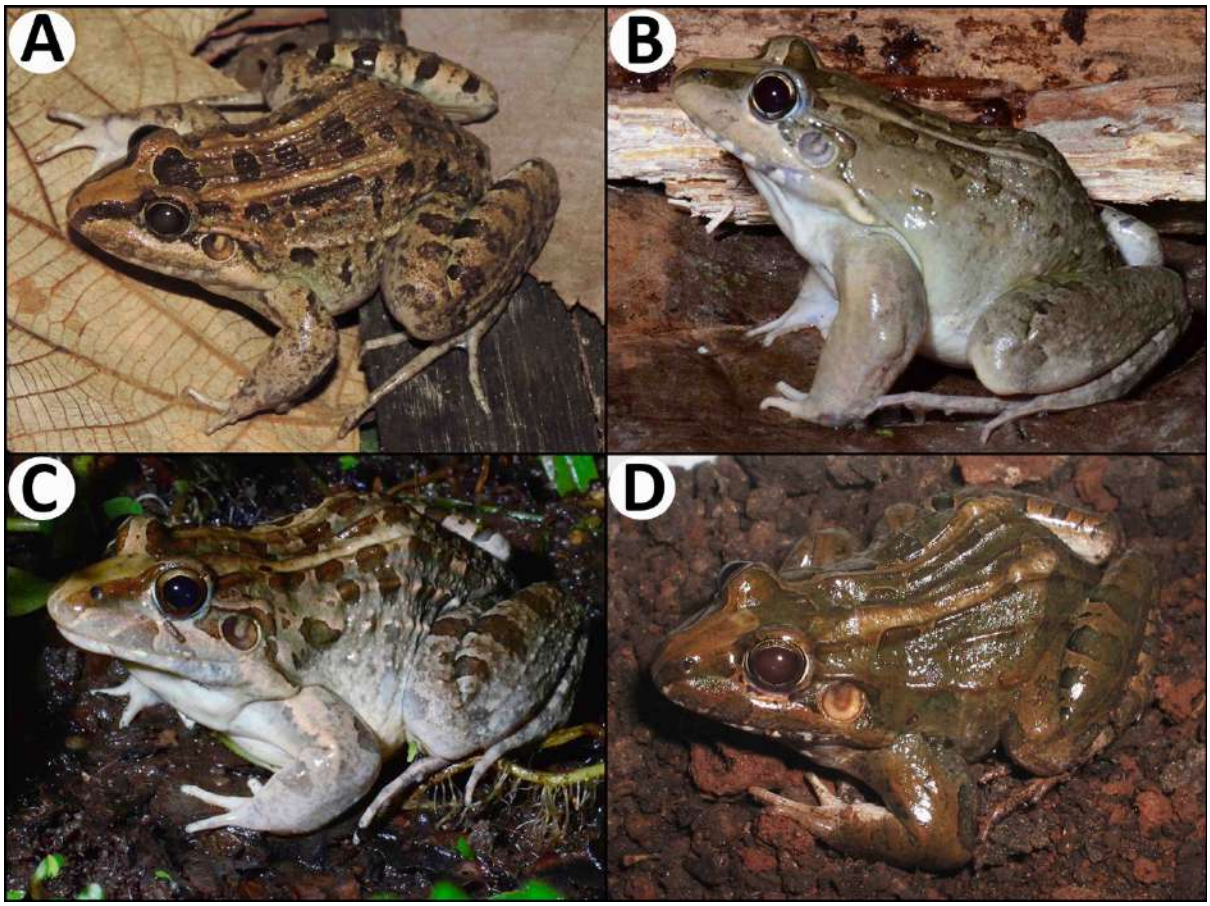

FIG. 15.—Geographic distribution of examined specimens and molecular samples of *Leptodactylus macrosternum* in South America. Star = type locality.

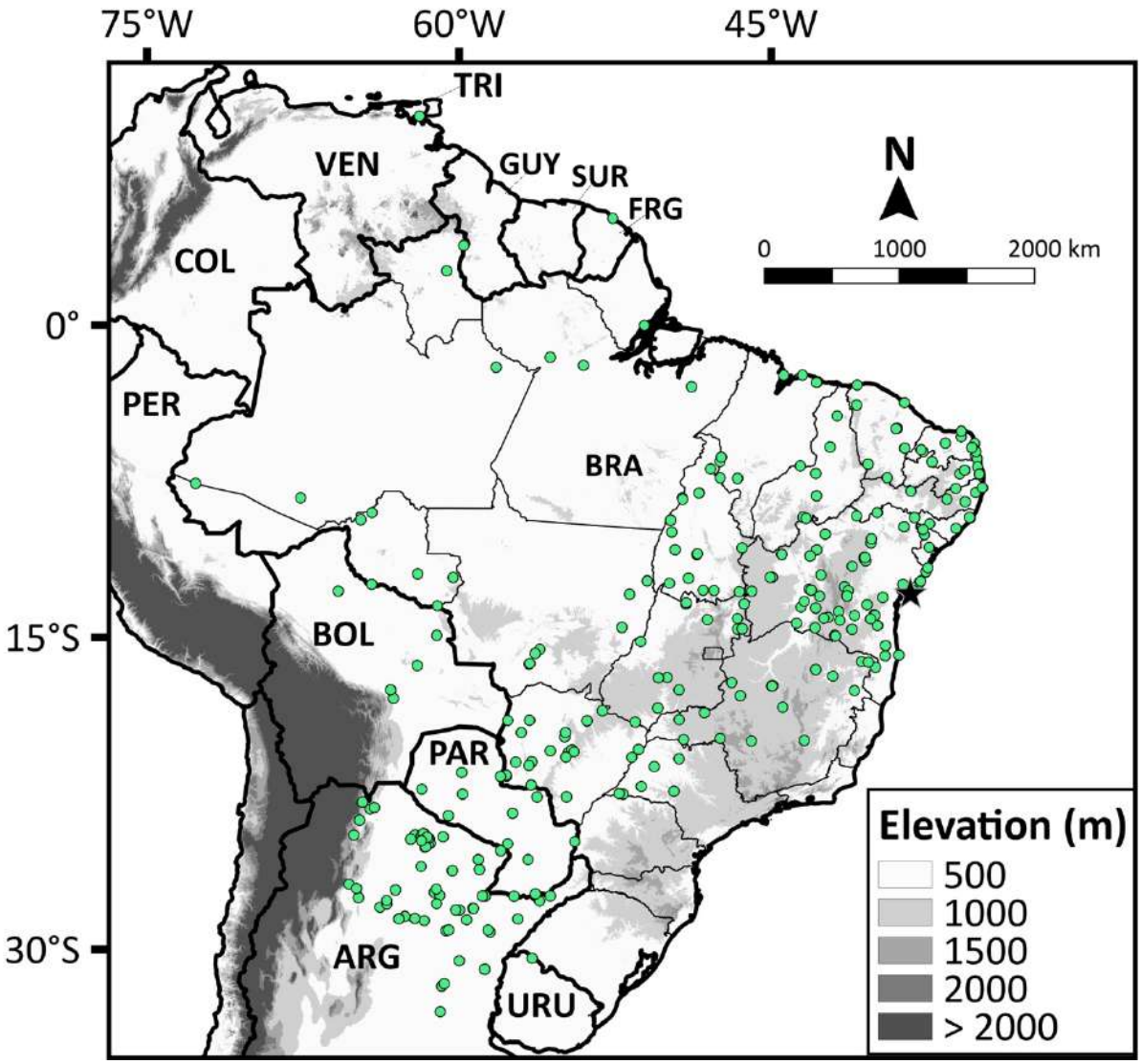

FIG. 16.—Representatives of nominal *Leptodactylus latrans*: (A) adult male (CFBH 42763) from Teresópolis municipality, Rio de Janeiro, Brazil; (B) adult male (AAG-UFU 6148) from Santa Teresa municipality, Espírito Santo, Brazil; (C) unvouchered adult male from Ubatuba municipality, São Paulo, Brazil; and (D) adult female (UFBA 15099) from Salvador municipality, Bahia, Brazil (photo by R.O. Abreu).

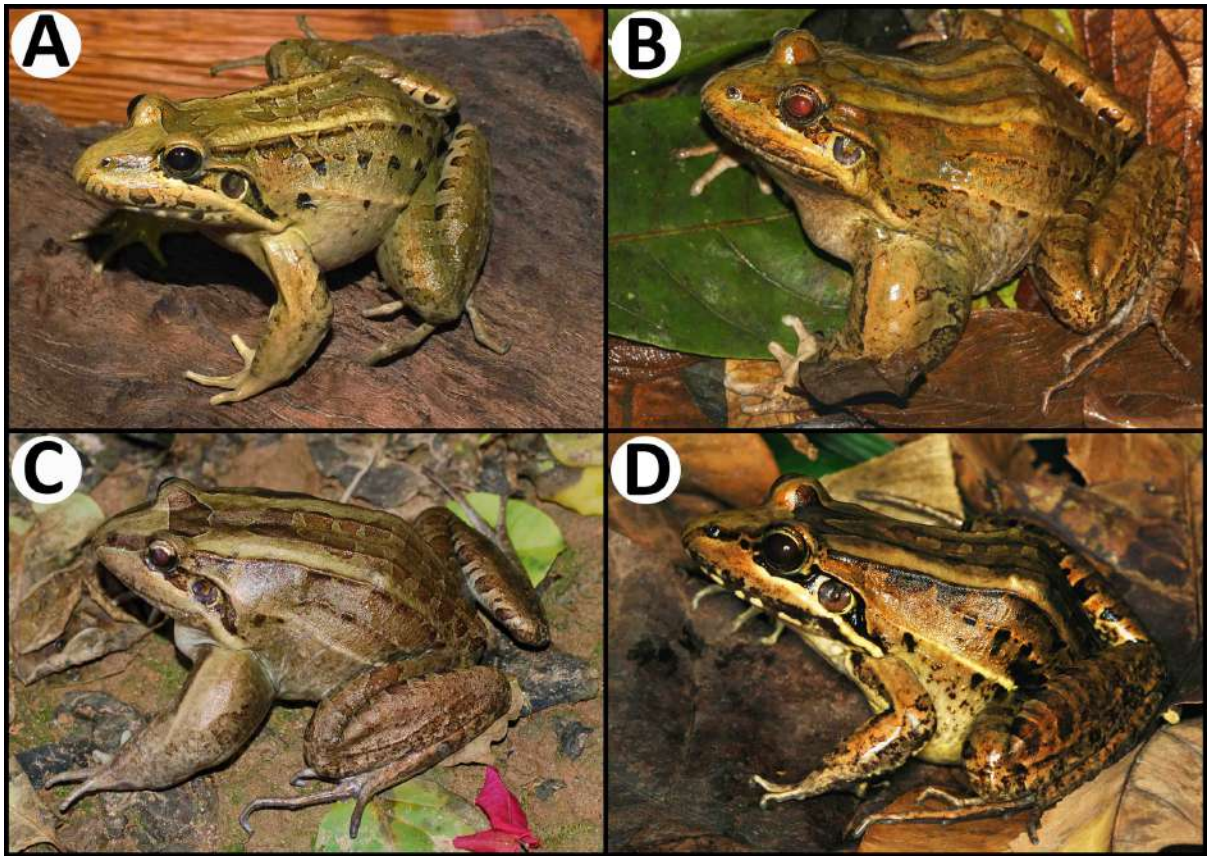

FIG. 17.—Geographic distribution of examined specimens and molecular samples of nominal *Leptodactylus latrans*. Star = type locality.

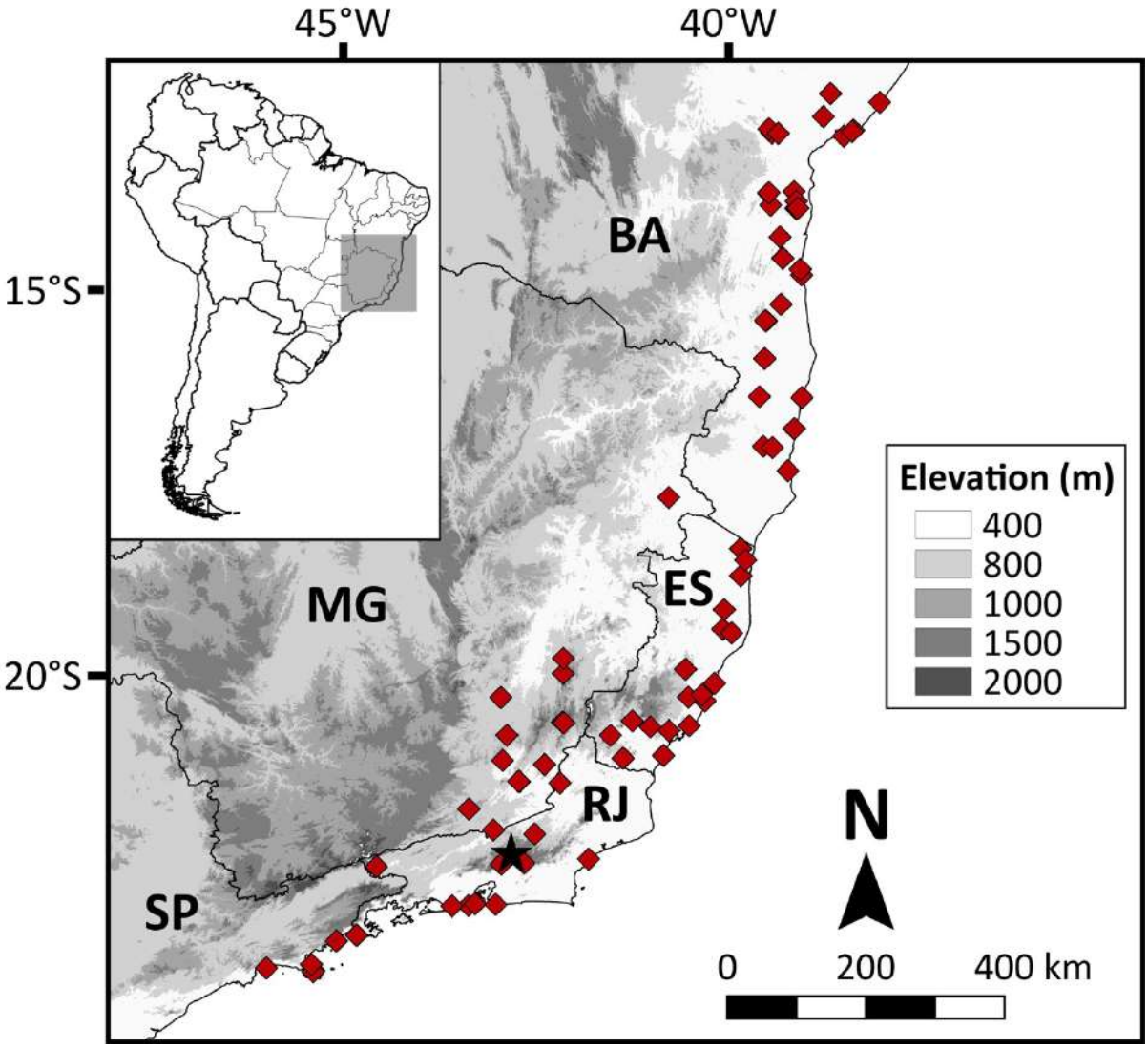

FIG. 18.—Neotype of *Leptodactylus luctator* (LGE 22146). (A) Dorsal and (B) ventral views of body. Views of (C) hand, (D) foot and (E) head. Scale = 1cm. Figures C, D and E not to scale.

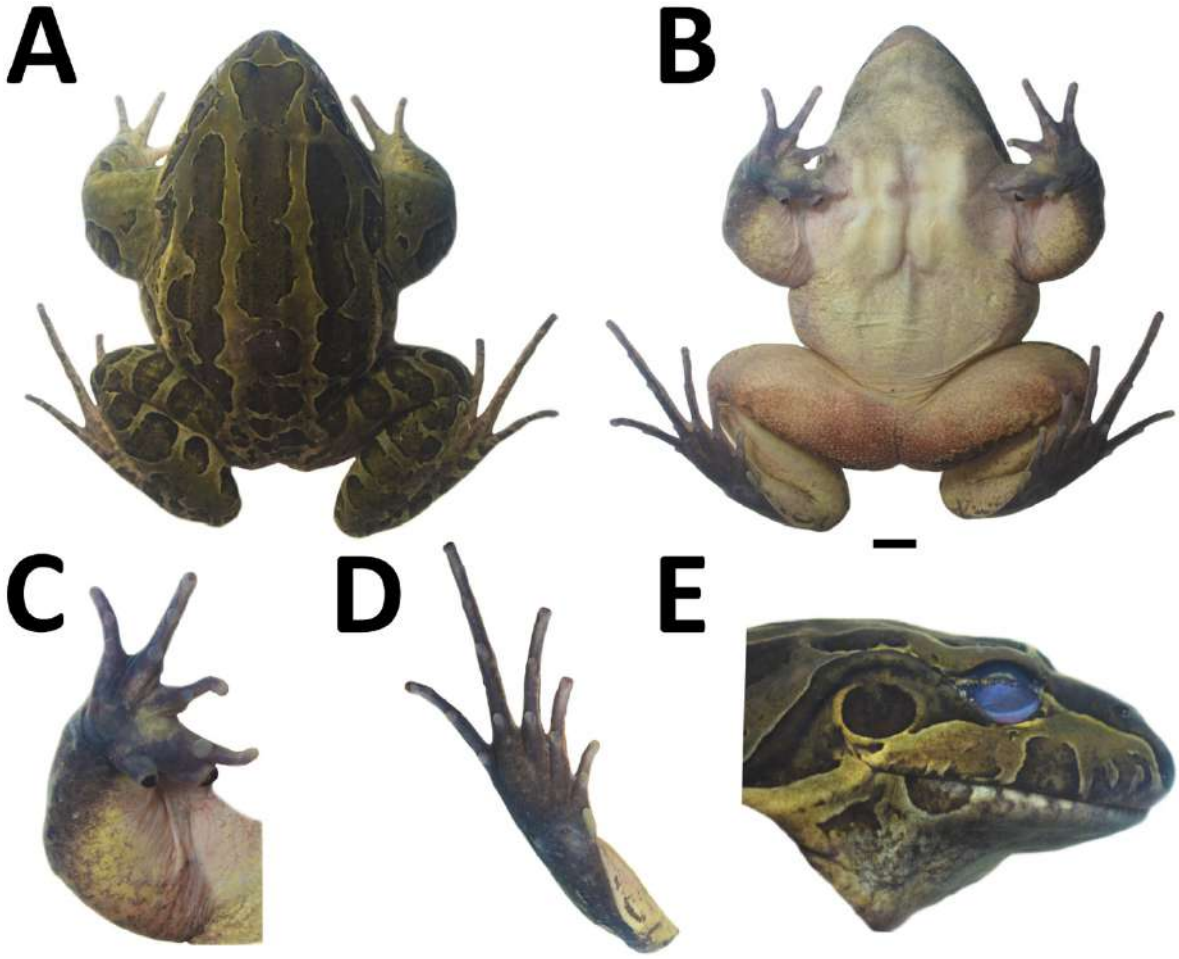

FIG. 19.—Representatives of *Leptodactylus luctator*: (A) neotype, adult male (LGE 22146) from La Plata municipality, Buenos Aires, Argentina; (B) adult male (MZFS 4438) from Piatã municipality, Bahia, Brazil; (C) adult male (voucher MAP1530) from Corumbá municipality, Mato Grosso do Sul, Brazil; and (D) adult male (CFBH 42813) from Buri municipality, São Paulo, Brazil.

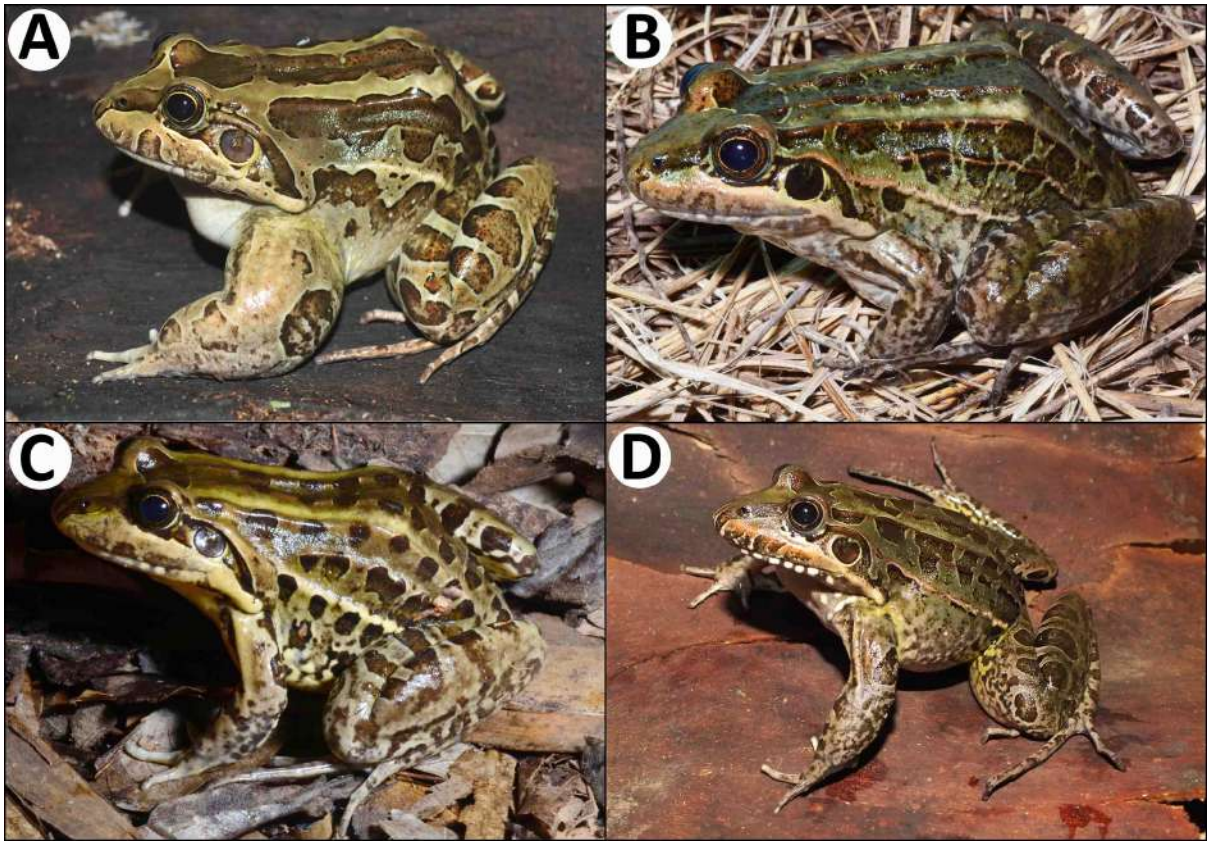

FIG. 20.—Geographic distribution of examined specimens and molecular samples of *Leptodactylus luctator*. Star = type locality.

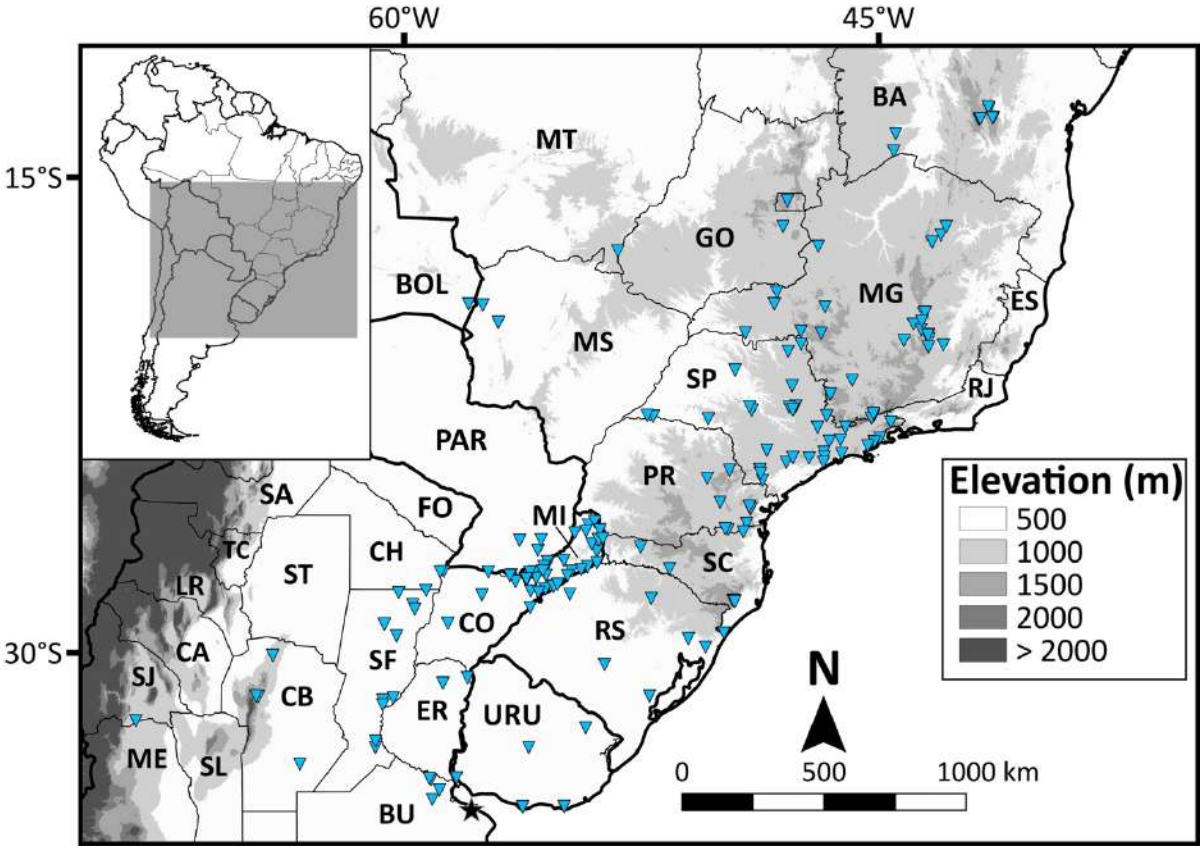

FIG. 21.—Holotype of *Leptodactylus* CS1 lineage (CHUFPB 28187). (A) Dorsal and (B) ventral views of body. Views of (C) hand, (D) foot and (E) head. Scale = 1cm. Figures C, D and E not to scale.

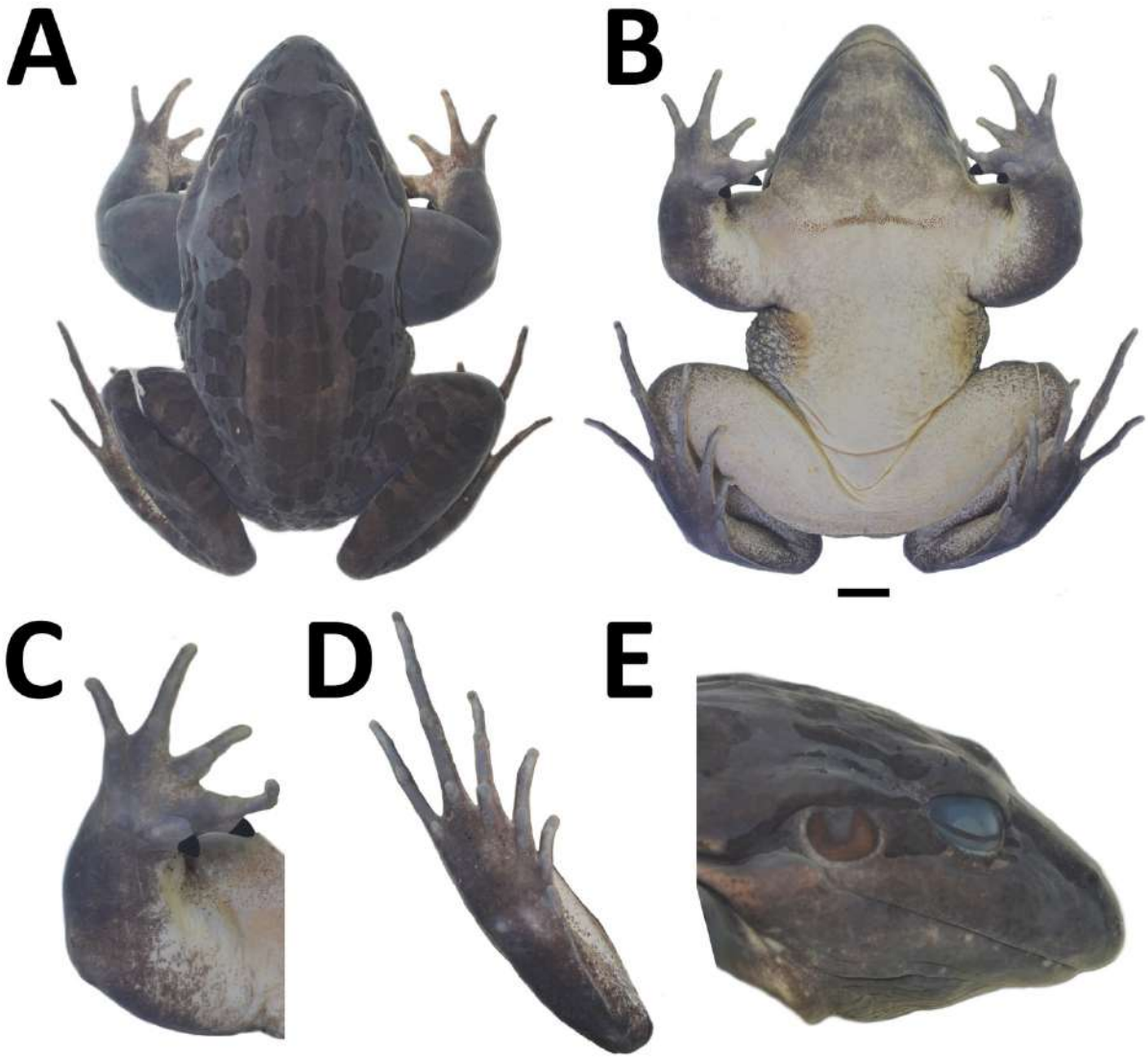

FIG. 22.—Representatives of *Leptodactylus* CS1 lineage: (A) holotype, adult male (CHUFPB 28187), (B) paratopotype, adult male (CHUFPB 28189); (C) paratopotype, adult male (CHUFPB 28184); and (D) paratopotype, adult female (CHUFPB 28193), all from Chapada Diamantina, Jacobina municipality, Bahia state, Brazil.

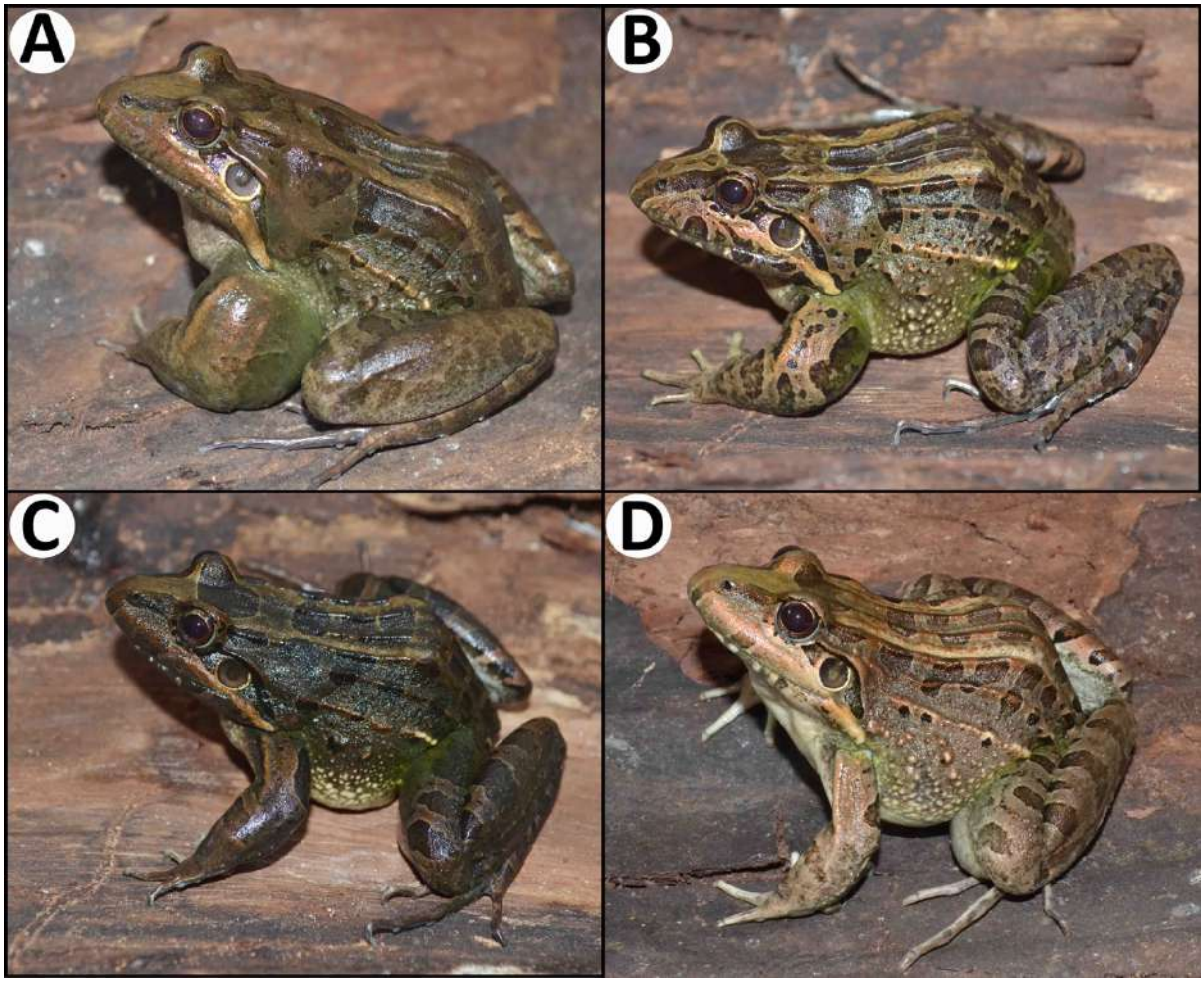

FIG. 23.—Geographic distribution of examined specimens and molecular samples of *Leptodactylus* CS1 lineage. Star = type locality. High altitudinal areas (above 1000 m) represent the boundaries of Chapada Diamantina ecoregion.

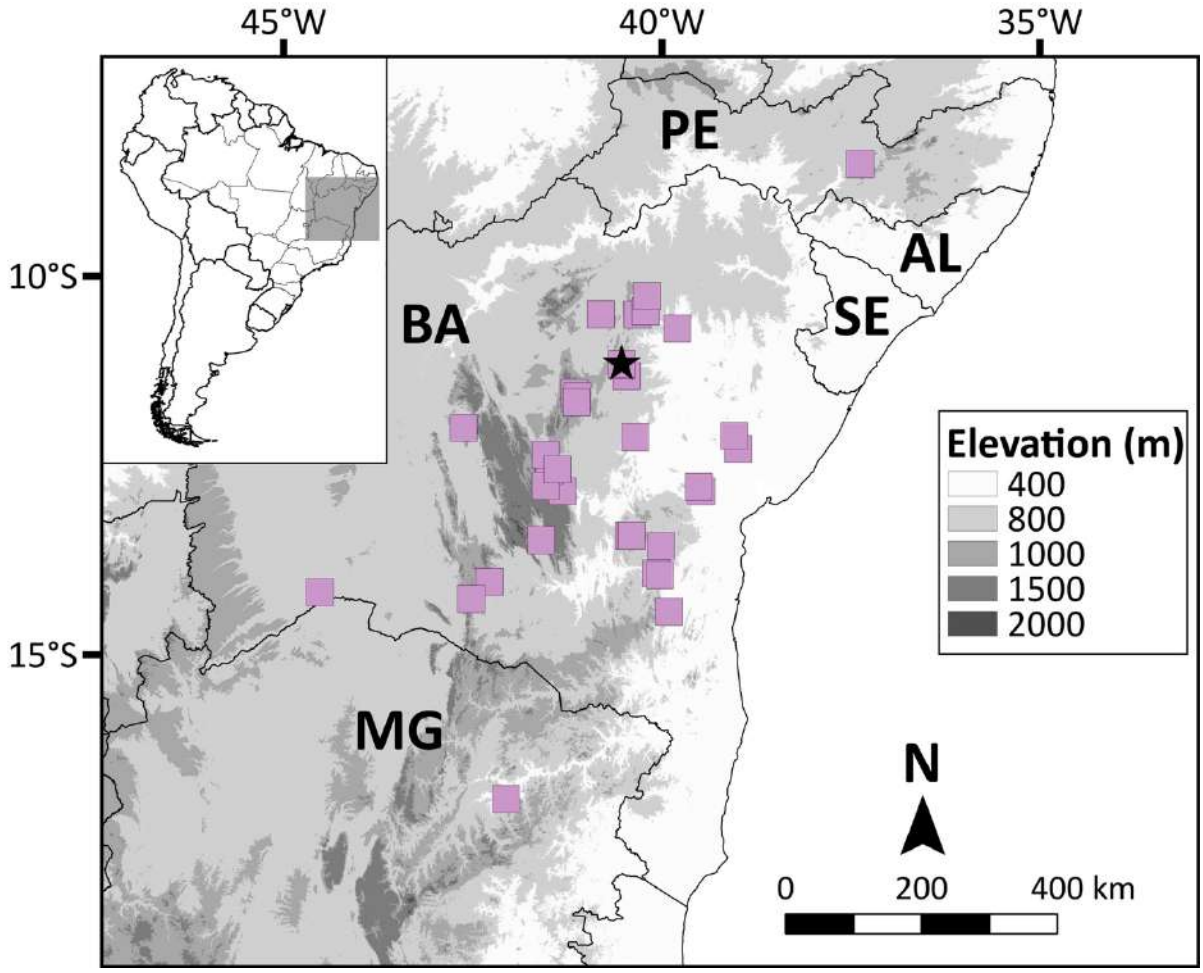

FIG. 24.—Holotype of *Leptodactylus* CS3 lineage (CFBH 42804). (A) Dorsal and (B) ventral views of body. Views of (C) hand, (D) foot and (E) head. Scale = 1cm. Figures C, D and E not to scale.

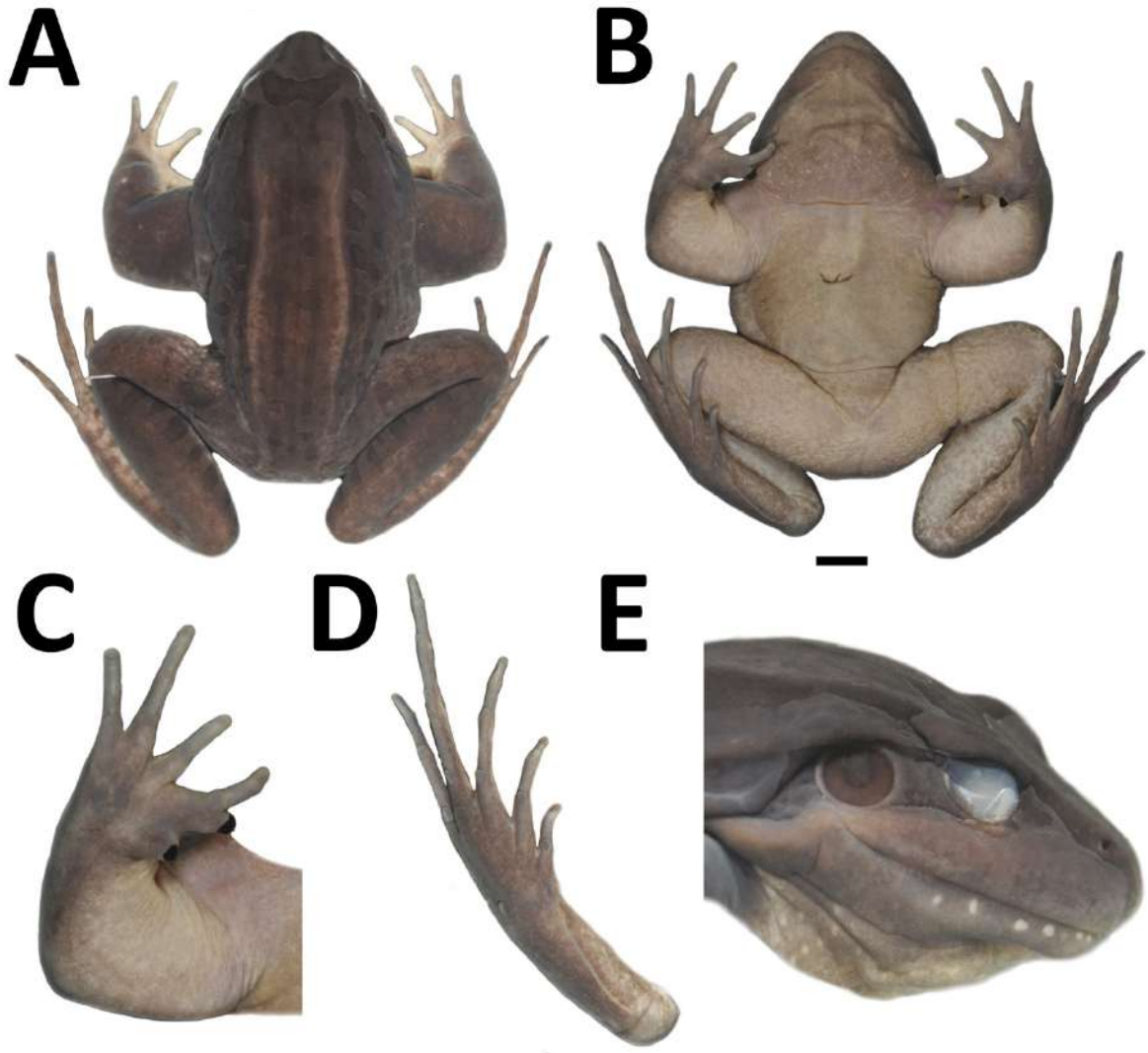

FIG. 25.—Representatives of the *Leptodactylus* CS3 lineage: (A) holotype, adult male (CFBH 42804); and (B) paratopotype, adult male (CFBH 42807) from Peruíbe municipality, São Paulo, Brazil.

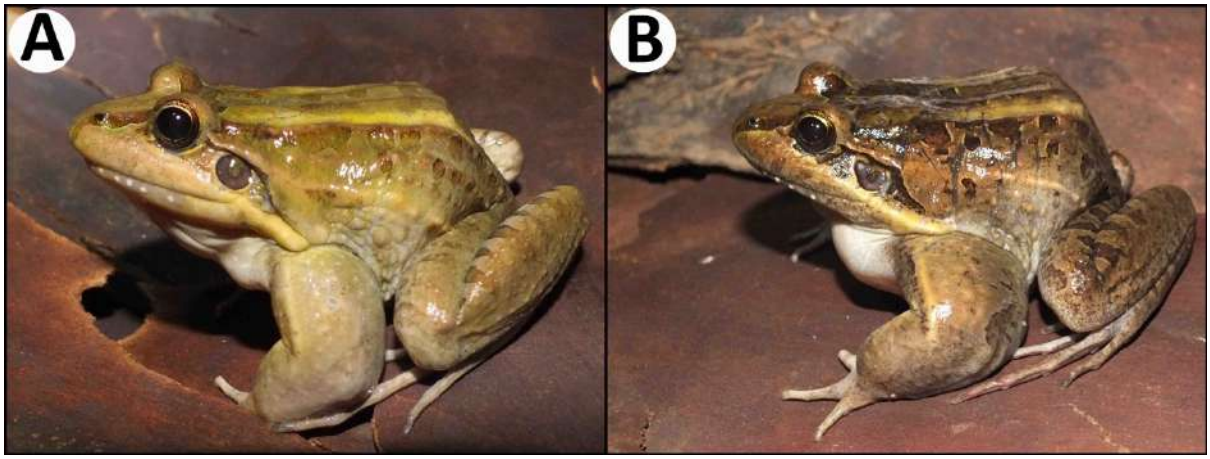

FIG. 26.—Geographic distribution of examined specimens and molecular samples of *Leptodactylus* CS3 lineage. Star = type locality

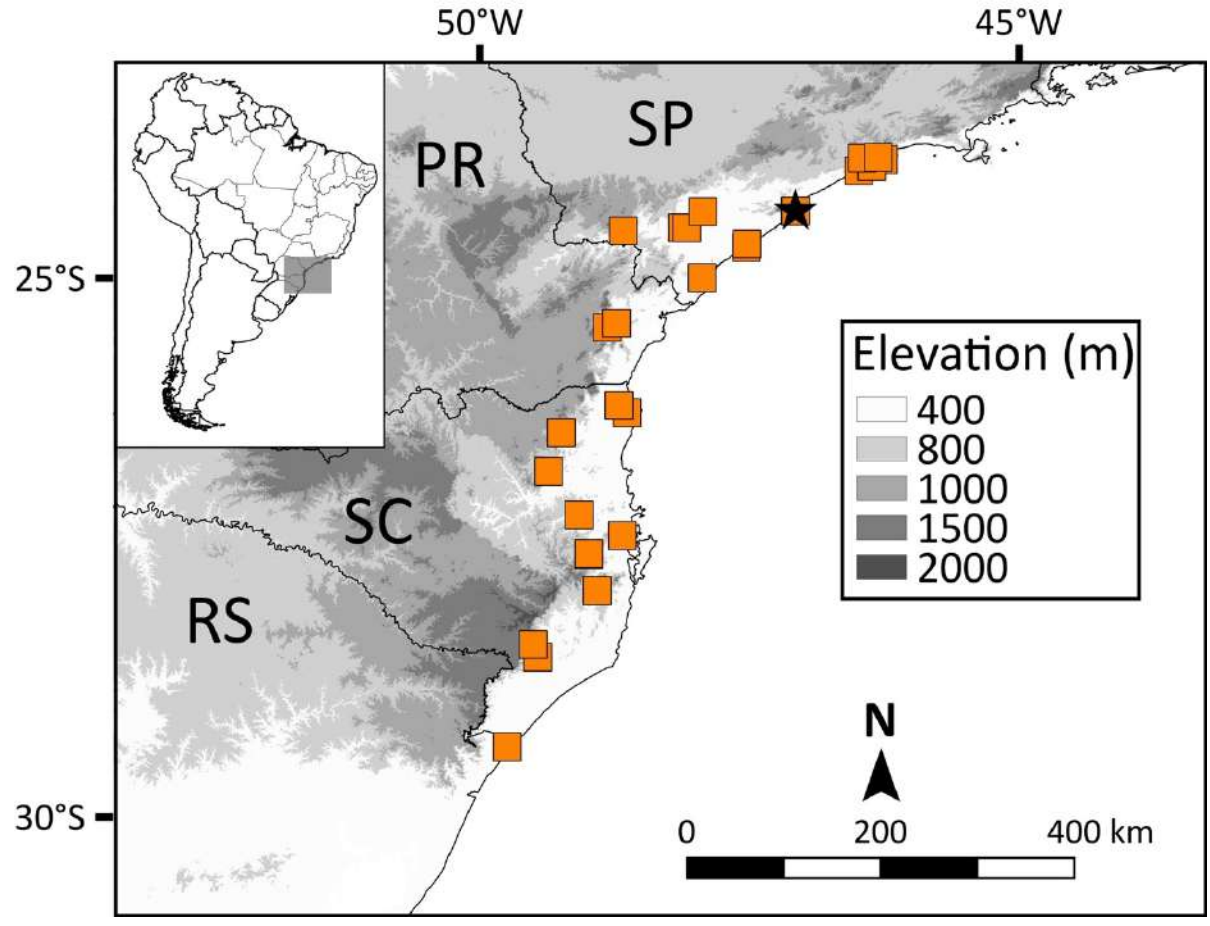

Capítulo II

Ecological isolation and Pleistocene climatic oscillations shaped genetic diversification in the widespread South American butter frogs

Felipe de M. Magalhães[a,*], Felipe Camurugi[a], Mariana Lyra[b], Diego Baldo[c], Marcelo C. Gehara[d], Célio F.B. Haddad[b], and Adrian A. Garda[e]

[a] *Programa de Pós-Graduação em Ciências Biológicas, Universidade Federal da Paraíba– UFPB, Centro de Ciências Exatas e da Natureza, Cidade Universitária, João Pessoa, PB 58000-000, Brazil*

[b] *Instituto de Biociências, Universidade Estadual Paulista, Campus Rio Claro, Departamento de Zoologia e Centro de Aquicultura (CAUNESP), Laboratorio de Herpetologia, Cx. Postal 199, 13506-900, Rio Claro, São Paulo, Brazil*

[c] *Instituto de Biología Subtropical (IBS, CONICET-UNaM), Laboratorio de Genética Evolutiva, Facultad de Ciencias Exactas, Universidad Nacional de Misiones, Félix de Azara 1552, CPA N3300LQF, Posadas, Misiones, Argentina*

[d] *American Museum of Natural History, Herpetology, Central Park West at 79th St., New York, NY 10024, USA*

[e] *Laboratório de Anfíbios e Répteis (LAR), Departamento de Botânica e Zoologia da Universidade Federal do Rio Grande do Norte, Campus Universitário. Lagoa Nova, CEP 59078-900, Natal, RN, Brazil*

*Author for Correspondence: felipemm17@gmail.com

Abstract: Phylogeographic studies primarily focus on the major role of landscape topography in driving lineage diversification. However, ecological isolation is also being evoked as a primary mode of genetic diversification in the absence of geographic barriers to gene flow. Furthermore, these two factors are not mutually exclusive and can act in concert, making difficult to evaluate their relative importance in shaping patterns of genetic variation in nature. Sister species that are both broadly distributed across environmental gradients are good models to investigate the relative importance of both geographic and ecologic factors on driving patterns of phylogeographic divergence. Herein, we use sequences of two mitochondrial and four nuclear genes to investigate the timing and diversification patterns of species pertaining to the *Leptodactylus latrans* complex, which harbors four morphologically cryptic species with broad distributions across eastern South America. We generated multilocus molecular dataset from 144 individuals out of a 327 COI mitochondrial genetic set, sampling species/populations throughout the group entire range. We identified that three species exhibited signals of populational genetic structure, which were highly supported in Bayesian clustering analysis. Mitochondrial gene tree and node supports were also congruent with the tree topology estimated using *BEAST. The origin of this species complex dates back to the Miocene (ca. 7.6 Mya), but most diversification events occurred during late Pleistocene likely as the result of climatic oscillations during interglacial cycles. Further, significant patterns of environmental niche divergences among species in the *L. latrans* complex imply that ecological isolation is the primary factor promoting diversification, mostly because phylogenetic breaks are associated with environmental transitions rather than topographic barriers at both species and populational scale. We provided new insights about diversification patterns and processes within a species complex of broadly and continuously distributed group of frogs along South America.

Key words: Atlantic Forest; Background tests; BPP; Cryptic diversity; Divergence Times; Diversification patterns; Leptodactylidae; *BEAST.

1. Introduction

Understanding patterns and processes underlying the diversification of organisms is of utmost interest to evolutionary biologists (Mayr 1964), which has intensified with the growing field of phylogeography. Since their dawn phylogeographic studies have primarily focused on the spatial distribution of lineages on a landscape and associated geographic factors such as distance, topography (e.g., geological events), and physical barriers to genetic differentiation throughout lineages evolutionary history (Avise, 2000). Nevertheless, recent phylogeographic studies are now evoking other isolation mechanisms that are not topography-driven and that are also important for promoting genetic differentiation (Irwin 2007). For instance, environmental and ecological divergence between lineages can also lead to phylogeographic structure posed by natural selection on populations in ecologically divergent habitats (Wang and Summers, 2010; Wang and Bradburd, 2014). Likewise, topographic heterogeneity (Rodriguez et al., 2015), climatic oscillations (Byrne 2008), sea-level fluctuations (Fazolato et al., 2017; Senczuk et al., 2019) and biotic interactions (Waters, 2011) have also been increasingly reported as primary modes of genetic diversification worldwide. Although alternative drivers of genetic differentiation are becoming more widely appreciated (Gehara et al., 2017a; Vasconcellos et al., 2019), relatively few studies have examined the roles of geographic and ecological factors in explaining phylogeographic patterns at different stages of diversification and throughout heterogeneous habitats at continental scales (e.g., Pyron and Burbrink, 2009; Wang et al., 2013).

The South America Neotropical region is one of the most species-rich regions of the world, harboring several hotspots of biodiversity (Mittermeier et al., 1998) and also highly

diverse in habitats (e.g., Ab'Saber, 1977; Vieira et al., 2015). Diversification processes along this region are mostly linked to geomorphological features and climatic fluctuations (Hoorn et al., 2010; Rull, 2011; Turchetto-Zolet et al., 2013; Smith et al., 2014). More recently, Carnaval and Moritz (2008) proposed that during glacial periods of the Pleistocene areas of climatic stability along the Atlantic Forest (AF) acted as refugees in a fragmented landscape as forests retracted due to colder and drier climatic conditions, prompting population isolation and genetic diversification, hereafter referred as CM model (Carnaval-Moritz). Therefore, AF species underwent a common set of processes resulting from fragmentation within glacial refugia (Carnaval et al., 2009; Tonini et al., 2013), range expansions via postglacial colonization (e.g., Martins, 2011; Thomé et al., 2014; Firkowski et al., 2016), and are likely experiencing secondary contacts among historically divergent lineages (Fitzpatrick et al., 2009; Sabbag et al., 2018). Indeed, the CM model expectations have been recurrently corroborated, in papers analyzing patterns of genetic diversity among distinct vertebrate and invertebrate organisms distributed along the AF (Batalha-Filho et al., 2010; D'Horta et al., 2011; Carnaval et al., 2014). Although diversification processes linked to Pleistocene climate oscillations are still controversial (Rull, 2008, 2011), the CM model was raised as a possible explanation for the high genetic diversity and elevated species richness found along the AF when compared to other Biomes (Morellato and Haddad, 2000; Carnaval and Moritz, 2008).

Conversely, Leite et al. (2016) proposed that during glacial cycles the AF expanded towards the exposed continental shelfs as global sea-levels decreased after the Last Interglacial (LIG) period, favoring AF associated taxa to expand instead of retract to climatically stable forest fragments, which played a minor role in shaping genetic diversification along the AF. Moreover, sea-level transgressions/regressions cycles intensified during repeated Pleistocene glaciation cycles (Hansen et al., 2013), which certainly caused modifications to the coastline (Suguio et al., 1988), and could have

promoted lineage diversification by creating physical barriers along lowland continuously distributed taxa (e.g., Fitzpatrick et al., 2009; Fazolato et al., 2017; Gehara et al., 2017a). Hence, geographic and ecological isolating mechanisms can act in concert, precluding the recognition of the primary mode of lineage diversification. This becomes especially intricate in regions where topography, climatic oscillations and biomes are changing constantly and concomitantly, as is the case of the South America Neotropical region (Vuilleumier 1971; Hoorn et al., 2010). Species that are distributed widely across environmentally and geographically heterogeneous landscapes offer opportunities to investigate distinct patterns of diversification, and are particularly valuable for understanding the role of geographic and ecological factors on genetic differentiation.

The *Leptodactylus latrans* complex (also known as butter frogs in Brazil) encompasses four large-sized (SVL varying from 80–120mm) morphologically cryptic species broadly and continuously distributed throughout 3,000 km across eastern South America with occurrence in five distinct biomes (taxonomy and species limits was thoroughly reviewed by Magalhães et al., Capítulo I). These four species cluster into a highly supported monophyletic clade (e.g., share a most recent common ancestor) within the *L. latrans* species group. They also exhibit a remarkably similar external morphology and advertisement calls (except for *L*. aff. *latrans* CS1), which is of paramount importance for intraspecific recognition in frogs, acting as isolating mechanisms precluding secondary contact and restricting hybridization (Wells, 2007). Nevertheless, multilocus molecular data revealed deep genetic structure, large genetic distances and apparent low gene exchange, as all four species were recovered robustly with high node supports (Magalhães et al., Capítulo I). Among these, two species are endemic to the AF (*L. latrans* and *L*. aff. *latrans* CS3), while *L. luctator* partially occurs across higher altitudes within the AF, but also along open formations within Pampas, Chaco and Pantanal Biomes. The fourth species, *L*. aff. *latrans* CS1, is mainly distributed throughout along open

formations associated to the Chapada Diamantina ecoregion and vicinities (for a characterization of this ecoregion see Lima and Nolasco, 2015) along interior of Bahia State, northeastern Brazil, which is surrounded by the Caatinga, a seasonally dry forest Biome (Lima and Nolasco, 2015). Despite being restricted to the Atlantic Forest Biome, *L. latrans* and *L.* aff. *latrans* CS3 are not forest-dependent species, and all four species share similar reproductive patterns: they all reproduce along temporary ponds in open fields or along forest edges, are abundant and generalist feeders, preying mostly on invertebrates and also vertebrates such small-medium sized frog species. Moreover, all four species are mostly low altitude specialists (predominantly occurring in areas below 700 meters above sea level), while *L. luctator* can reach high plain sites at 1400m above sea level across Brazil mainland.

The species in the *L. latrans* complex are widely and continuously distributed across environmental (e.g., from seasonally dry to tropical moist forests) and altitudinal (from sea-level to highlands) gradients, show strong signs of geographic and genetic structure, and low morphologic and acoustic divergence, making them an excellent biological group to address how geographic and ecological isolation shaped evolutionary history within this group of frogs. With recent advances in methods for assessing niche divergence through the use of ecological niche models (ENMs) allied to coalescent genetic analyses (Carstens and Richards, 2007), it is now possible to weigh the relative importance of these two factors in explaining patterns of phylogeographic structure between groups (Thorpe et al. 2008; Wang et al., 2013).

In this paper, we investigate populational genetic structure, divergence times and the effects of late Pleistocene climatic changes on the demographic history and genetic diversity in a complex of cryptic species broadly distributed along the eastern region of South America. Our goals are to clarify which processes and patterns are involved in the diversification of *Leptodactylus latrans* species complex, and to use these taxa to understand temporal and geographic patterns of diversification in eastern South America. We used a

multi-locus dataset (two mitochondrial and four nuclear loci) to characterize geographic populational structure relative to the presence of putative barriers (geographic) and transitional environmental (ecologic) areas in the range of these frog species. If diversification is driven by allopatric isolation, we expect that phylogeographic breaks match major topographic barriers to gene flow. Instead, if ecological isolation mechanisms are playing a major role in shaping diversification we expect that phylogeographic breaks coincident with environmental transition areas and that environmental niches are also divergent between sister lineages.

2. Material and Methods

2.1. Taxon and gene sampling and laboratory procedures

Magalhães et al. (Capítulo I) extensively sampled and delimited the major evolutionary lineages within the *Leptodactylus latrans* species group, which encompasses the *L. latrans* species complex. To further investigate genetic diversity and diversification patterns of the four species in the *L. latrans* complex, we sequenced two mitochondrial (mtDNA) and four nuclear (nuDNA) genes for 144 specimens from 131 localities along eastern South American region (see Table S1 for a full list of samples and localities), representing a subset of the 327-cytochrome oxidase I (COI) genetic dataset provided by Magalhães et al. (Capítulo I). Because species exhibit from restrict (e.g., *Leptodactylus* aff. *latrans* CS1 and CS3) to wide (e.g., *L. latrans* and *Leptodactylus* aff. *latrans* CS2) geographic ranges, we have distinct genetic sample sets per species, but we equally and continuously sampled across their entire distribution range. Specimens and tissues were obtained from distinct scientific collections from Argentina, Brazil, Paraguay, and Uruguay which are also listed in Table S1.

We extracted DNA from muscle/liver tissues using the standard ammonium (Maniatis et al. 1982) or salt (Bruford et al. 1992) precipitation methods. Polymerase chain reaction (PCR) amplifications were carried out using Taq DNA Polymerase Master Mix (Ampliqon S/A, Denmark) to amplify fragment sequences of mtDNA Cytochrome Oxidase I (COI) and 16S rRNA (16S) genes, and nuDNA c-myc exon 2 (cmyc2), tyrosinase precursor (Tyr), β-Fibrinogen Intron 7 (Fib7), and proopiomelanocortin (POMC) genes (for primers and PCR protocols see Table S2 in Supplementary material). In most occasions, we conducted PCR product cleaning using enzymatic purifications (shrimp alkaline phosphatase and exonuclease I; Werle et al. 1994). Purified or unpurified PCR products were sent to Macrogen Inc. (South Korea) for purification (when needed) and sequencing. We aligned all sequences using MAFFT algorithm (Katoh et al. 2002) default configuration implemented in Geneious v1.8.7 (Kearse et al. 2012). We sequenced the same genes for individuals of *L. viridis*, *L. bolivianus* and *L. guianensis* to use as outgroups when needed.

We assumed heterozygosity for nuclear sequences when the sequences of the chromatogram contained strong equal double peaks, typically more than 50% of neighboring homozygotic peaks height. We recovered phase information from nuclear sequences using PHASE algorithm (Stephens et al., 2001) implemented in DNAsp 5 (Librado and Rozas, 2009). To estimate the best substitution model of each gene fragment (Table S3), we used the Bayesian Information Criterion (BIC) implemented in jModelTest 2.1.4 (Darriba et al., 2012).

2.2. Haplotype network genealogies

To investigate genealogical relationships, we estimated gene trees using Bayesian inference in BEAST software v1.10.4 (Suchard et al. 2018). We estimated independent gene trees for each nuclear loci, while for the mitochondrial genes (16S+COI) we recovered single topology by concatenating the tree priors in BEAST, but partitioning among genes in order to

accommodate for evolutionary rate heterogeneity among partitions. We used the most appropriate substitution model for each gene (Table S3) and ran 20,000,000 generations sampled every 2,000 generations for all five genes using the Coalescent model as tree prior. We visually assessed convergence of the Monte Carlo Markov Chain (MCMC) runs and effective sample sizes (ESS values > 200) using Tracer 1.7 (Rambaut et al., 2018). We discarded 25% of generations as burn-in, and the consensus tree for each locus was inferred with TreeAnnotator v1.10.4 (http://beast.community/treeannotator). We used these gene trees (without outgroups) to estimate haplotype networks in HAPLOVIEWER (http://www.cibiv.at/~greg/haploviewer). Individuals were assigned to populations following STRUCTURE/Geneland results (see below).

2.3. Bayesian genetic assignment

Because missing data for POMC was considerably high (33% out of 144 individuals), we only used cmyc2, Fib7 and Tyr nuclear genes for subsequent assignment tests, including individuals with at least two loci. Moreover, we ran the following assignment tests separately for each of the four species to increase detectability of genetic populational structure rather than the species limits, which has been shown to be large by molecular means (Magalhães et al., Capítulo I).

To assign individuals to genetic clusters, we used a model-based clustering method implemented in STRUCTURE 2.3.4 (Pritchard et al., 2000). Using multi-locus genotypic data, STRUCTURE divides individuals into genetic clusters (K) that both minimizes deviations from Hardy–Weinberg and linkage equilibrium within each cluster and also calculates fractional membership of individuals to each cluster (Q). To convert sequences to STRUCTURE input, we used the program xmfa2struct (available at: http://www.xavierdidelot. xtreemhost.com/clonalframe.htm), which encodes each variable site as an allele. We performed ten independent runs for each K (ranging from 1 to 6

populations for each species). We ran the analyses for 50,000 iterations as burn-in and 100,000 additional iterations implementing the linkage model and uncorrelated allele frequencies. The most likely K was determined based on the method of Evanno et al. (2005) via the on-line program Structure Harvester v.0.6.94 (Earl and von Holdt, 2012).

Given the impossibility of validating K = 1 by means of Evanno's methods (Janes et al., 2017), we also estimated the optimal number of populations with the Bayesian program Geneland v4.0.8 (Geneland R library; Guillot et al., 2005) in the R 3.5.3 environment (R Corte Team 2018) to complement STRUCTURE assignment analysis. Unlike STRUCTURE, Geneland also consider geographic location on individual assignment to a given cluster K. We also ran Geneland population assignment model separately for each of the four species as follows: We performed 10 independent runs with K values ranging from 1 to 6 populations, assuming an uncorrelated allele frequency, and a spatial model with uncertainty on coordinates. Each run consisted of 5,000,000 MCMC iterations, thinning interval of 5,000 and a burn-in phase of 200 iterations. We assessed the MCMC posterior probability plot to determine runs convergence and compared with the posterior estimates of the number of populations.

Results of both STRUCTURE and Geneland assignment tests were largely congruent (Fig. 1a). Nevertheless, some populational breaks within CS1, CS3 and *L. luctator* lineages were only validated by one of these programs (see Fig. 1a). Therefore, we also implemented the Bayesian Phylogenetics and Phylogeography species delimitation method (BPP4) (Flouri et al., 2018) to test for all genetic breaks identified by both STRUCTURE and Geneland analyses combined. BPP is a multi-locus method that implements a reversible jump MCMC algorithm under the multispecies coalescent model to delimit species and estimate a species-tree. For this analysis we used two mitochondrial and three nuclear genes (POMC not included). We ran BPP with four different prior combinations for population size (theta = θ)

and divergence time (tau = τ) parameters as proposed by Leaché and Fujita (2010): (i) large ancestral population sizes and ancient divergence [IG(3,0.2) for both parameters]; (ii) large population sizes and recent divergences [IG (3,0.2) for theta; and IG(3,0.002) for tau]; (iii) small population sizes and recent divergences [IG(3,0.002) for both parameters]; and (iv) small population sizes and deep divergences [IG(3,0.002) for theta; and IG(3,0.2) for tau]. We ran all prior combinations at least twice using both algorithms available in BPP (0 and 1) and adjusted the finetuning to ensure swapping rates between 0.30 and 0.70. We performed the A11 analysis, which jointly delimit species and estimate a species-tree (Yang and Rannala, 2014), using the species tree estimated in *BEAST as the guide tree. Each run consisted of a burn-in phase of 10,000 iterations followed by a sampling phase of 400,000 iterations, with a frequency of 4 iterations per sampling.

2.4. Genetic diversity and historical demography

To assess genetic diversity, we estimated haplotype diversity (Hd) and per-site nucleotide diversity (Pi) using DnaSP (Librado and Rozas, 2009). We also applied the neutrality tests of Tajima's *D* (Tajima, 1989), Fu's Fs (Fu, 1997) and Ramos-Onsins and Rozas's R2 (Ramos-Onsins & Rozas, 2002) to detect significant deviations from the null hypothesis of neutral evolution and constant population size. We estimated significance levels of neutrality tests through 10,000 coalescent simulation replicates in DnaSP. Because neutrality tests were significant for some populations (Table S4), we then performed the multilocus coalescent-based extended Bayesian skyline plot (EBSP; Heled and Drummond, 2008) implemented in Beast 2.5.2 (Bouckaert et al., 2019) to estimate changes in effective population sizes over time. We used all loci, mitochondrial and nuclear (except for POMC), and the 16S substitution rate as a reference, with 0.007 substitutions/site/Mya (High Posterior Density [HPD] 95% = 0.005–0.009 substitutions/site/Mya) based on previous estimates of Weigt et al. (2005), and Gehara et al. (2017a). The COI mitochondrial segment

proportionally accumulates nucleotide mutation at a rate twice as fast as the 16S gene (Vences et al., 2005; Lyra et al., 2017). Therefore, we also set the COI mean substitution rate as 0.014, and relaxed the clock so that the HDP 95% confidence interval prior ranged from 0.008 to 0.03 substitutions/site/Mya. For both clock calibrations, we employed a strict molecular clock and uniform priors to set the HPD interval. We implemented the same substitution models provided in **Table S3**. We ran 50,000,000 MCMC simulations sampled every 5,000 chains. We checked for run convergence using Tracer 1.7 (Rambaut et al., 2018) by visually checking effective sample size (ESS > 200).

2.5. Species divergence times

We estimated a dated species tree using all loci, mitochondrial and nuclear, for all samples in *BEAST 1.8.4 software (Drummond et al., 2012). We grouped individuals into 8 populations that were identified by STRUCTURE/Geneland and supported as distinct evolving lineages with significant posterior probabilities (> 0.95) in BPP. To run the species-tree we also set mean substitution rates of 16S and COI at 0.007/site/Mya (HPD 95% = 0.003–0.009) and 0.014/site/Mya (HPD 95% = 0.009–0.03), respectively. Substitution rates of the nuclear gene were coestimated by the program. We assumed a relaxed clock model with uncorrelated lognormal distribution for the mitochondrial genes and a strict clock for the nuclear genes, and a Yule tree prior (see Table S3 for details about substitution models). We ran the MCMC chain for 500,000,000 iterations, sampling every 50,000 iterations, and discarded the initial 25% iterations as burn-in. To check for convergence among runs, we performed three independent analyses using different seed numbers and combined logs with LogCombiner v1.8.4. We checked for runs convergence by visually checking ESS (> 200) values in the log files using Tracer v1.7. We summarized the species tree in Tree Annotator, which was drawn in FigTree 1.6 (Rambaut, 2014).

2.6. Ecological niche models

To characterize the environmental niche of all deeply divergent species within the *L. latrans* complex (delimited by Magalhães et al., Capítulo I), we assembled a minimum of 40 localities for each species (Proosdij et al. 2016). Because species in the *L. latrans* complex exhibit high levels of cryptic morphology (Magalhães et al., Capítulo I), we used as occurrence point data all localities associated to molecular-vouchered individuals plus the database of species occurrences from museum records assembled by Magalhães et al. (Capítulo I). Occurrence points data are given as molecular voucher points (total point data considering museum records within brackets): 86(178) samples for *L. latrans*, 155(311) for *L. luctator*, 50(69) for *L*. aff. *latrans* CS1, and 31(42) for *L*. aff. *latrans* CS3, respectively.

We generated environmental niche models (ENM) using bioclimatic data from Worldclim (Hijmans et al. 2005) and elevation data from NASA Jet Propulsion Laboratory (available at https://landscape.jpl.nasa.gov/) at a spatial resolution of 2.5 arc-minutes. The first 19 "Bioclim" layers, reflecting aspects of precipitation and temperature, were used in addition to elevation data. Prior to analyses, raster layers were clipped to enclose the entire South American continental extent (-82 to -34 degrees of longitude and -58 to 15 degrees of latitude), which is reasonable considering *L. latrans* complex broad distribution along eastern South America (see Magalhães et. al., Capítulo I). We generated ENM with *dismo* package in R (Hijmans & Elith, 2013) using the Maxent 3.3 algorithm (Phillips et al., 2006). To avoid over-parameterization (Rissler & Apodaca, 2007), we excluded highly correlated bioclim variables (Pearson correlation coefficients < 0.8) keeping those biologically relevant for the group (Table S5). We used 75% of presence points withheld to train the model and 25% of the remaining points to test it, through 20 replications with cross-validation. The model performance was based on the area under the receiver-operating characteristic curve (AUC).

With no absence data for these frog species, AUC scores represent the model's effectiveness at distinguishing presence from the background (Phillips et al. 2006).

Finally, we projected present-day ENMs into bioclimatic variables predicted for two different past scenarios, Last Interglacial (LIG; ca. 130 kya) and Last Glacial Maximum (ca. 21 kya) from CCSM4 (Community Climate System Model) models. Because Pleistocene climatic oscillations directly shaped landscape and biomes ranges (Carnaval et al., 2014; Gehara et al., 2017b), we expect to correlate past environmental niche scenarios to populational demographic changes among species/lineages in the *L. latrans* species complex.

2.7. Niche overlap/divergence

To evaluate the degree of niche similarity among species in the *Leptodactylus latrans* complex, we compared ENMs produced for all species using *phyloclim* R package to perform background similarity tests between group pairs using 1,000 replications. For such purpose, we utilized the Schoener's *D* (Schoener, 1968) and Hellinger's based *I* metrics (Warren et al., 2008). Both metrics range from 0 to 1, with 0 representing no niche overlap and 1 corresponding to identical niches between the two compared groups. The list of variables used in each background similarity comparison is given in Appendix I (Table S6). To avoid drawing background values from areas without species occurrence, we used the minimum convex polygon surrounding the original occurrence records of each species as their respective geographic range, which was comprehensively evaluated using genetic and morphologic data by Magalhães et al. (Capítulo I).

In order to examine niche divergence at a finer scale, we also assembled datasets at populational level for species that showed genetic and geographic populational structure (identified in our phylogeographic analyses) and have a minimum of 15 localities sampled (only *L. latrans* and *L. luctator* fit these abovementioned requirements). For the niche

characterization at the populational scale, we only considered as occurrence data points molecular voucher specimens (depicted in Fig. 3a): we compiled 42 localities for the lucN and 28 for lucS lineages, respectively and 17 localities for the latN and 18 for latS lineages. We applied the same methodological procedure for species and populational scale.

3. Results

The final alignment for the 16S and COI mitochondrial genes comprises 350 bp and 507bp, respectively. Alignments of the nuclear gene segments included 852 bp of cmyc2 (43 haplotypes), 359 bp of FIB7 (29 haplotypes), and 510 bp of Tyr (54 haplotypes), and 407 bp of POMC (7 haplotypes) (Table S4**; Fig. 1b**). Among 144 sequenced individuals, the percentage of missing data for Fib7, Tyr, cmyc2 and POMC nuclear genes were 12%, 6%, 1% and 33%, respectively, and 11% for 16S and COI? mitochondrial DNA. Moreover, both mitochondrial gene tree topology and monophyly of the *Leptodactylus latrans* complex (Fig. 1) agree with previous proposals for the *L. latrans* species group (Magalhães et al., Capítulo I).

3.1. Haplotype network genealogies and genetic diversity

We found high nucleotide and haplotype diversity within COI, while summary statistics revealed slightly lower diversity within 16S and nuclear genes when compared to COI (Table S4). Nevertheless, haplotype networks showed a relatively high genetic variation in nuclear gene haplotypes within the *Leptodactylus latrans* species complex (Fig. 1b), except for POMC for which only 7 haplotypes were recovered. Moreover, among FIB7, POMC and Tyr nuclear genes only a single haplotype is shared between at least two of the four species delimited in Magalhães et al.'s (Capítulo I) taxonomic review, and haplotype sharing occurred in a slightly higher proportion at the populational level. For instance, we observed 43 haplotypes for cmyc2, of which 4 are shared between at least two distinct

lineages, 54 haplotypes for Tyr (9 shared), 29 haplotypes for FIB7 (8 shared), and 7 haplotypes for POMC (4 shared). Such amounts of incomplete lineage sorting could indicate that lineages diverged under presence of gene flow, lineages diversified in a short timespan relative to population sizes or is a result of secondary contact (Fig. 1). Additionally, species in the *L. latrans* complex are considered allopatric with very few sympatry/syntopy zones occurring along their distribution (Magalhães et al., Capítulo I). Likewise, we observed a similar spatial pattern of allopatric distribution within lineages, except for one locality in the Brazilian state of Minas Gerais where two lineages belonging to *L. latrans* (latN and latS) and the lucN lineage were sampled in sympatry, and another locality at Chapada Diamantina in central Bahia State where lucN and CS1S lineages are sympatric. In both cases, we found no evidence of admixture among individuals in any gene (mitochondrial and nuclear). Although lineages are not necessarily allopatric, there is a strong pattern of geographic structure at populational scale as well. Interestingly, CS3 seems to share haplotypes at a higher proportion with the southern population of *Leptodactylus latrans* (latS), than southern and northern populations of *L. latrans* are sharing between themselves (Fig. 1).

3.2. Bayesian genetic assignment

The population assignment test of STRUCTURE identified an optimal value of two clusters for all the four species in the *Leptodactylus latrans* complex (Fig. 1), totaling eight populations. Conversely, Geneland identified a total of nine genetic clusters with posterior probability over 0.65 (Supplementary Fig. 1). The results of both assignment tests were overall congruent, except that Genelend showed one additional break within CS1 (splitting between higher and lower altitudinal areas of Chapada Diamantina; Supplementary Fig. 1) and *luctator* (splitting apart the Serra Geral population in the Brazilian State of Santa

Catarina; Fig. 1, 3b), that were not identified by STRUCTURE. Moreover, Geneland did not detected genetic breaks within CS3 lineage, as identified by STRUCTURE.

All of the four prior combinations used in BPP consistently supported with high PP (1.0) the existence of six lineages (latN, latS, lucN, lucS, lucSC, and CS3) within the *Leptodactylus latrans* complex, which instead showed incongruences regarding the delimitation of CS1N and CS1S lineages. For instance, only the runs with theta prior assuming large population sizes [IG(3,0.2)] grouped the lineages CS1N and CS1S into a single species with significant probability > 0.95 (Fig. 1a), while theta priors assuming small population sizes [IG(3,0.002)] support these two lineages with significant probability (PP > 0.98). Moreover, all prior combinations lumped the two lineages within CS3 (identified only by STRUCTURE) into a single species with significant support (PP = 1.0). Indeed, this break within CS3 did not exhibit cohesive phylogenetic nor geographic structure and likely represent a program artifact, given the impossibility of validating K = 1 by means of Evanno's methods (Janes et al., 2017). Therefore, BPP analyses validated a total of seven or eight lineages with high posterior probability depending on theta prior we employ. Interestingly, all breaks validated by BPP, which were validated with nuclear data only, match the mitochondrial lineages recovered in the gene tree (Fig. 1a).

Despite mitochondrial and nuclear genes overall congruence, some mitochondrial introgressions were detected between lucN and lucS lineages, and between latN and latS individuals. For instance, six individuals clustered within lucS mitochondrial lineage were assigned to lucN by the nuclear genes-based assignment tests, while one individual from lucN was assigned to lucS lineage. Moreover, only a single individual from latN was assigned to the latS lineage.

3.3. Historical demography

The neutrality tests values were not consistent among algorithms, genes and within lineages. For instance, neutrality tests values were significant for mitochondrial genes (except for CS1 lineage), which instead were mostly not significant for nuclear genes (Table S4). The inconsistency among nuclear and mitochondrial genes may be attributed to differences in mutation-accumulation rates, which are overall more accelerated in the mitochondrial genome (Lynch, 2007). Therefore, abrupt changes in populational effective sizes are more efficiently detected by mitochondrial genes, especially when these changes occurred in a recent timespan, which might be the case. Nonetheless, these results may indicate signs of recent demographic expansion. According to Ramos-Onsins and Rozas (2002), Fs and R2 tests are more robust in detecting events of demographic expansion, and Fs is more suitable for larger samples while R2, for smaller samples.

The EBSP analysis revealed a pronounced increase in effective population size for all populations distributed within the AF boundaries such as latN, latS, lucN and CS3 at around 130,000 years ago. Moreover, a very subtle increase in effective population size was detected for lucS lineage at about 20,000 years ago (Fig. 2). Conversely, EBSP revealed no abrupt changes on effective populations sizes during the last 500,000 years for CS1S lineage (a lineage restricted to the Chapada Diamantina ecoregion).

3.4. Species divergence time

*BEAST and BPP recovered the same species tree topology with high probabilities (PP > 0.98) for all internal nodes (see Fig. 3b). The resulting tree from *BEAST shows that the origin of the *Leptodactylus latrans* species complex and the time to *L. luctator*, *L. latrans* and *L.* aff. *latrans* CS3 most recent common ancestor are both within the boundaries of late Neogene around 7.6 Mya (95% HPD = 4.7–10.8 Mya) and 4.7 Mya (95% HPD = 3.1–6.8

Mya), respectively. Diversification between the AF species (*L. latrans*, CS3) falls within the transition between Plio-Pleistocene boundaries around 2.3 Mya (95% HPD = 1.0–3.8 Mya). Conversely, all other splitting events within species started during the middle-to-late Pleistocene about 1 Mya (HPD 95% = 0.4–1.7 Mya) with the early divergence within *L. luctator* (Fig. 3b). Moreover, all lineages within *L. latrans*, *L. luctator* and *L.* aff. *latrans* CS1 exhibited an apparently synchronous diversification during late Pleistocene around 200,000–300,000 years ago (Fig. 3b). Because nuclear and mitochondrial genes are mostly reciprocally monophyletic (as showed by haplotype networks) and *BEAST topology was recovered with high node support indicates that lineages diversified under a scenario where gene flow is absent or very restricted (Degnan and Rosenberg, 2009).

3.5. Ecological niche models

The predicted suitable areas for species in the *Leptodactylus latrans* complex based on the ENMs matched their actual occurrences closely (Fig. 4). The mean value of the area under the operating receiver curve (AUC) was similar between the four species (> 0.95 for all species), indicating better than random predictions (0.5 = random, 1 = maximum). Considering pairwise comparisons between present projections of species ENMs, models consistently did not predict overlapping geographic areas well (e.g., the environmental niche of one species projected to the other). The background between pairwise comparisons among all four species in the *L. latrans* complex were all below 0.3 for Schoener's *D* index (Fig. 5a), and below 0.57 for Hellinger's based *I* index (Table S6) and are statistically lower ($p < .05$) than the null distribution (Fig. 5), indicating that species are more divergent in climate niche than expected from the available climate conditions (99% confidence intervals are mostly not overlapping). This pattern was also observed at populational scale as background tests indicated niche divergence between lucN and lucs

lineages with significative support (Fig. 5b). In contrast, background tests between latN and latS lineages exhibited higher levels of niche overlap without significative support (Fig. 5b), indicating niche conservatism.

We recovered a similar patterns of niche suitability influenced by Pleistocene climatic oscillations among all four species in the *L. latrans* complex (Fig. 4). For instance, we observed that there is a trend of habitat displacement toward northern areas during the LGM and towards southern areas during LIG period. Moreover, we found more fragmentation of suitable habitats during the LIG than in the LGM, especially for AF endemic species (e.g., *latrans* and CS3). Interestingly, the ENMs did not identify suitable areas where nowadays is the current distribution of *L.* aff. *latrans* CS3 during the LGM, and predicted the occurrence only in northern areas within AF biome.

4. Discussion

4.1. Timing of diversification and biogeographic patterns

We identified that three of the four species delimited in Magalhães et al. (Capítulo I) exhibit considerable genetic diversity with geographically structured populations that diverged during late Pleistocene, totaling eight independently evolving lineages. Considering populational phylogeographic breaks, all delimitation analyses validated two genetically structured populations belonging to *Leptodactylus latrans* (Fig. 1). The break between northern (latN) and southern (latS) populations matches the Doce River break, as predicted by CM model for AF associated taxa (Carnaval and Moritz, 2008). The Doce River has been considered a barrier to gene flow in previous phylogeographic studies (see Leite and Costa, 2012). However, its relative importance as a major barrier to gene flow is questionable because it runs through an area of noticeable environmental/climatic shift (Carnaval and Moritz, 2008; Carnaval et al., 2014). Hence, it is likely that vicariance is driven by climatic

isolation, rather than river-associated (Carnaval et al., 2014). Because species in the *L. latrans* complex are all large in size and likely not constrained to disperse over long distances, specially between riverbanks, a climatic-driven isolation scenario seems more reasonable than river-associated one. Moreover, if rivers were strong barriers to gene flow, we would expect that other main rivers along Bahia State (e.g., Jequitinhonha river) and Rio de Janeiro States (e.g., Paraíba do Sul river) also promoted phylogeographic breaks within *L. latrans*, what is not the case here. Therefore, it is likely that habitat fragmentation caused by Pleistocene climatic oscillations is the primary mode for lineage diversification within this species, also evidenced by niche suitability displacement when ENMs are projected to LIG (ca. 130 Kya; Fig. 4).

Moreover, both latN and latS populations showed signals of population expansions about 130,000 years ago, which corroborates the hypothesis that AF associated taxa expanded rather than retracted during LGM (Leite et al., 2016). This is especially interesting given that all AF associated populations (CS3 included) apparently exhibit synchronous populations expansions around 130,000 years ago (Fig. 2). Additionally, lineages distributed south of the climatically stable areas (e.g., lucN and latS) proposed by Carnaval and Moritz (2008) exhibited similar levels of genetic diversity in comparison to northern AF lineage (latN). This indicate that the LGM period did not have significative effects on population size changes nor environmental stable areas predicted genetic diversity as expected by the CM model (Carnaval and Moritz, 2008), a pattern also observed for another frog complex (Thomé et al., 2014) and birds (Cabanne et al., 2016).

Among all species in the *Leptodactylus latrans* complex, only *L*. aff. *latrans* CS3 did not exhibit signs of populational genetic structure, but this species is restricted to a narrow geographic area along low altitudinal sites (bearing sea-level) located east to the Serra do Mar Mountain range (Fig. 3). Our divergence time estimates indicate that the AF endemic

species (CS3 and *L. latrans*) diverged during the Plio-Pleistocene transition, around 2.3 Mya. The phylogenetic break between these two species occurs within Santos Basin in São Paulo State, a region where lies the Continental Rift of Southeastern Brazil (Vieira et al., 2015). Phases of tectonic reactivations of ancient structural faults have been promoting changes along this continental rift (Souza, 2015), and allied with sea-level changes transgressions/regressions related to Quaternary interglacial periods (Siddal et al. 2010; Hansen et al., 2013), may have isolated a once continually coastal distributed lineage. The diversification of a highly endemic fish fauna is mostly associated with such neotectonic activities (Ribeiro et al., 2006), with one of them (the Bertioga Fault; see Souza, 2015) matching our mean divergence time estimates for the split between CS3 and *L. latrans*. Additionally, the current CS3 lineage geographic distribution lies within an area where neotectonic barriers (e.g., the Guapiara lineament and the Cubatão shear zone; Saadi et al., 2002) coincides with phylogeographic breaks among several AF-associated taxa (e.g., Grazziotin et al., 2006; Thomé et. al., 2010; Menezes et al., 2017). However, the large confidence interval of divergence time estimates (HPD 95% = 1.0 to 3.8 Mya) and the uncertainty in establishing a single tectonic barrier to gene flow, hampered us to clearly distinguishes whether an ecological or vicariance based process explains this phylogenetic break. Although background tests indicate that environmental niches of CS3 and *L. latrans* are significantly divergent (Fig. 5), patterns of ecological isolation can also be a by-product of allopatric isolation mostly because CS3 lineage have been affected by at least three neotectonic pulses. Interestingly, latS and CS3 lineages still share haplotypes on a higher proportion. Nevertheless, we did not identify areas of sympatric occurrence between CS3 and *L. latrans* (indicating secondary contact), but *L. latrans* (latS lineage) was sampled about 25km northwards from the distribution limit of CS3 along São Paulo State coastal zone (Magalhães et al., Capítulo I). As proposed by the ENMs (Fig. 4), this lineage remained

restricted to a narrow geographic patch between northern Paraná and São Paulo States, a region of climatic refugia with high phylogeographic endemism index (Carnaval et al., 2014), showing recent signs of populational expansion as sea-levels continuously regressed during the last 130,000 years (Siddal et al., 2010; Hansen et al., 2013).

Leptodactylus luctator exhibited the highest uncovered diversity among species in the *L. latrans* complex and three genetically structured populations are recognized. Among these, individuals from a high-altitude site at Serra Geral region in the Brazilian State of Santa Catarina (lucSC) diverged from the sister lineages (lucN+lucS) during middle Pleistocene around 1 Mya. Recently, both Carnaval et al. (2014) and Barros et al. (2015) predicted that a narrow patch of higher altitudinal sites across Paraná and Santa Catarina States acted as forested microrefugia and played an important role in maintaining genetic diversity locally. Although not a forest-dependent taxon, our results corroborate the existence of a deeply divergent lineage within *L. luctator* that was only sampled from Serra Geral region in Santa Catarina State. Accordingly, Peçanha et al. (2017) identified that cryptic rodent lineages associated to open areas diversified around this same region, with divergence time estimates falling within the middle to late Pleistocene boundaries. Moreover, the ENMs consistently identified two main core areas that coincides with the geographic ranges of lucS (around northeastern Argentina/southern Paraguay) and lucN (around São Paulo and Minas Gerais State) lineages. These core areas are relatively fragmented during both LGM and LIG periods as ENM predicts low environmental suitability around the higher altitudinal sites within the AF region comprising the interior of São Paulo, Paraná and Santa Catarina States (Fig. 4). For instance, previous palynological studies showed that highlands in southern Brazil exhibited a relatively dry climate with a longer annual dry season and a cold climate with frosts during glacial cycles (Behling and Lichte, 1997). Only during late Holocene, the grassland fields were replaced by forests (related to increasingly moister climate change;

Behling, 1995), which expanded into the highlands southern Brazil (Behling, 2002) likely favoring lineages to disperse and to establish secondary contact. Indeed, we only observed mitochondrial introgression and sympatry between lucN and lucS lineages along AF and Chaco/Pampas Biomes transitional areas located around southern Brazil and northeastern Argentina (Fig. 3). Because there are no major geographic barriers to gene flow at the time lineages divergence (around 0.2 to 1.0 Mya) and background tests support environmental niche divergence (Fig. 5b), a climate/ecological based process likely explains the patterns of genetic diversification within *L. luctator*. Moreover, EBSP analyses indicated a subtle, but significative (as supported by neutrality testes; Table S4), sign of populational expansion around the LGM for both lucN and lucS lineages. Conversely to other AF species, populational viability of this cold-associated taxa was likely more impacted by Pleistocene glacial cycles than low altitude adapted ones, as indicated by post-LGM populational expansions.

The *L*. aff. *latrans* CS1 is the most divergent lineage within this complex of frog species and originated at about 7.6 Mya during late Neogene. This old divergence time reflects in a complete absence of haplotype sharing among species in the *L. latrans* complex (which are all exclusive to this lineage), and a unique and distinctively advertisement call among species in the *L. latrans* complex (Magalhães et al., Capítulo I). This species showed a populational break that split north (CS1N) and south (CS1S) populations around where currently the São Francisco River flows. The São Francisco River lower course previously flowed in a different direction northward towards the equatorial Atlantic Ocean and drastically shifted towards the southeast and to the eastern Atlantic Ocean coast about approximately 450,000 years ago (Mabesoone, 1994; Nascimento et al., 2013). The shift in the river course fells within the divergence time confidence interval estimated for the split between CS1N and CS1S populations (mean = 0.35 Mya; HPD 95% = 0.1–0.7 Mya),

indicating the role of a riverine barrier in shaping diversification of CS1 lineage (as previously reported for other taxa; Nascimento et al., 2013). On the other hand, Pleistocene interglacial cycles continuously promoted aridification of lowland Caatinga areas (Auler and Smart, 2001) with a prominent expansion of Caatinga and associated dry-adapted taxa during the last 260,000 years (Gehara et al., 2017b). However, several recurrent wetter periods occurred within the Caatinga Biome during middle to late Pleistocene (Wang et al., 2004; Auler et al., 2004) promoting the expansion of forest corridors that allowed species to disperse, especially along northern and central Bahia. These wetter pulses date back to middle Pleistocene about 900,000 years ago (Auler et al., 2004), which intensified during the last 210,000 years (Wang et al., 2004). This is interesting because the current location of the lower São Francisco river course was pointed in the ENMs as an area of high suitability for this species during both LIG and LGM, which is substantiated by evidences of wetter pulses within the Caatinga during these periods (Auler and Smart, 2001). Considering that *L.* aff. *latrans* CS1 is not a dry-adapted species, it is likely that these early wetter pulses favored populational dispersion outside its core distribution in central Bahia followed by isolation when Caatinga aridification intensified in late Pleistocene (Auler and Smart, 2001), which instead favored populational expansion of dry-adapted taxa (Gehara et al., 2017b). Therefore, both Pernambuco interior and Chapada Diamantina highlands (which are embedded within a semi-arid landscape; Vieira et al., 2015) could have acted as climatic refugium during dryness periods, and diversification was driven by climatic oscillations. This further explains why southern CS1 lineage population size remained constant (as show by EBSP analysis) or experience bottle necks as indicated by significant Tajima's *D* positive values for the COI mitochondrial gene (Table S4).

4.2. Patterns of ecological isolation

Phylogenetic sister species often exhibit differences on traits that are apparent responses to differing ecological conditions, revealing a primary mode of ecologic isolation on driving lineage divergence and speciation (Mayr, 1947; Shafer and Jochen, 2013). Nevertheless, except for some unique intraspecific phenotypic variations, external morphology among species in the *Leptodactylus latrans* complex is overall homogeneous (Magalhães et al., Capítulo I). Moreover, an extensive mitochondrial DNA barcoding sampling (with more than 300 sequenced individuals) detected relatively few sympatry zones among species in the *L. latrans* complex, despite their broad geographic occurrence area across South America. This is especially interesting considering that ENMs among species pertaining to the *L. latrans* complex are mostly not overlapping under current climatic conditions (Fig. 4). Thus, either sister species are adapted to different allopatric distributed environments, are too ecologically and morphologically similar to coexist and competition enforces allopatry, or had insufficient time to expand their ranges (Hutchinson, 1959; Mayr, 1964). Considering that acoustic and external morphological traits are not under strong divergent selection (Magalhães et al., Capítulo I), competition would enforce allopatry because morphological and/or acoustic (for frog species; Blair, 1964) divergence is required before two taxa could coexist (Hutchinson, 1959; Wang and Summers, 2010). Conversely, the lack of phenotypic differentiation may imply that other intrinsic sources for ecological isolation, such as specific physiological adaptations (Lexer and Fay, 2005), are constraining species to coexist in divergent habitats (Hutchinson, 1959; Zink 2014), therefore weakening selection towards morphological and acoustic differentiation. Moreover, a hypothesis of recent diversification is unlikely given that divergence among all four species in the *L. latrans* complex is old, dating back to late Neogene.

On the other hand, high levels of sympatry between species in the *L. latrans* complex and a sister taxon, *L. macrosternum*, were observed throughout several localities across Brazil and Argentina (Magalhães et al., Capítulo I). These species also share preferences for reproductive sites and a generalist feeding habits, making them potential competitors for spatial and energetic resources. Therefore, one could hypothesize that *L. macrosternum* is an additional biotic factor that could reinforce an allopatric isolation among species in the *L. latrans* complex. Nevertheless, these hypotheses should be tested in future contributions in order to assess the intrinsic variation of physiological traits within species in the *L. latrans* complex relative to adaptations along heterogeneous environments.

4.3. Final remarks

The scenario presented herein corroborates the existence of lineages that are phylogenetically structured at both species and populational scale (Fig. 3), each with idiosyncratic histories and processes affecting their intraspecific genetic differentiation. These groups were strongly supported by all analyses, including phylogenetic reconstruction, haplotype networks, and all assignment tests we performed. Interestingly, all divergent lineages are mostly allopatric and did not exhibit any major topographic barrier to gene flow (except for CS3 lineage). Instead, we found evidence that most interspecific genetic breaks coincide with areas of environmental transition with a second pulse of synchronous intraspecific diversification occurring during late Pleistocene, showing that climatic oscillations played a major role in shaping genetic diversity among the *Leptodactylus latrans* species complex. The recurrent pattern of ecological isolation implies that lineages in the *L. latrans* complex are relatively sensitive to climatic changes, which drastically shifts the paradigm from a widely distributed and not threatened species to a group that is suitable to negative effects regarding population viability due to global climatic changes. This is

furthermore aggravated by the fact that most lineages are distributed within the AF (most of them endemic), which suffers from major loss of natural vegetation cover due to human activity and/or occurs along a restricted geographic area (e.g., CS3 and lucSC lineages). Finally, recently proposed patterns of isolation mechanisms showed that isolation by environment (Wang and Summers, 2010; Wang and Bradburd, 2014), climatic instability (Vasconcellos et al., 2019) and natural selection against immigrants (Nosil et al., 2005) can influence both dispersal rate and population connectivity in ecological modes of speciation. Future works that explicitly test for contrasting models of isolation mechanisms under coalescent simulations will certainly shed light about the evolutionary processes underlying the cryptic environment-driven diversification patterns revealed for this widespread frog group.

Acknowledgments

This work would never be possible without the help and collaboration of several researches. FMM thanks the staff of Herpetology Laboratory and Zoology Museums from LGE (UNaM), UFBA, UFMS, UFPB, UNB, and UNESP-Rio Claro for their kind assistance and for all logistic support. FMM is indebted to E.F. Oliveira, E.M. Fonseca, F.M. Lanna, V.A. São-Pedro, and W. Pessoa for their support during field work. FMM thanks CNPq (Process number 167148) for his doctoral fellowship and Instituto Chico Mendes de Conservação da Biodiversidade (ICMBio, Process number 53175-1) for scientific collection permits. This research was supported by resources supplied by the High-Performance Computing Center (NPAD) at Universidade Federal do Rio Grande do Norte-Brazil and Cyberinfrastructure for Phylogenetic Research (CIPRES).

References

Ab'Saber, A.N., 1977. Domínios morfoclimáticos na América do Sul: primeira aproximação. Geomorfologia 52, 1–21.

Auler, A.S., Smart, P.L., 2001. Late Quaternary Paleoclimate in Semiarid Northeastern Brazil from U-Series Dating of Travertine and Water-Table Speleothems. Quaternary Research 55, 159–167. DOI: 10.1006/qres.2000.2213

Auler, A.S., Wang, X., Edwards, R.L., Cheng, H., Cristalli, P.S., Smart, P.L., Richards, D.A., 2004. Quaternary ecological and geomorphic changes associated with rainfall events in presently semi-arid northeastern Brazil. Journal of Quaternary Science 19, 693–701. DOI: 10.1002/jqs.876

Avise, J.C., 2000. Phylogeography: the history and formation of species. Harvard University Press, Cambridge, Massachusetts.

Barros, M.J.F., Silva-Arias, G.A., Fregonezi, J.N., Turchetto-Zolet, A.C., Iganci, J.R.V., Diniz-Filho, J.A.F., Freitas, L.B., 2015. Environmental drivers of diversity in Subtropical Highland Grasslands. Perspectives in Plant Ecology, Evolution and Systematics 17, 360–368. DOI: 10.1016/j.ppees.2015.08.001

Batalha-Filho, H., Waldschmidt, A.M., Campos, L.A.O., Tavares, M.G., Fernandes-Salomão, T.M., 2010. Phylogeography and historical demography of the neotropical stingless bee *Melipona quadrifasciata* (Hymenoptera, Apidae): incongruence between morphology and mitochondrial DNA. Apidologie 41, 534–547. DOI: 10.1051/apido/2010001

Behling, H., 1995. Investigations into the Late Pleistocene and Holocene history of vegetation and climate in Santa Catarina (S Brazil). Vegetation History and Archaeobotany 4, 127–152. https://www.jstor.org/stable/23417538

Behling, H., 2002. South and southeast Brazilian grasslands during Late Quaternary times: a synthesis. Palaeogeography, Palaeoclimatology, Palaeoecology 177, 19–27. DOI: 10.1016/S0031-0182(01)00349-2

Behling, H., Lichte, M., 1997. Evidence of Dry and Cold Climatic Conditions at Glacial Times in Tropical Southeastern Brazil. Quaternary Research 48, 348–358. DOI: 10.1006/qres.1997.1932

Blair, W.F., 1964. Isolating Mechanisms and Interspecies Interactions in Anuran Amphibians. The Quarterly Review of Biology 39, 334–344. DOI: 10.1086/404324

Bouckaert, R., Vaughan, T.G., Barido-Sottani, J., Duchêne, S., Fourment, M., Gavryushkina, A., Heled, J., Jones, G., Kühnert, D., Maio, N., Matschiner, M., Mendes, F.K., Müller, N.F., Ogilvie, H.A., Plessis, L., Popinga, A., Rambaut, A., Rasmussen, D., Siveroni, I., Suchard, M.A., Wu, C.H., Xie, D., Zhang, C., Stadler, T., Drummond, A.J., 2019. BEAST 2.5: An advanced software platform for Bayesian evolutionary analysis. PLoS computational biology 15, e1006650. DOI: 10.1371/journal.pcbi.1006650

Bruford, M.W., Hanotte, O., Brookfield, J.F.Y., Burke, T., 1992. Single and multilocus DNA fingerprinting, in: Hoelzel, A.R. (Ed.) Molecular Genetic Analysis of Populations: A Practical Approach. I. R. L. Press, Oxford, pp. 225–269.

Byrne, M., 2008. Evidence for multiple refugia at different time scales during Pleistocene climatic oscillations in southern Australia inferred from phylogeography. Quaternary Science Reviews 27, 2576–2585. DOI: 10.1016/j.quascirev.2008.08.032

Cabanne, G.S., Calderón, L., Arias, N.T., Flores, P., Pessoas, R., d'Horta, F.M., Miyaki, C.Y., 2016. Effects of Pleistocene climate changes on species ranges and evolutionary processes in the Neotropical Atlantic Forest. Biological Journal of the Linnean Society 119, 856–872. DOI: 10.1111/bij.12844

Carnaval, A.C., Hickerson, M.J., Haddad, C.F.B., Rodrigues, M.T., Moritz, C., 2009. Stability predicts genetic diversity in the Brazilian Atlantic Forest hotspot. Science 323, 785–789. DOI: 10.1126/science.1166955

Carnaval, A.C., Moritz, C., 2008. Historical climate modelling predicts patterns of current biodiversity in the Brazilian Atlantic forest. Journal of Biogeography 35, 1187–1201. DOI: 10.1111/j.1365-2699.2007.01870.x.

Carnaval, A.C., Waltari, E., Rodrigues, M.T., Rosauer, D., VanDerWal, J., Damasceno, R., Prates, I., Strangas, M., Spanos, Z., Rivera, D., Pie, M.R., Firkowski, C.R., Bornschein, M.R., Ribeiro, L.F., Moritz, C., 2014. Prediction of phylogeographic endemism in an environmentally complex biome. Proceedings of the Royal Society B: Biological Sciences 281, 20141461. DOI: 10.1098/rspb.2014.1461

Carstens, B., Richards, C.L., 2007. Integrating coalescent and ecological niche modeling in comparative phylogeography. Evolution 61, 1439–1454. DOI: 10.1111/j.1558-5646.2007.00117.x

d'Horta, F.M., Cabanne, G.S., Meyer, D., Miyaki, C.Y., 2011. The genetic effects of Late Quaternary climatic changes over a tropical latitudinal gradient: diversification of an Atlantic Forest passerine. Molecular Ecology 20, 1923–1935. DOI: 10.1111/j.1365-294X.2011.05063.x.

Darriba, D., Taboada, G.L., Doallo, R., Posada, D., 2012. jModelTest 2: more models, new heuristics and parallel computing. Nature Methods 9, 772. DOI: http://dx.doi.org/10.1038/nmeth.2109.

Degnan, J.H., Rosenberg, N.A., 2009. Gene tree discordance, phylogenetic inference and the multispecies coalescent. Trends in Ecology & Evolution 24, 332–340. DOI: 10.1016/j.tree.2009.01.009.

Drummond, A.J., Suchard, M.A., Xie, D., Rambaut, A., 2012. Bayesian phylogenetics with BEAUti and the BEAST 1.7. Molecular Biology And Evolution 29, 1969–1973.

Earl, D.A., vonHoldt, B.M., 2012. STRUCTURE HARVESTER: a website and program for visualizing STRUCTURE output and implementing the Evanno method. Conservation Genetics Resources 4, 359–361. DOI: 10.1007/s12686-0119548-7.

Evanno, G., Regnaut, S., Goudet, J., 2005. Detecting the number of clusters of individuals using the software STRUCTURE: a simulation study. Molecular Ecology 14, 2611–2620. DOI: 10.1111/j.1365-294X.2005.02553.x

Fazolato, C., Fernandes, F., Batalha-Filho, H., 2017. The effects of Quaternary sea-level fluctuations on the evolutionary history of an endemic ground lizard (*Tropidurus hygomi*). Zoologischer Anzeiger 270, 1–8. DOI: 10.1016/j.jcz.2017.08.007

Firkowski, C.R., Bornschein, M.R., Ribeiro, L.F., Pie, M.R., 2016. Species delimitation, phylogeny and evolutionary demography of co-distributed, montane frogs in the southern Brazilian Atlantic Forest. Molecular Phylogenetics and Evolution 100, 345–360. DOI: 10.1016/j.ympev.2016.04.023

Fitzpatrick, S.W., Brasileiro, C.A., Haddad, C.F.B., Zamudio, K.R., 2009. Geographical variation in genetic structure of an Atlantic Coastal Forest frog reveals regional differences in habitat stability. Molecular Ecology 18, 2877–2896. DOI: 10.1111/j.1365-294X.2009.04245.x

Flouri, T., Jiao, X., Rannala, B., Yang, Z., 2018. Species tree inference with BPP using genomic sequences and the multispecies coalescent. Molecular Biology and Evolution 35, 2585–2593. DOI: 10.1093/molbev/msy147

Fu, Y.X., 1997. Statistical tests of neutrality of mutations against population growth, hitchhiking and background selection. Genetis 147, 915–925.

Gehara, M., Barth, A., Oliveira, E.F., Costa, M.A., Haddad, C.F.B., Vences, M., 2017a. Model-based analyses reveal insular population diversification and cryptic frog species in the *Ischnocnema parva* complex in the Atlantic forest of Brazil. Molecular Phylogenetics and Evolution 112, 68–78. DOi: 10.1016/j.ympev.2017.04.007

Gehara, M., Garda, A.A., Werneck, F.P., Oliveira, E.F., Fonseca, E.M., Camurugi, F., Magalhães, F.M., Lanna, F.M., Sites Jr., J.W., Marques, R., Silveira-Filho, R., São-Pedro, V.A., Colli, G.R., Costa, G.C., Burbrink, F.T., 2017b. Estimating synchronous demographic changes across populations using hABC and its application for a herpetological community from northeastern Brazil. Molecular Ecology 18, 4756–4771. DOI: 10.1111/mec.14239

Grazziotin, F.G., Monzel, M., Echeverrigaray, S., Bonatto, S.L., 2006. Phylogeography of the *Bothrops jararaca* complex (Serpentes: Viperidae): past fragmentation and island colonization in the Brazilian Atlantic Forest. Molecular Ecology 15, 3969-3982. DOI: 10.1111/j.1365-294X.2006.03057.x

Guillot, G., Mortier, F., Estoup, A., 2005. Geneland: A computer package for landscape genetics. Molecular Ecology Notes 5, 712–715. DOI: 10.1111/j.1471-8286.2005.01031.x

Hansen, J., Sato, M., Russel, G., Kharecha, P., 2013. Climate sensitivity, sea level and atmospheric carbon dioxide. Philosophical Transactions of the Royal Society A 371, 20120294. DOI: 10.1098/rsta.2012.0294

Heibl, C., Calenge, C., 2013. Phyloclim: integrating phylogenetics and climatic niche modelling. Available at: http://cran.r-project.org/web/packages/phyloclim/index.html.

Heled, J., Drummond, A.J., 2008. Bayesian inference of population size history from multiple loci. Bmc Evolutionary Biology 8, 289. DOI: 10.1186/1471-2148-8-289

Hijmans, R.J., Cameron, S., Parra, J., 2005. WorldClim, version 1.3. . University of California, Berkeley, CA. Available at: http://biogeo.berkeley.edu/worldclim/worldclim.htm.

Hijmans, R.J., Elith, J., 2013. Species distribution modeling with R. R CRAN Project.

Hoorn, C., Wesselingh, F.P., ter Steege, H., Bermudez, M.A., Mora, A., Sevink, J., Sanmartin, I., Sanchez-Meseguer, A., Anderson, C.L., Figueiredo, J.P., Jaramillo, C., Riff, D., Negri, F.R., Hooghiemstra, H., Lundberg, J., Stadler, T., Sarkinen, T., Antonelli, A., 2010. Amazonia through time: Andean uplift, climate change, landscape evolution, and biodiversity. Science 330, 927–931. DOI: 10.1126/science.1194585

Hutchinson, G.E., 1959. Homage to Santa Rosalia or why are there so many kinds of animals? The American Naturalist 93, 145–159. DOI: 10.1086/282070

Irwin, D.E., 2002. Phylogeographic breaks without geographic barriers to gene flow. Evolution 56, 2383–2394. DOI: 10.1111/j.0014-3820.2002.tb00164.x

Janes, J.K., Miller, J.M., Dupuis, J.R., Malenfant, R.M., Gorrel, J.C., Cullingham, C.I., Andrew, R.L., 2017. The K = 2 conundrum. Molecular Ecology 26, 3594–3602. DOI: 10.1111/mec.14187

Katoh, K., Misawa, K., Kuma, K., Miyata, T., 2002. MAFFT: a novel method for rapid multiple sequence alignment based on fast Fourier transform. Nucleic Acids Research 30, 3059–3066. https://doi.org/10.1093/nar/gkf436

Kearse, M., Moir, R., Wilson, A., Stones-Havas, S., Cheung, M., Sturrock, S., Buxton, S., Cooper, A., Markowitz, S., Duran, C., Thierer, T., Ashton, B., Meintjes, P., Drummond, A., 2012. Geneious basic: an integrated and extendable desktop software platform for the organization and analysis of sequence data. Bioinformatics 28, 1647–1649. DOI:10.1093/bioinformatics/bts199

Leaché, A.D., Fujita, M.K., 2010. Bayesian species delimitation in West African forest geckos (Hemidactylus fasciatus). Proceedings of the Royal Society B 277, 3071–3077. DOI: 10.1098/rspb.2010.0662

Leite, F.S.F., Pezzuti, T.L., Garcia, P.C.A., 2012. A new species of the *Bokermannohyla pseudopseudis* group from the Espinhaço range, central Bahia, Brazil (Anura: Hylidae). Herpetologica 68, 401–409.

Leite, Y.L.R., Costa, L.P., Loss, A.C., Rocha, R.G., Batalha-Filho, H., Bastos, A.C., Quaresma, V.S., Fagundes, V., Paresque, R., Passamani, M., Pardini, R., 2016. Neotropical forest expansion during the last glacial period challenges refuge hypothesis. Proceedings of the National Academy of Sciences of the USA 113, 1008–1013. DOI: 10.1073/pnas.1513062113

Lexer, C., Fay, M.F., 2005. Adaptation to environmental stress: a rare or frequent driver of speciation? Journal of Evolutionary Biology 18, 893–900.

Librado, P., Rozas, J., 2009. DnaSP v5: A software for comprehensive analysis of DNA polymorphism data. Bioinformatics 25, 1451–1452. DOI: 10.1093/bioinformatics/btp187

Lima, C.C.U., Nolasco, M.C., 2015. Chapada Diamantina: a remarkable landscape dominated by mountains and plateaus, in: Vieira, B.C., Salgado, A.A.R., Santos, L.J.C. (Eds.). Landscapes and Landforms of Brazil. World Geomorphological Landscapes. Springer, Dordrecht, pp. 211–220. DOI: 10.1007/978-94-017-8023-0_19

Lynch, M., 2007. The origins of genome architecture. Sinauer Associates, Sunderland.

Lyra, M.L., Haddad, C.F.B., Azeredo-Espin, A.M.L., 2017. Meeting the challenge of DNA barcoding Neotropical amphibians: polymerase chain reaction optimization and new COI primers. Molecular Ecology Resources 17, 966–980. https://doi.org/10.1111/1755-0998.12648

Mabesoone, J.M., 1994. Sedimentary basins of Northeast Brazil. 1ª ed. Recife: Editora Universitária, Universidade Federal de Pernambuco.

Maniatis, T., Fritsch, E.F., Sambrook, J., 1982. Molecular Cloning: A Laboratory Manual. Cold Spring Harbour Laboratory, USA.

Martins, F.M., 2011. Historical biogeography of the Brazilian Atlantic forest and the Carnaval–Moritz model of Pleistocene refugia: what do phylogeographical studies tell us? Biological Journal of the Linnean Society 104, 499–509. DOI: 10.1111/j.1095-8312.2011.01745.x

Mayr, E., 1947. Ecological factors in speciation. Evolution 1, 263–288. DOI: 10.2307/2405327

Mayr, E., 1964. Animal species and evolution. Harvard University Press, Cambridge, MA.

Menezes, R.S.T., Brady, S.G., Carvalho, A.F., Del Lama, M.A., Costa, M.A., 2017. The roles of barriers, refugia, and chromosomal clines underlying diversification in Atlantic Forest social wasps. Scientifc Reports 7, 7689. DOI: 10.1038/s41598-017-07776-7

Mittermeier, R.A., Myers, N., Thomsen, J.B., Fonseca, G.A.B., Oliveiri, S., 1998. Biodiversity hotspots and major tropical wilderness areas: approaches to setting conservation priorities. Conservation Biology 12, 516–520. DOI: 10.1046/j.1523-1739.1998.012003516.x

Morellato, L.P.C., Haddad, C.F.B., 2000. Introduction: the Brazilian Atlantic forest. Biotropica 32, 786–792. DOI: 10.1111/j.1744-7429.2000.tb00618.x

Nascimento, F.F., Lazar, A., Menezes, A.N., M., D.A., Moreira, J.C., Salazar-Bravo, J., D'Andrea, P.S., Bonvicino, C.R., 2013. The role of historical barriers in the diversification processes in open vegetation formations during the Miocene/Pliocene using an ancient rodent lineage as a model. PLoS ONE 8, e61924. DOI: 10.1371/journal.pone.0061924

Nosil, P., Vines, T.H., Funk, D.J., 2005. Perspective: Reproductive isolation caused by natural selection against immigrants from divergent habitats. Evolution 59, 705–719. DOI: 10.1554/04-428

Peçanha, W.T., Althoff, S.L., Galiano, D., Quintela, F.M., Maestri, R., Gonçalves, G.L., Freitas, T.R.O., 2017. Pleistocene climatic oscillations in Neotropical open areas: Refuge isolation in the rodent *Oxymycterus nasutus* endemic to grasslands. PloS ONE 12, e0187329. DOI: 10.1371/journal.pone.0187329

Phillips, S.J., Anderson, R.P., Schapire, R.E., 2006. Maximum entropy modeling of species geographic distributions. Ecological Modelling 190, 231–259. DOI: 10.1016/j.ecolmodel.2005.03.026

Pritchard, J.K., Stephens, M., Donnelly, P., 2000. Inference of population structure using multilocus genotype data. Genetics 155, 945–959.

Proosdij, A.S., Sosef, M.S., Wieringa, J.J., Raes, N., 2016. Minimum required number of specimen records to develop accurate species distribution models. Ecography 39, 542–552. DOI: 10.1111/ecog.01509

Pyron, R.A., Burbrink, F.T., 2009. Lineage diversification in a widespread species: roles for niche divergence and conservatism in the common kingsnake, *Lampropeltis getula*. Molecular Ecology 18, 3443–3457. DOI: 10.1111/j.1365-294X.2009.04292.x

R Core Team. 2018. R: A language and environment for statistical computing. Vienna, R Foundation for Statistical Computing, Austria. Available at: http://www.R-project.org.

Rambaut, A., 2014. FigTree: a graphical viewer of phylogenetic trees, version 1.4.2. Available at: http://tree.bio.ed.ac.uk/software/figtree/.

Rambaut, A., Drummond, A.J., Xie, D., Baele, G., Suchard, M.A., 2018. Posterior summarisation in Bayesian phylogenetics using Tracer 1.7. Systematic Biology 67, 901–904. DOI:10.1093/sysbio/syy032

Ramos-Onsins, S.E., Rozas, J., 2002. Statistical properties of new neutrality tests against population growth. Molecular Biology and Evolution 19, 2092–2100. DOI: 10.1093/oxfordjournals.molbev.a004034

Ribeiro, A.C., Lima, F.C.T., Riccomini, C., Menezes, N.A., 2006. Fishes of the Atlantic Rainforest of Boracéia: testimonies of the Quaternary fault reactivation within a Neoproterozoic tectonic province in Southeastern Brazil. Ichthyological Exploration of Freshwaters 17, 157–164.

Rissler, L.J., Apodaca, J.J., 2007. Adding more ecology into species delimitation: ecological niche models and phylogeography help define cryptic species in the black salamander (*Aneides flavipunctatus*). Systematic Biology 56, 924–942. DOI: 10.1080/10635150701703063

Rodríguez, A., Borner, M., Pabijan, M., Gehara, M., Haddad, C.F.B., Vences, M., 2015. Genetic divergence in tropical anurans: deeper phylogeographic structure in forest specialists and in topographically complex regions. Evolutionary Ecology 29, 765–785. DOI 10.1007/s10682-015-9774-7

Rull, V., 2008. Speciation timing and neotropical biodiversity: the Tertiary-Quaternary debate in the light of molecular phylogenetic evidence. Molecular Ecology 17, 2722–2729. DOI: 10.1111/j.1365-294X.2008.03789.x

Rull, V., 2011. Neotropical biodiversity: timing and potential drivers. Trends in Ecology & Evolution 26, 508–513. DOI: 10.1016/j.tree.2011.05.011

Saadi, A., Machette, M.N., Haller, K.M., Dart, R.L., Bradley, L., Souza, A.M.P.D., 2002. Map and database of Quaternary faults and lineaments in Brazil. U.S. Geological

Survey. Open-File Report 02-230, Version 1.0. Available from: <http://pubs.usgs.gov/of/2002/ofr-02-230/>.

Sabbag, A.F., Lyra, L.M., Zamudio, K.R., Haddad, C.F.B., Feio, R.N., Leite, F.S.F., Gasparini, J.L., Brasileiro, C.A., 2018. Molecular phylogeny of Neotropical rock frogs reveals a long history of vicariant diversification in the Atlantic forest. Molecular Phylogenetics and Evolution 2018, 142–156. DOI:https://doi.org/10.1016/j.ympev.2018.01.017

Schoener, T.W., 1968. The *Anolis* lizards of Bimini: resource partitioning in a complex fauna. Ecology 49, 704–726. DOI: 10.2307/1935534

Senczuk, G., Harris, D.J., Castiglia, R., Mizan, V.L., Colangelo, P., Canestrelli, D., Salvi, D., 2019. Evolutionary and demographic correlates of Pleistocene coastline changes in the Sicilian wall lizard *Podarcis wagleriana*. Journal of Biogeography 46, 224–237. DOI: 10.1111/jbi.13479

Shafer, A.B.A., Jochen, B.W.W., 2013. Widespread evidence for incipient ecological speciation: a meta-analysis of isolation-by-ecology. Ecology Letters 16, 940–950. DOI: 10.1111/ele.12120

Siddal, M., Rohling, E.J., Blunier, T., Spahni, R., 2010. Patterns of millennial variability over the last 500 ka. Climate of the Past 6, 295–303. DOI: 10.5194/cp-6-295-2010

Smith, B.T., McCormack, J.E., Cuervo, A.M., Hickerson, M.J., Aleixo, A., Cadena, C.D., Pérez-Emán, J., Burney, C.W., Xie, X., Harvey, M.G., Faircloth, B.C., Glenn, T.C., Derryberry, E.P., Prejean, J., Fields, S., Brumfield, R.T., 2014. The drivers of tropical speciation. Nature 515, 406–409. DOI: 10.1038/nature13687

Souza, C.R.G., 2015. The Bertioga coastal plain: an example of morphotectonic evolution, in: Vieira, B.C., Salgado, A.A.R., Santos, L.J.C. (Eds.). Landscapes and Landforms of

Brazil. World Geomorphological Landscapes. Springer, Dordrecht, pp. 115–134. DOI: 10.1007/978-94-017-8023-0_11

Stephens, M., Smith, N.J., Donnelly, P., 2001. A new statistical method for haplotype reconstruction from population data. American Journal of Human Genetics 68, 978–989. DOI: 10.1086/319501

Suchard, M.A., Lemey, P., Baele, G., L., A.D., Drummond, A.J., Rambaut, A., 2018. Bayesian phylogenetic and phylodynamic data integration using BEAST 1.10. Virus Evolution 4, vey016. DOI:10.1093/ve/vey016

Suguio, K., Martins, L., Bittencourt, A.C.S.P., Dominguez, J.M.L., Flexor, J., Azevedo, A.E.G., 1985. Flutuações do nível relativo do mar durante o Quaternário superior ao longo do litoral brasileiro e suas implicações na sedimentação costeira. Revista Brasileira de Geociências 15, 273–286.

Tajima, F., 1989. Statistical method for testing the neutral mutation hypothesis by DNA polymorphism. Genetis 123, 585–595.

Thomé, M.T., Zamudio, K.R., Giovanelli, J.G., Haddad, C.F.B., Baldissera, F.A., Alexandrino, J., 2010. Phylogeography of endemic toads and post-Pliocene persistence of the Brazilian Atlantic Forest. Molecular Phylogenetics and Evolution 55, 1018–1031.

Thomé, M.T., Zamudio, K.R., Haddad, C.F.B., Alexandrino, J., 2014. Barriers, rather than refugia, underlie the origin of diversity in toads endemic to the Brazilian Atlantic Forest. Molecular Ecology 23, 6152–6164. DOI: doi.org/10.1111/mec.12986

Thorpe, R.S., Surget-Groba, Y., Johansson, H., 2008. The relative importance of ecology and geographic isolation for speciation in anoles. Philosophical Transactions of the Royal Society B: Biological Sciences 27, 3071–3081. DOI: 10.1098/rstb.2008.0077

Tonini, J.F.R., Costa, L.P., Carnaval, A.C., 2013. Phylogeographic structure is strong in the Atlantic Forest; predictive power of correlative paleodistribution models, not always. Journal of Zoological Systematics and Evolutionary Research 51, 114–121. 10.1111/jzs.12014

Turchetto-Zolet, A.C., Pinheiro, F., Salgueiro, F., Palma-Silva, C., 2013. Phylogeographical patterns shed light on evolutionary process in South America. Molecular Ecology 22, 1193–1213. DOI: 10.1111/mec.12164

Vasconcellos, M.M., Colli, G.R., Weber, J.N., Ortiz, E.M., Rodrigues, M.T., Cannatella, D.C., 2019. Isolation by instability: Historical climate change shapes population structure and genomic divergence of treefrogs in the Neotropical Cerrado savanna. Molecular Ecology 28, 1748–1764. DOI: 10.1111/mec.15045

Vences, M., Thomas, M., Bonett, R.M., Vieites, D.R., 2005. Deciphering amphibian diversity through DNA barcoding: chances and challenges. Philosophical Transactions of the Royal Society B: Biological Sciences 360, 1859–1868. DOI: 10.1098/rstb.2005.1717

Vieira, B.C., Salgado, A.A.R., Santos, L.J.C., 2015. Landscapes and Landforms of Brazil. World Geomorphological Landscapes. Springer, Dordrecht. DOI: 10.1007/978-94-017-8023-0

Vuilleumier, B.S., 1971. Pleistocene changes in the fauna and flora of South America. Science 173, 771–780. DOI: 10.1126/science.173.3999.771

Wang, I.J., Bradburd, G.S., 2014. Isolation by environment. Molecular Ecology 23, 5649–5662. DOI: 10.1111/mec.12938

Wang, I.J., Glor, R.E., Losos, J.B., 2013. Quantifying the roles of ecology and geography in spatial genetic divergence. Ecology Letters 16, 175–182. DOI: 10.1111/ele.12025

Wang, I.J., Summers, K., 2010. Genetic structure is correlated with phenotypic divergence rather than geographic isolation in the highly polymorphic strawberry poison-dart frog. Molecular Ecology 19, 447–458.

Wang, X., Auler, A.S., Edwards, R.L., Cheng, H., Cristalli, P.S., Smart, P.L., Richards, D.A., Shen, C., 2004. Wet periods in northeastern Brazil over the past 210 kyr linked to distant climate anomalies. Nature 432, 740–743. DOI: 10.1038/nature03067

Warren, D.L., Glor, R.E., Turelli, M., 2008. Environmental niche equivalency versus conservatism: quantitative approaches to niche evolution. Evolution 62, 2868–2883. DOI: 10.1111/j.15585646.2008.00482.x

Waters, J.M., 2011. Competitive exclusion: phylogeography's 'elephant in the room'? Molecular Ecology 20, 4388–4394. DOI: 10.1111/j.1365-294X.2011.05286.x

Weigt, L.A., Crawford, A.J., Rand, A.S., Ryan, M.J., 2005. Biogeography of the tungara frog, *Physalaemus pustulosus*: a molecular perspective. Molecular Ecology 14, 3857-3876. 10.1111/j.1365-294X.2005.02707.x

Wells, K.D., 2007. The Ecology and Behavior of Amphibians. The University of Chicago Press, USA.

Werle, E., Schneider, C., Renner, M., Völker, M., Fiehn, W., 1994. Convenient single-step, one tube purification of PCR products for direct sequencing. Nucleic Acids Research 22, 4354–4355.

Yang, Z., Rannala, B., 2014. Unguided species delimitation using DNA sequence data from multiple loci. Molecular Biology and Evolution 31, 3125–3135. DOI: 10.1093/molbev/msu279

Zink, R.M., 2014. Homage to Hutchinson, and the role of ecology in lineage divergence and speciation. Journal of Biogeography 41, 999–1006. DOI: 10.1111/jbi.12252

Supplementary material

Table S1. Sampling information. Zoological museum acronyms: CAUFJF = Coleção de Anfíbios da Universidade Federal de Juiz de Fora, Minas Gerais, Brazil; CFBHT = Tissue Samples Amphibian Collection Célio F. B. Haddad, UNESP-Rio Claro, São Paulo, Brazil; CHUFPB = Coleção de Herpetologia da Universidade Federal da Paraíba, João Pessoa, Paraíba, Brazil; CHUNB = Coleção Herpetológica da Universidade de Brasília, Brasília, Brazil; IIBPH = Herpetology Collection of the Instituto de Investigación Biológica del Paraguay, Asunción, Paraguay; LGE = Laboratorio de Genética e Evolução de Misiones, Posadas, Argentina; MZSF = Museu de Zoologia de Feira de Santana, Feira de Santana, Bahia, Brazil; UFBA = Coleção da Universidade Federal da Bahia, Salvador, Bahia; UFES = Tissue samples from Universidade Federal do Espírito Santo, Vitória, Espírito Santo, Brazil; UFMGT = Tissue samples from Universidade Federal de Minas Gerais, Belo Horizonte, Minas Gerais, Brazil; ZVCB = Collección de Zoología Vertebrados, Facultad de Ciencias, Universidad de la República, Montevideo, Uruguay. Other acronyms represent field series.

#	Sampling ID	species	COI	16S	cmyc2	Fib7	Tyr	POMC	Municipality	State/Province	Country	Lat	Long
1	AAGARDA00660	*luctator*	**seq**	**seq**	**seq**	**seq**	**seq**	**seq**	Lagoa Santa	Minas Gerais	Brazil	-19.63	-43.91
2	AAGARDA03281	*latrans*	**seq**	**seq**	**seq**	**seq**	**seq**	**seq**	Cataguases	Minas Gerais	Brazil	-21.37	-42.72
3	AAGARDA03356	*luctator*	**seq**	**seq**	**seq**	**seq**	**seq**	**seq**	Bom Jardim da Serra	Santa Catarina	Brazil	-28.36	-49.54
4	AAGARDA03688	*latrans*	**seq**	**seq**	**seq**	**seq**	**seq**	**seq**	Vicosa	Minas Gerais	Brazil	-20.78	-42.88
5	AAGARDA06784	CS1	**seq**	NA	**seq**	**seq**	**seq**	**seq**	Palmeiras	Bahia	Brazil	-12.57	-41.49
6	AAGARDA07017	CS1	**seq**	**seq**	**seq**	**seq**	**seq**	**seq**	Palmeiras	Bahia	Brazil	-12.57	-41.49
7	AAGARDA07244	*luctator*	**seq**	**seq**	**seq**	**seq**	**seq**	**seq**	Guiné	Bahia	Brazil	-12.77	-41.54
8	AAGARDA07245	CS1	**seq**	**seq**	**seq**	**seq**	**seq**	**seq**	Guiné	Bahia	Brazil	-12.77	-41.54
9	AAGARDA08165	CS1	**seq**	NA	**seq**	**seq**	**seq**	**seq**	Buíque	Pernambuco	Brazil	-8.52	-37.38
10	AAGARDA08166	CS1	**seq**	**seq**	**seq**	**seq**	**seq**	**seq**	Buíque	Pernambuco	Brazil	-8.52	-37.38
11	AAGARDA09084	CS1	**seq**	**seq**	**seq**	**seq**	**seq**	**seq**	Macajuba	Bahia	Brazil	-12.13	-40.36
12	AAGARDA09098	CS1	**seq**	**seq**	**seq**	**seq**	**seq**	**seq**	Jaguaquara	Bahia	Brazil	-13.56	-40.01
13	AAGARDA09102	*latrans*	**seq**	**seq**	**seq**	**seq**	**seq**	**seq**	Igrapiúna	Bahia	Brazil	-13.85	-39.12
14	AAGARDA09648	*latrans*	**seq**	NA	**seq**	**seq**	**seq**	**seq**	Elísio Medrado	Bahia	Brazil	-12.91	-39.48
15	AAGARDA09722	*latrans*	**seq**	NA	**seq**	**seq**	**seq**	**seq**	Varzedo	Bahia	Brazil	-12.97	-39.36
16	AAGARDA10077	*luctator*	**seq**	**seq**	**seq**	**seq**	**seq**	**seq**	Piatã	Bahia	Brazil	-13.15	-41.80
17	AAGARDA12103	*luctator*	**seq**	**seq**	**seq**	**seq**	**seq**	**seq**	Lindoia	São Paulo	Brazil	-22.52	-46.64
18	AAGARDA12212	*latrans*	**seq**	**seq**	**seq**	**seq**	**seq**	**seq**	Teresópolis	Rio de Janeiro	Brazil	-22.32	-42.82
19	AAGARDA12214	*latrans*	**seq**	NA	**seq**	**seq**	**seq**	NA	Teresópolis	Rio de Janeiro	Brazil	-22.32	-42.82
20	AAGARDA12226	*latrans*	**seq**	**seq**	**seq**	**seq**	**seq**	NA	Itatiaia	Rio de Janeiro	Brazil	-22.48	-44.57
21	AAGARDA12233	*luctator*	**seq**	**seq**	**seq**	**seq**	**seq**	NA	Buri	São Paulo	Brazil	-23.61	-48.53
22	AAGARDA12254	CS3	**seq**	**seq**	**seq**	**seq**	**seq**	**seq**	Peruibe	São Paulo	Brazil	-24.38	-47.07
23	AAGARDA12302	CS1	**seq**	**seq**	NA	**seq**	**seq**	**seq**	Jacobina	Bahia	Brazil	-11.16	-40.53

24	CAUFJF1350	*luctator*	**seq**	**seq**	**seq**	**seq**	**seq**	**seq**	Ponte Nova	Minas Gerais	Brazil	-20.29	-42.96
25	CAUFJF1352	*latrans*	**seq**	**seq**	**seq**	**seq**	**seq**	**seq**	Ponte Nova	Minas Gerais	Brazil	-20.29	-42.96
26	CAUFJF1355	*latrans*	**seq**	NA	**seq**	**seq**	**seq**	**seq**	Ponte Nova	Minas Gerais	Brazil	-20.29	-42.96
27	CAUFJF1550	*latrans*	**seq**	**seq**	**seq**	**seq**	**seq**	**seq**	Ubá	Minas Gerais	Brazil	-21.10	-42.93
28	CC06	*latrans*	**seq**	**seq**	**seq**	**seq**	**seq**	NA	Ilha Bela	São Paulo	Brazil	-23.84	-45.39
29	CFBH30247	CS1	**seq**	NA	**seq**	**seq**	**seq**	**seq**	Jussiape	Bahia	Brazil	-13.49	-41.60
30	CFBH31115	CS1	**seq**	**seq**	**seq**	NA	**seq**	NA	Araçuai	Minas Gerais	Brazil	-16.91	-42.06
31	CFBHT00382	*latrans*	**seq**	**seq**	**seq**	**seq**	**seq**	NA	Guarapari	Espirito Santo	Brazil	-20.65	-40.51
32	CFBHT00832	*luctator*	**seq**	KU495335	**seq**	**seq**	**seq**	NA	Camanducaia	Minas Gerais	Brazil	-22.89	-46.05
33	CFBHT00969	*luctator*	**seq**	**seq**	**seq**	NA	**seq**	NA	Nova Itapirema	São Paulo	Brazil	-21.07	-49.54
34	CFBHT01030	*luctator*	**seq**	**seq**	**seq**	**seq**	NA	NA	Ribeirao Branco	São Paulo	Brazil	-24.34	-48.74
35	CFBHT01166	*luctator*	**seq**	**seq**	**seq**	**seq**	**seq**	NA	Capinzal	Santa Catarina	Brazil	-27.34	-51.61
36	CFBHT01169	*luctator*	**seq**	**seq**	**seq**	NA	NA	NA	Ipuacu	Santa Catarina	Brazil	-26.67	-52.53
37	CFBHT01611	*luctator*	**seq**	**seq**	**seq**	NA	NA	NA	Pilar do Sul	São Paulo	Brazil	-23.83	-47.71
38	CFBHT01723	*luctator*	**seq**	KU495332	**seq**	NA	NA	NA	Tijucas do Sul	Paraná	Brazil	-25.92	-49.17
39	CFBHT01758	CS3	**seq**	**seq**	**seq**	**seq**	**seq**	NA	Angelina	Santa Catarina	Brazil	-27.56	-48.99
40	CFBHT01860	*luctator*	**seq**	KU495334	**seq**	**seq**	**seq**	**seq**	Mafra	Santa Catarina	Brazil	-26.09	-49.85
41	CFBHT01926	CS3	**seq**	**seq**	**seq**	NA	**seq**	NA	Treviso	Santa Catarina	Brazil	-28.51	-49.46
42	CFBHT02037	*luctator*	**seq**	**seq**	**seq**	**seq**	**seq**	NA	Conceicao do Mato Dentro	Minas Gerais	Brazil	-19.29	-43.58
43	CFBHT02266	*latrans*	**seq**	KU495328	**seq**	**seq**	**seq**	**seq**	São Sebastião	São Paulo	Brazil	-23.75	-45.41
44	CFBHT02530	*luctator*	**seq**	**seq**	**seq**	**seq**	**seq**	NA	Bairro Alto	São Paulo	Brazil	-23.47	-45.34
45	CFBHT02635	CS3	**seq**	**seq**	**seq**	**seq**	**seq**	NA	Eldorado	São Paulo	Brazil	-24.53	-48.08
46	CFBHT02748	CS3	**seq**	**seq**	**seq**	**seq**	**seq**	NA	Cananeia	São Paulo	Brazil	-25.00	-47.94
47	CFBHT02990	CS3	**seq**	**seq**	**seq**	**seq**	**seq**	NA	Botuvera	Santa Catarina	Brazil	-27.20	-49.08
48	CFBHT03039	*luctator*	**seq**	**seq**	**seq**	**seq**	**seq**	NA	Bom Jardim da Serra	Santa Catarina	Brazil	-28.39	-49.55
49	CFBHT03087	CS3	**seq**	**seq**	**seq**	**seq**	**seq**	**seq**	Antonina	Paraná	Brazil	-25.42	-48.73
50	CFBHT03182	*luctator*	**seq**	**seq**	**seq**	NA	NA	NA	Santa Isabel	São Paulo	Brazil	-23.28	-46.21
51	CFBHT03259	CS3	**seq**	**seq**	**seq**	NA	**seq**	NA	Corupa	Santa Catarina	Brazil	-26.43	-49.24
52	CFBHT03296	*luctator*	**seq**	**seq**	**seq**	NA	**seq**	NA	Sapiranga	Rio Grande do Sul	Brazil	-29.55	-51.02
53	CFBHT03698	*latrans*	**seq**	**seq**	**seq**	**seq**	**seq**	NA	Rio de Janeiro	Rio de Janeiro	Brazil	-22.96	-43.29
54	CFBHT04051	*latrans*	**seq**	**seq**	**seq**	**seq**	**seq**	NA	Caraiva	Bahia	Brazil	-16.80	-39.15
55	CFBHT04053	*latrans*	**seq**	**seq**	**seq**	NA	NA	NA	Anchieta	Espirito Santo	Brazil	-20.72	-40.77
56	CFBHT04058	*latrans*	**seq**	**seq**	**seq**	**seq**	**seq**	**seq**	Conceicao da Barra	Espirito Santo	Brazil	-18.50	-39.78
57	CFBHT04086	CS1	**seq**	**seq**	**seq**	NA	NA	NA	Feira de Santana	Bahia	Brazil	-12.28	-38.99
58	CFBHT04399	*luctator*	**seq**	**seq**	**seq**	**seq**	**seq**	NA	Pedregulho	São Paulo	Brazil	-20.25	-47.45
59	CFBHT05235	CS3	**seq**	**seq**	**seq**	**seq**	**seq**	**seq**	Ilha Comprida	São Paulo	Brazil	-24.71	-47.53
60	CFBHT06487	*luctator*	**seq**	KU495329	**seq**	NA	**seq**	NA	Rio Claro	São Paulo	Brazil	-22.33	-47.72
61	CFBHT07680	*latrans*	**seq**	**seq**	**seq**	**seq**	**seq**	NA	Prado	Bahia	Brazil	-17.35	-39.23
62	CFBHT07725	*luctator*	**seq**	KU495333	**seq**	NA	NA	NA	Bauru	São Paulo	Brazil	-22.24	-49.08

63	CFBHT08134	*luctator*	**seq**	**seq**	**seq**	NA	**seq**	NA	Quatro Barras	Paraná	Brazil	-25.38	-49.09
64	CFBHT08618	CS3	**seq**	**seq**	**seq**	**seq**	**seq**	NA	Cananeia	São Paulo	Brazil	-25.00	-47.94
65	CFBHT08695	CS3	**seq**	**seq**	**seq**	NA	NA	NA	Iguape	São Paulo	Brazil	-24.68	-47.52
66	CFBHT09153	*latrans*	**seq**	**seq**	**seq**	NA	NA	NA	Urucuca	Bahia	Brazil	-14.59	-39.30
67	CFBHT09167	CS1	**seq**	**seq**	**seq**	NA	NA	NA	Jequie	Bahia	Brazil	-13.95	-40.03
68	CFBHT09221	*latrans*	**seq**	**seq**	**seq**	**seq**	**seq**	NA	Linhares	Espirito Santo	Brazil	-19.15	-40.06
69	CFBHT09245	*latrans*	**seq**	**seq**	**seq**	**seq**	**seq**	NA	Aurelino Leal	Bahia	Brazil	-14.31	-39.33
70	CFBHT09392	CS1	**seq**	**seq**	**seq**	NA	NA	NA	Maracás	Bahia	Brazil	-13.43	-40.44
71	CFBHT09399	CS1	**seq**	**seq**	**seq**	NA	NA	NA	Maracás	Bahia	Brazil	-13.43	-40.44
72	CFBHT09560	*luctator*	**seq**	**seq**	**seq**	**seq**	**seq**	NA	Cerro Largo	Rio Grande do Sul	Brazil	-28.15	-54.76
73	CFBHT09578	*luctator*	**seq**	**seq**	**seq**	NA	**seq**	NA	Sao Sepe	Rio Grande do Sul	Brazil	-30.37	-53.66
74	CFBHT09612	*luctator*	**seq**	**seq**	**seq**	NA	**seq**	NA	Teodoro Sampaio	São Paulo	Brazil	-22.51	-52.32
75	CFBHT09673	*luctator*	**seq**	**seq**	**seq**	NA	**seq**	NA	Mato Castelhano	Rio Grande do Sul	Brazil	-28.28	-52.19
76	CFBHT10455	*latrans*	**seq**	KU495331	**seq**	**seq**	**seq**	NA	Marataizes	Espirito Santo	Brazil	-21.04	-40.85
77	CFBHT10542	*latrans*	**seq**	KU495336	**seq**	NA	NA	NA	Niteroi	Rio de Janeiro	Brazil	-22.97	-43.02
78	CFBHT11565	CS3	**seq**	**seq**	**seq**	**seq**	**seq**	**seq**	Santos	São Paulo	Brazil	-23.88	-46.31
79	CFBHT11864	*luctator*	**seq**	KU495330	**seq**	**seq**	**seq**	NA	Tibagi	Paraná	Brazil	-24.50	-50.42
80	CFBHT11881	*luctator*	**seq**	**seq**	**seq**	**seq**	**seq**	NA	Jaguariaiva	Paraná	Brazil	-24.24	-49.71
81	CFBHT12637	*luctator*	**seq**	**seq**	**seq**	**seq**	**seq**	**seq**	Brasilia	Distrito Federal	Brazil	-15.74	-47.88
82	CFBHT12812	*latrans*	**seq**	**seq**	**seq**	**seq**	**seq**	**seq**	Camamu	Bahia	Brazil	-13.94	-39.10
83	CFBHT12834	*latrans*	**seq**	NA	**seq**	**seq**	**seq**	NA	Camamu	Bahia	Brazil	-13.94	-39.10
84	CFBHT13480	*latrans*	**seq**	NA	**seq**	**seq**	**seq**	NA	Gandu	Bahia	Brazil	-13.74	-39.48
85	CFBHT14337	*luctator*	**seq**	**seq**	**seq**	**seq**	**seq**	**seq**	Sao Jose do Barreiro	São Paulo	Brazil	-22.72	-44.62
86	CFBHT15828	*latrans*	**seq**	NA	**seq**	**seq**	**seq**	NA	Porto Seguro	Bahia	Brazil	-16.40	-39.05
87	CFBHT18461	CS1	**seq**	NA	**seq**	NA	**seq**	NA	Brejinho das Ametistas	Bahia	Brazil	-14.27	-42.52
88	CFBHT18858	CS3	**seq**	**seq**	**seq**	**seq**	**seq**	NA	Sete Barras	São Paulo	Brazil	-24.38	-47.93
89	CFBHT18860	*luctator*	**seq**	NA	**seq**	**seq**	**seq**	NA	Sacramento	Minas Gerais	Brazil	-19.86	-47.46
90	CFBHT19433	CS3	**seq**	**seq**	**seq**	**seq**	**seq**	**seq**	Apiai	São Paulo	Brazil	-24.59	-48.59
91	CFBHT19776	CS3	**seq**	**seq**	**seq**	**seq**	**seq**	**seq**	São Francisco do sul	Santa Catarina	Brazil	-26.18	-48.71
92	CFBHT21008	*luctator*	**seq**	**seq**	**seq**	**seq**	**seq**	NA	Campo Alegre	Santa Catarina	Brazil	-26.18	-49.28
93	CFBHT21063	CS3	**seq**	**seq**	**seq**	NA	**seq**	**seq**	Torres	Rio Grande do Sul	Brazil	-29.35	-49.75
94	CHUNB25169	*luctator*	**seq**	**seq**	**seq**	**seq**	**seq**	NA	Paracatu	Minas Gerais	Brazil	-17.17	-46.91
95	CHUNB43427	*luctator*	**seq**	**seq**	**seq**	**seq**	**seq**	NA	Luziânia	Goias	Brazil	-16.55	-48.02
96	CHUNB53237	CS1	**seq**	**seq**	**seq**	**seq**	**seq**	**seq**	Dário Meira	Bahia	Brazil	-14.44	-39.91
97	FSCHUFPB7162	CS1	**seq**	**seq**	**seq**	**seq**	**seq**	**seq**	Morro do Chapeu	Bahia	Brazil	-11.59	-41.12
98	FSCHUFPB7170	CS1	**seq**	**seq**	**seq**	**seq**	**seq**	**seq**	Campo Formoso	Bahia	Brazil	-10.51	-40.81
99	FSCHUFPB7174	CS1	**seq**	**seq**	**seq**	**seq**	**seq**	**seq**	Jaguarari	Bahia	Brazil	-10.27	-40.20
100	FSCHUFPB7175	CS1	**seq**	NA	**seq**	**seq**	**seq**	**seq**	Jaguarari	Bahia	Brazil	-10.27	-40.20
101	IGA103	*luctator*	**seq**	**seq**	**seq**	**seq**	**seq**	NA	Atucha	Buenos Aires	Argentina	-33.96	-59.20

102	IIBPH0619	*luctator*	**seq**	**seq**	**seq**	NA	**seq**	NA	Yegros	Caazapa	Paraguay	-26.45	-56.35
103	IIBPH1208	*luctator*	**seq**	**seq**	**seq**	NA	NA	NA	Alto Vera	Itapua	Paraguay	-26.76	-55.77
104	IIBPH1570	*luctator*	**seq**	**seq**	**seq**	NA	NA	NA	Alto Vera	Itapua	Paraguay	-26.76	-55.77
105	JL2030	*luctator*	**seq**	**seq**	**seq**	**seq**	**seq**	NA	Monte Vera	Santa Fe	Argentina	-31.49	-60.67
106	JLEjemp5	*luctator*	**seq**	**seq**	**seq**	NA	**seq**	NA	La Capital	Santa Fe	Argentina	-31.64	-60.67
107	JLsj3	*luctator*	**seq**	**seq**	**seq**	**seq**	**seq**	**seq**	San Carlos	San Juan	Argentina	-32.14	-68.48
108	JLsj4	*luctator*	**seq**	NA	**seq**	**seq**	**seq**	NA	San Carlos	San Juan	Argentina	-32.14	-68.48
109	LGE01211	*luctator*	**seq**	**seq**	**seq**	**seq**	**seq**	NA	Cainguás	Misiones	Argentina	-27.09	-54.95
110	LGE02007	*luctator*	**seq**	**seq**	**seq**	**seq**	**seq**	NA	San Miguel	Corrientes	Argentina	-28.17	-57.54
111	LGE02278	*luctator*	**seq**	**seq**	**seq**	**seq**	**seq**	NA	General Manuel Belgrano	Misiones	Argentina	-26.12	-53.81
112	LGE03417	*luctator*	**seq**	**seq**	**seq**	**seq**	**seq**	**seq**	Estancia Macaca	Misiones	Argentina	-26.39	-53.72
113	LGE03574	*luctator*	**seq**	**seq**	**seq**	NA	**seq**	NA	StoDomingo	Corrientes	Argentina	-27.63	-56.14
114	LGE03658	*luctator*	**seq**	**seq**	**seq**	**seq**	**seq**	NA	Garupa	Misiones	Argentina	-27.47	-55.88
115	LGE06178	*luctator*	**seq**	**seq**	**seq**	**seq**	**seq**	NA	ResStoTome	Corrientes	Argentina	-28.57	-56.01
116	LGE07305	*luctator*	**seq**	**seq**	**seq**	**seq**	**seq**	NA	SanJavier	Misiones	Argentina	-27.84	-55.15
117	LGE07805	*luctator*	**seq**	NA	**seq**	**seq**	NA	NA	EstHollada	Cordoba	Argentina	-31.36	-64.68
118	LGE09027	*luctator*	**seq**	**seq**	**seq**	**seq**	**seq**	NA	StoTome	Corrientes	Argentina	-28.09	-55.75
119	LGE18721	*luctator*	**seq**	**seq**	**seq**	**seq**	**seq**	NA	Luis Palacios	Santa Fe	Argentina	-32.78	-60.90
120	MAPT0968	CS3	**seq**	**seq**	**seq**	**seq**	**seq**	NA	São Bonifacio	Santa Catarina	Brazil	-27.90	-48.91
121	MAPT1362	*luctator*	**seq**	**seq**	**seq**	**seq**	**seq**	**seq**	Corumbá	Mato Grosso do Sul	Brazil	-19.58	-57.02
122	MAPT1372	*luctator*	**seq**	**seq**	**seq**	**seq**	**seq**	NA	Corumbá	Mato Grosso do Sul	Brazil	-19.58	-57.02
123	MLPDB2510	*luctator*	**seq**	**seq**	**seq**	NA	**seq**	NA	Perugorria	Corrientes	Argentina	-29.20	-58.53
124	MLPDB2632	*luctator*	**seq**	**seq**	**seq**	NA	**seq**	NA	Tulumba	Cordoba	Argentina	-30.08	-64.15
125	MLPDB3325	*luctator*	**seq**	**seq**	**seq**	NA	**seq**	NA	Vera	Santa Fe	Argentina	-29.47	-60.23
126	MLPDB4190	*luctator*	**seq**	**seq**	**seq**	**seq**	**seq**	**seq**	Lujan	Buenos Aires	Argentina	-34.63	-59.11
127	MLPDB4421	*luctator*	**seq**	**seq**	**seq**	**seq**	**seq**	NA	Candelario	Misiones	Argentina	-27.41	-55.62
128	MLPDB6080	*luctator*	**seq**	**seq**	**seq**	**seq**	**seq**	NA	Chajari	Entre Ríos	Argentina	-30.79	-58.00
129	MLPDB6679	*luctator*	**seq**	**seq**	**seq**	NA	**seq**	NA	Juarez Celman	Cordoba	Argentina	-33.51	-63.29
130	MLPDB8140	*luctator*	**seq**	**seq**	**seq**	**seq**	**seq**	NA	General Obligado	Santa Fe	Argentina	-28.62	-59.66
131	MZFS4360	CS1	**seq**	**seq**	**seq**	**seq**	**seq**	**seq**	Elísio Medrado	Bahia	Brazil	-12.84	-39.48
132	TRC011	*latrans*	**seq**	**seq**	**seq**	**seq**	**seq**	**seq**	Santa Tereza	Espirito Santo	Brazil	-19.92	-40.56
133	TRC116	*latrans*	**seq**	**seq**	**seq**	**seq**	**seq**	NA	Cachoeira de Macacu	Rio de Janeiro	Brazil	-22.44	-42.65
134	UFBA14650	*latrans*	**seq**	**seq**	**seq**	**seq**	**seq**	NA	Itapebi	Bahia	Brazil	-15.89	-39.53
135	UFBA15099	*latrans*	**seq**	**seq**	**seq**	**seq**	**seq**	**seq**	Vale Encantado, Salvador	Bahia	Brazil	-12.95	-38.40
136	UFES3511	*latrans*	**seq**	**seq**	**seq**	**seq**	**seq**	NA	Castelo	Espirito Santo	Brazil	-20.59	-41.25
137	UFMGT2137	*luctator*	**seq**	**seq**	**seq**	**seq**	**seq**	**seq**	Serra do salitre	Minas Gerais	Brazil	-19.09	-46.70
138	UFMGT3008	*luctator*	**seq**	NA	**seq**	**seq**	**seq**	NA	Itacambira	Minas Gerais	Brazil	-17.04	-43.32
139	UFMGT3539	*luctator*	**seq**	**seq**	**seq**	**seq**	**seq**	**seq**	Botumirim	Minas Gerais	Brazil	-16.82	-43.03
140	UFMGT4377	*luctator*	**seq**	**seq**	**seq**	**seq**	**seq**	NA	Grão Mogol	Minas Gerais	Brazil	-16.55	-42.87

141	UFMGT5160	*latrans*	**seq**	**seq**	**seq**	**seq**	**seq**	**seq**	Caratinga	Minas Gerais	Brazil	-19.78	-42.14
142	UFMGT5744	*latrans*	**seq**	**seq**	**seq**	**seq**	**seq**	**seq**	Carlos Chagas	Minas Gerais	Brazil	-17.69	-40.78
143	ZVCB04714	*luctator*	**seq**	**seq**	**seq**	**seq**	**seq**	**seq**	Maldonado	Maldonado	Uruguay	-34.85	-54.94
144	ZVCB11749	*luctator*	**seq**	**seq**	NA	NA	**seq**	NA	Durazno	Durazno	Uruguay	-32.99	-56.06

Table S2. Substitution model as selected by the Bayesian Information Criterion for each locus in jModelTest.

Locus	Substitution model
COI	HKY + I
16S	HKY + I
cmyc2	HKY + Γ
Fib7	F81
Tyr	K80 + I
POMC	F81

Table S3. Primers and PCR protocol used to amplify each locus. COI = mitochondrial cytochrome c oxidase I; cmyc2 = c-myc exon 2; Fib7 = β-Fibrinogen Intron 7; POMC = nuclear proopiomelanocortin; TYR = nuclear tyrosinase precursor.

Primer		Gene	Sequence	PCR protocol	Reference
dgLCO1490	F	COI	GGTCAACAAATCATAAAGAYATYGG	[94 (30"), 48 (30"), 72 (45")] × 35	Meyer, 2003
dgHCO2198	R	COI	TAAACTTCAGGGTGACCAAARAAYCA		
AnF1	F	COI	ACHAAYCAYAAAGAYATYGG		Lyra et al., 2017
AnR1	R	COI	CCRAARAATCARAADARRTGTTG		
16SA-L	F	16S	CGCCTGTTTATCAAAAACAT		Palumbi et al. 1991
16SB-H	R	16S	CCGGTCTGAACTCAGATCACGT		
Tyr I Lepto14	F	Tyr	GTCSTGTCCAACTCTCCYGTG	[94 (30"), 58 (30"), 72 (45")] × 40	Fouquet et al., 2012
Tyr E Lepto29	R	Tyr	CGTTGCTGGTTGGGTGGKTTC		
POMC_DRV_F1	F	POMC	ATATGTCATGASCCAYTTYCGCTGGAA	[94 (30"), 56 (30"), 72 (45")] × 40	Vieites et al., 2007
POMC_DRV_R1	R	POMC	GGCRTTYTTGAAWAGAGTCATTAGWGG		
FIB-I7U	F	Fib7	GGAGAAAACAGGACAATGACAATTCAC	[94 (30"), 54 (30"), 72 (45")] × 40	Prychitko and Moore, 1997
FIB-I7L	R	Fib7	TCCCATATATCTGCCATTAGGGTT		
cmyc1U	F	cmyc2	GAGGACATCTGGAARAARTT	[94 (30"), 59 (30"), 72 (120")] × 40	Crawford, 2003
cmyc3L	R	cmyc2	GTCTTCCTCTTGTCRTTCTCYTC		
cmyc3cat (seq)	R	cmyc2	GTTGYTGCTGATCTGTTTGAG		Brunes et al., 2010

Table S4. Population genetic summary metrics. Neutrality tests values in bold indicates statistically significative results.

Locus	Population	Summary statistics						Neutrality tests		
		n	bp	*S*	H	Hd	pi	D	R2	Fs
16S mtDNA	**total**	125	348							
	CS1S	15	–	1	2	0.133	0.000	-1.159	0.249	-0.649
	lucN	40	–	7	6	0.432	0.004	-0.314	0.103	-0.162
	lucS	25	–	16	11	0.827	0.008	-1.325	**0.075***	**-3.509***
	latN	12	–	7	7	0.894	0.005	-0.946	**0.103***	**-2.976***
	latS	16	–	3	4	0.442	0.002	-1.002	**0.112***	**-1.415***
	CS3	17	–	6	7	0.596	0.002	**-1.825***	**0.078***	**-4.799***
COI mtDNA	**total**	140	507							
	CS1S	19	–	16	6	0.725	0.014	**2.093***	0.22	4.086
	lucN	42	–	39	22	0.916	0.014	-0.838	0.0852	**-5.352***
	lucS	27	–	42	17	0.892	0.016	-1.001	0.087	-3.196
	latN	17	–	20	13	0.949	0.012	-0.243	0.129	**-4.104***
	latS	18	–	30	13	0.961	0.010	-1.687	0.092	**-4.36***
	CS3	17	–	6	6	0.654	0.002	-1.631	**0.098***	**-2.848***
Fib7 (nuDNA)	**total-phased**	210	359							
	CS1S	26	–	3	4	0.702	0.004	1.791	0.227	1.049
	lucN	62	–	6	6	0.594	0.002	-0.809	0.072	-1.296
	lucS	32	–	5	5	0.542	0.004	0.119	0.129	0.135
	latN	32	–	3	3	0.365	0.001	-0.829	0.13	0.014
	latS	32	–	6	6	0.806	0.005	0.399	0.139	0.004
	CS3	26	–	4	5	0.625	0.002	-0.782	0.096	-1.576
Tyr (nuDNA)	**total-phased**	246	510							
	CS1S	30	–	4	4	0.490	0.001	-0.855	0.0842	-0.532
	lucN	74	–	17	24	0.948	0.008	0.524	0.121	**-8.399***
	lucS	46	–	11	12	0.831	0.006	0.884	0.147	-1.517
	latN	32	–	2	3	0.433	0.001	-0.190	0.13	-0.104
	latS	32	–	5	5	0.631	0.002	-0.805	0.088	-0.93
	CS3	32	–	5	6	0.782	0.003	0.123	0.129	-0.79
cmyc2 (nuDNA)	**total-phased**	276	852							
	CS1S	36	–	4	4	0.410	0.001	-1.123	0.101	-0.968
	lucN	84	–	9	12	0.501	0.001	-1.764	**0.039***	**-10.123***
	lucS	52	–	5	9	0.729	0.002	0.424	0.13	-2.839
	latN	34	–	5	6	0.670	0.001	-0.567	0.108	-1.606
	latS	36	–	6	8	0.687	0.001	-0.952	0.092	**-3.109***
	CS3	34	–	3	4	0.604	0.001	0.339	0.14	0.102

Table S5. List of variables used for climatic niche models construction (in bold variables selected after correlation test).

Variables	ID
Altitude	Altitude
BIO01	Annual mean temperature
BIO02	Mean diurnal range (mean of monthly (max temp - min temp))
BIO03	Isothermality (BIO2/BIO7) (* 100)
BIO04	Temperature seasonality
BIO05	Maximum temperature of warmest month
BIO06	Minimum temperature of coldest month
BIO07	Temperature annual range
BIO08	Mean temperature of wettest quarter
BIO09	Mean temperature of driest quarter
BIO10	Mean temperature of warmest quarter
BIO11	Mean temperature of coldest quarter
BIO12	Annual precipitation
BIO13	Precipitation of wettest month
BIO14	Precipitation of driest month
BIO15	Precipitation seasonality (Coefficient of Variation)
BIO16	Precipitation of wettest quarter
BIO17	Precipitation of driest quarter
BIO18	Precipitation of warmest quarter
BIO19	Precipitation of coldest quarter

Table S6. Variables used to test background similarity between pairs of lineages belonging to the *Leptodactylus latrans* species complex and AUC values from the observed dataset for the pairwise comparison. Results from the background similarity test using Hellinger's I metric.

Lineage pairs (X – Y)	Variables	AUC (lineage 1/ lineage 2)	Hellinger's I metric		
			observed	null-model 95%(X>Y)	null-model 95% (Y>X)
CS1 - luc	alt, bio12, bio16, bio18, bio19, bio2, bio4, bio5, bio8, bio9	0.983/0.847	0.292	0.40–0.46	0.80–0.90
CS1 - lat	alt, bio16, bio19, bio3, bio4, bio5, bio7	0.917/0.920	0.47	0.79–0.85	0.64–0.80
CS1 - CS3	alt, bio16, bio19, bio2, bio4, bio5, bio6, bio7	0.904/0.968	0.173	0.77–0.87	0.43–0.62
luc - lat	alt, bio12, bio16, bio18, bio19, bio2, bio5, bio7, bio8, bio9	0.844/0.956	0.576	0.87–0.91	0.65–0.72
luc - CS3	alt, bio12, bio16, bio18, bio19, bio2, bio5, bio8, bio9	0.838/0.993	0.54	0.83–0.92	0.42–0.49
lat - CS3	alt, bio16, bio19, bio2, bio4, bio5,	0.869/0.966	0.437	0.79–0.89	0.53–0.62
lucN - lucS	alt, bio12, bio16, bio19, bio2, bio5, bio7, bio8, bio9	0.853/0.859	0.753	0.86–0.95	0.77–0.89
latN - latS	alt, bio12, bio16, bio19, bio2, bio4, bio5	0.857/0.861	0.87	0.80–0.93	0.88–0.96

Supplementary Fig. 1. Geneland results showing cluster membership probabilities.

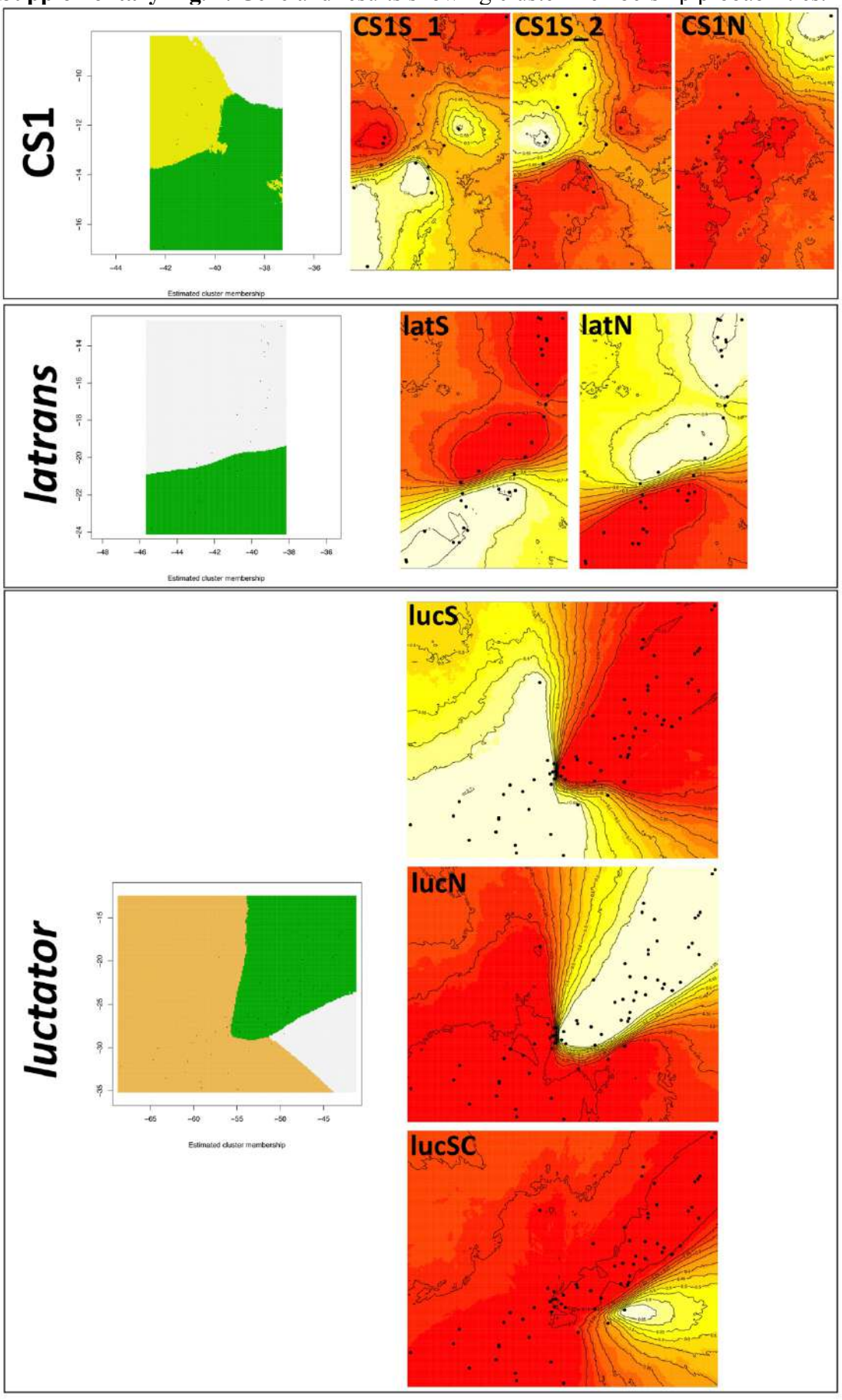

References:

Brunes, T.O., Sequeira, F., Haddad, C.F.B., Alexandrino, J., 2010. Gene and species trees of a Neotropical group of treefrogs: Genetic diversification in the Brazilian Atlantic Forest and the origin of a polyploid species. Molecular Phylogenetics and Evolution 57, 1120–1133. DOI: 10.1016/j.ympev.2010.08.026

Crawford, A.J., 2003. Huge populations and old species of Costa Rican and Panamanian dirt frogs inferred from mitochondrial and nuclear gene sequences. Molecular Ecology 12, 2525–2540. DOI: 10.1046/j.1365-294X.2003.01910.x

Fouquet, A., Noonan, B.P., Rodrigues, M.T., Pech, N., Gilles, A., Gemmell, N.J., 2012. Multiple quaternary refugia in the eastern Guiana Shield revealed by comparative phylogeography of 12 frog species. Systematic Biology 61, 461–489. DOI:10.1093/sysbio/syr130

Lyra, M.L., Haddad, C.F.B., Azeredo-Espin, A.M.L., 2017. Meeting the challenge of DNA barcoding Neotropical amphibians: polymerase chain reaction optimization and new COI primers. Molecular Ecology Resources 17, 966–980. DOI: 10.1111/1755-0998.12648

Meyer, C., 2003. Molecular systematics of cowries (Gastropoda: Cypraeidae) and diversification patterns in the tropics. Biological Journal of Linnean Society 79, 401–459. https://doi.org/10.1046/j.1095-8312.2003.00197.x

Palumbi, S.R., Martin, A., Romano, S., McMillan, W.O., Stice, L., Grabowski, G., 1991. The Simple Fool's Guide to PCR, Version 2.0. Department of Zoology, Kewalo Marine Laboratory, University of Hawaii.

Prychitko, T.M., Moore, W.S., 1997. The utility of DNA sequences of an intron from the beta-fibrinogen gene in phylogenetic analysis of woodpeckers (Aves: Picidae). Molecular Phylogenetics and Evolution 8, 193–204. DOI: 10.1006/mpev.1997.0420

Vieites, D.R., Min, M.-S., Wake, D.B., 2007. Rapid diversification and dispersal during periods of global warming by plethodontid salamanders. Proceedings of the National Academy of Sciences of the USA 104, 19903–19907. https://doi.org/10.1073/pnas.0705056104

Figure Captions

Fig. 1. Inter and intraspecific genetic diversity among L*eptodactylus latrans* species complex. (a) mitochondrial gene tree recovered in BEAST and genetic breaks found by STRUCTURE (STR) and Geneland (GNL) for each species. The first column refers to species delimited by Magalhães et al. (MAG; Capítulo I). Values on nodes indicate posterior probabilities, while black circles denote posterior probability = 1.0. Scale indicates rate of base substitutions per site. Asterisks indicate lineages identified by BPP with probabilities above 0.95. Lineages are named as north and south populations relative to the geographic break, while lucSC is named with after the Brazilian state it occur (Santa Catarina). (b) Haplotype networks for the four nuclear genes, cmyc2, Tyr, Fib7, and POMC. Numbers within circles refers to haplotype frequency. Branches without dots represent a single mutational step. Dots along haplotype networks indicate additional mutational steps for branches with more than one mutation. Colors of haplotypes denote all populations validated by STRUCTURE/Geneland and BPP.

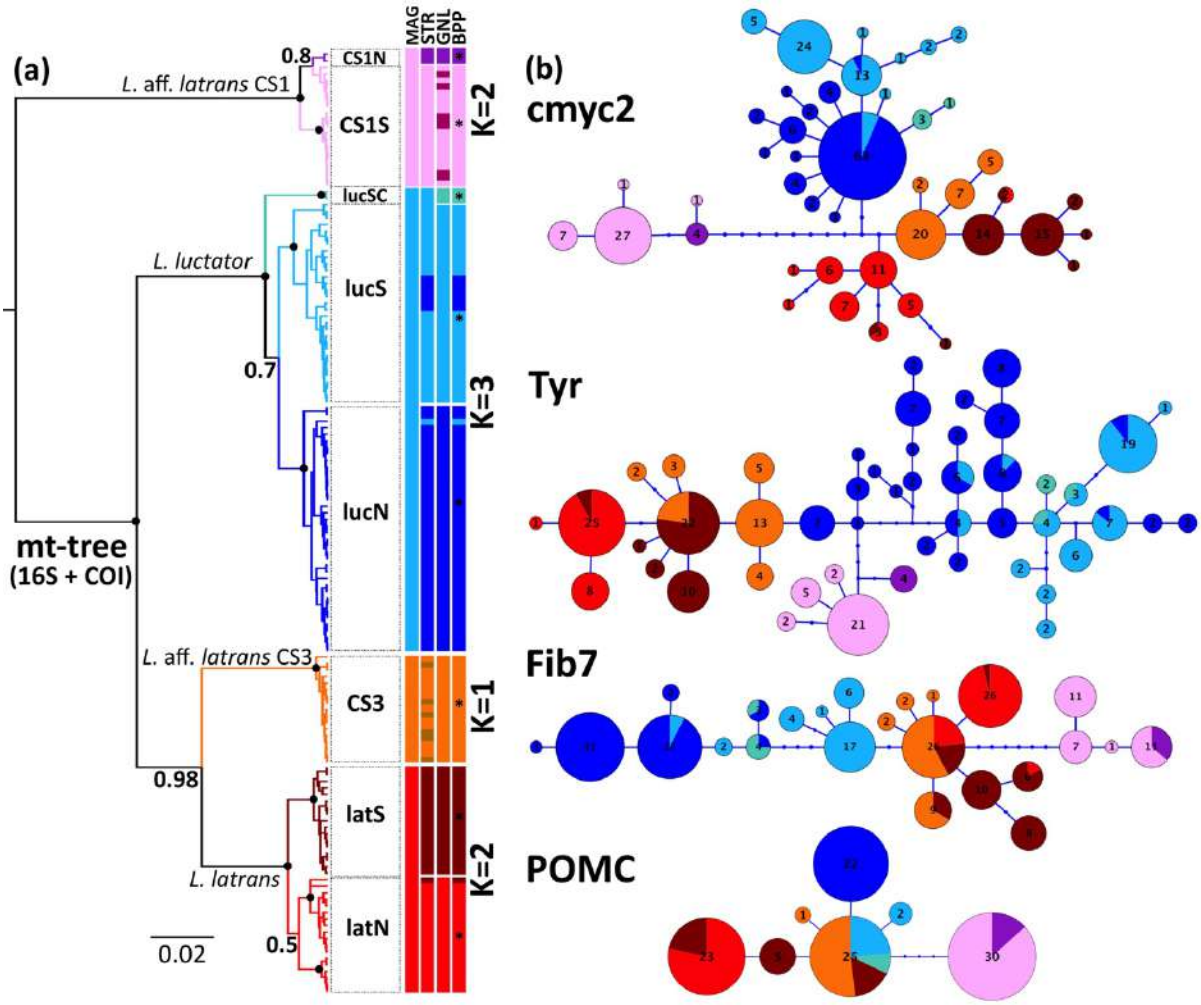

Fig. 2. Extended Bayesian skyline plot (EBSP) showing changes in effective population size through time for lineages in the *Leptodactylus latrans* species complex based on mitochondrial and nuclear genes. Y-axis shows the effective population size with respective mean (dashed lines) and 95% highest posterior density limits (The surrounding green area delimited by the continuous line). The x-axis shows time in millions of years as time goes backwards from left to right. The thick and thinner grayish horizontal bars along all plots indicate the Last Interglacial (LIG, ca. 130 kya) and Last Glacial Maximum (LGM, ca. 21 kya) periods, respectively.

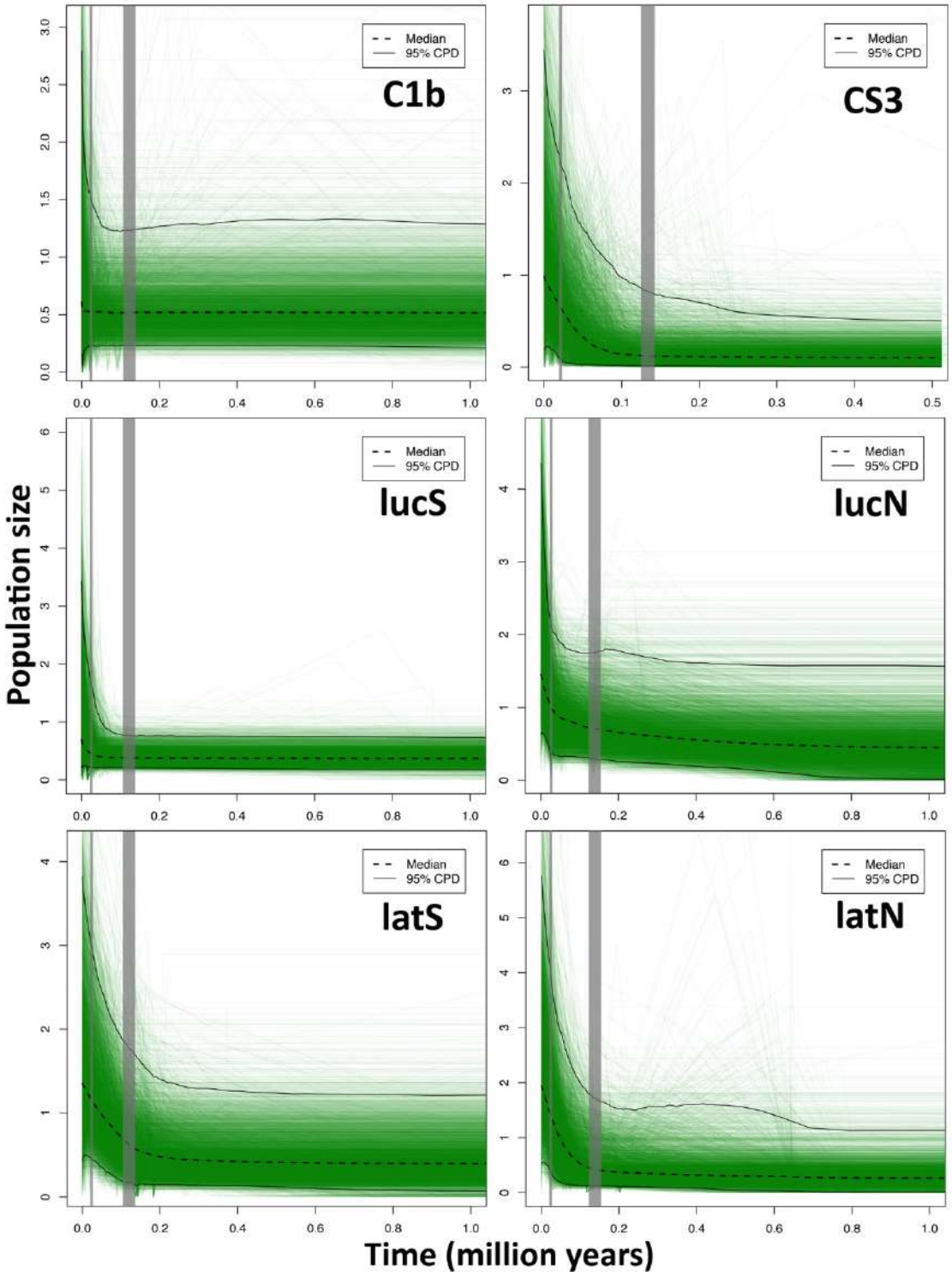

Fig. 3. (a) Geographic distribution along eastern South America of all genetic samples from all eight supported lineages belonging to the *Leptodactylus latrans* species complex; (b) Time-calibrated species tree of lineages in the *Leptodactylus latrans* species complex estimated with *BEAST. Terminals represent the genetic breaks found by Geneland and STRUCTURE and validated by BPP. Values above nodes indicate Bayesian posterior probabilities, while values below indicate mean divergence time estimated in *BEAST. Asterisks indicate posterior probabilities values = 1.0. Scale indicates time in millions of years (Mya). Two main rivers that could be related to populational genetic breaks are also depicted. Country acronyms: ARG: Argentina, BRA: Brazil, PAR: Paraguai, URU: Uruguay. A representative from the nominal *Leptodactylus latrans* lineage (latN) is also depicted.

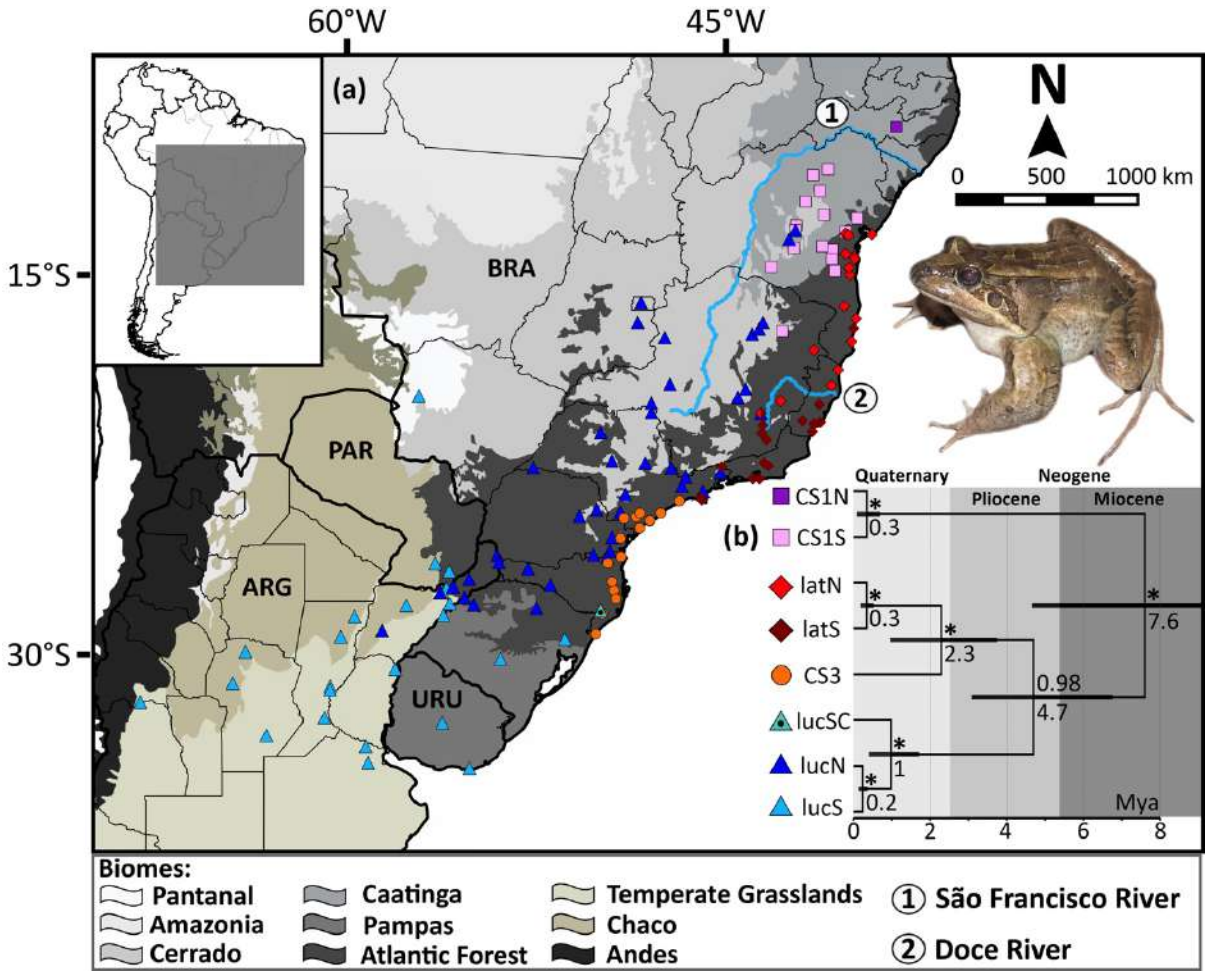

Fig. 4. Ecological niche models constructed in Maxent for all four species in the *Leptodactylus latrans* complex projected to the present, last glacial maximum (LGM), and last interglacial (LIG) periods. Hot colors indicate high habitat suitability, while cold colors indicate low habitat suitability.

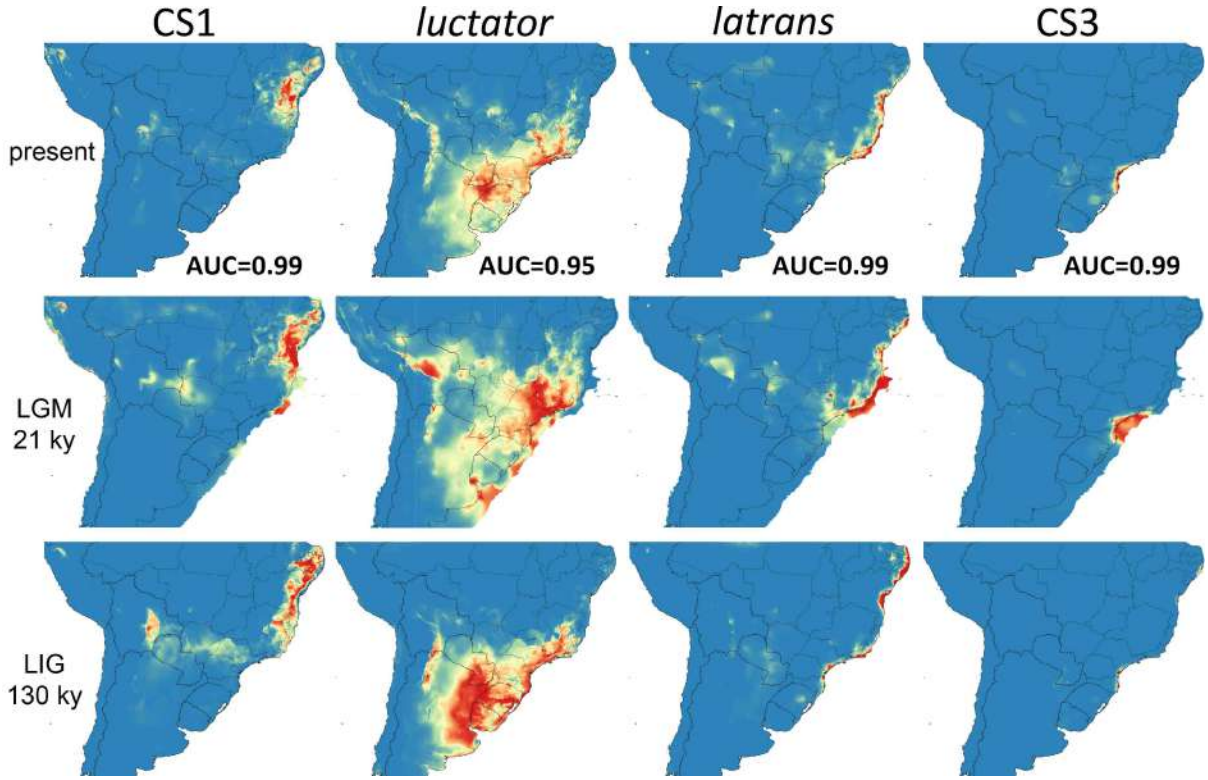

Fig. 5. Pairwise background similarity tests (a) among species belonging to the *Leptodactylus latrans* complex and, (b) among genetically structured sister lineages of both *L. luctator* and *L. latrans*. Niche overlap values were based on Schoener's *D* statistics. Observed values are shown as red line and null distribution is shown as a histogram.